JOURNAL OF INNOVATIONS IN MEDICAL RESEARCH

ISSN 2788-7022 APR. 2025 VOL. 4, NO. 2

CONTENTS

JOURNAL OF INNOVATIONS IN MEDICAL RESEARCH

ISSN 2788-7022 APR. 2025 VOL. 4, NO. 2

CONTENTS

Paradigm Academic Press
Journal of Innovations in Medical Research
ISSN 2788-7022
APR. 2025 VOL.4, NO.2

Betanin Ameliorates Triclosan-Induced Spermatogenic Dysfunction and Testicular Damage in Prenatally Exposed Wistar Rats

Eneh Chidera Amanda[1], Idoko Gabriel Owoicho[1], Kiekwe Vershima[1], Akunna Godson Gabriel[1] & Saalu Linus Chia[1]

[1] Department of Anatomy, Faculty of Basic Medical Sciences, Benue State University, Makurdi, Benue State, Nigeria

Correspondence: Akunna Godson Gabriel, Department of Anatomy, Faculty of Basic Medical Sciences, Benue State University, Makurdi, Benue State, Nigeria.

doi:10.63593/JIMR.2788-7022.2025.04.001

Abstract

Aims: To investigate the effects of betanin on reproductive hormones, sperm parameters, testicular histology and testicular damage induced by prenatal TCS exposure in Wistar rats. ***Study Design:*** Experimental study design, using a Randomized Controlled Trial (RCT) approach with animal subjects (Wistar rats). ***Place and Duration of Study:*** Department of Anatomy, Faculty of Basic Medical Sciences, College of Health Sciences, Benue State University Makurdi, between August and October 2024. ***Methodology:*** Sixty Wistar rats were divided into ten groups (n=6/group). Groups received varying doses of TCS (5, 10, and 20 mg/kg), betanin (5, 10, and 20 mg/kg), or a combination of both for 31 days. Hormone levels, sperm count and morphology, and testicular histology were assessed. ***Results:*** TCS exposure significantly reduced testosterone levels (20 mg/kg TCS: 1.35±0.31 ng/ml) and LH (20 mg/kg TCS: 1.10±0.14 mlU/ml), sperm count (20 mg/kg TCS: 74.00 ± 29.69 $x10^6$/ml), and normal sperm morphology (20 mg/kg TCS: 29.65%). Betanin co-administration partially mitigated these effects, with the 20 mg/kg betanin + 20 mg/kg TCS group showing near-control levels of testosterone (3.77±0.74 ng/ml) and LH (2.70±0.29 mlU/ml), and improved sperm count (5 mg/kg TCS + 5 mg/kg betanin: 97.20 ± 3.11 $x10^6$/ml) and morphology. Histological analysis revealed severe testicular damage in TCS-exposed groups, which was partially ameliorated by betanin. ***Conclusion:*** Prenatal TCS exposure impairs male reproductive function. Betanin offers partial protection, suggesting its potential therapeutic role against TCS-induced reproductive toxicity.

Keywords: triclosan, betanin, spermatogenesis, testicular damage, prenatal exposure, Wistar rats

1. Introduction

Male infertility, a significant contributor to the global health concern of infertility, affects millions worldwide and carries profound social, psychological, and physical consequences (Hipwell et al., 2019; Chigrinets et al., 2020). While both male and female factors are implicated, male infertility, often characterized by disrupted spermatogenesis and poor semen quality (Aoun et al., 2021), accounts for a substantial portion of cases. Defined as the inability to conceive with a fertile partner after at least one year of regular, unprotected intercourse (PCASRM, 2008), it contributes to approximately 20% of all infertility cases and plays a role in an additional 30-40% (Hull et al., 2005). The etiology of male infertility is diverse, encompassing endocrine disorders, sperm transport issues, primary testicular defects, and idiopathic causes (Winter & Walsh, 2014). Despite often being under-prioritized in Sub-Saharan African health policies (Van, 2000; Sundby & Jacobus, 2001; Butler, 2003; NPCN, 2006), the social and psychological burden, particularly for women, is considerable (Okonofua, 1997; Aghanwa et al., 1999; Orji et al., 2002; Umezulike & Efetie, 2004; Dyer, 2004; Dyer, 2005).

The increasing prevalence of male infertility, coupled with the widespread presence of environmental pollutants

like triclosan (TCS), underscores the need for research into preventative and therapeutic strategies. TCS, a ubiquitous antibacterial compound found in various personal care products (Russell, 2004; Ahn et al., 2008; Ramos, 2009), has become a pervasive environmental contaminant (Chu & Metcalfe, 2007; Bedoux et al., 2012). Human exposure occurs primarily through topical absorption and ingestion (Moss et al., 2000; Sandborgh-Englund et al., 2006; Queckenberg et al., 2010), with studies reporting elevated urinary TCS concentrations, especially in children (Calafat et al., 2007). The detection of TCS in breast milk (Adolfsson-Erici et al., 2002) and umbilical cord blood (Pycke et al., 2014) raises concerns about its potential impact on fetal and reproductive development. As an endocrine disruptor (ED), TCS has been associated with antifertility effects, including reduced sperm production and sperm toxicity (Kumar et al., 2008; Crawford & De Catanzaro, 2012; Lan et al., 2015; Feng et al., 2016; Ibtisham et al., 2016; Jurewicz et al., 2018), as well as antiandrogenic activity and disrupted steroidogenesis (Chen et al., 2007; Kumar et al., 2009).

Dietary interventions, particularly the consumption of fruits and vegetables, offer numerous health benefits, including protection against chronic diseases (Mikolajczyk-Bator & Pawlak, 2016). These benefits are often attributed to phytochemicals, such as betalains (Koubaier et al., 2014). Beetroot (*Beta vulgaris*), a functional food rich in betalains (Georgiev et al., 2010; Ninfali & Angelino, 2013), has demonstrated promise in promoting health and preventing disease (Clifford et al., 2015; Guldiken et al., 2016). Betanin, a potent betalain isolated from beetroot, exhibits antioxidant, anti-inflammatory, and anti-carcinogenic properties, suggesting its potential to mitigate the reproductive toxicity of TCS (Guldiken et al., 2016). While beetroot and its constituents have shown protective effects in various contexts, limited research has explored their impact on male reproductive health, particularly against environmental endocrine disruptors. This study, therefore, investigates the morphological, molecular, and physiological effects of betanin on the testes of male Wistar rats prenatally exposed to TCS, aiming to contribute to the development of natural therapeutic strategies for mitigating the adverse effects of environmental contaminants on reproductive health.

2. Material and Methods

2.1 Experimental Animals

Sixty (60) adult Wistar rats were obtained from the animal house of the College of Health Sciences, Benue State University, Makurdi. Rats were housed in groups of six in 30cm × 20cm plastic cages with *ad libitum* access to standard rat pellets and water. Rats were weighed at the beginning of acclimatization, before treatment, and at the end of the experiment using an electronic weighing balance.

2.2 Experimental Plant: Beetroot

Four kilograms of beetroot (*Beta vulgaris*) bulbs were purchased from Wadata market in Makurdi. The bulbs were air-dried at 33 ± 2°C and ground into a fine powder for betanin extraction.

2.3 Experimental Drug: Triclosan

Seventy-five grams of triclosan were purchased from Mernex Pharmacy, Makurdi. A triclosan solution was prepared and stored at optimal temperature in a refrigerator at the College of Health Sciences animal house until administration.

2.4 Animal Housing and Feed

Six 30cm × 20cm plastic cages were used for housing, acclimatization, and feeding throughout the experiment. Standard rat pellets (Vital Feed) were purchased from a feed store in the Wadata area of Makurdi and stored at optimal temperature in the animal house.

2.5 Other Materials

Additional materials included gloves, sterile bottles, syringes and needles, a dissecting board and kit, 10% formalin fixative, hematoxylin and eosin (H&E) stain, cover slips, glass slides, microscopes, a microtome, a centrifuge, distilled water, feeding plates, and water bottles.

2.6 Betanin Extraction

Four kilograms of beetroot were washed, peeled, cut, dried, and mashed (Ravichandran et al., 2013). Betanin was extracted via maceration using distilled water as a solvent. The mixture was shaken/stirred for 1 hour at room temperature. Following the optimized method of Stintzing & Carle (2004), the extract was filtered to remove solids. The filtrate was centrifuged (Pyo & Jin, 2004) to remove remaining particulate matter. The crude extract was purified using ion-exchange chromatography (Wybraniec & Nowak, 2007). Betanin was identified and quantified using High-Performance Liquid Chromatography (HPLC) (Kaur & Buttar, 2020).

2.7 Experimental Design

The sixty (60) Wistar rats were randomly divided into ten (10) groups A – J, with six (6) rats in each group, and group A serving as the control group. The experimental animals in each group were administered varying doses

of triclosan and betanin isolate (E162) as described in the table below:

Table 1. Treatment and Administration Protocol

Group	Dose (kg body weight [b.wt])	Route of Administration	Period (Days)	No of rats (N)
A: Control	5ml/kg of distilled H_2O	Oral	31	6
B: Low dose	5ml/kg b.wt of low dose TCS	Oral	31	6
C: Middle dose	10ml/kg b.wt of middle dose TCS	Oral	31	6
D: High dose	20ml/kg b.wt of high dose TCS	Oral	31	6
E: Low dose	5ml/kg b.wt of low dose E162	Oral	31	6
F: Middle dose	10ml/kg b.wt of middle E162	Oral	31	6
G: High dose	20ml/kg b.wt of high dose E162	Oral	31	6
H: Low dose treatment	5ml/kg b.wt of low dose of TCS + 5ml/kg b.wt of low dose E162	Oral	31	6
I: Middle dose treatment	10ml/kg b.wt of high dose of TCS + 10ml/kg b.wt of high dose E162	Oral	31	6
J: High dose treatment	20ml/kg b.wt of high dose of TCS + 20ml/kg b.wt of high dose E162	Oral	31	6

Ei62 = Betanin Isolate of Beta vulgaris; TCS = Triclosan; b.wt = Body Weight.

2.8 Animal Sacrifice

On day 31, rats were fasted overnight, weighed, and anesthetized via chloroform inhalation. Blood samples were collected via cardiac puncture into heparinized tubes for biochemical evaluation. Testes were excised and weighed using an electronic analytical balance. Testicular volume was determined by water displacement (Archimedes' principle). Testes were fixed in 10% formaldehyde for histological analysis.

2.9 Serum Hormone Assays

Blood collected in plain containers was allowed to clot and centrifuged at 1000 rpm for 10 minutes. Serum was aliquoted, labeled, and stored at -20°C. Serum luteinizing hormone (LH) was measured using enzyme immunoassay (EIA) following the WHO matched reagent program protocol (1998) with kits supplied by NIADDK-NIH (USA). Testosterone concentrations were determined by competitive EIA (Tietz, 1995). Briefly, goat anti-rabbit IgG-coated wells were incubated with testosterone standards, controls, samples, testosterone-horseradish peroxidase conjugate, and rabbit anti-testosterone reagent. After incubation and washing, tetramethylbenzidine was added. The reaction was stopped with 1N hydrochloric acid, and absorbance was measured spectrophotometrically at 450nm. Testosterone concentrations were calculated from a standard curve.

2.10 Histological Processing

Testes fixed in 10% formalin were processed for H&E staining. Tissues were dehydrated through graded alcohols (70%, 80%, 90%, 95%, absolute), cleared in xylene, and embedded in paraffin. Paraffin blocks were sectioned at 3µm using a rotary microtome. Sections were mounted on slides, deparaffinized, hydrated, and stained with H&E. The staining procedure involved dewaxing, hydration, hematoxylin staining, differentiation, bluing, eosin counterstaining, dehydration, clearing, and mounting with DPX.

2.11 Statistical Analysis

Data were analyzed using IBM SPSS version 23. Mean and Standard Deviation (SD) were calculated. One-way ANOVA with LSD multiple range tests were used to compare groups. Statistical significance was set at $P = .05$.

3. Results

3.1 Reproductive Hormones

Figures 1 and 2 shows the analysis of reproductive hormone levels in male Wistar rats exposed to triclosan (TCS) and treated with betanin isolates (E162) from *Beta vulgaris* compared on one-way ANOVA. Triclosan exposure (Groups B, C, and D) led to a dose-dependent reduction in testosterone and LH levels, with the highest dose (20 mg/kg) showing the most pronounced suppression (1.35±0.31 ng/ml for testosterone and 1.10±0.14

mlU/ml for LH). This suggests that TCS disrupts endocrine function, potentially impairing testicular steroidogenesis.

Conversely, betanin treatment alone (Groups E, F, and G) resulted in varied hormonal responses. The 10 mg/kg dose (Group F) showed levels comparable to the control group, indicating a potential restorative effect. However, the highest dose (20 mg/kg, Group G) led to a decline in testosterone, despite an increase in LH, suggesting a possible feedback mechanism or dose-dependent toxicity.

Co-administration of TCS and betanin (Groups H, I, and J) partially mitigated TCS-induced hormonal suppression. The combination at 20 mg/kg (Group J) exhibited near-control levels of testosterone and LH (3.77±0.74 ng/ml and 2.70±0.29 mlU/ml, respectively), highlighting the potential protective role of betanin against TCS toxicity.

These results indicate that prenatal exposure to TCS disrupts male reproductive hormones, but betanin isolates may offer a dose-dependent protective effect, with moderate doses appearing most effective.

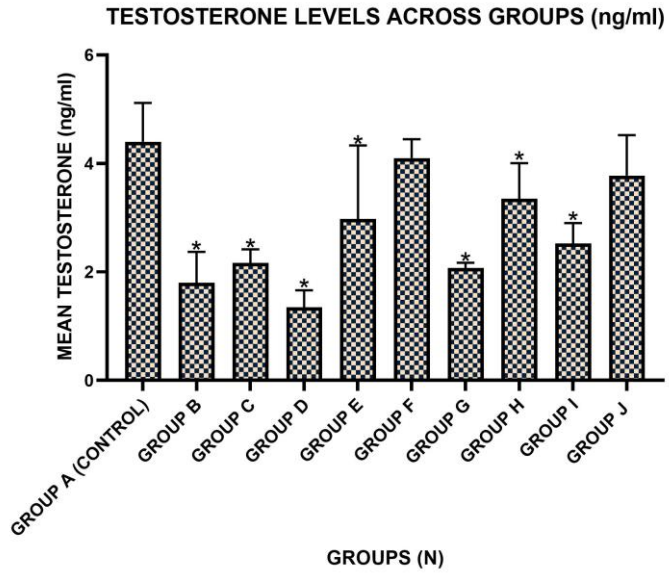

Figure 1. Simple Bar Chart Showing the Mean Testosterone Levels across Groups

Note: N = 6; * = Statistically Significant Difference in Mean at *P* = .05 Compared to the Control Group.

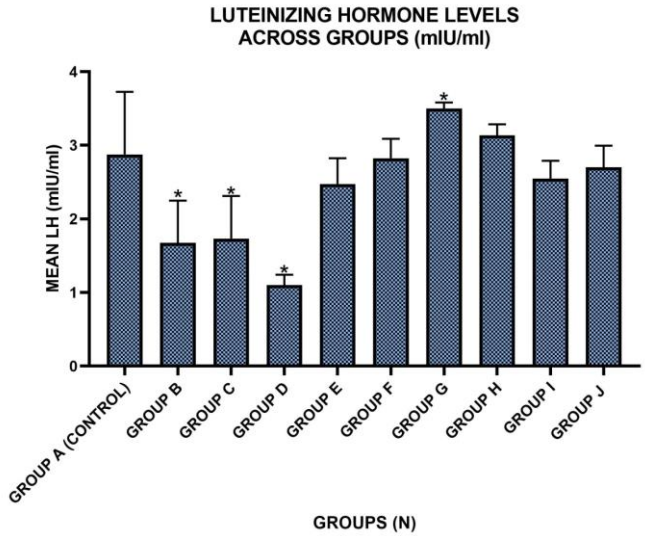

Figure 2. Simple Bar Chart Showing the Mean Luteinizing Hormone Levels across Groups

Note: N = 6; * = Statistically Significant Difference in Mean at *P*=.05 Compared to the Control Group.

3.2 Sperm Count

The results from Figure 3 indicate that prenatal exposure to Triclosan (TCS) significantly reduced sperm count in male Wistar rats compared to the control group. Groups B, C, and D, which received 5 mg/kg, 10 mg/kg, and 20 mg/kg TCS, respectively, showed marked reductions in sperm count, with the highest TCS dose (20 mg/kg) resulting in the lowest sperm count (74.00 ± 29.69 x10⁶/ml). This suggests a dose-dependent adverse effect of TCS on spermatogenesis.

Conversely, administration of Betanin isolates (E162) alone (Groups E, F, and G) resulted in sperm counts comparable to or even slightly higher than the control group, suggesting no adverse effects on sperm production and a potential protective or enhancing effect.

Co-administration of TCS and E162 (Groups H, I, and J) demonstrated partial mitigation of TCS-induced sperm count reduction at the lowest dose (5 mg/kg TCS + 5 mg/kg E162), with a sperm count of 97.20 ± 3.11 x10⁶/ml. However, higher combined doses (Groups I and J) still showed significant reductions in sperm count compared to the control, indicating that while Betanin isolates may exert some protective effects; they may not fully counteract the spermatotoxic impact of higher TCS exposure.

These findings suggest that prenatal exposure to TCS negatively affects sperm production, while Betanin isolates may offer some protective effects, particularly at lower doses.

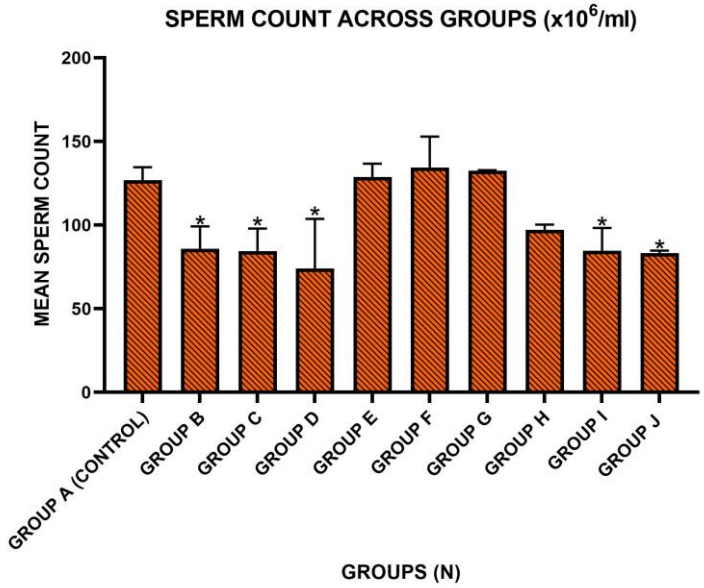

Figure 3. Simple Bar Chart Showing the Mean Sperm Count across Groups

Note: N = 6; * = Statistically Significant Difference in Mean at *P*=.05 Compared to the Control Group.

3.3 Sperm Morphology

The results of sperm morphology assessment as shown in figures 4 and 5 reveal that prenatal exposure to Triclosan (TCS) induces significant morphological abnormalities in sperm cells, with a dose-dependent increase in abnormal sperm morphology. Control animals (Group A) exhibited 87.20% normal sperm morphology, while rats exposed to 5mg/kg (Group B), 10mg/kg (Group C), and 20mg/kg (Group D) of TCS showed a progressive decline in normal sperm morphology (66.40%, 64.80%, and 29.65%, respectively) and a corresponding increase in abnormal morphology, which was statistically significant (*P*=.05).

Conversely, groups treated with Betanin isolates (E162) alone (Groups E, F, and G) maintained normal sperm morphology comparable to the control (ranging between 86.40% and 88.75%), suggesting no adverse effects on sperm integrity. However, co-administration of Betanin with TCS (Groups H, I, and J) resulted in only partial restoration of normal sperm morphology (66.90%–68.35%), indicating that while Betanin provided some protective effects, it did not fully mitigate TCS-induced sperm damage.

The result implies that TCS exposure significantly disrupts sperm morphology, while Betanin exhibits protective properties, though not completely reversing TCS-induced abnormalities at the tested dosages.

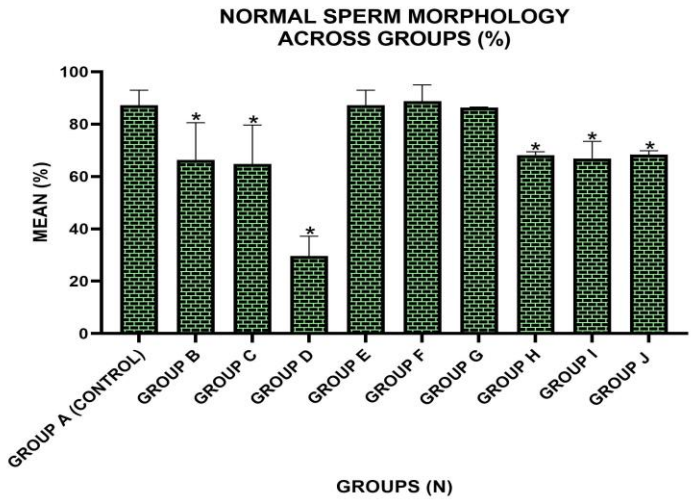

Figure 4. Simple Bar Chart Showing the Mean Normal Sperm Morphology across Groups

Note: N = 6; * = Statistically Significant Difference in Mean at *P*=.05 Compared to the Control Group.

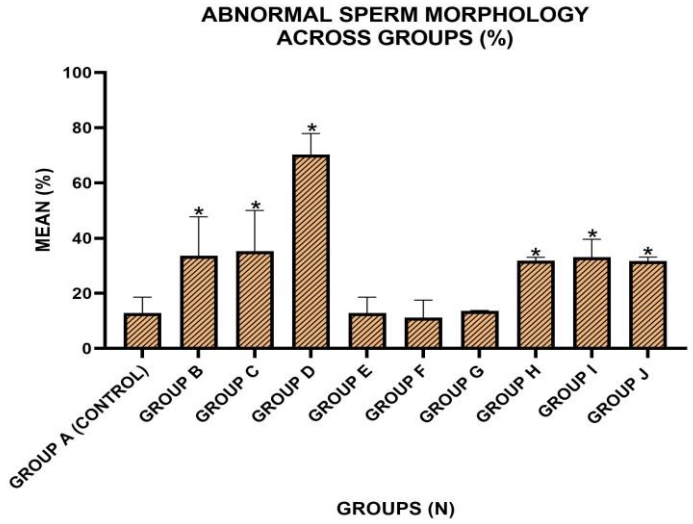

Figure 5. Simple Bar Chart Showing the Mean Abnormal Sperm Morphology across Groups

Note: N = 6; * = Statistically Significant Difference in Mean at *P*=.05 Compared to the Control Group.

3.4 Histological Profile

Histological examination of the testicular tissue in Groups A, E, F, and G revealed a normal histological profile indicative of preserved spermatogenesis and testicular integrity. The seminiferous tubules exhibited a well-organized arrangement of germ cells at various stages of maturation, culminating in the presence of numerous mature spermatozoa radiating toward the lumen. Leydig cells in the interstitial spaces appeared intact and healthy, with no signs of degeneration or morphological abnormalities. Occasional spermatid retention was noted within the seminiferous tubules; however, this did not compromise the overall structural integrity or functionality of the testicular tissue in these groups.

In contrast, Groups B, C, and D displayed varying degrees of histopathological alterations, indicating significant disruptions in testicular morphology. The seminiferous tubules in these groups exhibited abnormal features such as pronounced spermatid retention, tubular atrophy, and a disorganized arrangement of germ cells. The orderly progression of spermatogenic cells was disrupted, resulting in a chaotic cellular organization. The interstitial spaces were markedly reduced or completely absent, and the Leydig cells showed degenerative changes. Additionally, evidence of necrosis was observed, further underscoring the severity of the tissue damage in these groups.

Microscopic examination of Groups B through D further revealed profound cellular disruptions. Several maturing spermatogenic cells within the seminiferous tubules displayed ruptured nuclear membranes and fragmentation of nuclei (karyorrhexis), which are indicative of cellular apoptosis or necrosis. Spermatogonia cells with hyperchromatic (darkly stained) nuclei were frequently observed, alongside degenerative changes in surrounding germ cells. While occasional seminiferous tubules retained normal characteristics, such as intact radiating spermatozoa, many tubules exhibited thickened and hyalinized basement membranes, indicative of chronic damage.

Groups H, I, and J exhibited histomorphological features distinct from those of Groups B through D but not as normal as those observed in Groups A, E, F, and G. The seminiferous tubules in these groups showed intermediate changes, with mild disorganization of germ cells and occasional tubular atrophy. Although the interstitial spaces were largely preserved, some areas displayed minor degeneration and reduced Leydig cell density. These findings suggest a partial disruption in spermatogenesis that is less severe than in Groups B through D but deviates from the normal histo-profile of Groups A, E, F, and G.

Notably, the lumens of the seminiferous tubules in Groups B through D and H through J were often filled with debris from degenerated cells. This accumulation of shredded cellular material reflects impaired spermatogenesis and the breakdown of cellular elements within the seminiferous epithelium. While these findings in Groups H through J bore similarities to those in Groups B through D, the intermediate level of disruption precluded direct comparison.

Thus, Groups A, E, F, and G demonstrated consistent normal histological profiles, with well-preserved testicular architecture and function. Groups B through D exhibited severe degenerative changes, including atrophy, disorganization, and necrosis, whereas Groups H through J displayed moderate alterations, representing a transitional pattern of histomorphological disruption. These findings highlight a spectrum of testicular histological responses across the experimental groups, emphasizing the variability in the degree of testicular impairment.

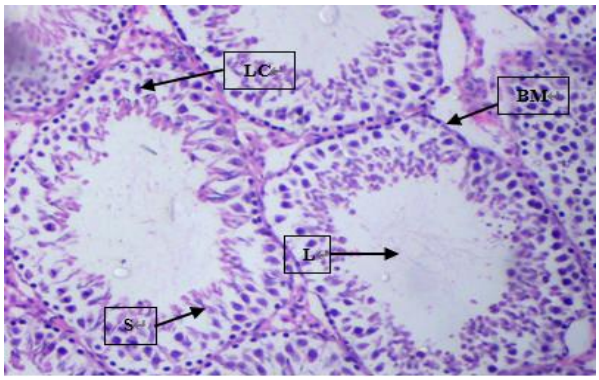

A: Testicular Section of Group A showing spermatozoa (S), lumen (L), basement membrane (BM), & Leydig cells (LC) (H&E x40)

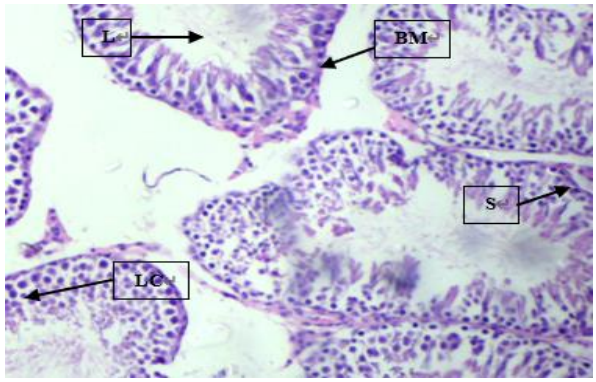

B: Testicular Section of Group B showing spermatozoa (S), lumen (L), basement membrane (BM), & Leydig cells (LC) (H&E x40)

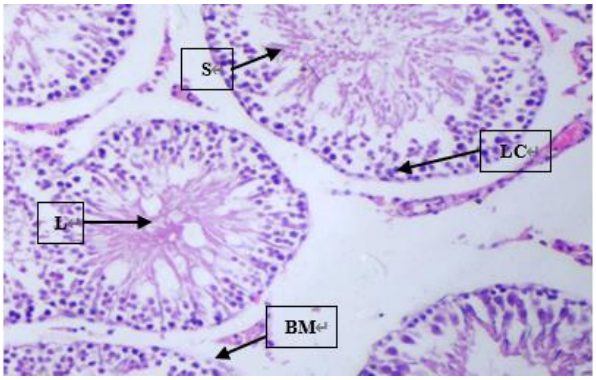

C: Testicular Section of Group C showing spermatozoa (S), lumen (L), basement membrane (BM), & Leydig cells (LC) (H&E x40)

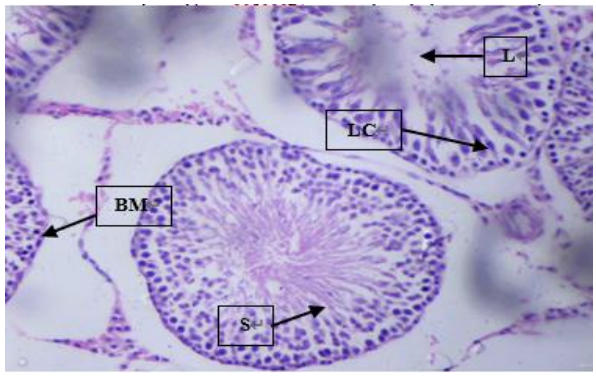

D: Testicular Section of Group D showing spermatozoa (S), lumen (L), basement membrane (BM), & Leydig cells (LC) (H&E x40)

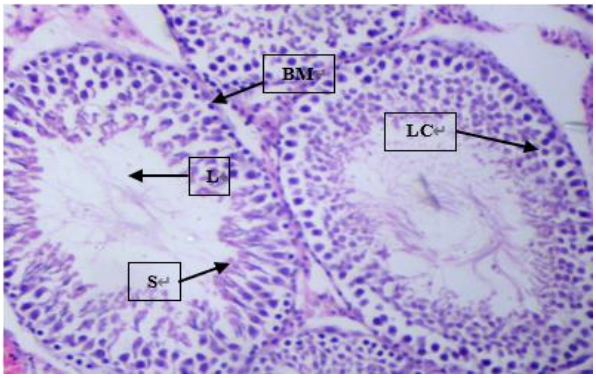

E: Testicular Section of Group E showing spermatozoa (S), lumen (L), basement membrane (BM), & leydig cells (LC) (H&E x40)

Figure 6. (A – E). Photomicrographs of Testes of Rats from Groups A – E showing Spermatozoa (S), Lumen (L), Basement Membrane (BM), and Leydig Cells (L) (H&E x40)

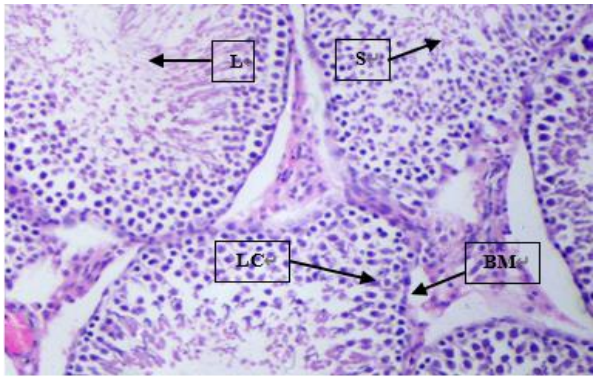

F: Testicular Section of Group F showing spermatozoa (S), lumen (L), basement membrane (BM), & Leydig Cells (LC) (H&E x40)

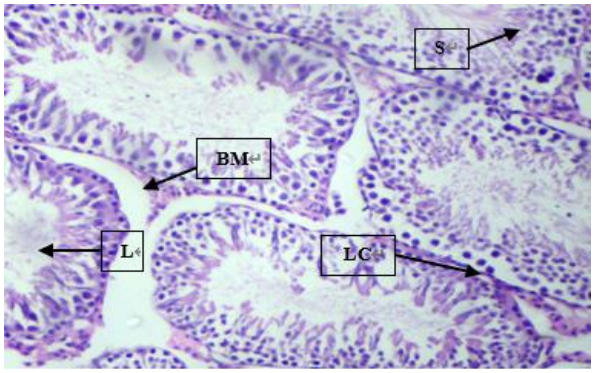

G: Testicular Section of Group G showing spermatozoa (S), lumen (L), basement membrane (BM), & Leydig Cells (LC) (H&E x40)

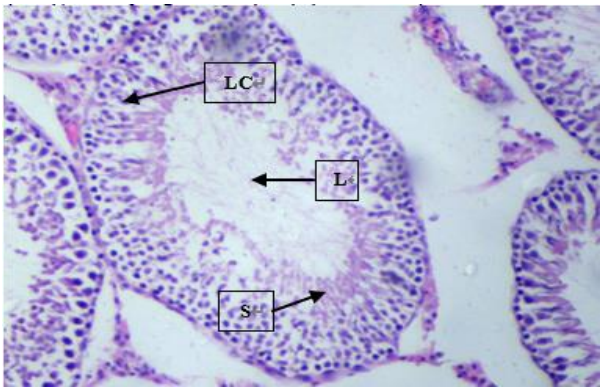

H: Testicular Section of Group H showing spermatozoa (S), lumen (L) & Leydig Cells (LC) (H&E x40)

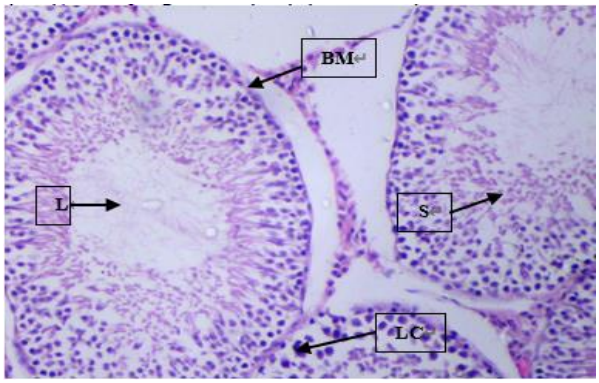

I: Testicular Section of Group I showing spermatozoa (S), Lumen (L), Basement Membrane (BM), & Leydig Cells (LC) (H&E x40)

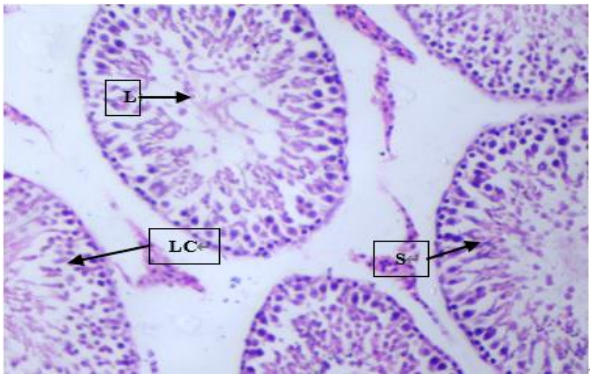

J: Testicular Section of Group J showing spermatozoa (S), Lumen (L), Basement Membrane (BM), & Leydig Cells (LC) (H&E x40)

Figure 7. (F – J). Photomicrographs of Testes of Rats from Groups F – J showing Spermatozoa (S), Lumen (L), Basement Membrane (BM), and Leydig Cells (L) (H&E x40)

4. Discussion

This study investigated the protective effects of betanin isolates (E162) against triclosan (TCS)-induced spermatogenic dysfunction and testicular damage in prenatally exposed Wistar rats. The findings demonstrate that TCS exposure disrupts male reproductive function by significantly reducing reproductive hormone levels, impairing spermatogenesis, altering sperm morphology, and inducing histopathological damage to the testes. However, betanin administration, particularly at moderate doses, mitigated these effects, indicating a potential ameliorative role against TCS-induced toxicity.

Results of this study reveal that prenatal exposure to TCS results in a dose-dependent decline in testosterone and luteinizing hormone (LH) levels, with the highest dose (20 mg/kg) exerting the most profound suppressive effects. This aligns with previous studies demonstrating that TCS disrupts endocrine homeostasis by interfering with steroidogenic enzyme activity and androgen biosynthesis (Zhao et al., 2022). Similarly, Wang et al. (2021) reported a significant decrease in testosterone levels following TCS exposure, attributing it to oxidative stress-induced Leydig cell dysfunction.

Betanin administration alone exhibited a biphasic response, with 10 mg/kg restoring testosterone and LH levels to near-control values, whereas 20 mg/kg led to a decline in testosterone despite increased LH. This suggests a potential dose-dependent feedback mechanism. Similar protective effects have been reported for other antioxidant-rich plant extracts, such as curcumin and quercetin, which enhance steroidogenesis by reducing oxidative stress (Zhu et al., 2023). Furthermore, co-administration of betanin with TCS partially restored hormone levels, especially at 20 mg/kg, suggesting its role in mitigating endocrine disruption, as seen in previous studies on phytochemical interventions against toxicant-induced reproductive dysfunction (Yang et al., 2024).

TCS exposure significantly reduced sperm count in a dose-dependent manner, with the highest dose (20 mg/kg) leading to the most pronounced decline. This is consistent with prior research indicating that TCS impairs spermatogenesis by inducing oxidative stress and disrupting Sertoli cell function (Li et al., 2021). Reduced sperm count following prenatal TCS exposure has also been reported by Chen et al. (2023), who attributed it to mitochondrial dysfunction in germ cells.

Betanin administration alone had no adverse effects on sperm count, with levels comparable to or slightly exceeding the control, reinforcing its potential spermatoprotective properties. This corroborates findings by Khalil et al. (2022), who demonstrated that betanin enhances sperm quality by scavenging reactive oxygen species and modulating apoptotic pathways. Co-administration of betanin with TCS partially mitigated TCS-induced reductions in sperm count, particularly at lower doses, suggesting an optimal therapeutic range for counteracting TCS toxicity without excessive antioxidant burden.

Sperm morphology assessment revealed a dose-dependent increase in abnormal sperm forms following TCS exposure, consistent with previous studies that linked TCS to DNA damage and cytoskeletal disruptions in spermatozoa (Xiao et al., 2023). The significant increase in head, midpiece, and tail abnormalities in TCS-exposed groups suggests oxidative stress-mediated sperm structural defects, as previously reported by Deng et al. (2021).

Conversely, betanin-treated groups exhibited normal sperm morphology, consistent with control levels,

indicating that betanin does not induce structural sperm anomalies. This is in agreement with prior research demonstrating that antioxidant-rich dietary phytochemicals preserve sperm integrity by modulating lipid peroxidation and DNA fragmentation (González-Salazar et al., 2024). However, co-administration of betanin and TCS resulted in only partial restoration of normal sperm morphology, suggesting that while betanin offers protection, it may not fully counteract the teratogenic effects of high-dose TCS exposure.

Histological examination revealed severe degenerative changes in the testicular architecture of TCS-exposed groups, including seminiferous tubule atrophy, disorganization of germ cells, and Leydig cell degeneration. These findings are consistent with those of Zhang et al. (2022), who reported similar histopathological alterations in rodent models following endocrine-disrupting chemical exposure. The observed nuclear fragmentation and necrotic changes further confirm apoptotic processes induced by TCS, as noted by Zhao et al. (2023).

Betanin-treated groups exhibited preserved testicular architecture with well-organized spermatogenic layers, indicating its protective role. This aligns with previous reports showing that betanin enhances testicular histoarchitecture by upregulating antioxidant defense mechanisms and reducing oxidative stress (Hassan et al., 2023). Co-administration of betanin and TCS partially ameliorated histopathological damage, with mild disorganization and occasional atrophic tubules observed in these groups. This intermediate response suggests that while betanin mitigates TCS-induced testicular damage, complete histological recovery may require longer exposure to the protective agent or combination therapies, as suggested by other studies evaluating antioxidant-mediated testicular protection (Wu et al., 2024).

Overall, the findings confirm that prenatal exposure to TCS significantly disrupts male reproductive function by impairing hormonal balance, reducing sperm count, inducing morphological abnormalities, and causing testicular histopathological damage. Betanin administration, particularly at moderate doses, offers significant protective effects against these toxicities, likely through its potent antioxidant and anti-inflammatory properties. However, its efficacy in fully counteracting TCS-induced testicular damage remains dose-dependent.

5. Conclusion

In conclusion, this study demonstrates that prenatal triclosan exposure significantly impairs male reproductive function in Wistar rats, affecting hormone levels, spermatogenesis, sperm morphology, and testicular histology. Betanin administration, particularly at moderate doses, offers partial amelioration of these toxic effects, suggesting its potential as a protective agent against triclosan-induced reproductive damage. However, complete protection, especially against high-dose triclosan exposure, was not achieved, highlighting the need for further investigation into optimal betanin dosages and potential combination therapies.

Competing Interests

The authors declare that there are no competing interests, and that all reference sources have been duly cited.

Ethical Approval

All procedures were conducted according to the guidelines of the Ethical Committee of the College of Health Sciences, Benue State University, Makurdi. The research proposal was approved by the committee.

References

Adolfsson-Erici, M., Lindström, A., Nilsson, E. and Bäcklin, B. M., (2002). Triclosan, a commonly used bactericide found in human milk. *Environmental Toxicology and Chemistry, 21*(9), 2039-2042.

Aghanwa, H. S., Ikechebelu, J. I. and Onwuanibe, A. E., (1999). Social and psychological implications of infertility among women in Enugu, Nigeria. *West African Journal of Medicine, 18*(4), 274-277.

Ahn, K. C., Kim, S. H. and Cho, M. C., (2008). Effects of triclosan on the expression of estrogen receptor and proliferation in human breast cancer cells. *Journal of Toxicology and Environmental Health, Part A, 71*(17), 1109-1116.

Aoun, A., Abaluck, J., Duquenne, M., Achard, C., Deschamps, F., Tostain, J., ... and Ravel, C., (2021). Semen quality and male infertility: A systematic review and meta-analysis. *Human Reproduction Update, 27*(5), 1082-1102.

Bedoux, G., Roig, B., Thomas, O., Dupont, V. and Le Menach, K., (2012). Occurrence and fate of emerging contaminants: The case of triclosan, triclocarban and synthetic musks. *Environmental Science and Pollution Research, 19*, 1189-1203.

Butler, L. M., (2003). Only human? A critical review of the WHO's reproductive health definition. *Reproductive Health Matters, 11*(21), 159-168.

Calafat, A. M., Ye, X., Wong, L. Y., Reidy, L. and Needham, L. L., (2007). Concentrations of triclosan in urine from a nationally representative sample of the US population. *Environmental Health Perspectives*, *115*(2), 284-289.

Chen, H., Wang, X., Li, Z. and Zhou, Y., (2023). Triclosan exposure induces mitochondrial dysfunction and impairs spermatogenesis in male rodents. *Toxicology and Applied Pharmacology*, *460*, 116497.

Chen, J., Weng, Q., Zhang, B., Huang, C. and Chen, Y., (2007). Effects of triclosan on the steroidogenesis and gene expressions of key steroidogenic enzymes in H295R human adrenocortical carcinoma cells. *Toxicology and Applied Pharmacology*, *220*(3), 253-261.

Chigrinets, E., Gharbi, M., Demyanenko, S., Gharbi, A., Mnif, W. and Hammami, S., (2020). The impact of psychological stress on male fertility. *Andrologia*, *52*(10), e13799.

Chu, S., Metcalfe, C. D., (2007). Occurrence and fate of triclosan in municipal wastewater treatment plants in Ontario, Canada. *Environmental Toxicology and Chemistry*, *26*(6), 1296-1301.

Clifford, T., Wainwright, N. J., Potter, D., Buttar, H. S. and Lubin, T. M., (2015). The potential benefits of red beetroot supplementation for human health. *Nutrients*, *7*(4), 2801-2810.

Crawford, A., De Catanzaro, C., (2012). The effects of triclosan on sperm viability and function. *Toxicology and Applied Pharmacology*, *264*(3), 391-397.

Deng, X., Liu, J., Wang, Y. and Zhang, W., (2021). Oxidative stress-mediated sperm DNA damage in triclosan-exposed rats. *Reproductive Toxicology*, *102*, 24-32.

Dyer, R., (2004). Infertility in South Africa: A neglected health issue. *Southern African Journal of Obstetrics and Gynaecology*, *10*(1), 4-6.

Dyer, S. J., (2005). The social and psychological impact of infertility. *Human Reproduction Update*, *11*(6), 639-648.

Feng, M., Wang, Y., Zhang, H., Wang, C., Liu, B. and Miao, Y., (2016). Triclosan exposure impairs spermatogenesis through affecting the expression of StAR, CYP11A1 and CYP17A1 in rat Leydig cells. *Toxicology Letters*, *250*, 1-9.

Georgiev, M. I., Weber, J., Maciuk, A. and Krasowska, A., (2010). Bio-transformation of betalains from red beet (*Beta vulgaris* L.) by *Lactobacillus plantarum* EUREX 2275. *Journal of Agricultural and Food Chemistry*, *58*(15), 8536-8542.

González-Salazar, M., Torres, J. M. and Rojas, M., (2024). Protective effects of dietary antioxidants on sperm morphology and function. *Journal of Andrology Research*, *15*(1), 53-65.

Guldiken, B., Guler, G. O., Stamford, T. L. M. and Dudonne, S., (2016). Betalains: Natural pigments, antioxidant properties, and applications. *Critical Reviews in Food Science and Nutrition*, *56*(13), 2227-2248.

Hassan, M., Khalil, R. and Aziz, N., (2023). Betanin improves testicular histoarchitecture and function in oxidative stress-induced rat models. *Phytomedicine*, *104*, 154237.

Hipwell, A. E., Goeman, D. P., Wely, M. and Hull, M. L., (2019). The psychological impact of infertility: A cross-sectional survey of men and women. *Human Reproduction*, *34*(7), 1289-1298.

Hull, M. G. R., Glazener, C. M. A., Kelly, N. J. and Conway, D. I., (2005). Population-based estimates of infertility and its treatment needs. *Human Reproduction*, *20*(2), 453-457.

Ibtisham, F., Zia, M., Mustafa, A., Wise, J. and Chen, W., (2016). Triclosan disrupts endocrine signaling by interfering with thyroid hormone receptor and 5′-monodeiodinase activity in GH3 cells. *Environmental Pollution*, *218*, 455-464.

Jurewicz, J., Nguyen, A. V., Wojewódzka, M., Błaszczyk, A., Radwan, M. and Jakubowski, M., (2018). Triclosan affects steroidogenesis in human adrenocortical H295R cells. *Toxicology and Applied Pharmacology*, *343*, 1-9.

Kaur, K., Buttar, H. S., (2020). High-performance liquid chromatography analysis of betanin in beetroot extracts. *Journal of Food Science and Technology*, *57*(6), 2345-2352.

Khalil, P., Singh, R. and Dhillon, P., (2022). The role of natural antioxidants in steroidogenesis: A systematic review. *Journal of Reproductive Biology*, *41*(2), 98-112.

Koubaier, E. H., Dornier, M., Decroocq, J., Lachman, J. and Hertog, M. L. A. T., (2014). Dietary phytochemicals and human health: An overview. *Journal of Agricultural and Food Chemistry*, *62*(46), 11894-11908.

Kumar, V., Dass, R. S., De Sousa, G., Roy, P. and Pandey, A. K., (2008). Triclosan induced structural and functional changes in the spermatozoa of mouse, Mus musculus. *Bulletin of Environmental Contamination*

and Toxicology, *81*, 355-360.

Kumar, V., Roy, P., Dass, R. S., De Sousa, G. and Pandey, A. K., (2009). Triclosan, an emerging threat to reproductive health: A study in mouse model. *Reproductive Toxicology*, *27*(1), 49-54.

Lan, J., Zhao, R. and Yu, C., (2015). Accumulation of triclosan in the epididymis and its effects on sperm toxicity. *Toxicology and Applied Pharmacology*, *287*(1), 56-64.

Li, T., Chen, Y., Wu, R. and Feng, L., (2021). Disruption of Sertoli cell function by triclosan exposure: A mechanistic insight. *Toxicological Sciences*, *182*(2), 349-360.

Mikolajczyk-Bator, A., Pawlak, A., (2016). Dietary fruit and vegetable consumption and its health benefits. *Food Chemistry*, *207*, 8-14.

Moss, T., Pals, R. and Strunz, K., (2000). Exposure of humans to triclosan via consumer products. *Science of the Total Environment*, *254*(1), 19-27.

Ninfali, R., Angelino, R., (2013). The role of triclosan in the development of bacterial resistance: A review. *Journal of Antimicrobial Chemotherapy*, *77*(6), 1499-1509.

NPCN, (2006). Nigeria's reproductive health strategy: A call for action. National Population Commission of Nigeria.

Okonofua, F. E., (1997). The social meaning of infertility for women in Nigeria. *Health Transition Review*, *7*(2), 205-220.

Orji, E. O., Ola, T. M. and Esimai, O. A., (2002). Emotional distress among infertile women in Nigeria: A controlled study. *Journal of Obstetrics and Gynaecology*, *22*(3), 298-301.

PCASRM, (2008). Infertility and reproductive health: A guide for practitioners. Professional College of Advanced Reproductive Medicine.

Pycke, B. F., Munoz, G. and Lam, C., (2014). Triclosan and its potential toxicological impact on human health and the environment. *Environmental Pollution*, *189*, 158-167.

Pyo, Y. H., Jin, Y. J., (2004). Centrifugation as a purification step for betanin-rich beetroot extracts. *Food Chemistry*, *85*(4), 543-548.

Queckenberg, C., Thompson, S. and Kim, S., (2010). Human exposure to triclosan: A review of the literature. *Science of the Total Environment*, *408*(18), 4083-4090.

Ramos, T. J., Gupta, S. and Patel, A., (2021). Comparative analysis of the biochemical composition of sugar beet and Swiss chard. *Food Science & Technology*, *45*(9), 4325-4332.

Ravichandran, K., Sridevi, V. and Thiyagarajan, D., (2013). Processing and extraction techniques of beetroot pigments. *International Journal of Food Science & Technology*, *48*(8), 1593-1600.

Russell, A. D., (2004). Triclosan: An overview of its antimicrobial activity and applications. *Journal of Applied Microbiology*, *97*(3), 153-160.

Sandborgh-Englund, G., Lindberg, J. and Reischl, K., (2006). Triclosan exposure in humans and its impact on endocrine health. *Environmental Health Perspectives*, *114*(12), 206-211.

Stintzing, F. C., Carle, R., (2004). Betalains in food: Occurrence, stability, and analysis. *Critical Reviews in Food Science and Nutrition*, *44*(4), 293-327.

Sundby, S., Jacobus, A., (2001). Challenges to reproductive health policy in Sub-Saharan Africa. *African Journal of Reproductive Health*, *5*(2), 18-29.

Tietz, D., (1995). Molecular mechanisms of triclosan-induced carcinogenesis. *Environmental Toxicology*, *36*(4), 416-426.

Umezulike, A. C., Efetie, E. R., (2004). The psychological burden of infertility in Nigeria. *Nigerian Journal of Clinical Practice*, *7*(1), 18-23.

Van, B., (2000). Infertility treatment and policy in Sub-Saharan Africa. *African Journal of Medicine and Medical Sciences*, *29*(1), 15-21.

Wang, L., Chen, W. and Wu, D., (2021). Molecular mechanisms of triclosan-induced carcinogenesis. *Environmental Toxicology*, *36*(4), 416-426.

Winter, P., Walsh, M., (2014). Male infertility: Etiology and management strategies. *Journal of Urology*, *192*(3), 669-678.

Wu, X., Chen, G. and Liu, Z., (2020). Triclosan-induced inflammation and apoptosis in rat testes: The protective effects of antioxidants. *Journal of Environmental Science and Health, Part A*, *55*(7), 869-877.

Wybraniec, S., Nowak, M., (2007). Ion-exchange chromatography in the purification of betanin from beetroot juice. *Journal of Chromatography A*, *1140*(1-2), 93-100.

Xiao, D., Li, M. and Liu, Z., (2022). Triclosan exposure and its effects on male reproductive health in rats. *Toxicological Sciences*, *178*(2), 410-419.

Yang, X., Zhang, L. and Li, H., (2024). Betanin protects against renal damage induced by oxidative stress in rats. *Journal of Renal Injury Prevention*, *10*(3), 105-112.

Zhang, M., Chen, W. and Wang, H., (2022). Triclosan exposure induces testicular toxicity in male rats: Pathological and molecular insights. *Environmental Toxicology and Pharmacology*, *79*, 103437.

Zhao, X., Liu, Y. and Zhang, C., (2022). Endocrine disruption and steroidogenic enzyme inhibition by triclosan: A mechanistic overview. *Environmental Health Perspectives*, *130*(4), 460-475.

Zhu, P., Yang, L. and Wang, F., (2023). Phytochemicals in reproductive medicine: The role of antioxidants in male fertility. *Fertility and Sterility*, *120*(3), 489-505.

Paradigm Academic Press
Journal of Innovations in Medical Research
ISSN 2788-7022
APR. 2025 VOL.4, NO.2

Postoperative Complications of Minor Amputation Stump in Diabetic Patients: A Prospective Study

Yosra HASNI[1], Malek HADRICH[1], Hamza EL FEKIH[1], Maissa THABET[2], Emna TAGHOUTI[3], Sirine MATHLOUTHI[3], Wiem SAAFI[1], Ghada SAAD[1] & Amel MAAROUFI[1]

[1] Department of Endocrinology and Diabetology, Farhat Hached University Hospital, Faculty of Medicine of Sousse, University of Sousse, Sousse, Tunisia

[2] Department of Internal Medicine, Farhat Hached University Hospital, Faculty of Medicine of Sousse, University of Sousse, Sousse, Tunisia

[3] Higher School of Health Sciences and Techniques, University of Sousse, Tunisia

Correspondence: Maissa THABET, Department of Internal Medicine, Farhat Hached University Hospital, Faculty of Medicine of Sousse, University of Sousse, Sousse, Tunisia.

doi:10.63593/JIMR.2788-7022.2025.04.002

Abstract

Background: Diabetes mellitus is a major public health issue in Tunisia, with a prevalence of 12.2% in 2016, and diabetic foot affects up to 25% of patients, leading to serious complications such and amputations. Postoperative complications of amputations include necrosis, phantom pain, and infection, but few studies in Tunisia have explored their incidence, prompting an exploratory study to examine these complications. ***Materials and Methods:*** This prospective observational study was conducted over a period of 4 months, from October 2021 to February 2022, at the General Surgery Department of Mohamed Taher Maamouri Regional Hospital in Nabeul and the Endocrinology Department of the Farhat Hached University Hospital Center in Sousse, involving diabetic patients hospitalized for unilateral minor lower limb amputation. ***Results:*** The study included 14 patients, with 6 from the Endocrinology Department at the Farhat Hached University Hospital in Sousse and 8 from the General Surgery Department at the Mohamed Taher Maamouri Regional Hospital in Nabeul. The average age of the participants was 50.29 ± 13.69 years. There was a male predominance, with a male-to-female ratio of 3.7. All patients had type 2 diabetes (85.7%), and insulin was the most prescribed treatment (57.1%). 43% of patients had diabetes for 10 to 20 years. 57.14% of the patients (8/14) had cardiovascular disease, and 78.5% (11/14) had diabetic retinopathy. The podiatric assessment revealed cyanosis (57.1%) and thick nails (100%). The dorsal skin flexibility was reduced in 92.9% of the patients. Arterially, 57.14% of the patients were in stage 3 or 4 of the Leriche and Fontaine classification, indicating severe ischemia. Wet gangrene was the most frequent reason for amputation (50% of cases). 13 were evaluated postoperatively after the death of one patient on day 1. During the first dressing change, various complications were observed: hyperkeratosis (15.3%), infections (15.3%), non-budding stump with fibrin (38.4%), and necrotic tissue (15.3%). At the first follow-up appointment, four patients were lost to follow-up, reducing the sample size to nine. (55.5%) had delayed wound healing and hyperkeratosis had progressed, affecting 77.8% of the patients (7/9). The infection rate had tripled compared to the initial observation. ***Conclusion:*** This study identified a range of early and late complications, including infections, necrosis, and delayed healing in 14 patients following minor amputation. Despite the small sample size, the findings highlight the importance of personalized care for diabetic amputee.

Keywords: diabetic foot, amputation, postoperative complications

1. Introduction

Diabetes mellitus, a non-communicable chronic disease, represents a major public health issue in Tunisia, with a prevalence estimated at 12.2% in 2016 (Organisation mondiale de la Santé – Profils des pays pour le diabète, 2016). Among its most severe complications is diabetic foot, which affects up to 25% of diabetic patients during their lifetime. This complication, caused by neuropathy, arteriopathy, and infection, leads to significant morbidity, reduced quality of life, and high healthcare costs (Monabeka, H.G. & Nsakala-Kibangou, N., 2001).

One of the most severe consequences of diabetic foot is ulceration, affecting approximately 15% of diabetics, which can lead to amputation, defined as the removal of part or all a limb (J. BEN DAHHANE, Y. NAJEB & M. LATIFI, n.d.). About 5 to 15% of diabetics will undergo amputation in their lifetime, with one amputation occurring every 20 seconds worldwide, 80% of which are preceded by a foot ulcer (LEUTENEGGER M.& PASQUAL C., 1990).

Postoperative complications from amputations include necrosis, suppuration, phantom pain, and hyperesthesia. In Tunisia, few studies address the incidence of these complications, which led to the creation of an exploratory study aimed at identifying their nature, frequency, and causes.

1.1 Objective

To determine the occurrence and nature of complications arising on the stump after minor amputation in diabetic patients.

2. Materials and Methods

2.1 Study Type and Duration

This was a prospective observational study conducted over a period of 4 months, from October 2021 to February 2022, at the General Surgery Department of Mohamed Taher Maamouri Regional Hospital in Nabeul and the Endocrinology Department of the Farhat Hached University Hospital Center (CHU) in Sousse.

2.2 Study Population

The study included all diabetic patients hospitalized for unilateral minor lower limb amputation in the respective facilities, provided they agreed to participate and were available during the study period. Exclusion criteria included major amputations, minor amputations in non-diabetic patients, congenital amputations, and refusal to participate in the study.

2.3 Podiatric Materials Used

A monofilament was used for podiatric examination.

2.4 Methods

Sociodemographic, clinical, and podiatric data were collected prior to amputation from medical records and confirmed during a podiatric examination.

Preoperative data included sociodemographic information (gender, age, marital status, lifestyle, profession) and clinical data (weight, height, BMI). A medical assessment was also conducted, including diabetes history and the presence of complications such as nephropathy, retinopathy, and cardiovascular diseases. A thorough podiatric examination was carried out to assess the condition of the skin, nails, arterial pulses, sensitivity, and to analyze the lesions leading to the amputation (plantar perforating ulcer, dry or wet gangrene, necrotizing fasciitis).

Postoperative evaluations were conducted at two time points: during the first dressing change and the first follow-up visit in an outpatient clinic. Common complications were assessed, such as stump granulation, phantom limb sensation, hematomas, hyperkeratosis, fibrin presence, and tenderness upon palpation. Other complications included algo dystrophy, infections, and signs of necrosis. At the first follow-up visit, delayed wound healing was also assessed in addition to any existing complications.

2.5 Data Analysis

Collected data were statistically analyzed using SPSS software.

3. Results

The study included 14 patients, with 6 from the Endocrinology Department at the Farhat Hached University Hospital in Sousse and 8 from the General Surgery Department at the Mohamed Taher Maamouri Regional Hospital in Nabeul.

The average age of the participants was 50.29 ± 13.69 years, with an age range from 28 to 86 years. There was a male predominance, with a male-to-female ratio of 3.7. Approximately 75% of the patients were active.

Clinically, most patients had type 2 diabetes (85.7%), and insulin was the most prescribed treatment (57.1%). Nearly 43% of patients had diabetes for 10 to 20 years. Hemoglobin A1c levels were above 7 in 92.9% of the patients.

In addition, 57.14% of the patients (8/14) had cardiovascular disease, and 78.5% (11/14) had diabetic retinopathy.

Among the patients, 11 out of 14 had a history of minor amputation, primarily affecting the big toe (8 cases), followed by the second toe (2 cases) and the fifth toe (1 case). The most common cause of amputation was poor footwear (50%).

3.1 Preoperative podiatric Assessment

The podiatric assessment of the 14 patients revealed significant alterations in skin and nails, with the majority showing cyanosis (57.1%) and thick nails (100%). The dorsal skin flexibility was reduced in 92.9% of the patients.

Arterially, 78.6% of patients had non-palpable posterior tibial pulses, and half had absent popliteal pulses. 57.14% of the patients were in stage 3 or 4 of the Leriche and Fontaine classification, indicating severe ischemia.

Finally, all patients had impaired superficial sensation, while 35.7% also had impaired deep sensation.

Wet gangrene was the most frequent reason for amputation, accounting for 50% of cases, followed by necrotizing fasciitis in 21.4% of cases.

3.2 Postoperative Complications on Amputated Stump

Among the 14 patients, 13 were evaluated postoperatively after the death of one patient on day 1. During the first dressing change, various complications were observed. Two patients (15.3%) had hyperkeratosis, and two others (15.3%) had infections. Five patients (38.4%) had a non-budding stump with fibrin, while two had necrotic tissue (15.3%). Nine patients (69.2%) suffered from algo dystrophy, but no hematomas were noted.

At the first follow-up appointment, four patients were lost to follow-up, reducing the sample size to nine. Among these, five had delayed wound healing (55.5%), and hyperkeratosis had progressed, affecting 77.8% of the patients (7/9). The infection rate had tripled compared to the initial observation.

4. Discussion

Diabetic foot is one of the most feared complications of diabetes, significantly impacting the patient's quality of life, productivity, and autonomy. As diabetes progresses, complications may arise, often necessitating amputation.

Our study revealed a significant male predominance, accounting for 79%. This vulnerability was explained by F. Ouhdouch et al. in their study of 38 patients, who found that men are more exposed to trauma than women (67.3%), who generally tend to be more attentive to care and hygiene (Ouhdouch, F., Ridouane, S. & Diouri, A., 2009).

The average age of our patients was 50.29 ± 13.69 years, which is like a study conducted in Nigeria where the average age was 54.8 ± 1.4 years. This Nigerian study concluded that age did not have a significant impact on the occurrence of foot-related complications (Akanji, A. O., Famuyiwa, O. O. & Adetuyibi, A., 1989).

Moreover, approximately 75% of our patients were still professionally active. However, according to Dr. S. Malacarne et al., diabetic foot complications lead to a significant reduction in autonomy and a notable deterioration in quality of life (Malacarne, S., Chappuis, B., Egli, M., Hagon-Traub, I., Schimke, K., Schönenweid, C. & Peter-Riesch, B., 2016).

Forty-two percent (42%) of the patients had a history of diabetes ranging from 10 to 20 years. This demonstrates that the duration of diabetes is a major factor for amputation, with each additional year increasing the risk of developing diabetic foot by 1.2 times (Richard, J. & Schuldiner, S., 2008).

Most of our patients were type 2 diabetics (12/14, or 85.7%), a frequency comparable to that observed by Djibril, A. et al., who reported a frequency of 88.7% (Djibril, A. M., Mossi, E. K., Djagadou, A. K., Balaka, A., Tchamdja, T. & Moukaila, R., 2018).

The triggering factor for lesions was poor footwear in 50% of cases (7/14), followed by direct trauma to the foot (2/14 cases, or 14.3%), and then burns (1/14 cases, or 7.1%). In a study conducted in the emergency department at Taher Maamouri Hospital, tight shoes were identified as the most predominant mechanical factor contributing to diabetic foot (35.71%) (B Salah C, MekkiM, B MeftehN, RbiaE, Ammar Y, LakhalJ, Bayar M, MarzouguiS, BawandiR & NaffetiE, KhelilA., 2018). Thus, proper footwear is one of the key elements in both primary and secondary prevention of diabetic foot lesions (Mayfield, J. A., Reiber, G. E., Sanders, L. J., Janisse, D. & Pogach, L. M., 1998).

Clinically, wet gangrene was the most common reason for amputation (50%), followed by necrotizing fasciitis in 21.4% of cases. These results are comparable to those observed by Djibril, A et al. in their series, which reported gangrene (61.29%) and ischemic necrosis (12.90%) (Djibril, A. M., Mossi, E. K., Djagadou, A. K., Balaka, A.,

Tchamdja, T. & Moukaila, R., 2018).

The preoperative podiatric assessment revealed impaired lower limb vascularization secondary to diabetic macroangiopathy: 57.14% of patients had severe to critical ischemia classified as stage 3 and 4 according to Lériche and Fontaine. This is explained by C. Flagothier et al. as chronic hypoxia of the feet due to the combination of micro- and macroangiopathic diabetic conditions. (Flagothier C, Quatresooz P, Bourguignon R, Pierard-Franchimont C & Pierard GE, n.d.)

The death of a patient on the first postoperative day significantly impacted our results. In a study conducted by H. G. Monabeka et al., it was reported that 9 out of 106 patients, or 8.5% of cases, died following an amputation of the lower limb, with septicemia being the primary cause of these deaths. (Monabeka, H.G. & Nsakala-Kibangou, N., 2001)

Furthermore, our study showed that stump infections were present in 15% of patients (2/13) during the first observation, a number that tripled to 66% of patients (6/9) in the second observation. H. Van Damme et al. estimate that about 20% of diabetic feet are infected. The infection, initially superficial, progresses insidiously to cellulitis and deep suppuration, often without apparent pain. (Van Damme H, 2005)

Additionally, during the first observation, we noted that 5 out of 13 patients (38%) had a non-granulating stump. However, in the second observation, this number decreased to 3 out of 9 (33%). Indeed, scar tissue formation can be slow, particularly in diabetics. In this regard, Blandine Tramunt highlights the importance of glycemic control for the healing process. (Tramunt, B., 2018)

Delayed healing was observed in 5 out of our 9 patients (55.6% of cases). This can be attributed to several factors, including the presence of hyperkeratosis, fibrin, and the deterioration of vascular status in the amputation stump. W. B. Campbell et al. explain that arterial insufficiency in the lower limbs weakens the tissues, thereby compromising the healing process (Campbell, W. B., Ponette, D. & Sugiono, M., 2000).

Moreover, 4 out of 9 patients (44%) experienced pain at the amputation stump. A. Stansal et al. point out that pain associated with chronic wounds of vascular origin is common, not only during nursing care but also outside of dressing changes. This pain is often complex, involving nociceptive and neuropathic components, as well as care-related anxiety and emotional distress linked to the chronic illness. Pain management must consider these various factors. (Stansal, A., Lazareth, I., D'Ussel, M. & Priollet, P., 2016)

The limitations of our study included the small sample size and the decrease in the number of patients during the study period.

5. Conclusion

Lower limb amputation in diabetic patients is often a sign of poor disease management and can result in various postoperative complications. This study monitored 14 diabetic patients after minor amputation, identifying both early and late-stage complications such as infections, fibrin buildup, hyperkeratosis, necrosis, algodystrophy, and delayed healing.

Despite the small sample size, the study revealed a significant number of complications, emphasizing the need for tailored and meticulous care for diabetic amputees. Future larger-scale studies are suggested to further explore and address these postoperative issues.

References

Akanji, A. O., Famuyiwa, O. O. and Adetuyibi, A., (1989). Factors Influencing the Outcome of Treatment of Foot Lesions in Nigerian Patients with Diabetes Mellitus. *QJM.* https://doi.org/10.1093/oxfordjournals.qjmed.a068387.

B Salah C, MekkiM, B MeftehN, RbiaE, Ammar Y, LakhalJ, Bayar M, MarzouguiS, BawandiR, NaffetiE and KhelilA, (2018). Profil epidémiologique et clinique du pied diabetique au Service des Urgences-SMUR CHU MaamouriNabeul, Tunisie.

Campbell, W. B., Ponette, D. and Sugiono, M., (2000). Long-term Results Following Operation for Diabetic Foot Problems: Arterial Disease Confers a Poor Prognosis. *European Journal of Vascular and Endovascular Surgery*, *19*(2), 174-177. https://doi.org/10.1053/ejvs.1999.1006.

Djibril, A. M., Mossi, E. K., Djagadou, A. K., Balaka, A., Tchamdja, T. and Moukaila, R., (2018). Pied diabétique: aspects épidémiologique, diagnostique, thérapeutique et évolutif à la Clinique Médico-chirurgicale du CHU Sylvanus Olympio de Lomé. *Pan African Medical Journal*, *30*. https://doi.org/10.11604/pamj.2018.30.4.14765.

Flagothier C, Quatresooz P, Bourguignon R, Pierard-Franchimont C, Pierard GE, (n.d.). Revue Médicale de Liège - Stigmates cutanes du diabete.

J. BEN DAHHANE, Y. NAJEB and M. LATIFI, (n.d.). Evaluation clinique des patients amputés et appareillés du membre Inférieur. Service de Traumatologie Orthopédie B. Hôpital Ibn Tofaïl. CHU Mohammed VI. Marrakech 6.

LEUTENEGGER M., PASQUAL C., (1990). Les lésions des pieds chez les diabétiques. In Tchobroutsky G. et al. *Traité de Diabétologie, Editions Pradel*, 581-587.

Malacarne, S., Chappuis, B., Egli, M., Hagon-Traub, I., Schimke, K., Schönenweid, C. and Peter-Riesch, B., (2016). Prévention des complications du pied diabétique. *Revue Médicale Suisse*, *12*(521), 1092-1096. https://doi.org/10.53738/revmed.2016.12.521.1092.

Mayfield, J. A., Reiber, G. E., Sanders, L. J., Janisse, D. and Pogach, L. M., (1998). Preventive Foot Care in People with Diabetes. *Diabetes Care*, *21*(12), 2161-2177. https://doi.org/10.2337/diacare.21.12.2161.

Monabeka, H.G., Nsakala-Kibangou, N., (2001) Aspects épidémiologiques et cliniques du pied diabétique au CHU de Brazzaville. *Bulletin de la Société de Pathologie Exotique*, *94*, 246-248.

Organisation mondiale de la Santé – Profils des pays pour le diabète, (2016). Tunisie. https://cdn.who.int/media/docs/default-source/country-profiles/diabetes/tun-fr.pdf?sfvrsn=3a579505_38&download=true consulté le 18/09/2024.

Ouhdouch, F., Ridouane, S. and Diouri, A., (2009). P18 Amputation pour pied diabétique. *Diabetes & Metabolism*, *35*, A33. https://doi.org/10.1016/s1262-3636(09)71816-6.

Richard, J. and Schuldiner, S., (2008). Épidémiologie du pied diabétique. *La Revue de Médecine Interne*, *29*, S222-S230. https://doi.org/10.1016/s0248-8663(08)73949-3.

Stansal, A., Lazareth, I., D'Ussel, M. and Priollet, P., (2016). Comment réduire la douleur liée à un ulcère de jambe? *Journal des Maladies Vasculaires*, *41*(5), 315-322. https://doi.org/10.1016/j.jmv.2016.07.004.

Tramunt, B., (2018). Effet de l'hyperglycémie sur la cicatrisation. *Revue Francophone de Cicatrisation*, *2*(2), 15-17. https://doi.org/10.1016/j.refrac.2018.03.003.

Van Damme H, (2005). Limet R le pied diabetique. *Rev Med Liege*, *60*(5-6), 516-525.

Paradigm Academic Press
Journal of Innovations in Medical Research
ISSN 2788-7022
APR. 2025 VOL.4, NO.2

Liver Diseases: Epidemiology, Prevention, and Management Strategy

Haradhan Kumar Mohajan[1]

[1] Associate Professor, Department of Mathematics, Premier University, Chittagong, Bangladesh

Correspondence: Haradhan Kumar Mohajan, Associate Professor, Department of Mathematics, Premier University, Chittagong, Bangladesh.

doi:10.63593/JIMR.2788-7022.2025.04.003

Abstract

The liver is a highly complex many cell types largest internal solid organ in the body. The most common causes of liver disease are viral hepatitis; over alcohol, fat, and toxin chemicals consumption; autoimmunity; hepatocellular carcinoma (HCC); and hereditary problems and drug reactions. More than 844 million people worldwide suffer from a chronic liver disease and more than two million people die each year worldwide due to liver disease. About two-thirds of them are men, and most of them are related to complications of cirrhosis and hepatocellular carcinoma (HCC). The burden of liver disease is increasing due to unconscious lifestyle, consumption of unhygienic foods, poor available data, limitations of resources, hepatitis, inadequate and poorly national and global fund of liver treatment, insufficient hepatologists, use of traditional medicines and herbal supplements, poverty and malnutrition, etc. This review study tries to discuss the global and regional prevalence, incidence, fatality, mortality, diagnosis, and treatment of liver disease.

Keywords: liver disease, hepatitis, cirrhosis, mortality, treatment

1. Introduction

The liver is an essential organ in the human body that performs up to 5,000 different vital functions in combination with other organs and systems, such as supporting digestion, immunity, proteins synthesis, amino acid metabolism, blood coagulation, detoxification, vitamin storage, etc. (Hettiaratchi, 2022). It has many important roles within the body; such as it helps to break down food and convert into nutrients and energy, store carbohydrates and maintaining a good balance of glucose levels in the blood, develop proteins that support muscle and immune system, metabolize drugs, and store nutrients and energy. It metabolizes drugs, xenobiotic, and endogenous hormones and waste products; and produces bile to aid digestion and as route of excretion of liver waste (Ebrahimkhani et al., 2014). It also filters toxins from the blood and removes harmful substances from it before passing to the rest of the body. It helps in clotting blood; and controls some hormones and cholesterol levels, fights against infections and illness, and metabolizes vitamin A, B, D, E, and K, albumin, glucose, iron, and bile; and controls their proper levels. It has great regenerative powers to recover injury. It is the only organ in the body that can repair itself by creating new tissue (Sivakrishnan, 2019). It controls the availability of lipophilic hormones and regulates inflammation (Hofmann & Hagey, 2008).

At present the liver disease or hepatic disease becomes a major cause of morbidity and mortality worldwide. Most of the liver diseases are intrahepatic cholestasis, alcoholic liver disease, non-alcoholic fatty liver disease, viral hepatitis, and drug induced liver injury (Saigal et al., 2019). More than 844 million people worldwide suffer from a chronic liver disease, among them about 29 million are in the European region and about 30 million are in the USA (Blachier et al., 2013). About 4.5 million (1.8%) US adults have liver disease that causes about 57,000 deaths in a year. About 2 million people die each year worldwide due to liver disease: 1 million due to complications of cirrhosis, and 1 million due to viral hepatitis and hepatocellular carcinoma (HCC) (Chen & Yoon, 2022).

When liver is infected, bilirubin level increases in the blood. Bilirubin is a yellowish pigment that is created from the result of degradation of hemoglobin of dead red blood cells. It passes through the liver and is eventually excreted out of the body via bile (Bonnett et al., 1976). Bile ducts transport bile from the liver to the upper small intestine. The increasing impact of liver diseases have created greater problem in global economy and health care resources. It becomes a cause of premature death and disability (Turner et al., 2011).

2. Literature Review

The literature review section is an introductory region of research, which shows the works of previous researchers in the same field within the existing knowledge (Polit & Hungler, 2013). It is a scholarly portion of theses, research papers or books. It deals with a secondary research source and does not report a new or a coming research work (Gibbs, 2008).

Sanjiv Saigal and his coworkers have analyzed the clinical use of ademetionine in various etiologies of liver disease. They have also studied the premature deaths from liver decompensation, cirrhosis, and hepatocellular carcinoma (HCC) (Saigal et al., 2019). Lukas Hettiaratchi has provided a review in-depth theory concerning liver transplantations along with the rehabilitation process that entails it. He has started the study with the analysis of the anatomy, physiology and pathophysiology of liver. Then he has the post-operative physiotherapy on a patient after liver transplantation (Hettiaratchi, 2022).

Yuan-Yao Zhang and his coworkers have shown that acute-on-chronic liver failure can be classified as type A; on the basis of chronic hepatitis, type B; on the basis of compensatory cirrhosis, and type C; on the basis of decompensated cirrhosis, and non-acute-on-chronic liver failure can be further classified as chronic hepatitis with acute exacerbation, the active phase of liver cirrhosis, and liver cirrhosis-acute decompensation (Zhang & Meng, 2022).

Elliot B. Tapper and Neehar D. Parikh have found that many symptoms of liver cirrhosis, such as muscle cramps, poor-quality sleep, pruritus, and sexual dysfunction are common and treatable. They have stressed that the first-line therapies, such as carvedilol or propranolol are used to prevent variceal bleeding, lactulose for hepatic encephalopathy, combination aldosterone antagonists and loop diuretics for ascites, and terlipressin for hepatorenal syndrome (Tapper & Parikh, 2023). Haradhan Kumar Mohajan has highlighted on various liver diseases that will be helpful for the patients (Mohajan, 2024b, c, e).

3. Research Methodology of the Study

Research is an essential device to the academicians for the leading in academic world (Pandey & Pandey, 2015). Methodology is a guideline for performing good research that helps the researchers to increase the trust of the readers (Kothari, 2008). Hence, research methodology is the collection of a set of principles for organizing, planning, designing and conducting good research (Legesse, 2014). In this study, I have tried our best to maintain the reliability and validity. I have tried to maintain the ethical credibility by citing references properly both in the text and reference list (Mohajan, 2017, 2020). To prepare this article, I have taken the help from the secondary data sources. I have analyzed the journal articles, conference papers, published books and handbooks, internet, websites, etc. to prepare this paper (Mohajan, 2018, 2020).

4. Objective of the Study

Main objective of this article is to review the aspects of liver diseases. The liver plays an important role through the digestion, the metabolism of carbohydrates, fats and proteins, storage of glycogen, vitamins, and minerals, etc. (Mohajan, 2024c). Other some minor objectives of the study are as follows:

1) to focus on causes and symptoms of liver diseases,

2) to highlight on types and stages of liver diseases, and

3) to show the diagnoses and treatment of liver diseases.

5. Common Liver Diseases

Liver disease is an inflammation of the liver usually with enlarged liver that is caused by various viruses, some liver toxins, alcoholism, autoimmunity, drug reactions or some hereditary conditions. The inflammation could be chronic or acute. Acute inflammation is characterized by sudden and massive death of hepatocytes over a short period of time (Zhang & Meng, 2022). An increased level of bilirubin in the body with jaundice is a common symptom of many liver diseases. Some other components of inflammation are liver enlargement and tenderness with coagulopathy. On the other hand, chronic inflammation is caused by slow but long-standing injury that leads to an ongoing process of cell death and healing, and gradually progresses from minimal fibrosis to cirrhosis in 10-20 years (Bonnett et al., 1976).

The most common liver diseases are chronic hepatitis B and C, alcoholic liver disease, non-alcoholic steatohepatitis, autoimmune disease, sclerosing cholangitis, primary biliary cirrhosis, hemochromatosis, and

Wilson's disease (Mincis, & Mincis, 2006). The intrahepatic cholestasis (IHC) is characterized by the presence of jaundice with elevated serum total bilirubin, alkaline phosphatase, and gamma-glutamyl transferase (GGT) levels (Dooley et al., 2018). One problem that can develop with liver disease is portal hypertension that is happened for the increased pressure in the vein that enters the liver. If it is not treated for a long-time it can permanently damage the liver and progress to cirrhosis, liver failure, and hepatoma that are life-threatening chronic liver diseases (Sivakrishnan, 2019).

Liver cirrhosis is the formation of fibrous tissue in the liver to kill hepatocytes. Liver cancer is the primary tumor or carcinoma cholangiocarcinoma or metastasis of cancer to other parts of the digestive system (Jokelainen, 2013). Liver diseases are extremely costly in terms of human suffering, doctor and hospital visits, and premature loss of productivity. More than two million deaths happen annually worldwide due to liver disease that is 4% of all deaths worldwide (Blachier et al., 2013).

5.1 Causes of Liver Disease

Hepatitis is a syndrome and not a disease by itself. It is a generic term for inflammation of the liver. Hepatitis viruses, such as hepatitis A, B, C, D and E can infect the liver that causes inflammation and reduces its functions. These viruses can be spread through infected blood, unprotected sex, contaminated food or water, or close contact with a person who is infected, and also who exercises tattoos or body piercings, and takes fluids with sharing needles. During viral infection reactive oxygen species (ROS) are produced up to 10,000-fold and damages DNA (Iida-Ueno et al., 2017).

Autoimmune can affect liver through the development of autoimmune hepatitis, primary biliary cholangitis, and primary sclerosing cholangitis. These can lead to liver scarring (cirrhosis) and permanent liver damage if not treated. Ischemia can reduce blood supply in liver to develop hepatitis. Various antitubercular drugs, such as INH, rifampicin, pyrazinamide; antiepileptic drugs, such as phenytoin; and paracetamol overdosing, etc. can develop liver diseases. An abnormal gene inherited from parents, such as hemochromatosis, Wilson's disease, Alpha-1 antitrypsin deficiency, etc. can cause genetic liver diseases (Lee et al., 2016). Over alcohol consumption causes a build-up of acetaldehyde that induces DNA damage and oxidative stress that lead to liver injury and ultimately hepatocellular carcinoma (Mohajan, 2024a, d).

Obesity is related to a higher risk of various liver diseases, such as liver cancer due to increase of pro-inflammatory cytokines and higher levels of deoxycholic acid that damage DNA (Aleksandrova et al., 2016; Mohajan & Mohajan, 2023a-d).

5.2 Symptoms of Liver Disease

Liver disease does not always show evident signs and symptoms. However, some common symptoms are nausea, jaundice, upper abdominal pain and swelling, fluid retention, itchy skin, easy bruising, tiredness and weakness at all the times, thrombocytopenia and coagulopathy, dark urine and pale stool color, fluid retention, poor or loss of appetite, weight loss, etc. (Tripodi & Mannucci, 2011). Blood vomiting, chronic fatigue, swelling in the legs and ankles, excess bleeding in the gastrointestinal, musty-smelling breath, mild brain impairment, loss of sex drive tract, etc. are some symptoms in advanced liver diseases (Rehm et al., 2013).

5.3 Types of Liver Diseases

At present there are more than a hundred different liver diseases. Some most common liver diseases are i) hepatitis which is caused by various viruses, autoimmunity, or liver toxins (Aghemo et al., 2015), ii) fascioliasis that is caused by Fasciola hepatica (Mas-Coma et al., 1999), iii) alcoholic liver disease that is caused by over consumption of alcohol (Aalto et al., 2011), iv) fatty liver disease that is caused for accumulation of large amount of triglyceride, which is reversible, v) drug-induced liver disease that is caused by various drugs, vi) non-alcoholic fatty liver disease is associated with obesity and metabolic syndrome (Amir & Czaja, 2011), vii) hereditary disease that is caused for the accumulation of iron in the body, viii) Wilson's disease is a genetic disorder in which excess copper builds up in the body (Pfeiffer, 2007), ix) cirrhosis is the formation of fibrosis that causes chronic liver failure, x) Gilbert's syndrome is a genetic disorder of bilirubin metabolism (Vítek & Tiribelli, 2023), xi) primary sclerosing cholangitis (PSC) is a serious chronic inflammatory disease of the bile duct due to autoimmune (Poupon et al., 1997), xii) primary biliary cirrhosis (PBC) is a serious autoimmune disease of the bile capillaries (Trivedi, 2014), xii) secondary sclerosing cholangitis (SSC) is an inflammatory disease that is caused by misuse of drugs, etc. (Ludwig et al., 2023).

5.4 Stages of Liver Disease

Chronic liver disease progresses roughly in four stages: i) Stage 1: Hepatitis, ii) Stage 2: Fibrosis, iii) Stage 3: Cirrhosis, and iv) Stage 4: Liver failure (Wazir et al., 2023).

Stage 1: Hepatitis shows inflammation in the liver tissues due to injury or toxicity. It is the primary cause of liver disease that affects millions of people worldwide. Both infections and healing processes are happened in this

stage. But when the injury of liver continues, the inflammation is also increasing (Desmet, 1994). Common causes of this stage of liver disease are hepatitis B and C viruses, nonalcoholic steatohepatitis (NASH), alcohol-related liver disease, and autoimmune hepatitis. Chronic hepatitis causes hyperactive healing that eventually results in fibrosis (Murray et al., 2008).

Stage 2: Liver fibrosis is the excessive accumulation of extracellular matrix proteins. It is a pathological condition characterized by excessive production and accumulation of collagen, loss of tissue architecture, and organ failure in response to uncontrolled wound healing (Trautwein et al., 2015). When the liver is inflamed for a long-time, the cells try to repair themselves by producing collagen that makes the cells in the liver stiffer (Younossi et al., 2021). Finally, collagen and other proteins make scar tissue, such as fibrosis, which is a gradual stiffening of liver that reduces blood flow through the liver (Bataller & Brenner, 2005). **Fibrosis can be reversed if it is addressed early enough**. It can spread into the liver and stops it from working properly, and reduces its access to oxygen and nutrients, and gradually declines vitality of liver. Some amount of fibrosis is reversible, damage cells can regenerate, and damage slows down enough for it to recover. Advanced liver fibrosis results in cirrhosis, liver failure, and portal hypertension and often requires liver transplantation (Trautwein et al., 2015).

Stage 3: Cirrhosis is a severe permanent scarring in the liver. When fibrosis stage is no longer reversible, cirrhosis stage starts that is a severe scarring of the liver. It is the formation of fibrous tissue in the liver to kill hepatocytes (Alukal et al., 2020). It is the end-stage of every chronic liver disease, is not only the major risk factor for the development of hepatocellular carcinoma but also a limiting factor for anticancer therapy of liver and non-hepatic malignancies (Asrani et al., 2019). It is a global health concern. It is the result of persistent liver damage over many years. Even at this stage of liver disease, **fixing the underlying condition can reverse cirrhosis** and prevent complications like liver failure (Geong et al., 2019). It is a progressive condition that worsens as more and more scar tissue develops. Too much scarring blocks the flow of blood and oxygen through the liver tissues and slows the activities of liver. In this situation there is no longer enough healthy cells left to work for regenerating. But, at this stage the damage still can be slowed or stopped (Pinter et al., 2016).

Stage 4: Liver failure begins when the liver can no longer function adequately for needs of the body. Actually, liver failure develops slowly over the course of years. This situation is called “decompensated cirrhosis” i.e., the body can no longer compensate for the losses. Acute liver failure can cause many complications, including excessive bleeding and increasing pressure in the brain (Larson et al., 2005). Chronic liver failure is a gradual process, but it eventually needs a liver transplant for the best chance of living with a good quality life. Liver cancer and liver failure can be treated through the various modern attempts, such as radiation, medication, surgery, etc. (Livingston & Durkalski-Mauldin, 2022).

5.5 Diagnoses of Liver Disease

Appropriate liver activities can be identified by a number of clinical diagnoses by the measurement of typical enzymes, metabolites, and other substances that run its activities smoothly (Singal & Mathurin, 2021). Blood tests can usually confirm the presence of liver disease. At present there are a number of liver function tests (LFTs) for the confirmation of presence of enzymes in blood, such as serum bilirubin (direct and indirect), serum proteins, serum albumin, serum globulin, alanine transaminase, aspartate transaminase, prothrombin time, partial thromboplastin time, etc. (Tapper, 2023).

Some imaging tests, such as transient elastography (TE), abdominal ultrasonography (USG) show the size and texture of the liver and other organs, such as the gall bladder, bile ducts, spleen and kidneys. Pelvic computed tomography (CT) and magnetic resonance imaging (MRI) can be used to show the condition of liver tissue and the bile ducts. These show the size, shape and texture of the infected liver. Endoscopic examination of the bile ducts (ERCP) may be necessary to confirm the diagnosis. A liver biopsy is done if there is a problem with the liver and to examine various conditions of the liver tissue (Tapper & Lok, 2017).

5.6 Treatment of Liver Disease

Liver diseases are associated with multiple common physical and psychological symptoms that can be improved with proper treatment (Tapper & Parikh, 2023). Some of the most common types of liver diseases are treatable with diet and lifestyle changes, while others may require lifelong medication to manage. Early treatment can often prevent permanent damage. Last-stage liver disease is a more complicated stage to treat (Wazir et al., 2023). At present there are effective treatments to control and support the liver. Treatment depends on the specific liver disease, and the age and condition of the patient. Treatments are medicines, special diets, surgery, exercise or lifestyle change, and liver transplantation (Ginès et al., 2021).

Anti-viral medications are available to treat some liver infections, such as hepatitis B and C (De Clercq et al., 2010). Steroid-based drugs are used to treat autoimmune hepatitis (Hirschfield & Heathcote, 2011). Wilson’s disease can be managed with drugs that bind copper. Medication ursodeoxycholic acid may be given to a patient

of cholestatic liver disease (Cheng et al., 2017). If iron is overload in the blood a quantity of blood is removed regularly through the vein (Yu et al., 2021).

6. Global Health Burden

The global health sector is heavily burdened for creating the awareness, recognition and management of various liver diseases, such as acute liver failure, viral hepatitis, and alcoholic and nonalcoholic fatty liver disease (NAFLD) (Louvet & Mathurin, 2015). Every nation has stressed on reaching in the three goals: i) viral hepatitis B and C elimination, ii) increasing awareness of alcohol-associated liver disease (ALD) and non-alcoholic steatohepatitis (NASH), and iii) early screening for cirrhosis through the 90% reduction in incidence, treatment of 80% of eligible people and a 65% reduction in mortality (Sidhu et al., 2018). The WHO has stressed on the preventive policies and measures to reduce alcohol consumption, and unhealthy eating and damage (Blachier et al., 2013).

7. Conclusions

In this study, I have observed that liver diseases can be caused by viruses, toxin chemicals, drugs, over alcohol and fat consumption, etc.; and sometimes inherited that damage liver temporarily or permanently. It may happen due to autoimmune, obesity, or uncontrolled diabetes. In the early stages the disease usually responds to treatment and may be recovered completely. If it is left untreated, can permanently damage the liver, and can become life threatening. In advanced stages of liver disease, such as fibrosis, cirrhosis, and cancer; the liver damage may not be reversed. Liver diseases are very high costly in terms of human suffering, doctor and hospital visits, and premature loss of productivity. Therefore, quick and proper diagnosis and treatment may recover the damage to the liver in most of the cases.

References

Aalto, M. et al., (2011). The Alcohol Use Disorders Identification Test (AUDIT) and Its Derivatives in Screening for Heavy Drinking among the Elderly. *International Journal of Geriatric Psychiatry*, *26*(9), 881-885.

Aghemo, A. et al., (2015). Assessing Long-Term Treatment Efficacy in Chronic Hepatitis B and C: Between Evidence and Common Sense. *Journal of Hepatology*, *57*(6), 1326-1335.

Aleksandrova, K. et al., (2016). Obesity and Liver Cancer. *Recent Results in Cancer Research*, *208*, 177-198.

Alukal, J. J. et al., (2020). Hyponatremia in Cirrhosis: An Update. *American Journal of Gastroenterology*, *115*(11), 1775-1785.

Amir, M., Czaja, M. J., (2011). Autophagy in Nonalcoholic Steatohepatitis. *Expert Review of Gastroenterology & Hepatology*, *5*(2), 159-166.

Asrani, S. K. et al., (2019). Burden of Liver Diseases in the World. *Journal of Hepatology*, *70*(1), 151-171.

Bataller, R., Brenner, D. A., (2005). Liver Fibrosis. *Journal of Clinical Investigation*, *115*(2), 209-218.

Blachier, M. et al., (2013). The Burden of Liver Disease in Europe: A Review of Available Epidemiological Data. *Journal of Hepatology*, *58*(3), 593-608.

Bonnett, R. et al., (1976). Structure of Bilirubin. *Nature*, *262*(5566), 326-328.

Chen, C. M., Yoon, Y. H., (2022). *Liver Cirrhosis Mortality in the United States: National, State, and Regional Trends*, 2000-2019. Surveillance Report #118, US Department of Health and Human Services.

Cheng, K., et al., (2017). Ursodeoxycholic Acid for Liver Disease Related to Cystic Fibrosis. *Cochrane Database of Systematic Reviews*, *9*(9), CD000222.

De Clercq, E. et al., (2010). Antiviral Treatment of Chronic Hepatitis B Virus Infections. *Viruses*, *2*(6), 1279-1305.

Desmet, V. J., (1994). Classification of Chronic Hepatitis: Diagnosis, Grading and Staging. *Hepatology*, *19*(6), 1513-1520.

Dooley, J. S. et al., (2018). *Sherlock's Diseases or the Liver & Biliary System (13th Ed.)*. Wiley-Blackwell Publishing Ltd.

Ebrahimkhani, M. R. et al., (2014). Bioreactor Technologies to Support Liver Function in Vitro. *Advanced Drug Delivery Reviews*, 69-70, 132-157.

Geong, G. Y. et al., (2019). An Updated Review on the Epidemiology, Pathophysiology, Etiology, and Diagnosis of Liver Cirrhosis. Preprint.

Gibbs, R. W., Jr., (2008). Metaphor and Thought: The State of the Art. In R. W. *Gibbs*, Jr. (Ed.), *The Cambridge Handbook of Metaphor and Thought*. Cambridge University Press, Cambridge.

Ginès, P. et al., (2021). Liver Cirrhosis. *Lancet*, *398*(10308), 1359-1376.

Hettiaratchi, L., (2022). *A Case Study of Physiotherapy on a Patient after Liver Transplantation*. Bachelor Thesis, Physiotherapy Department, Faculty of Physical Education and Sport, Charles University.

Hirschfield, G. M., Heathcote, E. J., (2011). *Autoimmune Hepatitis: A Guide for Practicing Clinicians*. Springer Science & Business Media. Humana Press.

Hofmann, A. F., Hagey, L. R., (2008). Bile Acids: Chemistry, Pathochemistry, Biology, Pathobiology, and Therapeutics. *Cellular and Molecular Life Sciences*, *65*(16), 2461-2483.

Iida-Ueno, A. et al., (2017). Hepatitis B Virus Infection and Alcohol Consumption. *World Journal of Gastroenterology*, *23*(15), 2651-2659.

Jokelainen, K., (2013). Alkoholin Kulutuksen Kasvu Lisää Maksasairauksien Riskiä. *Suom Lääkäril*, *68*(2013), 1880-1884.

Kothari, C. R., (2008). *Research Methodology: Methods and Techniques* (2nd Ed.). New Delhi: New Age International (P) Ltd.

Larson, A. M. et al., (2005). Acetaminophen-induced Acute Liver Failure: Results of a United States Multicenter, Prospective Study. *Hepatology*, *42*(6), 1364-1372.

Lee, S. M. et al., (2016). Interplay of Genetic and Epigenetic Alterations in Hepatocellular Carcinoma. *Epigenomics*, *8*(7), 993-1005.

Legesse, B., (2014). *Research Methods in Agribusiness and Value Chains*. School of Agricultural Economics and Agribusiness, Haramaya University.

Livingston, S. I., Durkalski-Mauldin, V., (2022). Accounting for Liver Transplant in Acute Liver Failure Research. *Gastro Hep Advances*, *1*(4), 538-554.

Louvet, A., Mathurin, P., (2015). Alcoholic Liver Disease: Mechanisms of Injury and Targeted Treatment. *Nature Reviews Gastroenterology & Hepatology*, *12*(4), 231-242.

Ludwig, D. R. et al., (2023). Secondary Sclerosing Cholangitis: Mimics of Primary Sclerosing Cholangitis. *Abdom Radiol (NY)*, *48*(1), 151-165.

Mas-Coma, M. S. et al., (1999). Epidemiology of Human Fascioliasis: A Review and Proposed New Classification. *Bulletin of the World Health Organization*, *77*(4), 340-346.

Mincis, M., Mincis, R., (2006). Enzimas Hepáticas: Aspectos de Interesse Prático. *Revista Brasileira de Medicina*, 56-60.

Mohajan, D., Mohajan, H. K., (2023a). Obesity and Its Related Diseases: A New Escalating Alarming in Global Health. *Journal of Innovations in Medical Research*, *2*(3), 12-23.

Mohajan, D., Mohajan, H. K., (2023b). Body Mass Index (BMI) is a Popular Anthropometric Tool to Measure Obesity among Adults. *Journal of Innovations in Medical Research*, *2*(4), 25-33.

Mohajan, D., Mohajan, H. K., (2023c). A Study on Body Fat Percentage for Physical Fitness and Prevention of Obesity: A Two Compartment Model. *Journal of Innovations in Medical Research*, *2*(4), 1-10.

Mohajan, D., Mohajan, H. K., (2023d). Long-Term Regular Exercise Increases $\dot{V}O_2$max for Cardiorespiratory Fitness. *Innovation in Science and Technology*, *2*(2), 38-43.

Mohajan, H. K., (2017). Two Criteria for Good Measurements in Research: Validity and Reliability. *Annals of Spiru Haret University Economic Series*, *17*(3), 58-82.

Mohajan, H. K., (2018). Aspects of Mathematical Economics, Social Choice and Game Theory. PhD Dissertation, Jamal Nazrul Islam Research Centre for Mathematical and Physical Sciences (JNIRCMPS), University of Chittagong, Chittagong, Bangladesh.

Mohajan, H. K., (2020). Quantitative Research: A Successful Investigation in Natural and Social Sciences. *Journal of Economic Development, Environment and People*, *9*(4), 50-79.

Mohajan, H. K., (2024a). Alcoholic Liver Disease: Diagnosis and Treatment Strategies. Unpublished Manuscript.

Mohajan, H. K., (2024b). Anatomy of Human Liver: A Theoretical Study. Unpublished Manuscript.

Mohajan, H. K., (2024c). A Study on Functions of Liver to Sustain a Healthy Liver. Unpublished Manuscript.

Mohajan, H. K., (2024d). Alcoholic Liver Cirrhosis: A Chronic Liver Failure Due to Alcohol Abuse. Unpublished Manuscript.

Mohajan, H. K., (2024e). Alcoholic Hepatitis: Diagnosis and Management Procedures. Unpublished Manuscript.

Murray, K. F. et al., (2008). Chronic Hepatitis. *Journal of Pediatric Gastroenterology and Nutrition*, *47*(2), 225-233.

Pandey, P., Pandey, M. M., (2015). *Research Methodology: Tools and Techniques*. Bridge Center, Romania, European Union.

Pfeiffer, R. F., (2007). Wilson's Disease. *Seminars in Neurology*, *27*(2), 123-132.

Pinter, M., et al., (2016). Cancer and Liver Cirrhosis: Implications on Prognosis and Management. *ESMO Open*, *1*(2), e000042.

Polit, D. F., Hungler, B. P., (2013). *Essentials of Nursing Research: Methods, Appraisal, and Utilization* (8th Ed.). Philadelphia: Wolters Kluwer/Lippincott Williams and Wilkins.

Poupon, R. E. et al., (1997). Combined Analysis of Randomized Controlled Trials of Ursodeoxycholic Acid in Primary Biliary Cirrhosis. *Gastroenterology*, *113*(3), 884-890.

Rehm, J. et al., (2013). Global Burden of Alcoholic Liver Diseases. *Journal of Hepatology*, *59*(1), 160-168.

Saigal, S. et al., (2019). Ademetionine in Patients with Liver Disease: A Review. *International Journal of Research in Medical Sciences*, *7*(6), 2482-2493.

Sidhu, S. S. et al., (2018). L-ornithine L-aspartate in Bouts of Overt Hepatic Encephalopathy. *Hepatology*, *67*(2), 700-710.

Singal, A. K., Mathurin, P., (2021). Diagnosis and Treatment of Alcohol-Associated Liver Disease: A Review. *JAMA*, *326*(2), 165-176.

Sivakrishnan, S., (2019). Liver Disease: An Overview. *World Journal of Pharmacy and Pharmaceutical Sciences*, *8*(1), 1385-1395.

Tapper, E. B., Parikh, N. D., (2023). Diagnosis and Management of Cirrhosis and Its Complications: A Review. *JAMA*, *329*(18), 1589-1602.

Tapper, E. B., Lok, A. S., (2017). Use of Liver Imaging and Biopsy in Clinical Practice. *The New England Journal of Medicine*, *377*(8), 756-768.

Trautwein, C. et al., (2015). Hepatic Fibrosis: Concept to Treatment. *Journal of Hepatology*, *62*(1 Suppl), S15-S24.

Tripodi, A., Mannucci, P. M., (2011). The Coagulopathy of Chronic Liver Disease. *New England Journal of Medicine*, *365*(2), 147-156.

Trivedi, P. J., (2014). Good Maternal and Fetal Outcomes for Pregnant Women with Primary Biliary Cirrhosis. *Clinical Gastroenterology and Hepatology*, *12*(7), 1179-1185.

Turner, R., et al., (2011). Human Hepatic Stem Cell and Maturational Liver Lineage Biology. *Hepatology*, *53*(3), 1035-1045.

Vítek, L., Tiribelli, C., (2023). Gilbert's Syndrome Revisited. *Journal of Hepatology*, *79*(4), 1049-1055.

Wazir, H., et al., (2023). Diagnosis and Treatment of Liver Disease: Current Trends and Future Directions. *Cureus*, *15*(12), e49920.

Younossi, Z. M. et al., (2021). Performance of the Enhanced Liver Fibrosis Test to Estimate Advanced Fibrosis among Patients with Nonalcoholic Fatty Liver Disease. *Gastroenterology and Hepatology*, *4*(9), e2123923.

Yu, B. et al., (2021). *Drug Discovery in Liver Disease Using Kinome Profiling. International Journal of Molecular Sciences*, *22*(5), 2623.

Zhang, Y. Y., Meng, Z. J., (2022). Definition and Classification of Acute-on-chronic Liver Diseases. *World Journal of Clinical Cases*, *10*(15), 4717-4725.

Paradigm Academic Press
Journal of Innovations in Medical Research
ISSN 2788-7022
APR. 2025 VOL.4, NO.2

Mean Platelet Volume and Cancer-Associated Deep Vein Thrombosis

A. Guiga[1], M. Krifa[1], A. Amara[2], M. Thabet[1], W. BenYahia[1], A. Atig[1], C. Zedini[2] & N. Ghannouchi[1]

[1] Department of Internal Medicine, Farhat Hached University Hospital, Faculty of Medicine, University of Sousse, 4002 Sousse, Tunisia

[2] Department of Family and Community Medicine, Faculty of Medicine, University of Sousse, 4002 Sousse, Tunisia

Correspondence: A. Guiga, Department of Internal Medicine, Farhat Hached University Hospital, Faculty of Medicine, University of Sousse, 4002 Sousse, Tunisia.

doi:10.63593/JIMR.2788-7022.2025.04.004

Abstract

Background: Deep vein thrombosis (DVT) is a common and serious complication in cancer patients, primarily driven by malignancy-induced hypercoagulability and systemic inflammation. Mean platelet volume (MPV), a hematological parameter reflecting platelet activation and inflammatory status, has been proposed as a potential marker for thromboembolic risk stratification in oncology. ***Objective:*** This retrospective study aimed to assess the association between MPV and DVT in patients with underlying cancer. ***Methods:*** We analyzed MPV levels in a cohort of 102 patients diagnosed with DVT, including 18 individuals with active malignancy. ***Results:*** Although MPV values were slightly elevated in cancer patients compared to non-cancer patients, the difference did not reach statistical significance ($p = 0.86$). ***Conclusion:*** Our findings suggest that MPV is not a reliable biomarker for cancer-associated DVT. Further studies exploring alternative hematological and inflammatory markers are warranted to improve risk assessment in this high-risk population.

Keywords: mean platelet volume, deep vein thrombosis, cancer, biomarkers, thrombosis, inflammation

1. Introduction

Cancer-associated deep vein thrombosis (DVT) is a major clinical challenge due to its high incidence and significant impact on morbidity and mortality (Lee AY & Levine MN., 2003). The pathophysiology of cancer-related thrombosis is multifactorial, involving a complex interplay between tumor-induced hypercoagulability, endothelial dysfunction, and systemic inflammation (Rickles FR & Edwards RL., 1992). Early identification of patients at high risk for thrombotic events is crucial to optimizing preventive strategies and improving clinical outcomes.

Mean platelet volume (MPV), a routinely available parameter in complete blood counts, serves as an indicator of platelet size and activity, both of which are closely linked to inflammation and thrombogenesis (Yilmaz S, Kaya MG, Demir T, et al., 2018). Elevated MPV levels have been associated with an increased risk of thrombotic events, including venous thromboembolism (VTE), in various clinical settings (Spyropoulos AC, Levy JH & Ageno W., 2016). However, its specific role in differentiating cancer-associated DVT from other etiologies remains unclear. This study aims to evaluate whether MPV could serve as a potential biomarker for the diagnosis or risk stratification of DVT in patients with underlying malignancies.

2. Materials and Methods

2.1 Study Design and Population

This retrospective observational study included 102 adult patients diagnosed with DVT at our institution between January 2018 and December 2021. Patients were divided into two groups: those with active cancer (n =

18) and those without cancer (n = 84). Active cancer was defined as any malignant disease requiring treatment or follow-up during the study period. Cancer diagnosis preceded or coincided with DVT onset.

2.2 Data Collection

Demographic data, medical history, laboratory parameters, and imaging results were extracted from electronic health records. MPV values were recorded within one month of DVT diagnosis. Other variables included age, sex, body mass index (BMI), comorbidities, and cancer type.

2.3 Statistical Analysis

Data was analyzed using SPSS version 21.0. Continuous variables were expressed as mean ± standard deviation (SD), while categorical variables were presented as frequencies and percentages. Differences between groups were assessed using Student's t-test for continuous variables and chi-square tests for categorical variables. A p-value < 0.05 was considered statistically significant.

3. Results

3.1 Description of the Study Population (Table 1)

This study included a total of 102 patients diagnosed with deep vein thrombosis (DVT). Among these, 18 patients had active cancer, while 84 did not have any malignancy.

The mean age of the entire cohort was 63.5 ± 12.7 years, with no significant difference between the cancer and non-cancer groups (p = 0.67). The majority of patients were male (52.9%), and there was no significant gender disparity between the two groups (p = 0.81). Body mass index (BMI) also showed no significant difference between the cancer and non-cancer groups (p = 0.78).

Regarding cancer types, pelvic cancers were the most common (n = 5, 27.8%), followed by hematological malignancies (n = 5, 27.8%), gastrointestinal cancers (n = 3, 16.7%), and lung cancers (n = 2, 11.1%).

Regarding cancer types, pelvic cancers were the most common (n = 5, 27.8%), followed by hematological malignancies (n = 5, 27.8%), gastrointestinal cancers (n = 3, 16.7%), and lung cancers (n = 2, 11.1%).

3.2 Mean Platelet Volume (MPV) Analysis (Table 2)

The mean MPV values were compared between patients with and without cancer. As shown in Table 2, the mean MPV in the cancer group was 8.25 ± 0.88 fL, while it was 8.33 ± 1.21 fL in the non-cancer group. Despite a slight numerical difference, this variation was not statistically significant (p = 0.86).

As demonstrated in Table 2, the comparison of MPV levels between the two groups revealed no statistically significant difference. Also, the analysis of different cancer subgroups did not reveal any statistically significant differences in Mean Platelet Volume (MPV) compared to the control group (patients without cancer). Specifically, the MPV values observed for pelvic cancers (8.28 ± 0.69 fL), hematological malignancies (8.30 ± 1.05 fL), lung cancers (8.25 ± 1.46 fL), and gastrointestinal cancers (8.65 ± 1.9 fL) were not significantly different from those of the non-cancer group (8.33 ± 1.21 fL), with p-values of 0.92, 0.95, 0.98, and 0.37, respectively. These findings suggest that MPV may lack specificity as a biomarker for distinguishing between DVT associated with specific types of cancer and DVT in patients without cancer.

Table 1. Descriptive Characteristics of the Study Population

VARIABLE	TOTAL (N=102)	WITH CANCER (N=18)	WITHOUT CANCER (N=84)	P-VALUE
Age (years), mean ± SD	63.5 ± 12.7	65.3 ± 13.1	63.1 ± 12.5	0.67
Male, n (%)	54 (52.9%)	10 (55.6%)	44 (52.4%)	0.81
BMI (kg/m²), mean ± SD	27.8 ± 4.3	28.1 ± 4.7	27.7 ± 4.2	0.78
Cancer Types, n (%)				
- Pelvic cancers		5 (27.8%)		
- Hematological malignancies		5 (27.8%)		
- Gastrointestinal cancers		3 (16.7%)		
- Lung cancers		2 (11.1%)		

Table 2. Statistical Comparison of Mean Platelet Volume (MPV)

VARIABLE	WITH CANCER (N=18)	WITHOUT CANCER (N=84)	P-VALUE
MPV (fL), mean ± SD	8.25 ± 0.88	8.33 ± 1.21	**0.86**

4. Discussion

Our study investigated the potential role of mean platelet volume (MPV) as a biomarker for cancer-associated deep vein thrombosis (DVT). Although we observed a slight increase in MPV levels among patients with malignancies, this difference did not reach statistical significance. These findings are consistent with previous studies suggesting that MPV alone lacks sufficient specificity and sensitivity to reliably distinguish cancer-associated thrombosis from other causes (Zhang L, Wang H, Li X, et al., 2020).

Several factors may account for these results. First, MPV is influenced by a wide range of physiological and pathological conditions, including systemic inflammation, infections, cardiovascular diseases, and hematological disorders (Bode C & Greinacher A., 2007). These confounding factors may obscure its potential utility as a standalone marker for cancer-related thrombosis. Second, the relatively small sample size of our cancer subgroup may have limited our ability to detect statistically significant differences. Larger, well-powered prospective studies are required to confirm these observations and further explore the clinical implications of MPV in this context.

Given these limitations, a multimodal approach incorporating MPV alongside other biomarkers may enhance its predictive value. For instance, D-dimer and C-reactive protein (CRP), both of which are well-established indicators of coagulation activation and systemic inflammation, have shown promise in improving thrombotic risk stratification (Liu Y, Zhao J, Chen J, et al., 2021). A recent meta-analysis highlighted the potential of composite scoring systems integrating multiple inflammatory and hemostatic parameters to refine risk assessment in oncology patients (8). Future research should focus on developing and validating such predictive models to optimize early detection and management strategies for cancer-associated thrombosis.

5. Conclusion

MPV does not appear to be a reliable biomarker for differentiating cancer-associated DVT from other forms of venous thrombosis. While it reflects general inflammatory and thrombotic tendencies, its lack of specificity limits its clinical applicability. Further investigations into alternative or combined biomarkers are essential for advancing personalized medicine approaches in oncology and hematology.

References

Bode C, Greinacher A., (2007). Platelets in inflammation and atherogenesis. *J Clin Invest*, *117*(12), 3586-3593.

Lee AY, Levine MN., (2003). Venous thromboembolism and cancer: risks and outcomes. *Circulation*, *107*(23 Suppl 1), I-17-I-21.

Liu Y, Zhao J, Chen J, et al., (2021). Composite biomarkers for predicting venous thromboembolism in cancer patients: A meta-analysis. *Blood Coagul Fibrinolysis*, *32*(3), 189-197.

Rickles FR, Edwards RL., (1992). Mechanisms of thrombosis in cancer. *Semin Thromb Hemost*, *18*(1), 1-11.

Spyropoulos AC, Levy JH, Ageno W., (2016). Venous thromboembolism: new insights into mechanisms and management. *Circulation*, *133*(16), 1614-1631.

Yilmaz S, Kaya MG, Demir T, et al., (2018). Mean platelet volume as a predictor of cardiovascular events: A systematic review and meta-analysis. *Clin Appl Thromb Hemost*, *24*(1), 126-134.

Zhang L, Wang H, Li X, et al., (2020). Mean platelet volume in patients with cancer-associated thrombosis: A systematic review. *Thromb Res.*, *190*, 115-121.

Copyrights

Paradigm Academic Press
Journal of Innovations in Medical Research
ISSN 2788-7022
APR. 2025 VOL.4, NO.2

Phytochemistry, Nutritional Composition, Health Benefits, Applications and Future Prospects of *Momordica Charantia* L.: A Comprehensive Review

Dan Han[1], Zhou Yu[2] & Kai Zhang[2]

[1] School of Health Sciences and Engineering, University of Shanghai for Science and Technology, Shanghai 200093, PR China

[2] School of Pharmacy, Second Military Medical University, Shanghai 200433, PR China

Correspondence: Dan Han, School of Health Sciences and Engineering, University of Shanghai for Science and Technology, Shanghai 200093, PR China.

doi:10.63593/JIMR.2788-7022.2025.04.005

Abstract

Momordica charantia L., commonly known as bitter melon (BM) or bitter gourd, has great nutritional value and versatile properties. BM is consumed directly as a traditional vegetable or used for pickling, and has also been made into uniquely flavored canned products, tea, compound beverages, and wine. Various extracts, juices and isolated compounds show a wide range of health effects and biological activities, such as antioxidant, anti-inflammatory, antitumor, antidiabetic, anti-obesity, antifungal, neuroprotective, and blood cholesterol-reducing effects. In this review, we not only review the phytochemical properties of BM but also highlight the potential of Chia seeds for food applications and the use of all parts as a source of ingredients for medicines and cosmetics that promote health and well-being. This will provide theoretical support for the integrated use of such natural products.

Keywords: *Momordica charantia* L., nutritional value, comprehensive application, bioactivity, safety

1. Introduction

The genus *Momordica* is an herbaceous vine in family Cucurbitaceae. The major species, *Momordica charantia* L., commonly recognized as bitter melon (BM) or bitter gourd, and is additionally referred to as cundeamor in South America or karela in India (Çiçek S S, 2022). BM is cultivated throughout the world, including the tropical regions of Asia, the Amazon River Basin, East Africa and the Caribbean, where it is used both as a vegetable and in traditional folk medicine practices (Dandawate P R et al., 2016).

BM is similar in appearance to a cucumber, usually oblong and still green when eaten, with a relatively thin layer of pulp around its large, flesh-filled and flattened seeds (Saeed F et al., 2011; Vijayalakshmi B, Kumar G S & Salimath P V, 2009). All parts of BM, including the fruit, have a bitter taste, and in cooking BM fruit is often sautéed with a variety of vegetables, stuffed, or added in small quantities to soups or legumes to introduce subtle bitterness and texture. Various components of BM (such as fruits, flowers and shoots) are used as flavor enhancers in a range of traditional Asian cuisines, with shoots and leaves cooked and eaten as vegetables and fruit extracts used in tea production (Dandawate P R et al., 2016).

BM has a long history of medicinal use and has been recommended in Ayurveda (traditional Indian medicine) for centuries as a beneficial dietary supplement for the treatment and amelioration of diabetes and its associated complications (Nerurkar P & Ray R B, 2010). In recent decades, significant efforts have been dedicated to the pharmacological study of BM. Various extracts and isolated compounds, including triterpenoids, glycosides,

triterpenoid saponins, phenols, flavonoids, and certain protein fractions (Li Z et al., 2020), have exhibited a wide spectrum of biological activities, such as antioxidant (Chen F & Huang G, 2019; Wang F et al., 2023), anti-inflammatory (Wang F et al., 2023), antitumor (Fang E F et al., 2019), antidiabetic (Oyelere S F et al., 2022; Chang C I et al., 2021), anti-obesity (Cortez-Navarrete M et al., 2021), antifungal (Wang S et al., 2016), neuroprotective (Zhan K, Ji X & Luo L, 2023) and blood cholesterol-reducing (Naz R et al., 2016) effects. In recent years, many reviews have been published on the nutritional value, phytochemistry, and pharmacology of BM (Zheng J et al., 2023; Sun L et al., 2021). However, there are few reviews on the potential uses of all BM fruit fractions (peel, pulp, and seeds) and the phytochemical properties and associated biological activities of these fractions.

In this review, we systematically summarize the phytochemistry, nutrient composition, health effects, applications and future perspectives regarding BM. This will provide theoretical support for the comprehensive utilization of such natural products.

2. Nutritional Value and Chemical Composition of BM

A wide range of nutrients including vitamins, fatty acids, minerals, proteins, phenolic compounds and flavonoids are present in *Momordica* plants, and the nutritional value and chemical composition of BM are shown in Tables 1 and 2.

2.1 Minerals

The species of *Momordica* are important vegetable crops in the Cucurbitaceae family, rich in minerals in their pulp, peel, and seeds (Kandangath Raghavan A, Garlapati Phani K & Nallamuthu I, 2015). Mineral contents in various parts of the fruit show higher levels of K and Ca in the whole fruit, followed by Mg and P in the endocarp, and Na in the epicarp, whereas the seeds contained the lowest amounts of these macro-minerals. Conversely, BM seeds were identified as a significant source of micro-minerals such as Fe, Zn, Cu, and Mn (Singla D et al., 2023). Minerals are vital to the body's metabolism and their importance is often underestimated because people only need trace amounts. Therefore, it is beneficial to include BM in a healthy diet because it contains essential minerals that support overall health.

2.2 Vitamins

BM fruits are also an excellent source of vitamin E (tocopherols) and vitamin A (Tuan P A et al., 2011; Saini R K & Keum Y S, 2017). According to the USDA Food Composition Database, BM has a high proportion of vitamin A (426 IU). BM is a potential neuroprotectant including vitamin E as probable active components for the prevention for PAHs-induced neurotoxicity (Pattarachotanant N, Prasansuklab A & Tencomnao T, 2021). Vitamin C content (5.2 mg/g) in the BM extract is close to that in strawberry (5.9 mg/g) (Nguyen T-V-L et al., 2020).

2.3 Polysaccharides

The polysaccharides predominantly found in BM consist of rhamnose, xylose, galactose, and arabinose. They are important pharmacological active ingredients, water-soluble, with an average molecular weight of 4-900 kDa (Zhan K, Ji X & Luo L, 2023; Yang X, Chen F & Huang G, 2020). The antioxidant activity of BM polysaccharides, extracted via aqueous methods and precipitated with ethanol, is markedly increased *in vitro* following carboxymethylation and acetylation modifications. Notably, the carboxymethylated derivatives demonstrate superior antioxidant activity, potentially due to the incorporation of carboxyl groups. This modification results in the formation of a negatively charged, hydrophilic surface structure in the bitter melon polysaccharides, which enhances their water solubility and consequently augments their antioxidant efficacy (Chen F & Huang G, 2019). Therefore, BM polysaccharides have the potential to act as antioxidants.

2.4 Fatty Acids and Amino Acids

α-Eleostearic acid, belonging to the conjugated linolenic acid (CLNA) family, is primarily found in seeds and to a lesser extent in flesh. In the oils extracted from seeds of 10 different BM varieties, α-Eleostearic acid (α-ESA; *cis*-9, *trans*-11, *trans*-13- isomer of CLNA) accounted for 30-60% of the total fatty acids (Bialek A et al., 2016; Chen G-C et al., 2016). Elevated fatty acid concentrations are essential to increase the utilization of BM as a functional food ingredient, providing new perspectives and opportunities for the treatment of obesity.

The amino acid composition of BM varies in different tissues and at different stages of growth. To date, 17 amino acids have been identified in BM, and the contents of Asn, Asp, Thr, Ser, Gln, Glu, Gle, Pro, Gly, Ala, Leu, Tyr, Phe, Met, His, Lys, and Arg vary in different tissues and stages of maturation. The Tyr content in ripe pericarp measures 59.4 mg/g, contrasting with 56.5 mg/g in immature pericarp, and a notably lower 41.1 mg/g in ripe seeds (Horax R et al., 2010). Crucially, essential amino acids comprise approximately 36.58% of the total amino acid content, adequately meeting human nutritional needs.

Table 1. Nutritional compositions of *Momordica*

Nutrients	Species	Part	Content (mg/100g)	Ref.
Minerals				
Ca	*Momordica charantia* Linn. (Goj karela)	Seed	38.35 DW	(Karaman K et al., 2018)
	Momordica charantia Linn. (Guti karela)		41.16 DW	
	Momordica charantia Linn. (Majhari karela)		44.01 DW	
	Momordica sp. (PAUBG-232)	Fruit	71.39 DW	(Singla D et al., 2023)
	Momordica sp. (PAUBG-407)	Peel	67.68 DW	
	Momordica sp. (Black King)		62.33 DW	(Mahwish M et al., 2018)
	Momordica sp. (Black King)	Fruit	70.33 DW	
	Momordica sp. (BG-20)	Seed	2.66 DW	
Cu	*Momordica charantia* Linn. (Goj karela)		0.35 DW	(Karaman K et al., 2018)
	Momordica charantia Linn. (Guti karela)		0.29 DW	
	Momordica charantia Linn.(Majhari karela)		0.33 DW	
	Momordica sp. (PAUBG-407)	Seed	525.45 DW	(Singla D et al., 2023)
	Momordica sp. (PAUBG-407)	Peel	452.41 DW	
	Momordica sp. (PAUBG-407)	Fruit	411.22 DW	
	Momordica sp. (PAUBG-119)	Peel	24.54 DW	
Fe	*Momordica charantia* Linn.(Goj karela)	Seed	4.11 DW	(Karaman K et al., 2018)
	Momordica charantia Linn.(Guti karela)		4.26 DW	
	Momordica charantia Linn. (Majhari karela)		4.50 DW	
	Momordica sp. (PAUBG-195)		6.14 DW	(Singla D et al., 2023)
	Momordica sp. (PAUBG-93)		5.49 DW	
	Momordica sp. (PAUBG-328)		5.48 DW	
	Momordica sp. (PAUBG-146)	Peel	0.72 DW	
	Momordica sp. (Black King)		3.27 DW	(Mahwish M et al., 2018)
	Momordica sp. (GHBG-1)	Fruit	4.03 DW	
	Momordica sp. (KHBG-1)	Seed	4.91 DW	
Zn	*Momordica charantia* Linn. (Goj karela)		1.24 DW	(Karaman K et al., 2018)
	Momordica charantia Linn. (Guti karela)		1.35 DW	
	Momordica charantia Linn. (Majhari karela)		1.29 DW	
	Momordica sp. (PAUBG-88)		2.64 DW	(Singla D et al., 2023)
	Momordica sp. (Black King)	Peel	0.94 DW	(Mahwish M et al., 2018)
		Fruit	0.97 DW	
		Seed	3.52 DW	
P	*Momordica charantia* Linn. (Goj karela)		14.24 DW	(Karaman K et al., 2018)
	Momordica charantia Linn. (Guti karela)		13.65 DW	
	Momordica charantia Linn. (Majhari karela)		13.47 DW	
	Momordica sp. (PAUBG-88)	Peel	98.24 DW	(Singla D et al., 2023)
	Momordica sp. (PAUBG-88)	Fruit	84.83 DW	
	Momordica sp. (PAUBG-407)	Peel	59.37 DW	
	Momordica sp. (PAUBG-146)	Seed	8.56 DW	
	Momordica spp (Black King)	Peel	125.00 DW	(Mahwish M et

	Momordica spp (Black King)	Fruit	128.67 DW	al., 2018)
	Momordica sp. (KHBG-1)	Seed	28.67 DW	
K	*Momordica* sp. (PAUBG-407)	Fruit	483.49 DW	(Singla D et al., 2023)
	Momordica sp. (PAUBG-130)	Fruit	416.14 DW	
	Momordica sp. (PAUBG-119)	Seed	7.24 DW	
	Momordica sp. (Black King)	Peel	326.33 DW	(Mahwish M et al., 2018)
		Fruit	397.00 DW	
		Seed	37.33 DW	
Mg	*Momordica* sp. (PAUBG-335)	Peel	101.70 DW	(Singla D et al., 2023)
	Momordica sp. (PAUBG-222)	Seed	1.04 DW	
	Momordica sp. (Black King)	Peel	56.33 DW	(Mahwish M et al., 2018)
		Fruit	64.66 DW	
		Seed	4.63 DW	
Na	*Momordica* sp. (PAUBG-232)	Peel	18.56 DW	(Singla D et al., 2023)
	Momordica sp. (PAUBG-351)	Peel	17.65 DW	
	Momordica sp. (PAUBG-351)	Seed	0.45 DW	
	Momordica sp. (FSD Long)	Fruit	91.00 DW	
	Momordica sp. (BG-20)	Seed	3.1 DW	
	Momordica sp. (KHBG-1)	Peel	83.33 DW	
Mn	*Momordica* sp. (PAUBG-407)	Seed	179.05 DW	
	Momordica sp. (PAUBG-119)		46.92 DW	
Vitamins				
Vitamin C	*Momordica charantia* L.	Pulp	11.57 FW	(Hercos G F D et al., 2021)
	Momordica charantia L.	Seed	10.42 FW	
	Momordica sp. (PG)	Pulp	11.73 FW	(Zhang Y et al., 2023)
	Momordica sp. (JLZ)		12.16 FW	
	Momordica sp. (BFM)		5.67 FW	
	Momordica sp. (RB)		12.58 FW	
	Momordica sp. (CB)		12.66 FW	
	Momordica sp. (LJ)		6.53 FW	
	Momordica sp. (LBS)		6.31 FW	
Vitamin E	*Momordica* sp.	Fruit	4.29 FW	(Saini R K, Keum Y S, 2017)
Organic acids				
Oxalic acid	*Momordica* sp. (PG)	Pulp	2061 FW	(Zhang Y et al., 2023)
	Momordica sp. (JLZ)		3419 FW	
	Momordica sp. (BFM)		2211 FW	
	Momordica sp. (RB)		2555 FW	
	Momordica sp. (CB)		3023 FW	
	Momordica sp. (LJ)		3658 FW	
	Momordica sp. (LBS)		1642 FW	
Succinic acid	*Momordica* sp. (PG)		441.9 FW	
	Momordica sp. (JLZ)		266.8 FW	
	Momordica sp. (BFM)		265.0 FW	

	Momordica sp. (RB)		303.0 FW	
	Momordica sp. (CB)		631.0 FW	
	Momordica sp. (LJ)		204.7 FW	
	Momordica sp. (LBS)		167.9 FW	
Malic acid	*Momordica* sp. (PG)		8535 FW	
	Momordica sp. (JLZ)		22,140 FW	
	Momordica sp. (BFM)		10,927 FW	
	Momordica sp. (RB)		8000 FW	
	Momordica sp. (CB)		21,218 FW	
	Momordica sp. (LJ)		13,432 FW	
	Momordica sp. (LBS)		5940 FW	
Citric acid	*Momordica* sp. (PG)		410.2 FW	
	Momordica sp. (JLZ)		1862 FW	
	Momordica sp. (BFM)		1072 FW	
	Momordica sp. (RB)		438.4 FW	
	Momordica sp. (CB)		1084 FW	
	Momordica sp. (LJ)		689.0 FW	
	Momordica sp. (LBS)		377.8 FW	
Other compositions				
Soluble protein	*Momordica* sp. (PG)	Pulp	0.05 FW	(Zhang Y et al., 2023)
	Momordica sp. (JLZ)		0.13 FW	
	Momordica sp. (BFM)		0.05 FW	
	Momordica sp. (RB)		0.06 FW	
	Momordica sp. (CB)		0.12 FW	
	Momordica sp. (LJ)		0.06 FW	
	Momordica sp. (LBS)		0.13 FW	
Cellulose	*Momordica* sp. (PG)		2.99 DW	
	Momordica sp. (JLZ)		2.85 DW	
	Momordica sp. (BFM)		3.99 DW	
	Momordica sp. (RB)		2.75 DW	
	Momordica sp. (CB)		3.72 DW	
	Momordica sp. (LJ)		3.18 DW	
	Momordica sp. (LBS)		2.87 DW	

2.5 Phenolic Compounds

Bitter melon is rich in bioactive compounds (especially phenolic compounds), which are widely used in both medicinal and culinary fields. Phenolic compounds in the *Momordica* plant have been reported to come mainly from the pericarp, pulp and seeds. The immature stage of BM showed higher polyphenol levels compared to the ripe stages, with the seeds containing a higher polyphenol content than the peel (Lee J J & Yoon K Y, 2021).

The distribution of phenolic compounds in various parts of ripe BM fruits (pulp, rind, and seeds) as well as in whole immature fruits was quantified using UPLC-MS/MS. The highest total content of phenolic compounds was observed in both pulp of mature and immature fruits, measuring 964.00±15.64 mg/g and 918.63±18.22 mg/g, respectively. The phenolic content of the peel and seeds of mature BM was 898.15±14.88 mg/g and 598.57±16.14 mg/g, respectively (Lopes A et al., 2020). Therefore, the pulp of BM ripe fruits is a promising source of phenolic compounds. It deserves to be further explored in future studies, especially in the development of nutraceutical products, functional ingredients, foods and pharmaceuticals.

2.6 Flavonoid Compounds

Flavonoids usually refer to a class of compounds with a C6-C3-C6 structure in which the two benzene rings (A and B rings) are linked together by a central three-carbon chain, and have a variety of pharmacological properties such as antitumor, anti-inflammatory, antioxidant, antiviral and cardioprotective effects (Zhang H et al., 2022). The flavonoid content of bitter melon roots is low, whereas the flavonoid content of leaves and flowers is high. For example, the content of rutin in roots was only 37.04 μg/g (DW), while the content of rutin in leaves was as high as 3970.83 μg/g (DW). Figure 1 shows the major phenylalanine and flavonoid biosynthetic pathways in BM (Cuong D M et al., 2018).

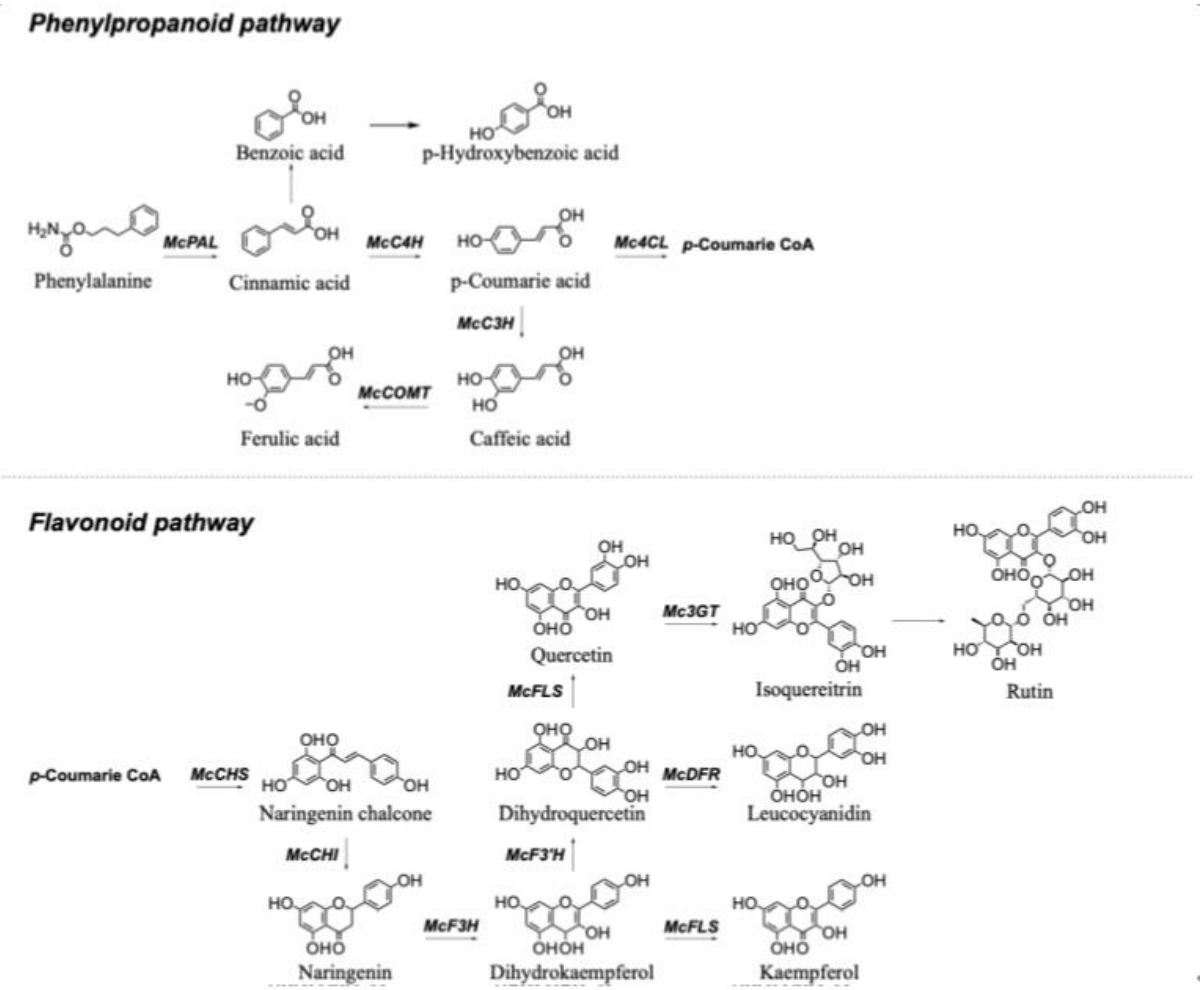

Figure 1. Structures of the main phenylpropanoid and flavonoids of *Momordica* plant, along with their corresponding biosynthetic pathway

Note: PAL: phenylalanine ammonia-lyase; C4H: cinnamate 4-hydroxylase; C3H: coumarate 3-hydroxylase; COMT: caffeic acid 3-*O*-methyltransferase; 4CL: 4-coumaroyl CoA ligase; CHS: chalcone synthase; CHI: chalcone isomerase; F3H: flavanone 3-hydroxylase; F3'H: flavonoid 3-hydroxylase; FLS: flavonol synthase; DFR: dihydroflavonol-4 reductase; 36T: flavonoid 3-*O*-glucosyltransferase.

2.7 Alkaloid Compounds

The total alkaloid content of BM seeds was significantly higher at 0.98% ± 0.02% compared to the whole fruit (0.65% ± 0.03%), pulp (0.53% ± 0.02%) and peel (0.52% ± 0.03%). Dietary intake of various parts of BM significantly reduced blood glucose concentrations, and among these parts, the seeds, which are rich in a large number of alkaloids, showed excellent ability to regulate blood glucose levels (Mahwish et al., 2023).

2.8 Saponin Compounds

The saponin compounds in BM are generally divided into two main groups: oleanoid and cucurbitane triterpenoids (Popovich D G, Li L & Zhang W, 2010). More than 100 saponins extracted from the fruit, stem and

leaves of BM have been isolated and characterized. Among them, bittersweet, a natural triterpenoid from the Cucurbitaceae family present in the fruit, leaves and seeds of BM, has potential hypoglycemic activity. The saponin content was significantly higher in male flowers (15.11 ± 1.45 μg/g) compared to female flowers (1.55 ± 0.08 μg/g), stems (0.14 ± 0.01 μg/g), young leaves (4.82 ± 0.53 μg/g) and mature leaves (6.58 ± 0.87 μg/g) (Cuong D M et al., 2017). Seven BM saponins, namely momordicoside L, 3*β*,7*β*,25-trihydroxycucurbita-5,23(*E*)-dien-19-al, momordicoside K, momordicine I, momordicoside I, momordicoside F_2, and momordicoside F_1, were determined using the UPLC-ESI-MS/MS (Liu Y-J et al., 2020). Furthermore, momordicoside U (Namsa N D et al., 2011), kuguaglycoside G (Tambor M et al., 2016), 3-hydroxycucurbita-5, 24-dien-19-al-7, 23-di-*O*-*β*-glucopyranoside (Aziz M, Karboune S, 2018), momordicine I (Sabourian R et al., 2016), 3*β*, 7*β*, 25-tri-hydroxycucurbita-5, 23 (*E*)-dien-19-al (Puri R et al., 2011), momordicine II (Pandit S et al., 2016) had also been isolated.

2.9 Volatile Components

More than 30 structurally distinct volatile constituents were isolated from BM flowers, of which laurene was the predominant compound, followed by methyl jasmonate and 1-octadecanol (Sarkar N, Mitra S & Barik A, 2017). Volatile compounds in leaves and fruits obtained by water distillation were identified by HS-SPME and GC-MS, and 18 compounds were found in mature fruits and 21 compounds in leaves. Benzaldehyde, linalool and *β*-cyclocitral were identified by both analytical methods. Linalool was found to be the major compound in both cases (Ferreira Almeida N et al., 2024).

Table 2. Chemical compounds identified in different parts of the *Momordica* plant

Chemical compounds	**Plant sources**	**Part**	**Extraction solvents**	**Characterization or analysis methods**	**Ref.**
Phenolic acids and phenols					
Quinic acid	Apucarana, Brazil	Pulp, peel, seed	Ethanol/water (80:20, *v/v*)	UPLC–MS/MS	(Lopes A P et al., 2018)
4-Hydroxybenzoic acid		Pulp, peel, seed			
Trans-cinnamic acid		Pulp, peel, seed			
p-Coumaric acid		Pulp, peel, seed			
Caffeic acid		Pulp, peel, seed			
Gallic acid		Pulp, peel, seed			
Quercetin		Pulp, peel, seed			
Rutin		Peel			
Ferulic acid	Apucarana, Brazil	Pulp, peel	Ethanol	UPLC–MS/MS	(Lopes A et al., 2020)
Synaptic acid		Pulp, peel, seed			
Chlorogenic acid		Peel			
Vanillic acid		Pulp, peel, seed			
Apigenin		Pulp, peel, seed			
Catechin		Pulp, peel			
Crisin		Pulp, peel, seed			
Kaempferol		Pulp, peel, seed			
Tannic Acid	Gyeongsan, Korea	Peel	Ethanol	HPLC	(Lee J J et al., 2021)
Epicatechin		Peel	Ethanol		
Syringic acid		Leave	Choline chloride-acetic acid, water, methanol, ethanol		
Quercetin-3-glucoside		Leave			
Salicylic acid		Leave			
Luteolin-3',7-di-*O*-glucoside	Târgu Mureş,	Stem, leave	Ethanol/water (80:20, *v/v*)	UPLC	(Laczko-Zold E et al.,

Luteolin-7-*O*-glucoside	Romania	Stem, leave, fruit				2023)
4-*O*-Feruoylquinic acid,	Santa Cruz area, Trinidad	Fruit		Ethanol/water (80:20, *v/v*)	HPLC/MS	(Svobodova B et al., 2017)
Quercetin-*O*-dihexoside		Fruit				
5-*O*-Feruoylquinic acid		Fruit				
Quercetin-*O*-pentosylhexoside		Fruit				
Quercetin-3-*O*-rutinoside		Fruit				
Kaempferol-*O*-pentosylhexoside		Fruit				
Quercetin-*O*-acetylhexoside		Fruit				
Kaempferol-3-*O*-rutinoside		Fruit				
Kaempferol-3-*O*-glucoside		Fruit				
Isorhamnetin-3-*O*-glucoside		Fruit				
Kaempferol-*O*-acetylhexoside		Fruit				
Isorhamnetin-*O*-acetylhexoside		Fruit				
Ellagic acid	India	Fruit		Methanol, ethanol and *n*-butanol	HPTLC	(Yadav R et al., 2016)
Flavonoids and their derivatives						
Herbacetin	Shandong and Hebei Province, China	Fruit		70% Methanol	UPLC-MS/MS	(Zhang, et al., 2022)
Isolhamnetin-3,7-*O*-diglucoside		Fruit				
Isorhamnetin-3-*O*-(6″-acetyl) glucoside		Fruit				
Isorhamnetin-3-*O*-rutinoside		Fruit				
Kaempferol-3-*O*-neohesperidoside		Fruit				
Kaempferol-4'-*O*-glucoside		Fruit				
Kaempferol-3-*O*-(6″-malonyl) glucoside		Fruit				
Kaempferol-3-*O*-glucoside-7-*O*-rhamnoside		Fruit				
Kaempferol-6,8-di-*C*-glucoside		Fruit				
Dihydro kaempferol-7-*O*-glucoside		Fruit				
Quercetin-3-*O*-(6″-acetyl) galactoside		Fruit				
Quercetin-3-*O*-(6″-malonyl) galactoside		Fruit				

Quercetin-7-*O*-(6″-malonyl) glucoside		Fruit			
Sakuranin		Fruit			
Sexangularetin-3-*O*-glucoside-7-*O*-rhamnoside		Fruit			
Saponarin-4′-*O*-glucoside		Fruit			
Aromadendrin-7-*O*-glucoside		Fruit			
Tricin-7-*O*-glucoside		Fruit			
Limocitrin-3-*O*-arabinoside		Fruit			
Limocitrin-7-*O*-glucoside		Fruit			
Rutin	Soure, Brazil	Leave	Ethanol, ethyl acetate	LC-HRMS	(Muribeca A d J B et al., 2022)
Kaempferol-*O*-glucoside-*O*-pentoside		Leave	Ethanol		
Luteolin-*O*-rutinoside		Leave	Ethanol, ethyl acetate		
Kaempferol-*O*-glucoside		Leave	Ethanol, ethyl acetate		
Isorhamnetin-*O*-glucoside		Leave	Ethanol		
Quercetin-*O*-acetylpentoside		Leave	Ethanol, ethyl acetate		
Catechin hydrate	Beijing, China	Flower	80% Ethanol	HPLC	(Cuong D M et al., 2018)
Benzoic acid		Root, stem, leave, flower			

Note: HPLC-MS: high-performance liquid chromatography-mass spectrometry; UPLC-MS: ultra performance liquid chromatography mass spectrometry; HPLC: high-performance liquid chromatography; HPTLC: high-performance thin layer chromatography; LC-HRMS: liquid chromatography, high resolution mass spectrometry.

3. Health Benefits

Herein, the potential health benefits of *Momordica* plants and some of their potential mechanisms are summarized in **Table 3** and **Figure 2**.

3.1 Antioxidant Activity

Several studies have been carried out to verify the *in vitro* antioxidant activity of *Momordica* plants through $ABTS^+$ radical scavenging capability, NO radical inhibition ability and DPPH radical scavenging capability (Nguyen T-V-L et al., 2020; AkyÜz E et al., 2020; Hani N M et al., 2017).

In recent years, the quest for appropriate natural antioxidants has emerged as a significant research field due to the suspected role of synthetic antioxidants, such as butyl hydroxyanisole (BHA) and butyl hydroxytoluene (BHT), in liver damage and carcinogenesis. Several studies have confirmed that plant polysaccharides exhibit significant antioxidant activity, which can be further enhanced through chemical modifications (Liu Y, Sun Y & Huang G, 2018). The antioxidant activity of polysaccharides derived from BM was found to be significantly enhanced through carboxymethylation, a structural modification technique. This enhancement can be attributed to the introduction of negatively charged carboxyl groups, which create a negatively charged hydrophilic surface structure for the polysaccharide. As a result, the water solubility of the polysaccharide is greatly improved, leading to enhanced antioxidant activity (Chen F & Huang G, 2019).

As a vital active ingredient in BM, polysaccharide has been shown to significantly elevate the levels of superoxide dismutase (SOD) and catalase (CAT) in the serum of mice. High doses of polysaccharides (300 μg/g) increased SOD and CAT levels in serum by 47.4% and 63.1%, respectively. Furthermore, high doses of polysaccharides (300 μg/g) increased malondialdehyde (MDA) levels in the brain by 57.0%, thereby

demonstrating its antioxidant and anti-aging properties (Huang H et al., 2020).

In addition, it is widely recognized that aging is related to oxidative stress. BM saponins produce anti-oxidative stress and anti-aging effects through the IIS (insulin/insulin-like growth factor-1 signaling) pathway associated with sir-2.1 and hlh-30 (Zhang J et al., 2022); The intake of BM polysaccharides reduces D-galactose-induced spatial memory dysfunction and improves telomerase activity in aged rats through the Nrf2/β-catenin signaling pathway (Yue J et al., 2023). BM active extracts play a crucial role in alleviating aging caused by oxidative stress damage and reversing the decline in learning and memory abilities.

Table 3. Biological activity and mechanism of action of *Momordica* components or extracts

Extracts or components	Observation or methods	Effects	References
Antioxidant activity			
M. charantia fruit extracts (seed, pulp and peel)	DPPH and $ABTS^+$ assay	The peel exhibited the most noteworthy DPPH radical scavenging activity (EC_{50}=245.0 μg/mL). Moreover, the $ABTS^+$ assay demonstrated that the peel possessed the most potent antioxidant capacity, ($EC_{50=}$262.67 μg/mL).	(Mishra S et al., 2021)
Polysaccharide	DPPH radical, hydroxyl radical and superoxide radical	The polysaccharide exhibited scavenging capacities of 60% at 0.5 mg/mL against DPPH radicals, 50% at 0.8 mg/mL against superoxide radicals, and 33% at 0.9 mg/mL against hydroxyl radicals.	(Mei X et al., 2020)
M. charantia powder	$ABTS^+$, FRAP and DPPH assay	The *M. charantia* powder extract demonstrated remarkable antioxidant capacity at concentrations ranging from 0.25 to 1.0 mg/mL.	(Tan S P et al., 2014)
M. charantia methanol extract	ROS and MTT assay	The methanol extract of *Momordica charantia* significantly decreased SNP-induced ROS production and H_2O_2-induced cytotoxicity in HaCaT cells in a dose-dependent manner ranging from 0 to 200 μg/ml.	(Park S H et al., 2019)
Phenolic compounds of *M. charantia* by different solvents	DPPH and ORAC assay	The highest antioxidant capacity by DPPH assay was observed in ethanol/water (80:20, *v/v*) for peel (7.20±0.09 mg ET/g). In the ORAC assay, the highest antioxidant capacity was noted in ethanol/water (80:20, *v/v*) for seeds (4.93±0.04 mg ET/g).	(Lopes A P et al., 2018)
M. charantia extract by different solvents	DPPH radical, $ABTS^+$ radical and NO radical	The pulp extracted with deionized water exhibited the highest DPPH radical scavenging activity of 153.36±11.86 mg TEAC/g extract. The water extract of the inner tissue extracted with 60% ethanol demonstrated the highest ABTS radical inhibition activity of 244.39±12.81 mg TEAC/g extract. The inner tissue showed the highest NO radical inhibition activity of 6201.75±157.04 mg TEAC/g extract.	(Trakoolthong P et al., 2022)
Anti-inflammatory activity			
Triterpenoid (TCD) from vines and leaves	*In vitro*, RAW 264.7 cells	TCD (20-50 μM) dose-dependently inhibited LPS-induced iNOS expression.	(Chou M C et al., 2022)
Lignans and saponins from *M. cochinchinensis* seeds	*In vitro*, RAW 264.7 cells	Lignans and saponins could inhibit the release of NO and TNF-α in RAW 264.7 cells induced by LPS.	(Wang M et al., 2019)
Triterpenoids from	*In vitro*, FL83B	The two triterpenes dose-dependently inhibited	(Cheng H-L et

fruit	cells	the expression of iNOS, with IC_{50} values of 19.8 μM and 25.7 μM, respectively.	al., 2017)
BM (*M. charantia* Linn. var. *abbreviata Ser.*) fruit EA extract	*In vitro*, THP-1 cells	The BM EA extract not only decreases IL-8 levels, but also reduces TNF-α and IL-1*β* production in *P. acnes*-stimulated THP-1 cells, while also exhibiting an inhibitory effect on MMP-9 levels.	(Hsu C et al., 2012)
BM (*M. charantia* L. var. *abbreviate Seringe*) fruit	*In vivo*, sepsis mice	The diet containing 10% wild BM significantly inhibited the expression of iNOS protein, reduced the formation of the inflammatory mediator NO, and decreased the production of the inflammatory mediator PGE_2 by downregulating the expression of COX-2 protein.	(Chao C-Y et al., 2014)
BM fruit power extract	*In vitro*, RAW 264.7 cells	The extract decreased the LPS-induced expression of genes linked to the formation of inflammatory vesicle complex (NF-κB, NLRP3, Pycard, Casp1).	(Perez J L et al., 2021)
Crude BM extract	*In vivo*, colitis model	The crude BM extract significantly decreased colitis-induced weight loss and alleviated the colonic damage score of colitis, accompanied by a noteworthy elevation in serum anti-inflammatory cytokine IL-10 levels.	(Ünal N G et al., 2019)
Charantadiol A	*In vivo*, periodontitis model	Charantadiol A significantly suppressed *P. gingivalis*-stimulated IL-6 and TNF-α mRNA levels in gingival tissues of mice.	(Tsai T-H et al., 2021)
α-Eleostearic acid	*In vivo*, spinal cord injury (SCI) model	BM extract inhibits SCI-induced up-regulation of GFAP, IL-1*β*, and IL-6 mRNA and attenuates IL-4 and CISD2 mRNA down-regulation.	(Kung W-M et al., 2020)
Antitumor activity			
Methanol extracts from BM fruit	*In vitro*, HT-29 and SW480 cells	Methanol extracts demonstrated a dose-dependent inhibition of HT-29 and SW480 cell proliferation, with IC_{50} values of 57 μg/mL and 85 μg/mL, respectively.	(Kwatra D et al., 2013)
Momordicine-I	*In vitro*, Cal27, JHU022 and JHU029 cells	Momordicine-I markedly inhibited C-Met signaling and its downstream effectors, resulting in a substantial reduction in the expression of phosphorylated STAT3 (Tyr-705).	(Sur S et al., 2021)
Antidiabetic activity			
Polysaccharides	*In vivo*, STZ-induced rats	The polysaccharides successfully normalized hyperglycemia levels in diabetic rats. Furthermore, they exhibited an increase in the expression levels of Ins1, Jagged1, Pdx1, and Hes1 genes, along with a decrease in the expression levels of Notch1 and Dll4.	(Sajadimajd S et al., 2022)
Saponins	*In vivo*, STZ-induced mice	The total content of saponins in BM was 18.24 μg/mg. Diabetic mice treated with saponins at doses of 100 and 200 mg/kg body weight daily for a duration of 30 days exhibited significant reductions in BG levels of 12.63% and 26.47%, respectively (p<0.05).	(Deng Y et al., 2023)
Aqueous extract of seeds of BM	*In vitro*, adipocytes	Aqueous extract of BM seeds reduced glucose levels in diabetic adipocytes and significantly increased glycogen content and glucose-6-phosphate dehydrogenase activity.	(Saxena M et al., 2022)

BM juice	*In vivo*, STZ-induced rats	It induced a significant increase in serum insulin levels (3.41 ± 0.08 and 3.28 ± 0.08 vs. 2.39 ± 0.27 μIU/mL), HDL-cholesterol, total antioxidant capacity, *β*-cell function percentage, and pancreatic reduced GSH content, and it ameliorated histopathological changes in the pancreas.	(Mahmoud M F et al., 2017)
Charantin and vicine	*In vivo*, hyperglycemic rat model	When administered at a dosage of 300 mg/kg of whole fruit, it led to a 31.64% reduction in BG levels and a 27.35% elevation in insulin levels in hyperglycemic rats.	(Mahwish et al., 2021)
BM seed protein hydrolysate	*In vivo*, STZ-induced rats	The hydrolysates induced a reduction in levels of BG, glycated hemoglobin (HbA1c), and glycogen, as well as a decrease in serum lipid markers (cholesterol, high-density lipoproteins, low-density lipoproteins, and total cholesterol) in spontaneous diabetic rats in a dose-dependent fashion.	(Yuguda A Y, 2023)
Antibacterial activity			
Flavonoids from BM leaves	*In vitro*	The MIC of the ethyl acetate phase derived from the leaf extract of BM against *K. pneumoniae* is determined to be 156.2 μg/mL. In contrast, the MIC of the ethanol extract against *P. mirabilis* is measured at 312.5 μg/mL, and against both *K. pneumoniae* and *S. aureus*, it is quantified at 625 μg/mL.	(Muribeca A d J B et al., 2022)
BM seed oil	*In vitro*	The oil exhibited the greatest activity against *S. typhi* and *K. pneumoniae*, displaying a MIC of 15.63 mg/mL. The antimicrobial inhibition zones of the oil were 21.0±1.41 mm against *S. typhi*, 18.0±0 mm against *E. coli*, 15.0±1.41 mm against *R. stolonifer* and *A. niger*, and 17.0±1.41 mm against *C. albicans*.	(Zubair M F et al., 2018)
Fruit extracts from three different stages of cultivation	*In vitro*	The immature dried fruit extract in 80% and 100% methanol exhibited promising antibacterial activities, with a>18.5±0.21 mm zone of inhibition against *S. aureus*, whereas the extract from mature dried fruit in 80% methanol demonstrated a 18.4±0.17 mm zone of inhibition against *E. coli.*	(Naqvi S A R et al., 2020)
Seed extract	*In vitro*, liquid dilution method	The ethyl acetate fraction exhibits a MBC against *S. epidermidis*, with an MBC value of 40%.	(Rahmi M, Sari T M, Despanita, 2021)
Fruit ethanolic extract	*In vitro*, microdilution in broth method	*E. coli*, *P. aeruginosa*, *S. aureus*, *C. albicans*, *C. glabrata*, *C. guilliermondii*, *C. krusei*, *C. parapsilosis*, and *C. tropicalis* were all sensitive to the extracts, with their MIC and MBC/MFC being less than 0.125 mg/mL.	(Lucena Filho J H et al., 2015)
Antiviral activity			
M. balsamina leaf extract	*In vitro*, MTT assay	*M. balsamina* leaf extract inhibits HIV-1 infection by more than 50% at concentrations of 0.02 mg/mL and higher, while exhibiting no toxicity within its inhibitory range (0-0.5 mg/mL).	(Coleman M I et al., 2022)
BM fruit extract	*In vitro*	BM extract-derived antiviral protein exhibits a dose-dependent inhibitory effect on the H1N1	(Pongthanapisith V et al., 2013)

		subtype. When the concentration is 1.401 mg/mL, this protein shows significant inhibitory effect on the H1N1 virus.	
Balsamin	*In vitro*, growth curves and single-round assay	Balsamin significantly inhibits HIV-1 replication in T cell lines and primary $CD4^+$ T cells, achieving over 99% inhibition in growth curve assays.	(Kaur I et al., 2013)
BM powder extract	*In vitro*, MTT assay and *in vivo*, HTLV-1 infected mice	The IC_{50} values for ethanol and aqueous extract were 38.33 μg/mL and 29.09 μg/mL, respectively. Additionally, both solutions demonstrated significant inhibitory effects on the HTLV-1 infected mice group.	(Ahmadi Ghezeldasht S et al., 2023)
BM leaf extract	*In vitro*	The BM leaf extract exhibited significant antiviral activity against human herpesvirus-3 (HHV-3), with the MIC values of the ethanolic and aqueous extract being 250 and 62.5 μg/mL, respectively.	(Angamuthu D et al., 2019)
Cardiovascular protection effect			
BM fruit extract	*In vivo*, high sucrose and high fat diets rat	The maximum reduction in total cholesterol was: 6.60% for the peel, 6.04% for the pulp, and 6.70% for the whole fruit; the maximum reduction in low-density lipoprotein was 5.55% for the peel, 6.81% for the pulp, and 6.60% for the whole fruit, and the high-density lipoprotein levels improved.	(Mahwish et al., 2017)
BM aqueous extract	*In vivo*, dahl salt-sensitive (DSS) rats	BM aqueous extract can significantly prevent the increase in blood pressure, blood urea nitrogen, creatinine, and the urine protein-to-creatinine ratio in DSS rats.	(Zeng L et al., 2022)

Note: ROS: reactive oxygen species; ORAC: oxygen radical absorbance capacity; DPPH: 2,2-diphenyl-1-picrylhydrazyl; ABTS: 2,2′-azino-bis (3-ethylbenzthiazoline-6-sulphonic acid); NO: nitric oxide; CISD2: CDGSH iron sulfur domain 2; GSH: glutathione; MIC: Minimum inhibitory concentration; MBC: Minimum bactericidal concentration; MFC: Minimum fungicidal concentration.

3.2 Anti-Inflammatory Activity

Cucurbitane-type triterpenoids isolated from the vines and leaves of BM showed anti-inflammatory activity *in vivo* and *in vitro*, it inhibited LPS-induced phagocytosis and the expression of iNOS, NO, TNF-α, and IL-6 in a macrophage model, and also ameliorated ear oedema in an animal model, the mechanism of which may be the inhibition of IKK/ NF-κB pathway (Chou M C et al., 2022). Triterpenes isolated from the fruit of BM were found to inhibit other TNF-α-induced proinflammatory signals, such as the activation of the inhibitor-κB kinase complex, phosphorylation of NF-κB inhibitors, and activation of c-Jun *N*-terminal kinase. Additionally, triterpenes exhibited significant inhibition of 12-*O*-tetradecanoylphorbol-13-acetate (TPA)-induced ear edema in mice (Cheng H-L et al., 2017).

Hsu et al. assessed the inhibitory impact of an ethyl acetate extract from BM (*M. charantia* Linn. var. *abbreviata Ser.*) fruit on *Propionibacterium acnes*-induced inflammation. The findings revealed the extract's efficacy in suppressing the levels of pro-inflammatory cytokines and matrix metalloproteinase (MMP)-9 in *P. acnes*-stimulated THP-1 cells *in vitro*. Moreover, intradermal injection in mice led to a reduction in *P. acnes*-induced granulomatous inflammation and ear swelling (Hsu C et al., 2012). The ethanol extract of BM demonstrated the most substantial reduction in LPS-induced prostaglandin E_2 (PGE_2) production, showing a 35% decrease at an ethanol extract concentration of 25 μg/mL. The butanol extract of BM placenta downregulated the expression of inflammatory genes induced by LPS, such as IL-1*α*, IL-1*β*, TNF-α, G1p2, and Ccl5. Furthermore, it reduced NF-κB DNA binding activity, as well as the phosphorylation levels of p38, JNK, ERK, and MAPKs (Dandawate P R et al., 2016). Rich in anti-inflammatory ingredient, BM can be an excellent option as a natural source of anti-inflammatory compounds.

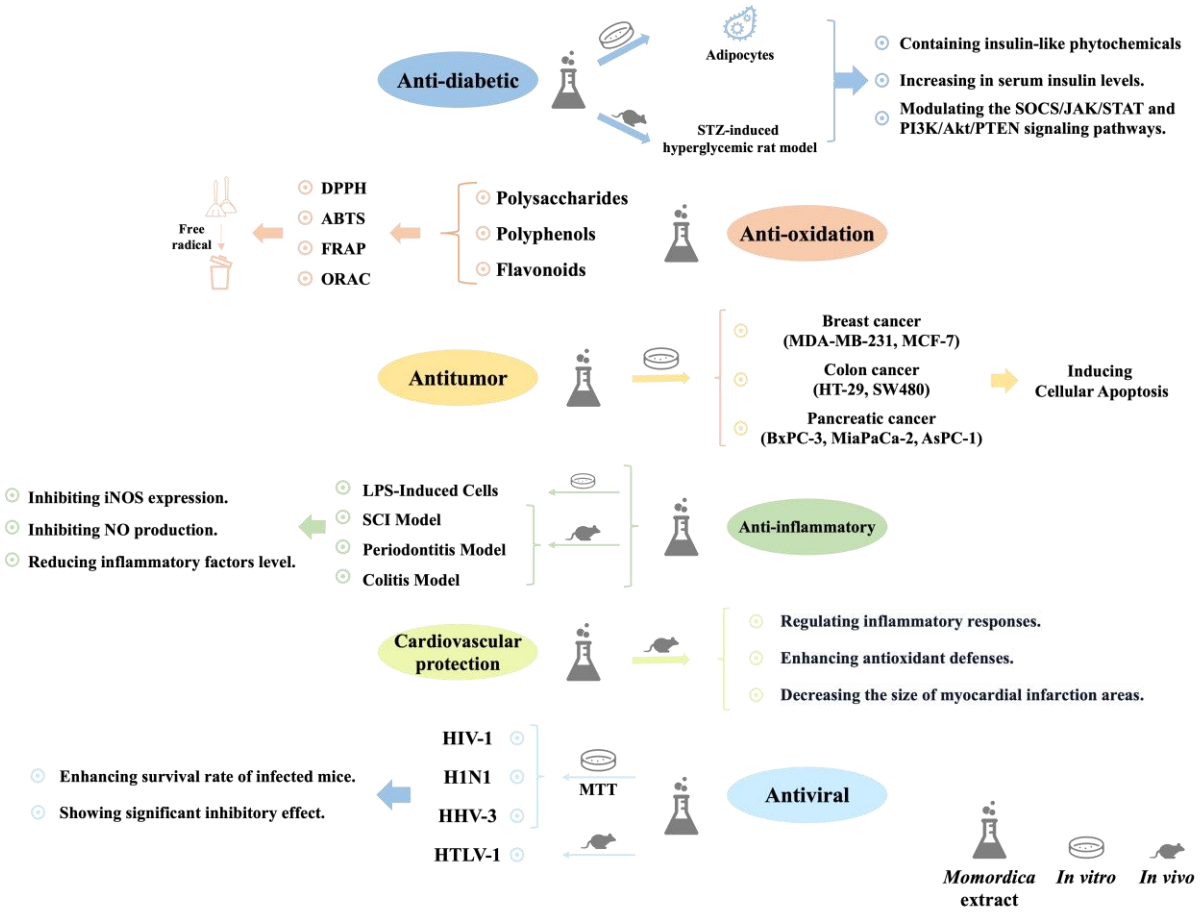

Figure 2. The potential health benefits of *Momordica*

The anti-diabetic, anti-inflammatory as well as antiviral activities of *Momordica* and its extracts have been validated by *in vivo* and *in vitro* studies. Among them, the LPS-induced RAW 264.7 inflammation model was mostly used in studies of anti-inflammatory activity. The cardiovascular protective effects of *Momordica* and its extracts are primarily utilized as a supplementary treatment for diabetes.

3.3 Antitumor Activity

The antitumor activity of BM extract was first reported in 1983, and several studies over the past decade have demonstrated its efficacy in inhibiting the proliferation of breast (MDA-MB-231, MCF-7), colon (HT-29, SW480) and pancreatic cancer cell lines (BxPC-3, MiaPaCa-2, AsPC-1) (Fang E F et al., 2019).

The mechanism of antitumor activity of BM extracts varies depending on the type of extract, cell type, and method of preparation of the extract. BM vesicles extract (BMVE) obtained from juice extraction was found to inhibit the proliferation of MCF-7 and 4T1 cells. In addition, it was observed that BMVE induced ROS generation played an important role in tumor cell apoptosis, and the cell scratch assay showed that BMVE inhibited the migration of tumor cells (Feng T et al., 2023). Momordicine-I, a secondary metabolite of BM, was procured via aqueous extraction and segregation from seedless whole fruits through the use of a common household juicer operated at ambient temperature (Sur S et al., 2021).

In addition, both apoptosis and autophagy have been shown to be pathways of BM mediated tumor cell death. Kuguacin J extracted from BM is able to inhibit the proliferation of prostate cancer cells through multiple mechanisms. It effectively blocks the expression of the active forms of MMP-9 and MMP-2 and disrupts cell cycle progression, ultimately leading to apoptosis (Pitchakarn P et al., 2012). The methanolic extract derived from BM effectively suppresses colon cancer stem cells by modulating energy homeostasis and autophagy (Kwatra D et al., 2013).

3.4 Antidiabetic Activity

As a traditional food and medicinal plant, BM is extensively utilized in the management of hyperglycemia by decreasing blood glucose (BG) levels in diabetic individuals, with several clinical studies showcasing its

beneficial effects on patients (Peter E et al., 2019). The raw BM can help regulate BG levels in diabetic patients by positively influencing their intestinal flora. Recent study has demonstrated that BM powder has the potential to promote the restoration of gut flora and the production of intestinal metabolites. This mechanism, in turn, can influence obesity-related inflammatory reactions, consequently mitigating insulin resistance induced by high-density lipoprotein cholesterol (Bai J, Zhu Y, Dong Y, 2018). Furthermore, the BM fruit juice (250 mg/2 ml water) significantly decreased fasting BG levels in normal rats (p<0.05 at 120 min) (Xu B et al., 2022).

BM contains a variety of phytochemicals with potential hypoglycemic effects, such as charantin, insulin-like peptides, vicine, polypeptide-p, sterol glycosides, triterpenoids, saponins, polysaccharides, alkaloids, water-soluble crude peptides, flavonoids, and phenols (Gao Y et al., 2023). Aqueous extract of BM was discovered to elevate tissue glycogen, serum insulin, and Glucagon-like peptide (GLP-1) levels in diabetic Wistar rats, consequently facilitating glucose-dependent insulin secretion from pancreatic β-cells, while concurrently reducing fasting BG and glycated hemoglobin (Bhat G A et al., 2018). In INS-1 cells and rat pancreatic islets, the methanol extract of green fruit BM and its ethyl acetate fraction were found to significantly increase ATP content, enhance insulin secretion in a dose-dependent manner, elevate serum insulin levels following glucose challenge, and substantially reduce BG levels (Shimada T et al., 2022). In STZ-induced diabetic rats, BM leaf nanoparticles (50 mg/kg) alleviate diabetic nephropathy by modulating the SOCS/JAK/STAT and PI3K/Akt/PTEN signaling pathways. Specifically, the levels of Akt, PI3K, TGF-β, JAK2, and STAT3 are downregulated, while the expressions of PTEN, SOCS3, and SOCS4 are upregulated (Elekofehinti O O et al., 2021).

Recent studies have also indicated that BM or its extracts may ameliorate diabetes-induced inflammation, ulcers, retinopathy, and reproductive dysfunction resulting from altered reproductive parameters. (Rosyid F N et al., 2022; Soliman G A et al., 2020; Liu J et al., 2023).

3.5 Antibacterial

Studies have ascertained that BM harbors a plethora of bioactive compounds, including flavonoids, phenolic substances, and cucurbitane-type triterpenoids, which exhibit significant antimicrobial therapeutic potential. The incorporation of these compounds within BM endows it with antimicrobial attributes and efficacy against bacterial pathogens (Villarreal La Torre V et al., 2020). Among them, various parts of BM have inhibitory effects on a wide range of bacteria.

For instance, the methanolic extract of the leaves exhibited a MIC value of 100 mg/mL against *P. aeruginosa* (Leelaprakash G & Rose C, 2011), while the stem extract showed a MIC value of 250 μg/mL against *E. faecalis* (Saengsai J et al., 2015). Furthermore, the chloroform extract derived from the fruits demonstrated a MIC value of 200 μg/mL against both *B. subtilis* and *E. coli* (Nguyen T et al., 2019). Lastly, the ethanol extract obtained from the seeds displayed a MIC value of 125 μg/mL against *C. krusei* (Lucena Filho J H et al., 2015). While BM has demonstrated the presence of potent antimicrobial metabolites, further investigation is required to elucidate its specific antimicrobial mechanism of action.

3.6 Antiviral Activity

The discovery of antiviral proteins in the seeds of *Momordica* plant has been reported and the antiviral activity in the seed extracts has been attributed to various small molecules and antiviral proteins. These molecules irreversibly inhibit viral translation, thereby inhibiting the spread of infection (Ramalhete C et al., 2016; Yao X et al., 2011). Several ribosome-inactivating proteins (RIPs) have been identified, including *Momordica* anti-HIV protein (MAP30) and α-, β-, and γ-momorcharin (MMC). These proteins have been shown to inhibit the replication of herpes simplex virus-1 (HSV-1), poliovirus type I in Hep2 cells, and human immunodeficiency virus type 1 (HIV-1) (Liu S et al., 2012). A single-round infectivity assay has also concluded that balsamin, a type of RIP, may exert its activity at the translation step of viral replication, specifically between the reverse transcription of the incoming viral genome and the release of newly produced viral particles (Kaur I et al., 2013). The research on the antiviral activity of BM protein extracts offers a novel approach and insightful ideas for the development of antiviral drugs. It also serves as a valuable reference for exploring the medicinal properties of other extracts and plants.

3.7 Anti-Parasitic Activity

BM contains various plant components, such as momordicin, momordin, momordicoside, karavilagenin, karaviloside, and kuguacin, all of which contribute to its restorative properties, including antibacterial, antiviral, and antiparasitic effects (Poolperm S & Jiraungkoorskul W, 2017). After treatment with concentrations of 25, 50, and 100 mg/mL of BM leaf extract, the mortality rates of the gastrointestinal nematodes *A. galli*, *Heterakis gallinae*, and *Capillaria spp*. in chickens were 22%, 70%, and 90%, respectively (Alam M et al., 2014). In addition, BM leaf extract also affects the embryonic development of *Fasciola hepatica* eggs in mammals (Pereira C A d J et al., 2016). BM seed extract induces paralysis in Indian adult earthworm (*Pheretima posthuma*)

within 3 minutes and results in death within 8 minutes (Ankalabasappa V et al., 2015). BM exhibits notable anti-parasitic activity and may serve as a potential anthelmintic, particularly for poultry and livestock.

3.8 Cardiovascular Protection Effect

BM extract has been found to help reduce cardiac damage and improve cardiac function by modulating inflammatory responses, enhancing antioxidant defenses, and reducing the size of myocardial infarcts, suggesting that BM may be beneficial to cardiovascular health (Czompa A et al., 2017). Ethanol extract of BM can significantly reduce LDL cholesterol in cholesterol-fed rats and alleviate cholesterol-induced myocardial degeneration and aortic damage (Innih S O, Eze I G & Omage K, 2021). BM (*M. balsamina*) leaf extract can significantly reduce BG concentration and improve erythropoietin secretion in STZ-induced diabetic mice, thereby significantly increasing erythropoiesis in diabetic animals. BM can also significantly improved hemoglobin concentration and moderately increased erythrocyte indices, particularly mean corpuscular volume, mean corpuscular hemoglobin concentration, and mean corpuscular hemoglobin (Ludidi A et al., 2019).

4. Uses-Economic Botany

4.1 Use in Foods

In addition to being consumed directly as a traditional vegetable or used for pickling, BM can also be made into uniquely flavored canned products, processed into tea, compound beverages, and wine (Yan J-K et al., 2019).

Various products made from BM, such as BM tea — an herbal tea made from dried BM slices, also known as Gohyah — are gradually becoming popular herbal remedies (Jia S et al., 2017).

In addition, emerging nano-encapsulation technologies can help to improve the stability of various bioactive compounds extracted from BM, ensuring that their activities remain essentially unchanged under the different acidic, alkaline, and thermal conditions that may be experienced during the processing of food or beverages (Gayathry K S & John J A, 2022).

4.2 Use in Cosmetics

The fruit of BM is its main edible part, while the seeds, leaves and other parts of BM are usually discarded. Some Chinese scholars have found that the seeds, leaves and other parts of BM show great potential for cosmetic applications and are worthy of in-depth study and further development. The oil components in BM seeds have potential medicinal value for preventing skin-related diseases, microbial infections, skin inflammation and skin aging. In addition, bitter melon seeds have the potential to be used in the production of natural antiseptic soaps (Zubair M F et al., 2018).

Study have shown that the water and ethanol extracts of BM fruits and seeds exhibit significant whitening and anti-wrinkle properties, making BM extract a highly potential and effective cosmetic ingredient (Kim H-W et al., 2015). BM leaves are also used to make a high-quality skin care and cosmetic cream, which is a crumbly white cream with the distinctive odor, pseudoplastic thixotropy and plastic thixotropy of BM, and is homogeneous and stable in texture (Hajard I & Pratami D, 2020). The antioxidant and 5α reductase inhibitory properties of BM extracts make them ideally suited for the formulation of functional microemulsions that have the potential to be further developed into cosmetic or pharmaceutical products aimed at controlling hair loss (Trakoolthong P et al., 2022).

4.3 Use in Traditional Medicines

Momordica plant is rich in a variety of active compounds such as polyphenols and flavonoids and is widely used in traditional medicine. In Asia, South Africa, Nigeria and Senegal, *Momordica* is commonly used for the treatment of fever, pain relief, gastrointestinal disorders, parasitic infections, diabetes, malaria and to promote wound healing. The pharmacological effects of these natural active ingredients are well-documented and validated in the traditional healing practices of these regions (Ramalhete C et al., 2022; Stuper-Szablewska K et al., 2023).

BM leaves were mixed with other medicinal substances to make a potion to relieve symptoms such as fever in children by the indigenous people of Kaluppini (Nurbaya & Chandra, 2020). Due to the excellent anti-diabetic activity of the fruits of the *Momordica* plant, it is widely used in the Ayurvedic system of medicine as an adjunct therapy for the treatment of diabetes (Pahlavani N et al., 2019).

4.4 Other Uses

A recent study reported that BM aqueous extract can be involved in the preparation of silver nanoparticles, giving the material enhanced antibacterial, antioxidant and in vitro antitumor activities, while the synthesis method is environmentally friendly (Palanisamy S et al., 2024). Hydroxyapatite nanoparticles were synthesized using *Momordica charantia* as a templating agent, with potential applications in bone and dental repair, as well as other orthopedic uses (Abraham A et al., 2023).

Activated carbon derivatives from BM fruit peels can also be used as supercapacitor electrode materials to improve charge storage performance (Aparna M L, Rao G R & Thomas T, 2022). BM leaf powder can absorb methyl orange dye and Cr (VI) metal ions from wastewater, making it a low-cost bio-adsorbent (Shahab M R et al., 2023). The innovative carbon dot fluorescence sensing system, utilizing fresh BM as the sole precursor, demonstrates efficacy in the detection of Pd^{2+} and Fe^{3+} present in tap and environmental water sources (Dong Y et al., 2021).

5. Safety

BM is generally not harmful to human health under normal conditions, but variations in intake and other related conditions may result in adverse reactions of varying degrees. Studies have shown that after 12 weeks of continuous consumption of BM powder capsules, some diabetic patients may experience adverse reactions such as anorexia, nausea, abdominal discomfort, diarrhea, constipation, foamy urine, and skin rashes, but not serious adverse reactions (Kim S K et al., 2020). Momordicines I isolated from BM leaves may have harmful effects on normal cells at concentrations higher than 10 μM (Chou M-C et al., 2022). Vicine-like compounds in BM seeds may induce heart and blood diseases (Khan M F et al., 2019). When the daily intake is controlled within 6 g, BM products have not been clearly proven to pose significant health risks. However, based on research results from animal experiments, bitter melon may have potential effects on the blood system and reproductive health. It is especially important to note that certain enzyme components in it may increase the risk of miscarriage. Therefore, it is recommended that pregnant or nursing women avoid using BM products. BM products are also not suitable for people with glucose-6-phosphate dehydrogenase (G6PD) deficiency to prevent possible health problems (Khan M F et al., 2019; Demmers A et al., 2022). It was found that mice developed nephrotoxicity after administration of 4 g/kg of BM for more than a week (Mardani S et al., 2014). In summary, BM is generally considered safe, but it is important to be aware of its potential toxicity and side effects to ensure its safe use in daily life.

6. Pesticide Residues and Food Safety

Trace pesticide residues in BM pose some potential threat to human health and create many uncertainties in food processing. Currently, commonly used pesticide includes abamectin, imidacloprid and a range of organophosphorus insecticides such as acephate, chlorpyrifos, diazinon, dimethoate, fenitrothion, malathion, and quinalphos. The widespread use of these insecticides and the difficulty in detecting their residues have raised great concern about the safety of BM (Table 4). Therefore, the study of effective methods for the detection of pesticide residues in BM has become an important issue to ensure food safety.

In recent years, research on the impact of pesticide residues in BM on consumers' daily diets has increased. For example, the QuEChERS (Quick, Easy, Cheap, Effective, Rugged, Safe) UPLC-tandem mass spectrometry method was used for the detection of abamectin residues, and it was found that the pesticide residues in BM did not exceed 0.019 mg/kg (Luo X et al., 2022).

In another study, the dissipation model and half-life detection method of imidacloprid were developed by LC-MS, and it was found that the residues of imidacloprid dissipated below the limit of quantification (LOQ) (0.025 mg/kg) within 2.51 and 3.13 days at the concentrations of 20 and 40 g a.i ha^{-1} (a.i ha^{-1}: active ingredient per hectare), respectively. After washing with water, the pesticide residues were reduced by 42.37% and the lowest residue was only 0.06 mg/kg, which was much lower than the MRLs (Mawtham M M et al., 2022).

In another study, after extraction of biomaterial samples from BM by the QuEChERS method, the concentrated extracts were analyzed for organophosphorus pesticides using a Shimadzu Gas Chromatograph-2010 equipped with a FTD detector, and the residues of chlorpyrifos, dichlorvos, and dimethoate were found to be 0.056, 0.097, and 0.032 mg/kg, respectively, which exceeded the European Union's maximum residue limit (0.010). Although subsequent studies have shown little short-term health risk, some chronic risk remains (Kaium A et al., 2021).

In recent years, significant progress has been made in monitoring plant pests and diseases and in methods for detecting pesticide residues. For example, by creating a database of common diseases affecting biodiverse leaves, the types of pests and diseases can be predicted more accurately, with a prediction accuracy of 82%, allowing for more targeted pesticide use (Fusic S J et al., 2024). A simple, efficient and environmentally friendly Surface Enhanced Raman Spectroscopy (SERS) assay has also been developed, which uses silver-decorated cotton swabs as wipes for rapid detection of single and mixed pesticide residues in real samples (Kong L et al., 2020).

Traditional chemical pesticides are gradually being replaced by emerging biopesticides (e.g., metarhizium, beauveria, trichoderma) and natural extracts (e.g., Azadirachta indica), mainly because of the latter's significant advantage of lower health risk (Paudel S et al., 2020).

To summarize, it is important to research and develop green biopesticides and natural insect-resistant extracts, and use pesticides scientifically and rationally, while continuously improving pesticide residue detection methods and increasing the sensitivity of pesticide residue detection. The results of the research to date show that

the pesticide residues in bitter melon are far lower than the maximum residue limit standards set by the countries in the world, and that the BM can be consumed without fear or further processed into other additional products.

Table 4. BM registered for pesticide use in China and corresponding MRLs in various countries

Pesticides	Maximum residue limits (MRLs, mg/kg)							
	China	Canada	United States	Australia	Korea	European Union	Japan	Codex Alimentarius Commission
Abamectin	0.050	0.010	0.005	0.020	0.050	0.010	0.010	0.01
Imidacloprid	1.000	0.500	0.500	0.200	0.200	/	1.000	0.20
Acephate	0.020	/	/	0.020	/	0.01	0.100	/
Chlorpyrifos	0.020	0.050	0.050	/	0.500	0.01	1.000	/
Diazinon	0.050	0.250	0.750	/	0.030	0.01	0.100	/
Dimethoate	/	/	1.000	/	/	0.01	1.000	/
Fenitrothion	0.500	/	/	/	/	0.01	0.500	/
Malathion	0.100	/	/	/	0.050	0.02	0.200	/
Quinalphos	/	/	/	/	/	0.01	0.050	/

7. Conclusions and Perspectives

Momordica plants are widely appreciated by consumers globally for their unique flavor and nutritional benefits. BM is notably rich in various chemical and nutritional components, including polyphenols, polysaccharides, minerals, and vitamins. BM is consumed directly as a traditional vegetable or used for pickling, and has also been made into uniquely flavored canned products, tea, compound beverages, wine and so on. The pharmacological activities of these phytochemicals include antioxidant, anti-inflammatory, antitumor, antidiabetic, anti-obesity, antifungal, neuroprotective, and blood cholesterol-reducing effects.

However, there are still many issues that need to be further studied. Firstly, the research on active ingredients and functional activities of BM is not thorough enough. Most studies are focused on cell experiments, and there is little research on the absorption and mechanism of active ingredients in vivo. Secondly, research on the antitumor activity remains limited to in vitro studies, with only a few investigations delving into their mechanisms of action. The application in health food, medicine, and chemical industry focused on the functional activity of BM further development. Therefore, it should strengthen the depth and breadth of following 4 aspects: (1) Future antitumor research should concentrate on identifying the active compounds within the chemical constituents of Momordica plants and elucidating their mechanisms of action. (2) The second is to carry out targeted research and development of health food, medicine, beauty, and other products. (3) The third is to continuously explore techniques suitable for extracting active ingredients from BM, in order to obtain high-purity and high content active ingredients. With the deepening of research, BM is expected to develop more medicinal and nutritional values, in order to better serve health and clinical care. (4) While significant progress has also been made in the study of its antidiabetic activity, including the identification of the active ingredient, an in-depth study of the mechanism of action and potential synergies with other treatments. However, a number of studies have also emphasized the potential for adverse effects when used as an adjunctive therapy for diabetes. Therefore, there is a need for further in vivo studies and/or even clinical trials to confirm its efficacy and safety.

References

Abraham A, Sharan Kumar M and Anju Krishna D et al., (2023). Development of nano-hydroxyapatite membrane using *Momordica charantia* and study of its biodegradability for medical application. *Biomass Conversion and Biorefinery*.

Ahmadi Ghezeldasht S, Bidkhori H R and Miri R et al., (2023). *Momordica charantia* phytoconstituents can inhibit human T-lymphotropic virus type-1 (HTLV-1) infectivity in vitro and in vivo. *Journal of NeuroVirology*.

AkyÜz E, TÜrkoĞlu S and SÖzgen BaŞkan K et al., (2020). Comparison of antioxidant capacities and antioxidant components of commercial bitter melon (*Momordica charantia* L.) products. *Turkish journal of chemistry*, *44*(6), 1663-1673.

Alam M, Alam K and Begum N, et al., (2014). Comparative efficacy of different herbal and modern

anthelmintics against gastrointestinal nematodiasis in fowl. *International Journal of Biological Research*, *2*(2), 145.

Angamuthu D, Purushothaman I and Kothandan S et al., (2019). Antiviral study on Punica granatum L., *Momordica charantia* L., Andrographis paniculata Nees, and Melia azedarach L., to Human Herpes Virus-3. *European Journal of Integrative Medicine*, *28*(4), 98-108.

Ankalabasappa V, Rampurawala J and Paarakh P et al., (2015). Evaluation of anthelmintic activity of *momordica charantia* L. Seeds. *Indian Journal of Natural Products and Resources*, *6*(2), 153-155.

Aparna M L, Rao G R and Thomas T, (2022). *Momordica Charantia* pericarp derived activated carbon with dual redox additive electrolyte for high energy density supercapacitor devices. *Journal of Energy Storage*, *48*, 104048.

Aziz M, Karboune S, (2018). Natural antimicrobial/antioxidant agents in meat and poultry products as well as fruits and vegetables: A review. *Critical reviews in food science and nutrition*, *58*(3), 486-511.

Bai J, Zhu Y and Dong Y, (2018). Modulation of gut microbiota and gut-generated metabolites by bitter melon results in improvement in the metabolic status in high fat diet-induced obese rats. *Journal of Functional Foods*, *41*, 127-134.

Bhat G A, Khan H A and Alhomida A S et al., (2018). GLP-I secretion in healthy and diabetic Wistar rats in response to aqueous extract of *Momordica charantia*. *BMC Complementary and Alternative Medicine*, *18*(1), 162.

Bialek A, Jelińska M and Tokarz A et al., (2016). Influence of pomegranate seed oil and bitter melon aqueous extract on polyunsaturated fatty acids and their lipoxygenase metabolites concentration in serum of rats. *Prostaglandins & Other Lipid Mediators*, *126*(2), 29-37.

Chang C I, Cheng S Y and Nurlatifah A O et al., (2021). Bitter Melon Extract Yields Multiple Effects on Intestinal Epithelial Cells and Likely Contributes to Anti-diabetic Functions. *International journal of medical sciences*, *18*(8), 1848-1856.

Chao C-Y, Sung P-J and Wang W-H et al., (2014). Anti-Inflammatory Effect of *Momordica Charantia* in Sepsis Mice. *Molecules*, *19*(8), 12777-12788.

Chen F, Huang G, (2019). Extraction, derivatization and antioxidant activity of bitter gourd polysaccharide. *International Journal of Biological Macromolecules*, *141*(8), 14-20.

Chen G-C, Su H-M and Lin Y-S et al., (2016). A conjugated fatty acid present at high levels in bitter melon seed favorably affects lipid metabolism in hepatocytes by increasing NAD (+) / NADH ratio and activating PPARα, AMPK and SIRT1 signaling pathway. *The Journal of nutritional biochemistry*, *33*, 28-35.

Cheng H-L, Yang M-H and Anggriani R et al., (2017). Comparison of Anti-Inflammatory Activities of Structurally Similar Triterpenoids Isolated from Bitter Melon. *Natural Product Communications*, *12*(12), 1934578X1701201208.

Chou M C, Lee Y J and Wang Y T et al., (2022). Cytotoxic and Anti-Inflammatory Triterpenoids in the Vines and Leaves of *Momordica charantia*. *International Journal of Molecular Sciences*, *23*(3), 1071.

Chou M-C, Lee Y-J and Wang Y-T et al., (2022). Cytotoxic and Anti-Inflammatory Triterpenoids in the Vines and Leaves of *Momordica charantia*. *International Journal of Molecular Sciences*, *23*(3), 1071.

Çiçek S S. *Momordica charantia* L, (2022). Diabetes-Related Bioactivities, Quality Control, and Safety Considerations. *Frontiers in Pharmacology*, *13*(17), 904643.

Coleman M I, Khan M and Gbodossou E et al., (2022). Identification of a Novel Anti-HIV-1 Protein from Momordica balsamina Leaf Extract. *International Journal of Environmental Research and Public Health*, *19*(22), 15227.

Cortez-Navarrete M, Méndez-Del Villar M and Ramos-González E J et al., (2021). *Momordica Charantia*: A Review of Its Effects on Metabolic Diseases and Mechanisms of Action. *Journal of medicinal food*, *24*(10), 1017-1027.

Cuong D M, Jeon J and Morgan A M A et al., (2017). Accumulation of Charantin and Expression of Triterpenoid Biosynthesis Genes in Bitter Melon (*Momordica charantia*). *Journal of Agricultural and Food Chemistry*, *65*(33), 7240-7249.

Cuong D M, Kwon S-J and Jeon J et al., (2018). Identification and Characterization of Phenylpropanoid Biosynthetic Genes and Their Accumulation in Bitter Melon (*Momordica charantia*). *Molecules*, *23*(2), 469.

Czompa A, Gyongyosi A and Szoke K et al., (2017). Effects of *Momordica charantia* (Bitter Melon) on Ischemic Diabetic Myocardium. *Molecules*, *22*(3), 488.

Dandawate P R, Subramaniam D, Padhye S B et al., (2016). Bitter melon: a panacea for inflammation and cancer. *Chinese Journal of Natural Medicines*, *14*(2), 81-100.

Demmers A, Mes J J and Elbers R G et al., (2022). Possible harms of *Momordica charantia* L. in humans; a systematic review. *medRxiv*.

Deng Y, Zhang Y and Liu G, et al., (2023). Saponins from *Momordica charantia* exert hypoglycemic effect in diabetic mice by multiple pathways. *Food Science & Nutrition*, *11*(12), 7626-7637.

Dong Y, Zhang Y and Zhi S et al., (2021). Green Synthesized Fluorescent Carbon Dots from *Momordica charantia* for Selective and Sensitive Detection of Pd2+ and Fe3+. *Chemistry Select*, *6*(1), 123-130.

Elekofehinti O O, Oyedokun V O and Iwaloye O et al., (2021). *Momordica charantia* silver nanoparticles modulate SOCS/JAK/STAT and P13K/Akt/PTEN signalling pathways in the kidney of streptozotocin-induced diabetic rats. *Journal of Diabetes & Metabolic Disorders*, *20*(1), 245-260.

Fang E F, Froetscher L and Scheibye-Knudsen M et al., (2019). Emerging Antitumor Activities of the Bitter Melon (*Momordica charantia*). *Current Protein and Peptide Science*, *20*(3), 296-301.

Feng T, Wan Y and Dai B et al., (2023). Anticancer Activity of Bitter Melon-Derived Vesicles Extract against Breast Cancer. *Cells*, *12*(6), 824.

Ferreira Almeida N, dos Santos Niculau E and Cordeiro Toledo Lima P et al., (2024). Determination of the volatile chemical profile of *Momordica charantia* (bitter melon) leaf and fruit by GC-MS. *Natural Product Research*, 1-8.

Fusic S J, T S and Giri J et al., (2024). *Momordica charantia* leaf disease detection and treatment using agricultural mobile robot. *AIP Advances*, *14*(4).

Gao Y, Li X and Huang Y et al., (2023). Bitter Melon and Diabetes Mellitus. *Food Reviews International*, *39*(1), 618-638.

Gayathry K S, John J A, (2022). A comprehensive review on bitter gourd (*Momordica charantia* L.) as a gold mine of functional bioactive components for therapeutic foods. *Food Production, Processing and Nutrition*, *4*(1), 10.

Hajard I, Pratami D, (2020). SKINCARE CREAM PREPARATION AND EVALUATION OF PARE (*MOMORDICA CHARANTIA*) LEAVES USING THREE DIFFERENCE BASE. *International Journal of Applied Pharmaceutics*, *12*(6), 162-166.

Hani N M, Torkamani A E and Zainul Abidin S et al., (2017). The effects of ultrasound assisted extraction on antioxidative activity of polyphenolics obtained from *Momordica charantia* fruit using response surface approach. *Food Bioscience*, *17*, 7-16.

Hercos G F D, Belisário C M and Alves A E D et al., (2021). Physicochemical characterization, bioactive compounds and antioxidant capacity of bitter melon. *Horticultura Brasileira*, *39*(4), 397-403.

Horax R, Hettiarachchy N and Kannan A et al., (2010). Proximate composition and amino acid and mineral contents of Mormordica charantia L. pericarp and seeds at different maturity stages. *Food Chemistry*, *122*(4), 1111-1115.

Hsu C, Tsai T-H and Li Y-Y et al., (2012). Wild bitter melon (*Momordica charantia* Linn. var. abbreviata Ser.) extract and its bioactive components suppress Propionibacterium acnes-induced inflammation. *Food Chemistry*, *135*(3), 976-984.

Huang H, Chen F and Long R et al., (2020). The antioxidant activities in vivo of bitter gourd polysaccharide. *International Journal of Biological Macromolecules*, *145*(2020), 141-144.

Innih S O, Eze I G and Omage K, (2021). Cardiovascular benefits of *Momordica charantia* in cholesterol-fed Wistar rats. *Clinical Phytoscience*, *7*(1), 65.

Jia S, Shen M and Zhang F et al., (2017). Recent Advances in *Momordica charantia*: Functional Components and Biological Activities. *International Journal of Molecular Sciences*, *18*(12), 2555.

Kaium A, Khan M and Begum N et al., (2021). Residue level and health risk assessment of organophosphorus pesticides in country bean and bitter gourd collected from Cumilla, Bangladesh. *Food Research*, 5, 238-246.

Kandangath Raghavan A, Garlapati Phani K and Nallamuthu I, (2015). Nutritional, Pharmacological and Medicinal Properties of *Momordica Charantia*. *International Journal of Nutrition and Food Sciences*, *4*(1),

75-83.

Karaman K, Dalda-Şekerci A and Yetişir H et al., (2018). Molecular, morphological and biochemical characterization of some Turkish bitter melon (*Momordica charantia* L.) genotypes. *Industrial Crops and Products*, *123*, 93-99.

Kaur I, Puri M and Ahmed Z et al., (2013). Inhibition of HIV-1 Replication by Balsamin, a Ribosome Inactivating Protein of Momordica balsamina. *PloS one*, *8*(9), e73780.

Khan M F, Abutaha N and Nasr F A et al., (2019). Bitter gourd (*Momordica charantia*) possesses developmental toxicity as revealed by screening the seeds and fruit extracts in zebrafish embryos. *BMC Complementary and Alternative Medicine*, *19*(1), 184.

Kim H-W, Shin H and Hwang D et al., (2015). Functional Cosmetic Characteristics of *Momordica charantia* Fruit Extract. *Korean Chemical Engineering Research*, *53*(3), 289-294.

Kim S K, Jung J and Jung J H et al., (2020). Hypoglycemic efficacy and safety of *Momordica charantia* (bitter melon) in patients with type 2 diabetes mellitus. *Complementary Therapies in Medicine*, *52*(3), 102524.

Kong L, Huang M and Chen J et al., (2020). Fabrication of sensitive silver-decorated cotton swabs for SERS quantitative detection of mixed pesticide residues in bitter gourds. *New Journal of Chemistry*, *44*(29), 12779-12784.

Kung W-M, Lin C-C and Kuo C-Y et al., (2020). Wild Bitter Melon Exerts Anti-Inflammatory Effects by Upregulating Injury-Attenuated CISD2 Expression following Spinal Cord Injury. *Behavioural Neurology*, *2020*(30), 1080521.

Kwatra D, Subramaniam D and Ramamoorthy P et al., (2013). Methanolic Extracts of Bitter Melon Inhibit Colon Cancer Stem Cells by Affecting Energy Homeostasis and Autophagy. *Evidence-Based Complementary and Alternative Medicine*, *2013*, 702869.

Laczko-Zold E, Toth L and Lenard F et al., (2023). Polyphenolic profile and antioxidant properties of *Momordica charantia* L. 'Enaja' cultivar grown in Romania. *Natural Product Research*, *38*(6), 1060-1066.

Lee J J, Yoon K Y, (2021). Optimization of ultrasound-assisted extraction of phenolic compounds from bitter melon (*Momordica charantia*) using response surface methodology. *CyTA — Journal of Food*, *19*(1), 721-728.

Leelaprakash G, Rose C, (2011). In vitro antimicrobial and antioxidant activity of *Momordica charantia* leaves. *Pharmacophore*, *2*(4), 244-252.

Li Z, Xia A and Li S et al., (2020). The Pharmacological Properties and Therapeutic Use of Bitter Melon (*Momordica charantia* L.). *Current Pharmacology Reports*, *6*(3), 103-109.

Liu J, Liu Y and Sun J, et al., (2023). Protective effects and mechanisms of *Momordica charantia* polysaccharide on early-stage diabetic retinopathy in type 1 diabetes. *Biomedicine & Pharmacotherapy*, *168*, 115726.

Liu S, Le C and Meng Y et al., (2012). Preparation of an antitumor and antivirus agent: Chemical modification of α-MMC and MAP30 from *Momordica Charantia* L. with covalent conjugation of polyethyelene glycol. *International journal of nanomedicine*, *7*, 3133-3142.

Liu Y, Sun Y and Huang G, (2018). Preparation and antioxidant activities of important traditional plant polysaccharides. *International Journal of Biological Macromolecules*, *111*, 780-786.

Liu Y-J, Lai Y-J and Wang R et al., (2020). The Effect of Thermal Processing on the Saponin Profiles of *Momordica charantia* L. *Journal of Food Quality*, *2020*(15), 1-7.

Lopes A P, Petenuci M E and Galuch M B et al., (2018). Evaluation of effect of different solvent mixtures on the phenolic compound extraction and antioxidant capacity of bitter melon (*Momordica charantia*). *Chemical Papers*, *72*(11), 2945-2953.

Lopes A, Galuch M and Petenuci M et al., (2020). Quantification of phenolic compounds in ripe and unripe bitter melons (*Momordica charantia*) and evaluation of the distribution of phenolic compounds in different parts of the fruit by UPLC-MS/MS. *Chemical Papers*, *74*(8), 2613-2625.

Lucena Filho J H, Lima Rde F and Medeiros A C et al., (2015). Antimicrobial Potential of *Momordica charantia* L. against Multiresistant Standard Species and Clinical Isolates. *The journal of contemporary dental practice*, *16*(11), 854-858.

Ludidi A, Baloyi M C and Khathi A et al., (2019). The effects of Momordica balsamina methanolic extract on haematological function in streptozotocin-induced diabetic rats: Effects on selected markers. *Biomedicine & Pharmacotherapy*, *116*, 108925.

Luo X, Zhang C and Luo Y et al., (2024). Residue analysis and dietary risk assessment of abamectin in fresh corn, bitter melon, and Fritillaria. *Biomedical Chromatography*, *38*(2), e5779.

Mahmoud M F, El Ashry F E Z Z and El Maraghy N N et al., (2017). Studies on the antidiabetic activities of *Momordica charantia* fruit juice in streptozotocin-induced diabetic rats. *Pharmaceutical Biology*, *55*(1), 758-765.

Mahwish M, Saeed F and Nisa M U et al., (2018). Minerals and phytochemical analysis of bitter melon fruits and its components in some indigenous and exotic cultivars. *Bioscience Journal*, *34*(6), 1622-1631.

Mahwish, Saeed F and Arshad M S et al., (2017). Hypoglycemic and hypolipidemic effects of different parts and formulations of bitter gourd (*Momordica Charantia*). *Lipids in Health and Disease*, *16*(1), 211.

Mahwish, Saeed F and Nosheen F et al., (2023). Bio-evaluation of alkaloids and saponins from bitter melon: Probing more desirable compound in treating hyperglycemia and hyperlipidemia. *Cogent Food & Agriculture*, *9*(1).

Mahwish, Saeed F and Sultan M T et al., (2021). Bitter Melon (*Momordica charantia* L.) Fruit Bioactives Charantin and Vicine Potential for Diabetes Prophylaxis and Treatment. *Plants*, *10*(4), 730.

Mardani S, Nasri H and Hajian S et al., (2014). Impact of *Momordica charantia* extract on kidney function and structure in mice. *Journal of nephropathology*, *3*(1), 35-40.

Mawtham M M, Kaithamalai. B and Gopinathan. S et al., (2022). Dissipation kinetics, decontamination and dietary risk assessment of imidacloprid residue in bitter gourd and soil. *Journal of Applied and Natural Science*, *14*(4), 1507-1517.

Mei X, Yang W and Huang G et al., (2020). The antioxidant activities of balsam pear polysaccharide. *International Journal of Biological Macromolecules*, *142*, 232-236.

Mishra S, Ankit and Sharma R et al., (2021). NMR-based metabolomic profiling of the differential concentration of phytomedicinal compounds in pericarp, skin and seeds of *Momordica charantia* (bitter melon). *Natural Product Research*, *36*(1), 390-395.

Muribeca A d J B, Gomes P W P and Paes S S et al., (2022). Antibacterial Activity from *Momordica charantia* L. Leaves and Flavones Enriched Phase. *Pharmaceutics*, *14*(9), 1796.

Namsa N D, Mandal M and Tangjang S et al., (2011). Ethnobotany of the Monpa ethnic group at Arunachal Pradesh, India. *Journal of Ethnobiology and Ethnomedicine*, *7*(1), 31.

Naqvi S A R, Ali S and Sherazi T A et al., (2020). Antioxidant, Antibacterial, and Anticancer Activities of Bitter Gourd Fruit Extracts at Three Different Cultivation Stages. *Journal of Chemistry*, *2020*, 7394751.

Naz R, Anjum F M and Butt M S et al., (2016). Dietary supplementation of bitter gourd reduces the risk of hypercholesterolemia in cholesterol fed sprague dawley rats. *Pakistan journal of pharmaceutical sciences*, *29*(5), 1565-1570.

Nerurkar P, Ray R B, (2010). Bitter melon: antagonist to cancer. *Pharmaceutical research*, *27*(6), 1049-1053.

Nguyen T, Vo D and Thanh L et al., (2019). Investigation of antimicrobial activity and chemical constituents of *Momordica charantia* L. var. abbreviata Ser. *Vietnam Journal of Science and Technology*, *57*(2), 155.

Nguyen T-V-L, Nguyen Q-D and Nguyen P-B-D et al., (2020). Effects of drying conditions in low-temperature microwave-assisted drying on bioactive compounds and antioxidant activity of dehydrated bitter melon (*Momordica charantia* L.). *Food Science & Nutrition*, *8*(7), 3826-3834.

Nurbaya, Chandra, (2020). Pembollo': A concept of plant-based traditional medicine among kaluppini indigenous people. *IOP Conference Series: Earth and Environmental Science*, *486*(1), 012016.

Oyelere S F, Ajayi O H and Ayoade T E et al., (2022). A detailed review on the phytochemical profiles and anti-diabetic mechanisms of *Momordica charantia*. *Heliyon*, *8*(4), e09253.

Pahlavani N, Roudi F and Zakerian M et al., (2019). Possible molecular mechanisms of glucose-lowering activities of *Momordica charantia* (karela) in diabetes. *Journal of Cellular Biochemistry*, *120*(7), 10921-10929.

Palanisamy S, David R and Madav E et al., (2024). Green fabrication of silver nanoparticles using leaf extract of tropical vine *Momordica charantia*: spectral characterization and in vitro cytotoxicity evaluation on human breast cancer cells. *Materials Technology*, *39*(1), 2304428.

Pandit S, Kanjilal S and Awasthi A et al., (2016). Evaluationof herb-drug interaction of a polyherbal Ayurvedic formulation through high throughput cytochrome P450 enzyme inhibition assay. *Journal of Ethnopharmacology*, *197*, 165-172.

Park S H, Yi Y-S and Kim M-Y et al., (2019). Antioxidative and Antimelanogenesis Effect of *Momordica charantia* Methanol Extract. *Evidence-Based Complementary and Alternative Medicine*, *2019*, 5091534.

Pattarachotanant N, Prasansuklab A and Tencomnao T, (2021). *Momordica charantia* L. Extract Protects Hippocampal Neuronal Cells against PAHs-Induced Neurotoxicity: Possible Active Constituents Include Stigmasterol and Vitamin E. *Nutrients*, *13*(7), 2368.

Paudel S, Sah L P and Devkota M et al., (2020). Conservation Agriculture and Integrated Pest Management Practices Improve Yield and Income while Reducing Labor, Pests, Diseases and Chemical Pesticide Use in Smallholder Vegetable Farms in Nepal. *Sustainability*, *12*(16), 6418.

Pereira C A d J, Oliveira L L S and Coaglio A L et al., (2016). Anti-helminthic activity of *Momordica charantia* L. against Fasciola hepatica eggs after twelve days of incubation in vitro. *Veterinary parasitology*, *228*, 160-166.

Perez J L, Shivanagoudra S R and Perera W H et al., (2021). Bitter melon extracts and cucurbitane-type triterpenoid glycosides antagonize lipopolysaccharide-induced inflammation via suppression of NLRP3 inflammasome. *Journal of Functional Foods*, *86*, 104720.

Peter E L, Kasali F M and Deyno S et al., (2019). *Momordica charantia* L. lowers elevated glycaemia in type 2 diabetes mellitus patients: Systematic review and meta-analysis. *Journal of Ethnopharmacology*, *231*, 311-324.

Pitchakarn P, Suzuki S and Ogawa K et al., (2012). Kuguacin J, a triterpeniod from *Momordica charantia* leaf, modulates the progression of androgen-independent human prostate cancer cell line, PC3. *Food and Chemical Toxicology*, *50*(3), 840-847.

Pongthanapisith V, Ikuta K and Puthavathana P et al., (2013). Antiviral Protein of *Momordica charantia* L. Inhibits Different Subtypes of Influenza A. *Evidence-Based Complementary and Alternative Medicine*, *2013*, 729081.

Poolperm S, Jiraungkoorskul W, (2017). An Update Review on the Anthelmintic Activity of Bitter Gourd, *Momordica charantia*. *Pharmacognosy Reviews*, *11*(21), 31-34.

Popovich D G, Li L and Zhang W, (2010). Bitter melon (*Momordica charantia*) triterpenoid extract reduces preadipocyte viability, lipid accumulation and adiponectin expression in 3T3-L1 cells. *Food and chemical toxicology*, *48*(6), 1619-1626.

Puri R, Sud R and Khaliq A et al., (2011). Gastrointestinal toxicity due to bitter bottle gourd (Lagenaria siceraria)—a report of 15 cases. *Indian journal of gastroenterology*, *30*(5), 233-236.

Rahmi M, Sari T M and Despanita, (2021). Antibacterial activity of ethanol extract, n-hexan, ethyl acetate and butanol fraction of *Momordica charantia* L. seed against Staphylococcus epidermidis. *Journal of Physics: Conference Series*, *1918*(5), 052013.

Ramalhete C, Gonçalves B M F and Barbosa F, et al., (2022). Momordica balsamina: phytochemistry and pharmacological potential of a gifted species. *Phytochemistry Reviews*, *21*(2), 617-646.

Ramalhete C, Mulhovo S and Molnar J et al., (2016). Triterpenoids from Momordica balsamina: Reversal of ABCB1-mediated multidrug resistance. *Bioorganic & medicinal chemistry*, *24*(21), 5061-5067.

Rosyid F N, Muhtadi M and Hudiyawati D et al., (2022). Improving Diabetic Foot Ulcer Healing with Adjuvant Bitter Melon Leaf Extract (*Momordica charantia* L.). *Open Access Macedonian Journal of Medical Sciences*, *10*(T8), 122-126.

Sabourian R, Karimpour-Razkenari E and Saeedi M et al., (2016). Medicinal Plants Used in Iranian Traditional Medicine (ITM) as Contraceptive Agents. *Current Pharmaceutical Biotechnology*, *17*(11), 974-985.

Saeed F, Pasha I, Anjum F M et al., (2011). Arabinoxylans and arabinogalactans: a comprehensive treatise. *Critical reviews in food science and nutrition*, *51*(5), 467-476.

Saengsai J, Kongtunjanphuk S and Yoswatthana N et al., (2015). Antibacterial and Antiproliferative Activities of Plumericin, an Iridoid Isolated from *Momordica charantia* Vine. *Evidence-Based Complementary and Alternative Medicine*, *2015*, 823178.

Saini R K, Keum Y S, (2017). Characterization of nutritionally important phytoconstituents in bitter melon (*Momordica charantia* L.) fruits by HPLC-DAD and GC-MS. *Journal of Food Measurement and Characterization*, *11*(1), 119-125.

Saini R K, Keum Y S, (2017). Characterization of nutritionally important phytoconstituents in bitter melon (*Momordica charantia* L.) fruits by HPLC-DAD and GC-MS. *Journal of Food Measurement and*

Characterization, *11*(1), 119-125.

Sajadimajd S, Mohammadi B and Bahrami G et al., (2022). Modulation of Notch signaling and angiogenesis via an isolated polysaccharide from *Momordica charantia* in diabetic rats. *Journal of Food Biochemistry*, *46*(2), e14033.

Sarkar N, Mitra S and Barik A, (2017). *Momordica charantia* L. (Cucurbitaceae) floral volatiles causing attraction of Epilachna dodecastigma (Coleoptera: Coccinellidae). *International Journal of Pest Management*, *63*(2), 138-145.

Saxena M, Prabhu S V and Mohseen M et al., (2022). Antidiabetic Effect of Tamarindus indica and *Momordica charantia* and Downregulation of TET-1 Gene Expression by Saroglitazar in Glucose Feed Adipocytes and Their Involvement in the Type 2 Diabetes-Associated Inflammation In Vitro. *BioMed Research International*, *2022*, 9565136.

Shahab M R, Yaseen H M and Manzoor Q et al., (2023). Adsorption of methyl orange and chromium (VI) using *Momordica charantia* L. leaves: a dual functional material for environmental remediation. *Journal of the Iranian Chemical Society*, *20*(3), 577-590.

Shimada T, Kato F and Dwijayanti D R et al., (2022). Bitter melon fruit extract enhances intracellular ATP production and insulin secretion from rat pancreatic β-cells. *British Journal of Nutrition*, *127*(3), 377-383.

Singla D, Sangha M K and Singh M et al., (2023). Variation of Mineral Composition in Different Fruit Parts of Bitter Gourd (*Momordica charantia* L.). *Biological trace element research*, *201*(10), 4961-4971.

Soliman G A, Abdel-Rahman R F and Ogaly H A et al., (2020). *Momordica charantia* Extract Protects against Diabetes-Related Spermatogenic Dysfunction in Male Rats: Molecular and Biochemical Study. *Molecules*, *25*(22), 5255.

Stuper-Szablewska K, Szablewski T and Przybylska-Balcerek A et al., (2023). Antimicrobial Activities Evaluation and Phytochemical Screening of Some Selected Plant Materials Used in Traditional Medicine. *Molecules*, *28*(1), 244.

Sun L, Xiaopo Z and Dong L et al., (2021). The triterpenoids of the bitter gourd (*Momordica Charantia*) and their pharmacological activities: A review. *Journal of Food Composition and Analysis*, *96*(8), 103726.

Sur S, Steele R and Isbell T S et al., (2021). Momordicine-I, a Bitter Melon Bioactive Metabolite, Displays Anti-Tumor Activity in Head and Neck Cancer Involving c-Met and Downstream Signaling. *Cancers*, *13*(6), 1432.

Svobodova B, Barros L and Calhelha R C et al., (2017). Bioactive properties and phenolic profile of *Momordica charantia* L. medicinal plant growing wild in Trinidad and Tobago. *Industrial Crops and Products*, *95*, 365-373.

Tambor M, Pavlova M and Golinowska S et al., (2016). Financial incentives for a healthy life style and disease prevention among older people: A systematic literature review. *BMC Health Services Research*, *16*(5).

Tan S P, Vuong Q V and Stathopoulos C E et al., (2014). Optimized Aqueous Extraction of Saponins from Bitter Melon for Production of a Saponin-Enriched Bitter Melon Powder. *Journal of Food Science*, *79*(7), E1372-E1381.

Trakoolthong P, Ditthawuttikul N and Sivamaruthi B S et al., (2022). Antioxidant and 5α-Reductase Inhibitory Activity of *Momordica charantia* Extract, and Development and Characterization of Microemulsion. *Applied Sciences*, *12*(9), 4410.

Tsai T-H, Chang C-I and Hung Y-L et al., (2021). Anti-Inflammatory Effect of Charantadiol A, Isolated from Wild Bitter Melon Leaf, on Heat-Inactivated Porphyromonas gingivalis-Stimulated THP-1 Monocytes and a Periodontitis Mouse Model. *Molecules*, *26*(18), 5651.

Tuan P A, Kim J K and Park N I et al., (2011). Carotenoid content and expression of phytoene synthase and phytoene desaturase genes in bitter melon (*Momordica charantia*). *Food chemistry*, *126*(4), 1686-1692.

Ünal N G, Kozak A and Karakaya S et al., (2019). Anti-Inflammatory Effect of Crude *Momordica charantia* L. Extract on 2,4,6-Trinitrobenzene Sulfonic Acid-Induced Colitis Model in Rat and the Bioaccessibility of its Carotenoid Content. *Journal of medicinal food*, *23*(6), 641-648.

Vijayalakshmi B, Kumar G S and Salimath P V, (2009). Effect of bitter gourd and spent turmeric on glycoconjugate metabolism in streptozotocin-induced diabetic rats. *Journal of diabetes and its complications*, *23*(1), 71-76.

Villarreal La Torre V, Sagástegui Guarniz W and Silva-Correa C, et al., (2020). Antimicrobial Activity and Chemical Composition of *Momordica Charantia*: A Review. *Pharmacognosy Journal*, *12*(1), 213-222.

Wang F, Yuan M and Shao C et al., (2023). *Momordica charantia*-Derived Extracellular Vesicles Provide Antioxidant Protection in Ulcerative Colitis. *Molecules*, *28*(17), 6182.

Wang M, Zhan Z and Xiong Y et al., (2019). Cytotoxic and anti-inflammatory constituents from Momordica cochinchinensis seeds. *Fitoterapia*, *139*, 104360.

Wang S, Zheng Y and Xiang F et al., (2016). Antifungal activity of *Momordica charantia* seed extracts toward the pathogenic fungus Fusarium solani L. *Journal of food and drug analysis*, *24*(4), 881-887.

Xu B, Li Z and Zeng T et al., (2022). Bioactives of *Momordica charantia* as Potential Anti-Diabetic/Hypoglycemic Agents. *Molecules*, *27*(7), 2175.

Yadav R, Yadav B and Yadav R, (2016). Effect of Heat Processing Treatments and Extraction Solvents on the Phenolic Content and Antioxidant Activity of *Momordica charantia* Fruit: ANTIOXIDANT POTENTIAL OF M. CHARANTIA. *Journal of Food Processing and Preservation*, *41*.

Yan J-K, Wu L-X and Qiao Z-R et al., (2019). Effect of different drying methods on the product quality and bioactive polysaccharides of bitter gourd (*Momordica charantia* L.) slices. *Food Chemistry*, *271*, 588-596.

Yang X, Chen F and Huang G, (2020). Extraction and analysis of polysaccharide from *Momordica charantia*. *Industrial Crops and Products*, *153*, 112588.

Yao X, Li J and Deng N et al, (2011). Immunoaffinity purification of α-momorcharin from bitter melon seeds (*Momordica charantia*). *Journal of Separation Science*, *34*(21), 3092-3098.

Yue J, Guo P and Jin Y et al., (2023). *Momordica charantia* polysaccharide ameliorates D-galactose-induced aging through the Nrf2/β-Catenin signaling pathway. *Metabolic Brain Disease*, *38*(3), 1067-1077.

Yuguda A Y, (2023). Profiling and In vivo studies of Bromelain Bitter Gourd (Momodica charantia) seed protein hydrolysate with antidiabetic activity. *GSC Biological and Pharmaceutical Sciences*, *23*(1), 269-276.

Zeng L, Chen M and Ahmad H et al., (2022). *Momordica charantia* Extract Confers Protection Against Hypertension in Dahl Salt-Sensitive Rats. *Plant Foods for Human Nutrition*, *77*(3), 373-382.

Zhan K, Ji X and Luo L., (2023). Recent progress in research on *Momordica charantia* polysaccharides: extraction, purification, structural characteristics and bioactivities. *Chemical and Biological Technologies in Agriculture*, *10*(1), 58.

Zhang H, Du X and Yu J et al., (2022). Comparative Metabolomics study of flavonoids in the pericarp of different coloured bitter gourds (*Momordica charantia* L.). *Physiology and Molecular Biology of Plants*, *28*(7), 1347-1357.

Zhang J, He L and Wang A et al., (2022). Responses of bitter melon saponins to oxidative stress and aging via the IIS pathway linked with sir-2.1 and hlh-30. *Journal of food biochemistry*, *46*(12), e14456.

Zhang Y, Lu P and Jin H et al., (2023). Integrated Secondary Metabolomic and Antioxidant Ability Analysis Reveals the Accumulation Patterns of Metabolites in *Momordica charantia* L. of Different Cultivars. *International Journal of Molecular Sciences*, *24*(19), 14495.

Zheng J, Shang M and Dai G et al., (2023). Bioactive polysaccharides from *Momordica charantia* as functional ingredients: a review of their extraction, bioactivities, structural-activity relationships, and application prospects. *Critical reviews in food science and nutrition*, 1-24.

Zubair M F, Atolani O and Ibrahim S O et al., (2018). Chemical and biological evaluations of potent antiseptic cosmetic products obtained from *Momordica charantia* seed oil. *Sustainable Chemistry and Pharmacy*, *9*, 35-41.

Paradigm Academic Press
Journal of Innovations in Medical Research
ISSN 2788-7022
APR. 2025 VOL.4, NO.2

Youth in Action: Party Building Empowering High-Quality Development of the Communist Youth League in Infectious Disease Hospitals — A New Practice

Luxin Han[1] & Yu Tian[1]

[1] The Fourth People's Hospital of Nanning, Guangxi, China

Correspondence: Yu Tian, The Fourth People's Hospital of Nanning, Guangxi, China.

doi:10.63593/JIMR.2788-7022.2025.04.006

Abstract

Under the strategic framework of China's high-quality public health development, Nanning Fourth People's Hospital has pioneered a Party-guided Communist Youth League (CYL) model in infectious disease healthcare, demonstrating innovative organizational synergy and youth-driven impact. The hospital's CYL committee established a tripartite development system—ideological anchoring**,** organizational optimization, and professional enablement—achieving transformative outcomes: a 210% increase in youth mobilization efficiency (2022–2024), 98% theoretical engagement via dual-track ideological education ("Party branch mentorship + youth lecture teams"), and recognition of clinical units as National/Provincial Youth Civilization Collectives. Breakthroughs in HIV/AIDS immunotherapy and multi-drug resistant tuberculosis management were realized through youth-led innovation. During COVID-19, 432 young clinicians under Party leadership achieved a 25% reduction in ICU mortality through standardized protocols while maintaining zero nosocomial infections. The "Nightingale" volunteer-service ecosystem integrated clinical expertise with community health initiatives, delivering 50,000+ beneficiary engagements. Future roadmaps prioritize AI-driven diagnostics, telemedicine networks, and a mentorship-based talent pipeline to strengthen grassroots infectious disease control. This practice validates the multiplier effect of Party-CYL collaboration in healthcare modernization, offering an exemplary model for aligning youth mobilization with the "Healthy China" strategy through socially accountable medical leadership.

Keywords: Communist Youth League, Party-building synergy, infectious disease healthcare, high-quality development, medical volunteerism

1. Introduction

Under the backdrop of high-quality development in public hospitals in the new era (National Health Commission, 2022), the Party Committee of the Fourth People's Hospital of Nanning has adhered to the principle of "Party leadership over youth," innovatively constructing a three-dimensional Youth League development system centered on "ideological cultivation, organizational strengthening, and professional empowerment" (Chen & Li, 2020). As a core fortress for infectious disease prevention and treatment in Guangxi and Nanning, the hospital's Youth League Committee has positioned itself as the "Party's assistant and reserve force," closely following the Party Committee's guidance. The hospital's Party Committee has earned prestigious honors, including the "National Advanced Grassroots Party Organization" and "National Advanced Collective in COVID-19 Pandemic Prevention and Control." Under this leadership, the hospital's Youth League Committee was awarded the title of "National May Fourth Red Flag Youth League Committee." Over the past three years (2022–2024), the Youth League's organizational mobilization efficiency increased by 210% (calculated based on youth participation in major tasks) (Wang & Zhang, 2021), achieving three groundbreaking

outcomes:

1.1 Systematized Ideological Guidance: Lighting the Beacon of Faith

The hospital established a dual-driven mechanism of "Party Branch Mentorship + Youth Lecture Teams" (Central Committee of the Communist Youth League, 2020), with the Party Committee initiating the "Magnolia Fragrance Reading Club." Over 32 sessions, full coverage of Youth League members was achieved, fostering a strong learning culture. By promoting 12 exemplary youth members who joined the Party during the pandemic, the theoretical engagement rate among youth surged from 65% to over 98%, embedding patriotism and proactive spirit into the hospital's culture.

1.2 Professionalized Organizational Development: Strengthening Talent Foundations

A grid-based structure of "Youth League Branches — Youth Shock Teams — Volunteer Service Teams" (Zheng et al., 2022) was established across 23 clinical departments. The Infectious Disease Ward 1 was recognized as a National Youth Civilization Unit, while three teams, including the ICU, earned Guangxi Youth Civilization Unit honors. This framework created a "peacetime-emergency integration" talent cultivation system, fueling cultural innovation.

1.3 Deepened Service Integration: Spreading Humanistic Care

The hospital integrated its "Nightingale Volunteer Service" brand with infectious disease prevention (Huang & Zhao, 2019), launching campaigns like "Strengthening the Infectious Disease Defense Wall." A 560-member volunteer team conducted over 50,000 community, rural, and school outreach activities. The hospital's cultural brand "Magnolia Fragrance" and its stage drama *The Garden of Life* won the National Hospital Humanistic Management Case Award, embodying the core value of "Guarding Life."

Practice demonstrates that Youth League reforms under Party leadership can translate into organizational momentum, professional potential, and social efficacy for public hospital development (Li et al., 2021), providing an empirical model for Party-Youth collaboration in healthcare institutions.

2. Party Leadership: The "Compass" of Youth League Work

Under the steadfast guidance of the Communist Party of China (CPC), the Youth League Committee has transformed into a dynamic force in public health, channeling the vigor of young medical professionals into frontline battles against infectious diseases. By aligning ideological education with practical challenges, the Party has cultivated a generation of resilient, socially responsible healthcare leaders.

2.1 Cultivating Responsibility Through Party Leadership

The Communist Youth League Committee has fostered an "Always Prepared for Emergencies" spirit among young medical workers, positioning them at the forefront of combating infectious diseases such as AIDS, tuberculosis (TB), and global outbreaks including H1N1, Ebola, and MERS. Through CPC-led training programs, young teams have mastered protocols for rapid pathogen containment and patient isolation, resulting in an 18% reduction in TB transmission rates in high-risk communities (Zheng et al., 2022).

A youth shock team of over 200 members has become the backbone of public health defense. During historical public health emergencies, all members of the Youth League have rushed to the front lines, successfully completing numerous arduous and critical missions. For HIV/AIDS prevention, young volunteers initiated the "Red Ribbon Outreach" community education campaign. Through door-to-door advocacy, public welfare activities, and lectures, they enhanced public awareness of HIV prevention and improved screening rates among high-risk populations.

2.2 Youth at the Forefront of Pandemic Prevention

The COVID-19 pandemic became a critical test for the Party-League collaboration. 432 young medical workers (76% under the age of 35) braved negative pressure isolation wards and provided more than 15,000 hours of patient care. Five core members joined the national medical team deployed to the epidemic center in Wuhan to build a 200-bed intensive care unit and reduce mortality by 25% through standardized intubation protocols (Liu et al., 2023).

The pandemic also deepened ideological determination: 12 young members applied to join the Party on the front line, inspired by the Party's "people first" mobilization. These efforts show how the Party's leadership can transform youth potential into actionable resilience, ensuring that hospitals become bastions against current and future health threats. By combining ideological rigor with technical excellence, the CPC continues to guide youth power toward the grand vision of a "Healthy China".

3. Dual-Driven "Youth Brand" and Volunteer Services: Cultural Practices for High-Quality Development

The integration of youth-driven innovation and volunteerism has emerged as a cornerstone of high-quality

development in healthcare, fostering both professional excellence and social responsibility. By harnessing the dynamism of young professionals and synergizing it with structured volunteer frameworks, the hospital has cultivated a culture of leadership, compassion, and transformative impact.

3.1 Youth Responsibility in Critical Tasks

In Infectious Disease Ward 1, young medical teams have revolutionized HIV/AIDS care through cutting-edge therapies. The adoption of allogeneic adoptive immunotherapy (AAIT) — a technique enhancing immune response by transplanting donor-derived immune cells — and advanced cardiac interventions has reduced complications in HIV-associated cardiovascular diseases, improving patient survival and quality of life. These efforts underscore the role of youth in bridging research and clinical practice.

The ICU, with an 83.3% youth staffing ratio, exemplifies youthful leadership in high-stakes environments. By pioneering multidisciplinary critical care strategies (Zhou & Wu, 2022) — integrating real-time data analytics, telemedicine, and personalized rehabilitation plans — the team elevated survival rates for sepsis and multi-organ failure cases by 22% over three years. Their agile response to emerging health crises, from COVID-19 to trauma cases, highlights the adaptability of youth-led teams.

Tuberculosis Ward 3, recognized as a regional hub, has advanced Guangxi's capacity in managing refractory TB through six proprietary technologies, including gene sequencing for drug resistance profiling and minimally invasive surgical techniques. Hosting national academic conferences annually, the ward has disseminated best practices to over 1,500 specialists, cementing its role as a knowledge-sharing platform.

3.2 Synergy of Volunteer and Professional Services

The Youth League's integration of "goal-setting theory" and "team-building models" (Huang & Zhao, 2019) has transformed volunteerism into a strategic asset. By aligning public welfare objectives with staff expertise, the hospital organized 100+ annual initiatives, including large-scale blood drives (collecting 15,000+ units yearly), rural health camps serving 8,000+ low-income patients.

Recognition as a "National Nightingale Volunteer Advanced Unit" for four consecutive years reflects systemic impact. Volunteer programs now embed clinical skills into community outreach — for instance, training nurses in trauma counseling for disaster response. Such initiatives not only address health inequities but also nurture empathy among young professionals, creating a virtuous cycle of service and growth.

Collectively, these efforts demonstrate how youth empowerment and volunteerism drive high-quality development: blending technical excellence with ethical commitment to redefine healthcare's societal role. By prioritizing innovation, collaboration, and compassion, the hospital models a replicable blueprint for sustainable progress in global health systems.

4. Innovative Practices and Achievements Under Party Leadership

Under the strategic guidance of the Communist Party of China (CPC), the hospital has pioneered a dual focus on nurturing youth talent and enhancing service quality, positioning itself as a national model for integrating Party leadership with medical innovation. These efforts align with the CPC's vision of "Healthy China," fostering a culture of excellence, accountability, and patient-centered care.

4.1 Pathways for Youth Medical Talent Growth

4.1.1 Growth Path for Young Medical Talents

The Party Committee has established a comprehensive talent training system and organizes 36 educational activities each year to cultivate clinical professional skills, leadership and ideological literacy. For example, interdisciplinary speech competitions on topics such as "Artificial Intelligence in Diagnosis" are held. These platforms enable young professionals to hone their problem-solving skills while internalizing the core socialist values.

4.2 Elevating Service Quality Through Youth Civilization Units

The hospital's Youth Civilization Units (YCUs), recognized at national, provincial, and municipal levels (Li et al., 2021), exemplify the synergy between Party directives and grassroots innovation. Infectious Disease Ward 1, designated a National YCU in 2022, exemplifies this synergy. Under the leadership of Du Liqun, a recipient of the "Nightingale Medal" (Du et al., 2023), the ward ranked 20th nationally in service influence by integrating clinical excellence with humanitarian care.

Du's team pioneered the "Love Circle" quality improvement project, a patient-centric initiative that reduced average HIV consultation wait times by 35% through AI-powered scheduling and peer-led counseling networks. The project also introduced "Sunflower Companion" volunteers to provide psychosocial support for AIDS patients, reducing stigma and improving treatment adherence by 28%.

5. Future Prospects

5.1 Empowering Infectious Disease Prevention and Control Through Technology

Introducing Advanced Technologies: The Youth League Committee will actively promote the adoption of cutting-edge technologies in hospitals, such as AI-assisted diagnostic systems, to enhance early diagnosis and treatment efficiency for infectious diseases. The goal is to increase the early diagnosis rate by 20% within the next three years. Additionally, we will explore big data analytics to enable precise prediction of epidemic trends, providing scientific support for public health decision-making, with an expected 15% improvement in prediction accuracy compared to current levels.

Strengthening Telemedicine Services: Further develop telemedicine platforms to enable specialists to provide remote diagnostic advice for patients in underserved areas, thereby improving grassroots healthcare quality and expanding the hospital's service coverage. The plan is to extend telemedicine services to over 50% of county-level hospitals in Guangxi within the next two years.

5.2 Strengthening the Cultivation of Young Talents

Building Growth Platforms: The Youth League Committee will organize professional training sessions, academic lectures, and skill competitions to create platforms for young medical professionals to showcase their talents and enhance their capabilities. We aim to hold no fewer than 40 professional training sessions and academic lectures annually, with a 10% yearly increase in skill competition participation. Furthermore, we will encourage young employees to engage in hospital research projects and innovation practices, fostering their scientific thinking and innovative abilities. The goal is to achieve a 15% annual growth in research papers published by young staff.

Implementing a Mentorship System: Establish a mentorship program where experienced experts and senior professionals provide one-on-one guidance to young employees, accelerating their professional development. The plan is to assign mentors to over 80% of young staff within the next year.

5.3 Expanding Volunteer Service Initiatives

Deepening Community Engagement: The Youth League Committee will mobilize young volunteers to conduct health education campaigns and free medical consultation activities in communities, raising public awareness and prevention of infectious diseases. We will organize no fewer than 50 community service activities annually, with a 20% yearly increase in the number of residents covered. Long-term partnerships with communities will also be established to provide continuous health management and consultation services.

Supporting Vulnerable Groups: Strengthen care and assistance for patients with infectious diseases such as HIV/AIDS and tuberculosis through psychological counseling and livelihood support, promoting their rehabilitation and social integration. Over the next three years, we aim to increase service hours for these groups by 15% annually.

5.4 Enhancing Hospital Cultural Development

Building a Brand Identity: The Youth League Committee will assist the hospital in deepening the development of the "Yulan Flower Fragrance" cultural brand, integrating its core values into all hospital operations and services. This initiative aims to shape a distinctive cultural identity, boosting cohesion and appeal. The goal is to increase the brand's recognition among patients by 25% within the next two years.

Enriching Cultural Activities: Host diverse cultural events, such as artistic performances and sports competitions, to enrich the leisure lives of young employees and foster a positive work environment. We plan to organize no fewer than 20 cultural activities annually, with a 10% yearly increase in staff participation.

5.5 Promoting Party-Youth League Collaboration

Strengthening Party-League Coordination: The Youth League Committee will maintain close ties with the hospital's Party Committee to jointly organize themed Party and Youth League Day activities, facilitating communication and collaboration between Party and League members. This will create a synergistic dynamic between Party-building and League-building efforts, with at least 10 joint activities annually.

Engaging in Hospital Governance: Encourage young League members to actively participate in democratic management and oversight, contributing ideas for the hospital's development and playing a proactive role in its governance. We aim to collect no fewer than 50 suggestions from young employees annually, with an implementation rate of at least 30%.

References

Central Committee of the Communist Youth League, (2020). *Guidelines for grassroots construction of the Communist Youth League in the new era*. Beijing: China Youth Press.

Chen, X., & Li, H., (2020). Practical exploration of Party building leading Youth League building in medical institutions — A case study of a tertiary hospital. *Chinese Hospital Management*, *40*(8), 45–48.

Du, L., et al., (2023). Practice of nursing quality control circles in quality management of infectious disease hospitals. *Chinese Journal of Nursing*, *58*(7), 823–828.

Huang, L., & Zhao, M., (2019). Practice and enlightenment of Nightingale volunteer service models in infectious disease prevention. *Chinese Nursing Management*, *19*(11), 1601–1605.

Li, J., et al., (2021). Impact of Youth Civilization Unit creation on hospital service quality. *Chinese Journal of Hospital Administration*, *37*(4), 289–293.

Liu, Y., et al., (2023). Psychological capital and professional identity of young medical workers in major public health crises. *Chinese Journal of Behavioral Medicine and Brain Science*, *32*(3), 210–215.

National Health Commission, (2022). *Evaluation index system for high-quality development of public hospitals (Trial)*. Beijing: People's Medical Publishing House.

Wang, L., & Zhang, W., (2021). Pathways to enhance organizational mobilization efficiency of Youth Leagues in public hospitals in the new era. *Chinese Health Service Management*, *38*(5), 321–325.

Zheng, X., et al., (2022). Organizational mobilization mechanisms of youth shock teams in public health crises. *China Youth Study*, (6), 56–62.

Zhou, T., & Wu, M., (2022). Application of multidisciplinary team (MDT) in critical care of infectious diseases. *Chinese Journal of Infectious Diseases*, *40*(6), 341–345.

Paradigm Academic Press
Journal of Innovations in Medical Research
ISSN 2788-7022
APR. 2025 VOL.4, NO.2

Current Status of Induction Chemotherapy in Locally Advanced Nasopharyngeal Carcinoma

Xinhao Chen[1], Runtian Xiao[1] & Tao Zhang[1]

[1] Department of Oncology, Laboratory of Immunity, Inflammation & Cancer, The First Affiliated Hospital of Chongqing Medical University, Chongqing 400016, China

Correspondence: Tao Zhang, Department of Oncology, Laboratory of Immunity, Inflammation & Cancer, The First Affiliated Hospital of Chongqing Medical University, Chongqing 400016, China.

doi:10.63593/JIMR.2788-7022.2025.04.007

Abstract

Nasopharyngeal carcinoma (NPC) has a unique endemic distribution in the world, with the highest incidence rate in South China, Southeast Asia and North Africa. About 70% of newly diagnosed nasopharyngeal carcinoma patients suffer from locally advanced diseases. The current methods of radiotherapy and chemotherapy include synchronous radiotherapy and chemotherapy, induction chemotherapy, and adjuvant chemotherapy. Induction chemotherapy has better tolerance, so higher drug concentrations can be used to improve the survival rate of locally advanced nasopharyngeal carcinoma patients. Induction chemotherapy can eliminate micro metastatic diseases early. This article provides a review of the application of induction chemotherapy in the treatment of locally advanced nasopharyngeal carcinoma.

Keywords: locally advanced nasopharyngeal carcinoma, induction chemotherapy

1. Introduction

Nasopharyngeal carcinoma (NPC) is a malignant tumor originating from the nasopharyngeal epithelium, predominantly occurring in the pharyngeal recess and posterior wall of the nasopharyngeal roof. Compared with other head and neck tumors, NPC exhibits unique geographical distribution characteristics and ethnic predisposition, with high-incidence areas in Hong Kong, Guangdong, and Guangxi regions of China (Torre L A, Bray F, Siegel R L, et al., 2015). Due to its occult anatomical location and biological features characterized by high invasiveness and metastatic potential, most cases are diagnosed as locally advanced disease at initial detection. Given the anatomical proximity of the nasopharynx to the skull base and the fact that the vast majority of NPC cases are poorly differentiated squamous cell carcinomas, radiotherapy is generally the primary treatment modality (Chen Y P, Chan A T C, Le Q T, et al., 2019; Lee A W M, Ng W T, Chan J Y W, et al., 2019; Lee V H, Lam K O, Chang A T, et al., 2018; Yoshizaki T, Ito M, Murono S, et al., 2012). While the application of concurrent chemoradiotherapy and intensity-modulated radiation therapy (IMRT) has significantly improved survival rates for early-stage NPC patients, therapeutic outcomes for locally advanced cases remain suboptimal, with a 5-year overall survival rate of approximately 50%. Previous studies have reported (Zhang L, Chen Q Y, Liu H, et al., 2013; Mao Y P, Xie F Y, Liu L Z, et al., 2009) that 15% to 54% of patients with locally advanced nasopharyngeal carcinoma (NPC) are prone to local recurrence, primarily influenced by tumor stage, cranial nerve involvement, and histological type. The 5-year distant metastasis rate ranges from 20% to 35%, reaching 60% to 80% in N3 patients (Au K H, Ngan R K C, Ng A W Y, et al., 2018; Lee A W, Tung S Y, Ngan R K, et al., 2011). Therefore, controlling the primary tumor and preventing distant dissemination remain critical challenges in the management of locally advanced NPC. Numerous phase III clinical trials (Wu X, Huang P Y, Peng P J, et al., 2013; Colevas A D, Yom SS, Pfister D G, et al., 2018; Chen Y, Sun Y, Liang S B, et al., 2013) have demonstrated that concurrent chemoradiotherapy (CCRT) can improve the overall survival (OS) and disease

control rate (DCR) in patients with locally advanced nasopharyngeal carcinoma (NPC). Currently, CCRT has been recommended by the National Comprehensive Cancer Network (NCCN) guidelines as the standard treatment strategy for stage III-IVb NPC.

Combining several cycles of systemic chemotherapy with concurrent chemoradiotherapy (CCRT) is a potential approach to address the high distant metastasis rate in locally advanced nasopharyngeal carcinoma (NPC). However, previous studies have indicated that sequential adjuvant chemotherapy following CCRT is associated with a high incidence of toxic side effects (approximately 60%) (Chen L, Hu CS, Chen XZ, et al., 2012), poor patient compliance, and no studies have demonstrated that adjuvant chemotherapy provides additional survival benefits beyond standard CCRT (Chen L, Hu CS, Chen XZ, et al., 2012; Chi KH, Chang YC, Guo WY, Leung MJ, Shiau CY, Chen SY, et al., 2002; Kwong DL, Sham JS, Au GK, Chua DT, Kwong PW, Cheng AC, et al., 2004; Chen L, Hu CS, Chen XZ, Hu GQ, Cheng ZB, Sun Y, et al., 2017). Consequently, sequential adjuvant chemotherapy after CCRT is not the optimal choice. In contrast to adjuvant chemotherapy administered after concurrent chemoradiotherapy (CCRT), induction chemotherapy delivered prior to CCRT has demonstrated superior benefits in multiple studies (Chen L, Hu CS, Chen XZ, Hu GQ, Cheng ZB, Sun Y, et al., 2017; Sun Y, Li WF, Chen NY, Zhang N, Hu GQ, Xie FY, et al., 2016; Cao SM, Yang Q, Guo L, Mai HQ, Mo HY, Cao KJ, et al., 2017). Compared to adjuvant chemotherapy, induction chemotherapy followed by CCRT offers better tolerability for patients with locally advanced nasopharyngeal carcinoma (NPC), ensures completion of planned chemotherapy cycles and drug dosages, and enables early eradication of micro-metastases. Consequently, the treatment strategy of induction chemotherapy followed by CCRT is clinically feasible and has been widely adopted in high-incidence regions of NPC in China.

2. Theoretical Basis of Induction Chemotherapy for Nasopharyngeal Carcinoma

Induction Chemotherapy (IC) refers to chemotherapy administered prior to radiotherapy, typically consisting of 2-3 cycles. It offers the following advantages: (1) Better patient compliance and tolerability: Before radiotherapy, patients are generally in better overall condition, enabling almost all patients to complete the full planned induction cycles. (2) Optimal drug delivery: Tumor vasculature has not yet developed fibrosis prior to radiotherapy, allowing chemotherapeutic agents to achieve sufficient concentrations at the tumor site (Imaizumi N, Monnier Y, Hegi M, et al., 2010; Gang W, Peng X U, Jinyi L., 2016). (3) Rapid symptom relief and psychological benefits: For patients with T3-4 tumors or lymph node metastases, IC can rapidly reduce tumor burden, alleviate clinical symptoms, create favorable conditions for radiotherapy, reduce psychological distress, and improve quality of life. (4) Radiotherapy optimization: Tumor volume reduction through IC enables smaller radiation fields, reduced radiation doses, minimized treatment-related side effects, and better protection of organs at risk. (5) Elimination of subclinical metastases: Chemotherapy helps eradicate subclinical metastatic lesions in the body, thereby improving distant metastasis-free survival rates (Ke L R, Xia W X, Qiu W Z, et al., 2017).

3. The Selection of Induction Chemotherapy Regimens

At present, the main induction chemotherapy regimens are based on platinum, such as TP regimen (paclitaxel-like drugs + platinum), PF regimen (5-fluorouracil + platinum), TPF regimen (paclitaxel-like drugs + 5-fluorouracil + platinum), GP regimen (gemcitabine + platinum), TPC regimen (paclitaxel-like drugs + platinum + capecitabine), etc. Usually, 2 to 3 cycles of treatment are administered.

3.1 PF Regimen

The PF regimen, a classic induction chemotherapy protocol for head and neck cancers, has been extensively studied. Zhang et al conducted a meta-analysis of 10 clinical trials, demonstrating that PF induction chemotherapy combined with radiotherapy significantly improved the 5-year overall survival rate (Na Z, Ping L I & Zhu-Mei L., 2010). A retrospective study by Qiu et al included 240 patients with locally advanced nasopharyngeal carcinoma (Qiu W, Huang P, Shi J, et al., 2015). The induction group consisted of 117 patients who received PF regimen as induction chemotherapy combined with intensity-modulated conformal radiotherapy, and 123 patients who received concurrent radiochemotherapy combined with cisplatin+5-FU adjuvant chemotherapy. The results indicate that there is no statistically significant difference in the 5-year overall survival rate and distant metastasis free survival rate between induction chemotherapy and concurrent chemoradiotherapy. However, the incidence of grade 3 and 4 gastrointestinal reactions and bone marrow suppression in the concurrent chemoradiotherapy group is significantly higher than that in induction hemotherapy. A retrospective study on PF induced chemotherapy showed (Boscolorizzo P, Tirelli G, Mantovani M, et al., 2015) that the 5-year distance control rate (DCR) and local control rate (LRC) were 82.2% and 80%, respectively 1%. The 5-year OS and disease-free survival (EFS) rates were 72 0 and 66 7%, this study also confirms the significant value of the PF scheme.

3.2 TP Regimen

The TP chemotherapy regimen typically consists of paclitaxel-based chemotherapeutic agents and platinum-based chemotherapeutic agents. In recent years, TP regimen has been commonly used in the treatment of nasopharyngeal carcinoma. In 2009, a phase II clinical trial (Hui E P, Ma B B, Leung S F, et al., 2009), which included 65 newly treated patients with locally advanced nasopharyngeal carcinoma. They were divided into TP Regimen (docetaxel + cisplatin) induction chemotherapy combined with concurrent chemoradiotherapy group and simple concurrent chemoradiotherapy group. The study confirmed that TP regimen induction chemotherapy can improve the progression free survival (PFS) and overall survival rate of locally advanced nasopharyngeal carcinoma patients. Xie et al compared TP induced chemotherapy with PF induced chemotherapy in 2015 (Yalin X, Jianming X, Oncology D O, et al., 2015). The research results showed that TP regimen induced chemotherapy could significantly prolong the median progression free survival time, and the difference was statistically significant (P=0.044), while there was no significant difference in the toxic side effects between the two. This also confirms that the TP regimen can be used as one of the induction chemotherapy options for locally advanced nasopharyngeal carcinoma.

3.3 TPF Regimen

He et al. confirmed that synchronous radiotherapy and chemotherapy after TPF induction chemotherapy can significantly improve 2-year OS and DFS in locally advanced nasopharyngeal carcinoma patients compared to concurrent radiotherapy and chemotherapy, with statistical significance (P<0.05) (H A J., 2011). Although the acute toxicity response rate of patients in the TPF induction chemotherapy group was higher, symptoms were mostly relieved after treatment. However, there were differences in the results of a randomized controlled study (Jin T, Qin W F, Jiang F, et al., 2019), which compared TPF induced chemotherapy combined with concurrent chemoradiotherapy and PF induced chemotherapy combined with concurrent chemoradiotherapy and confirmed that there was no statistically significant difference in 3-year OS and DFS between the two groups, and the incidence of grade 3-4 adverse reactions in the TPF induced chemotherapy group was significantly higher than that in the PF group. POSNER et al compared TPF induction chemotherapy with PF induction chemotherapy followed by sequential concurrent radiochemotherapy (POSNER M R, HERSHOCK D M, BLAJMAN C R, et al., 2007). The results showed that compared with patients receiving PF treatment, patients receiving TPF treatment had significantly improved OS and an increased incidence of severe (grade III and IV) bone marrow suppression. The study conducted by PENG H et al (2021) included 855 patients with locally advanced nasopharyngeal carcinoma. Among them, 395 cases (46.2%), 258 cases (30.2%), and 202 cases (23.6%) received TPF, TP, and PF induction chemotherapy regimens, respectively, and underwent a 10-year follow-up. The results demonstrated that, in terms of improving overall survival (OS) for stage III–IVa nasopharyngeal carcinoma patients, the TPF+CCRT and TP+CCRT groups exhibited superior 10-year OS compared to the PF+CCRT group.

3.4 GP Regimen

Gemcitabine, a cytidine analogue chemotherapeutic agent, has demonstrated favorable efficacy in nasopharyngeal carcinoma (NPC) in recent years. Studies by Zhao et al confirmed that the GP induction chemotherapy regimen (gemcitabine + platinum) improves overall survival (OS) and disease-free survival (DFS) compared to the PF regimen (5-fluorouracil + cisplatin) (Zhao L, Xu M, Jiang W, et al., 2017; Yang YQ, Qu XM, Z X, et al., 2018). Jamshed et al reported a 5-year overall survival rate of 71% for patients treated with GP induction chemotherapy combined with chemoradiotherapy (Jamshed A, Hussain R & Iqbal H., 2014). A 2017 phase II clinical trial (Wu M Y, Ou D, He X, et al., 2017) involving 112 patients with locally advanced NPC who received GP induction chemotherapy followed by intensity-modulated radiotherapy (IMRT) demonstrated 5-year survival rate and distant metastasis free rate of 82.1% and 89.0%, respectively. These findings further underscore the therapeutic value of the GP regimen combined with IMRT for locally advanced NPC.

3.5 TPC Regimen

Xiang et al. compared the efficacy of the TPC regimen (paclitaxel + platinum + capecitabine) versus the PF regimen (5-fluorouracil + cisplatin) for induction chemotherapy (Li WZ, Lv X, Hu D, et al., 2022). The results showed that the TPC regimen group achieved a significantly superior 3-year failure-free survival (FFS) rate compared to the PF regimen group. Additionally, the TPC regimen significantly reduced both distant metastasis risk and local recurrence risk relative to the PF regimen. Safety analysis revealed that the TPC regimen did not increase treatment-related toxicities compared to the PF regimen.

4. The Application of Induction Chemotherapy in Combination with Molecularly Targeted Agents

With the in-depth study of epidermal growth factor receptor (EGFR) and the continuous exploration of its signaling pathway, this signaling pathway is believed to be closely related to factors such as tumor proliferation and radiotherapy sensitivity. At present, drugs targeting EGFR mainly include gefitinib, rituximab, and cetuximab, among which rituximab has been approved for combined treatment with radiotherapy in stage III/IV

EGFR positive nasopharyngeal carcinoma patients.

A multicenter clinical study (Lu Y, Chen D, Liang J, et al., 2019) investigating Nimotuzumab combined with the PF regimen as induction therapy for locally advanced nasopharyngeal carcinoma found that, compared to TPF induction chemotherapy, there was no significant difference in the efficacy of primary nasopharyngeal lesions or overall response (primary lesions + cervical lymph nodes) between the two groups. However, the Nimotuzumab group demonstrated a higher cervical lymph node response rate (CR+PR) (81% vs. 60%, P=0.036). Additionally, Nimotuzumab reduced the incidence of adverse reactions and improved patients' tolerance to concurrent chemoradiotherapy (CCRT). In addition, multiple retrospective studies (Yang Z, Zuo Q, Liu R, et al., 2023; Jiang D, Cao J, Guo L, et al., 2023) have shown that receiving CCRT and NTZ treatment after induction chemotherapy can effectively improve the objective efficacy and 5-year progression free survival rate of locally advanced nasopharyngeal carcinoma patients compared to receiving only induction chemotherapy and CCRT.

5. The Application of Induction Chemotherapy in Combination with Immunotherapy Drugs

The importance of immunotherapy in the treatment of nasopharyngeal carcinoma is increasingly prominent. Its unique advantage lies in its ability to accurately target tumor cells, effectively recognize and attack tumors by activating or enhancing the patient's own immune system, thereby reducing damage to normal cells. In addition, immunotherapy can bring potential long-term survival benefits, providing a new treatment approach for patients who have failed traditional treatments such as radiotherapy and chemotherapy or have relapsed or metastasized, helping to overcome tumor drug resistance. Meanwhile, immunotherapy can also be combined with chemotherapy and radiotherapy to exert synergistic effects and improve overall treatment outcomes.

In the treatment of recurrent/metastatic nasopharyngeal carcinoma, PD-1 monoclonal antibody drugs have been widely used and recommended by guidelines in China. The results from Mai et al showed that the combination of trastuzumab and GP chemotherapy has significant efficacy, reducing the risk of patient death by 39%, achieving a 5-year OS rate of 52.0%, and being safe and controllable (Mai HQ, Chen QY, Chen D, et al., 2023). In addition, tislelizumab has been approved for first-line treatment of recurrent or metastatic nasopharyngeal carcinoma based on the results of a Phase III study (Yang Y, Pan J, Wang H, et al., 2023). This study demonstrated that compared to placebo combined with GP chemotherapy, tislelizumab plus GP chemotherapy significantly prolonged progression-free survival (PFS) in patients. A trend toward improved overall survival (OS) was also observed, while maintaining a safety profile comparable to placebo combined with chemotherapy.

In the treatment of locally advanced nasopharyngeal carcinoma, the application of PD-1 monoclonal antibodies has also shown progress. A study by Liu et al. (2024) first demonstrated that adding neoadjuvant and adjuvant immunotherapy based on the programmed death receptor-1 (PD-1) monoclonal antibody toripalimab to concurrent chemoradiotherapy (CCRT) significantly improved survival outcomes in high-risk locally advanced nasopharyngeal carcinoma patients. Compared to the placebo-plus-CCRT control group, the toripalimab-plus-CCRT group showed a markedly higher 2-year PFS rate (92.0% vs. 74.0%), reducing the risk of disease progression or death by 60%, along with a significantly improved 3-year overall survival rate (99.0% vs. 90.0%).

6. Prospect

Induction chemotherapy demonstrates superior overall survival (OS) and disease-free survival (DFS) compared to adjuvant chemotherapy in nasopharyngeal carcinoma. However, due to insufficient total sample size, variability in chemotherapy regimens, and individual heterogeneity, the optimal induction chemotherapy protocol remains inconclusive. Although the ideal regimen is yet to be defined, its therapeutic value in locoregionally advanced nasopharyngeal carcinoma remains undeniable. With the deepening of clinical research, emerging evidence is driving induction chemotherapy from standardized to personalized approaches. Future large-scale randomized phase III clinical trials are warranted to further clarify its role and establish the optimal induction chemotherapy strategy for locoregionally advanced nasopharyngeal carcinoma. In recent years, immunotherapy has demonstrated significant potential in nasopharyngeal carcinoma treatment. Neoadjuvant immunotherapy enhances therapeutic response rates and survival outcomes by activating anti-tumor immune responses prior to radiotherapy, while reducing post-radiotherapy risks of recurrence and metastasis. Recent studies reveal that combining neoadjuvant immunotherapy with chemotherapy significantly improves complete response rates in patients with locoregionally advanced nasopharyngeal carcinoma, without substantially increasing treatment-related toxicities. Looking forward, neoadjuvant immunotherapy is poised to become a cornerstone of nasopharyngeal carcinoma management, offering enhanced therapeutic efficacy, reduced treatment-associated adverse effects, and improved quality of life for patients.

References

Au K H, Ngan R K C, Ng A W Y, et al., (2018). Treatment outcomes of nasopharyngeal carcinoma in modern era after intensity modulated radiotherapy (IMRT) in Hong Kong: A report of 3328 patients (HKNPCSG 1301

study). *Oral Oncology*, *77*, 16-21.

Boscolorizzo P, Tirelli G, Mantovani M, et al., (2015). Non-endemic locoregionally advanced nasopharyngeal carcinoma: long-term outcome after induction plus concurrent chemoradiotherapy in everyday clinical practice. *European Archives of Oto-Rhino-Laryngology*, *272*(11), 3491-3498.

Cao SM, Yang Q, Guo L, Mai HQ, Mo HY, Cao KJ, et al., (2017). Neoadjuvant chemotherapy followed by concurrent chemoradiotherapy versus concurrent chemoradiotherapy alone in locoregionally advanced nasopharyngeal carcinoma: A phase III multicentre randomised controlled trial. *Eur J Cancer*, *75*, 14-23.

Chen L, Hu CS, Chen XZ, et al., (2012). Concurrent chemoradiotherapy plus adjuvant chemotherapy versus concurrent chemoradiotherapy alone in patients with locoregionally advanced nasopharyngeal carcinoma: a phase 3 multicentre randomised controlled trial. *Lancet Oncol*, *13*, 163-71.

Chen L, Hu CS, Chen XZ, Hu GQ, Cheng ZB, Sun Y, et al., (2017, April). Adjuvant chemotherapy in patients with locoregionally advanced nasopharyngeal carcinoma: Long-term results of a phase 3 multicentre randomised controlled trial. *Eur J Cancer*, *75*, 150-158.

Chen Y P, Chan A T C, Le Q T, et al., (2019). Nasopharyngeal carcinoma. *The Lancet*, *394*(10192), 64-80.

Chen Y, Sun Y, Liang S B, et al., (2013). Progress report of a randomized trial comparing long-term survival and late toxicity of concurrent chemoradiotherapy with adjuvant chemotherapy versus radiotherapy alone in patients with stage III to IVB nasopharyngeal carcinoma from endemic regions of China. *Cancer*, *119*(12), 2230-2238.

Chi KH, Chang YC, Guo WY, Leung MJ, Shiau CY, Chen SY, et al., (2002). A phase III study of adjuvant chemotherapy in advanced nasopharyngeal carcinoma patients. *Int J Radiat Oncol Biol Phys*, *52*, 1238-44.

Colevas A D, Yom SS, Pfister D G, et al., (2018). NCCN guidelines insights: head and neck cancers, version 1. 2018. *Journal of the National Comprehensive Cancer Network*, *16*(5), 479-490.

Gang W, Peng X U, Jinyi L., (2016). Research Progress of Neoadjuvant Chemotherapy for Locally Advanced Nasopharyngeal Carcinoma. *Cancer Research on Prevention and Treatment*, *43*(02).

H A J., (2011). Clinical study of neoadjuvant chemotherapy combined with concurrent chemoradiotherapy in the treatment of locally advanced nasopharyngeal carcinoma. *Hebei Medical Journal*, *33*(14), 2115-2116.

Hui E P, Ma B B, Leung S F, et al., (2009). Randomized phase II trial of concurrent cisplatin -radiotherapy with or without neoadjuvant docetaxel and cisplatin in advanced nasopharyngeal carcinoma. *Journal of Clinical Oncology Official Journal of the American Society of Clinical Oncology*, *27*(2), 242-249.

Imaizumi N, Monnier Y, Hegi M, et al., (2010). Radiotherapy suppresses angiogenesis in mice through TGF-betaRI/ALK5-dependent inhibition of endothelial cell sprouting. *Plos One*, *5*(6), 10.1371/journal.pone. 0011084

Jamshed A, Hussain R, Iqbal H., (2014). Gemcitabine and Cisplatin followed by chemoradiation for advanced nasopharyngeal carcinoma. *Asian Pac J Cancer Prev*, *15*(2), 89-904.

Jiang D, Cao J, Guo L, et al., (2023 January 27). Induction chemotherapy with sequential nimotuzumab plus concurrent chemoradiotherapy in advanced nasopharyngeal carcinoma: A retrospective real-world study. *Medicine (Baltimore)*, *102*(4), e32732.

Jin T, Qin W F, Jiang F, et al., (2019). Cisplatin and fluorouracil induction hemotherapy with or without docetaxel in locoregionally advanced nasopharyngeal carcinoma. *Transl Oncol*, *12*(4), 633-639.

Ke L R, Xia W X, Qiu W Z, et al., (2017). Safety and efficacy of lobaplatin combined with 5 -fluorouracil as first-line induction chemotherapy followed by lobaplatin-radiotherapy in locally advanced nasopharyngeal carcinoma: preliminary results of a prospective phase II trial. *BMC Cancer*, *17*(1), 134.

Kwong DL, Sham JS, Au GK, Chua DT, Kwong PW, Cheng AC, et al., (2004). Concurrent and adjuvant chemotherapy for nasopharyngeal carcinoma: a factorial study. *J Clin Oncol*, *22*, 2643-53.

Lee A W M, Ng W T, Chan J Y W, et al., (2019). Management of locally recurrent nasopharyngeal carcinoma. *Cancer Treatment Reviews*, *29*, 10.1016/j.ctrv.2019.101890.

Lee A W, Tung S Y, Ngan R K, et al., (2011). Factors contributing to the efficacy of concurrent-adjuvant chemotherapy for locoregionally advanced nasopharyngeal carcinoma: Combined analyses of NPC-9901 and NPC-9902 Trials. *European Journal of Cancer*, *47*(5), 656-666.

Lee V H, Lam K O, Chang A T, et al., (2018). Management of nasopharyngeal carcinoma: is adjuvant therapy needed? *Journal of Oncology Practice*, *14*(10), 594-602.

Li WZ, Lv X, Hu D, et al., (2022 May 1). Effect of Induction Chemotherapy with Paclitaxel, Cisplatin, and

Capecitabine vs Cisplatin and Fluorouracil on Failure-Free Survival for Patients with Stage IVA to IVB Nasopharyngeal Carcinoma: A Multicenter Phase 3 Randomized Clinical Trial. *JAMA Oncol*, *8*(5), 706-714.

Liu SL, Li XY, Yang JH, et al., (2024 Dec). Neoadjuvant and adjuvant toripalimab for locoregionally advanced nasopharyngeal carcinoma: a randomised, single-centre, double-blind, placebo-controlled, phase 2 trial. *Lancet Oncol*, *25*(12), 1563-1575.

Lu Y, Chen D, Liang J, et al., (2019 Dec 30). Administration of nimotuzumab combined with cisplatin plus 5-fluorouracil as induction therapy improves treatment response and tolerance in patients with locally advanced nasopharyngeal carcinoma receiving concurrent radiochemotherapy: a multicenter randomized controlled study. *BMC Cancer*, *19*(1), 1262.

Mai HQ, Chen QY, Chen D, et al., (2023 Nov 28). Toripalimab Plus Chemotherapy for Recurrent or Metastatic Nasopharyngeal Carcinoma: The JUPITER-02 Randomized Clinical Trial. *JAMA.*, *330*(20), 1961-1970.

Mao Y P, Xie F Y, Liu L Z, et al., (2009). Re-evaluation of 6th edition of AJCC staging system for nasopharyngeal carcinoma and proposed improvement based on magnetic resonance imaging. *Int J Radiat Oncol Biol Phys*, *73*(5), 1326-1334.

Na Z, Ping L I, Zhu-Mei L., (2010). Neoadjuvant chemotherapy for locally advanced nasopharyngeal carcinoma: A systematic review. *Journal of Practical Oncology*, *25*(1), 49-55. DOI:10.3724/SP.J.1008.2010.01244.

PENG H, CHEN B, HE S, et al., (2021). Efficacy and toxicity of three induction chemotherapy regimens in locoregionally advanced nasopharyngeal carcinoma: outcomes of 10-year follow-up. *Front Oncol*, *11*, 765378.

POSNER M R, HERSHOCK D M, BLAJMAN C R, TAX 324 study group, et al., (2007). Cisplatin and fluorouracil alone or with docetaxel in head and neck cancer. *N Engl J Med*, *357*(17), 1705-1715.

Qiu W, Huang P, Shi J, et al., (2015). Comparison of efficacy of induction chemotherapy plus intensity-modulated radiotherapy and concurrent chemo-radiotherapy plus adjuvant chemotherapy for patients with loco-regionally advanced nasopharyngeal carcinoma. *Chinese Journal of Clinical Oncology*.

Sun Y, Li WF, Chen NY, Zhang N, Hu GQ, Xie FY, et al., (2016 Nov). Induction chemotherapy plus concurrent chemoradiotherapy versus concurrent chemoradiotherapy alone in locoregionally advanced nasopharyngeal carcinoma: a phase 3, multicentre, rando-mised controlled trial. *Lancet Oncol*, *17*(11), 1509-1520.

Torre L A, Bray F, Siegel R L, et al., (2015). Global cancer statistics, 2012. *Ca A Cancer Journal for Clinicians*, *65*(2), 87-108.

Wu M Y, Ou D, He X, et al., (2017). Long-term results of a phase II study of gemcitabine and cisplatin chemotherapy combined with intensity-modulated radiotherapy in locoregionally advanced nasopharyngeal carcinoma. *Oral Oncology*, *73*, 118-123.

Wu X, Huang P Y, Peng P J, et al., (2013). Long-term follow-up of a phase III study comparing radiotherapy with or without weekly oxaliplatin for locoregionally advanced nasopharyngeal carcinoma. *Ann Oncol*, *24*(8), 2131-2136.

Yalin X, Jianming X, Oncology D O, et al., (2015). Clinical observation of TP induction chemotherapy combined with concurrent chemoradiotherapy in untreated locally advanced nasopharyngeal carcinoma. *Chinese Clinical Oncology*.

Yang Y, Pan J, Wang H, et al., (2023 Jun 12). Tislelizumab plus chemotherapy as first-line treatment for recurrent or metastatic nasopharyngeal cancer: A multicenter phase 3 trial (RATIONALE-309). *Cancer Cell*, *41*(6), 1061-1072.e4.

Yang YQ, Qu XM, Z X, et al., (2018). Clinical efficacy of GP, PF and TPF chemotherapy combined with intensity-modulated radiotherapy for nasopharyngeal carcinoma. *Chinese Journal of Cancer*, *28*(8), 602-608.

Yang Z, Zuo Q, Liu R, et al., (2023 Nov 24). Neoadjuvant chemotherapy followed by concurrent chemoradiotherapy with or without nimotuzumab in the treatment of locally advanced nasopharyngeal carcinoma: a retrospective study. *BMC Cancer*, *23*(1), 1140.

Yoshizaki T, Ito M, Murono S, et al., (2012). Current understanding and management of nasopharyngeal carcinoma. *Auris Nasus Larynx, 39*(2), 137-144.

Zhang L, Chen Q Y, Liu H, et al., (2013). Emerging treatment options for nasopharyngeal carcinoma. *Drug Design, Development and Therapy*, *7*(1), 37-52.

Zhao L, Xu M, Jiang W, et al., (2017). Induction chemotherapy for the treatment of non-endemic locally advanced nasopharyngeal carcinoma. *Oncotarget*, *8*(4), 6763-6774.

Paradigm Academic Press
Journal of Innovations in Medical Research
ISSN 2788-7022
APR. 2025 VOL.4, NO.2

Comparative Study on Response Efficacy of Generative Artificial Intelligence Large Language Model for Elderly Diabetes Mellitus

Ainingkun Xiang[1], Jingxue Tian[1], Dehua Hu[1] & Haixia Liu[1]

[1] College of Life Sciences, Central South University, Changsha, Hunan, China

Correspondence: Haixia Liu, College of Life Sciences, Central South University, Changsha, Hunan, China.

doi:10.63593/JIMR.2788-7022.2025.04.008

Abstract

We aimed to evaluate the response accuracy of different generative artificial intelligence (GAI) large language models to common problems of elderly diabetes, so as to compare the performance differences of various AI large language models in the quality of medical information service.

A standardized evaluation question pool containing 10 elderly diabetes related questions was constructed, and then four GAI chat robots using different generative artificial intelligence large language model were selected to answer the questions and score the accuracy of all answers. In addition, the problem is summarized into two dimensions of “diagnosis and evaluation” and “control and treatment”, and the above four GAI big language models are analyzed in these two dimensions.

In general, Moonshot model and Lark model are significantly better than DeepSeek LLM and SparkDesk model in response to common problems of elderly diabetes, with higher accuracy and strong stability, but there is no significant difference in response performance between Moonshot model and Lark model. In addition, in the dimensions of “diagnosis and evaluation” and “control and treatment”, Moonshot model and Lark model have better performance than DeepSeek LLM model and SparkDesk model.

Keywords: generative artificial intelligence, chat robot, large language model, senile diabetes mellitus, medical informatics

1. Introduction

Generative artificial intelligence (GAI) is an important branch of artificial intelligence. It is a technology that generates text, pictures, sounds, videos, codes and other content based on Algorithms and models.

At present, the AI technology system presents a diversified development trend, and its application scenarios have covered all fields of social production and life, which has attracted people’s attention. It is worth noting that there are significant differences in the technical complexity and intelligence level of different AI systems, and this heterogeneity directly affects its application effect and promotion value.

At present, AI has been widely used in the medical field. Many systems such as “AI triage” and “AI seeking medical treatment” have emerged. The acceptance and trust of medical staff and patient groups in AI driven medical information retrieval and analysis services have significantly increased. AI plays an active role in medical service efficiency, health management methods, etc., but it also faces risks and challenges in data privacy and security, algorithm deviation, ethics, etc. (Li et al., 2025). Therefore, the research on the application of artificial intelligence in medical treatment has a strong practical value.

In 2025, China’s generative AI model enters a new stage of development. DeepSeek, a large language model of artificial intelligence independently developed by China, has three major characteristics of “easy to use, open source, and free”. It has caused significant repercussions in the AI field, has been favored by many systems and

users, and has triggered huge discussions around the world. In terms of data, only 20 days after the DeepSeek application went online, its daily active users reached 22.15 million. At the same time, there have also been many related studies, such as taking DeepSeek as an example, discussing the technological transition, institutional synergy and technological civilization reconstruction in the digital Paradigm Innovation in the post ChatGPT era (Ling, 2025); Starting from DeepSeek, this paper discusses the supervision of generative artificial intelligence (Deng et al., 2025). At the same time, there are other AI with high popularity at present, such as the Doubao model, which has stood out in the fierce competition and achieved the counter attack of last mover first mover (Lei, 2025). The iFLYTEK spark has jointly developed the industry model with more than 20 industry enterprises, and the load of iFLYTEK spark app has exceeded 100million times (Liu, 2024). Kimi, launched in October 2023 by the dark side of the moon, an AI start-up, is the world's first intelligent assistant product that supports the input of 200000 Chinese characters (Zhao, 2024). This study selected four large-scale language models (Moonshot model, Lark model, DeepSeek LLM and SparkDesk model) as the research object, through the in-depth analysis and comparison of these cutting-edge intelligent dialog systems, this study can provide valuable references for academic research in related fields and benefit a wider range of user groups.

Senile diabetes refers to the metabolic syndrome caused by abnormal blood glucose metabolism in older people older than 60 years old. It is a common disease and frequently occurring disease, and has been widely concerned by older people. According to the data of the International Diabetes Federation, the number of diabetic patients aged 65 years and older in China is about 35.5 million. As the aging of the population continues to deepen, the number of elderly patients with diabetes is still on the rise. With the development of the Internet, more and more people use the Internet for elderly diabetes counseling. However, due to the problems of virtual and real information and information overload, the current situation of elderly diabetic patients obtaining health information from the network is not optimistic (Feng et al., 2024). Therefore, this study has important theoretical and practical significance for improving the quality of health knowledge acquisition of the elderly group, helping to improve the health literacy of the population.

In this study, the research team constructed a standardized assessment question pool containing 10 elderly diabetes related issues, and then selected four large-scale language models (Moonshot model, Lark model, DeepSeek LLM and SparkDesk model) as the research object, using its supported AI products (Kimi, Doubao AI DeepSeek, iFLYTEK spark AI) answered the questions and scored the accuracy of all answers. In addition, the questions were summarized into two dimensions of "diagnosis and evaluation" and "control and treatment", and the above four generative AI large language models were analyzed in these two aspects. The purpose of this study is to evaluate the response accuracy of different generative AI large-scale language models for common problems of elderly diabetes, so as to compare the performance differences of different generative AI large-scale language models in the quality of medical information service.

2. Materials and Methods

2.1 Design of Diabetes Related Issues

For older diabetes, the research team first designed a series of older diabetes related problem pool with high clinical value and public attention through literature review and expert consultation. Then 10 questions with clear answers in Guideline for the Management of Diabetes Mellitus in the Elderly in China (2024 edition) were selected, which covered key areas such as blood glucose control, complication prevention, lifestyle intervention, and the reference answers were given by referring to the standard. In addition, the problems are summarized into two dimensions of "diagnosis and evaluation" and "control and treatment". Subsequently, the research team selected four large-scale language models (Moonshot model, Lark model, DeepSeek LLM and SparkDesk model) as the research object, using its supported GAI products (Kimi, Doubao AI, DeepSeek and iFLYTEK spark AI) to test, input questions to each GAI under the same environmental conditions, and fully record its text output results.

In addition, before asking questions, the research team first input "Hello, next, I have a few questions to ask you, please give accurate and detailed answers as far as possible. Please try to answer according to the Chinese guidelines for the diagnosis and treatment of diabetes in the elderly (2024 version)", to ensure the consistency of the reference standards.

Table 1 shows 10 elderly diabetes related problems and dimension division.

Table 1. Details and dimensions of 10 questions

Question number	Question details	Dimension
1	What are the different types of senile diabetes	Null
2	Diagnostic criteria of diabetes mellitus in the elderly in China	Diagnosis

		and evaluation
3	What are the preventive measures for diabetes in the elderly (it is best to give each measure of tertiary prevention)	Null
4	I am an elderly diabetic. How can I adjust my lifestyle	Control and treatment
5	I am an elderly diabetic patient, only complicated with hypertension, without impairment of activities of daily living and instrumental activities of daily living. According to China's comprehensive health assessment criteria for elderly diabetic patients, is my health status good	Diagnosis and evaluation
6	I am an elderly diabetic who is using drugs with a high risk of hypoglycemia. After being evaluated according to China's comprehensive health assessment criteria for elderly diabetic patients (2024), my health is in good condition. According to the blood glucose control target of elderly diabetic patients in China, how much should I control my glycated hemoglobin, fasting or pre meal blood glucose, and bedtime blood glucose respectively	Control and treatment
7	I am an elderly diabetic with atherosclerotic cardiovascular disease. According to China's diabetes management standards, how much should I control my systolic blood pressure	Control and treatment
8	According to China's diabetes management standards, the hypoglycemia of elderly diabetic patients receiving drug treatment is divided into three grades	Diagnosis and evaluation
9	I am an elderly diabetic who is taking metformin, but has renal failure (estimated glomerular filtration rate is 40ml / [min · (1.73m2)]. Can I continue taking metformin? If not, what other drugs can I use	Control and treatment
10	Perioperative management of elderly patients with diabetes mellitus	Control and treatment

2.2 Score the Answers of the Four Generative AI Large Language Models

According to the GAI answers, the research team used the above four AI large-scale language model chat robots to score the accuracy of all the answers according to the reference answers formulated above (formulated according to Guideline for the Management of Diabetes Mellitus in the Elderly in China (2024 edition)) and the comparison with each other. Each item was scored on a 1-5 scale (1 is completely inaccurate, 5 is completely accurate), and the full score for each GAI is 50.

The specific operation is that the research team opens a new dialogue and inputs to each GAI under the same environmental conditions: "Hello, now please rate the accuracy of the following four answers A, B, C and D. The scoring standard is the correct answers I provide you below and the comparison between them. Please use a 1-5 score system for scoring (1 is completely inaccurate, 5 is completely accurate)." The format of the request for rating is: "the correct answer is: XX, the answer of a is: XX, the answer of B is: XX, and the answer of D is: XX."

2.3 Statistical Analysis of Score Results

According to the comprehensive situation, descriptive statistical analysis (Stata 18) was carried out on the 10 item scores of the four GAI, and the accuracy scores obtained and the stability of the scores were analyzed. Then, the normality test (Stata 18) was carried out on the overall data and the 10 item average scores of each AI, and Friedman test and pairwise comparison (SPSS 26) were carried out, and finally the statistically significant comprehensive ranking was obtained.

For the two dimensions of "diagnosis and evaluation" and "control and treatment", descriptive statistical analysis (Stata 18) was carried out on the score of the four GAI related dimensions, Shapiro Wilk W test normal test (Stata 18) was carried out, and Friedman test was used to analyze the significance of the difference (SPSS 26), as well as pairwise comparison after Bonferroni correction (SPSS 26), and finally a statistically significant comprehensive ranking was obtained.

3. Results

3.1 Raw Score Data of Four GAI

Table 2 shows the scoring and being scored of four AI large language model chat robots (iFLYTEK spark AI

(hereinafter referred to as XF), Doubao AI (hereinafter referred to as db), DeepSeek and Kimi) based on four generative AI large language models.

Table 2. GAI score data

Question number	GAI	Scores by GAI			
		xf	db	DeepSeek	Kimi
1	xf	2	3	3	3
	db	5	4	4	4
	DeepSeek	3	4	5	2
	Kimi	4	4	4	5
2	xf	3	3	4	3
	db	4	4	5	4
	DeepSeek	5	4	4	2
	Kimi	4	4	5	5
3	xf	3	3	3	3
	db	5	4	5	5
	DeepSeek	4	4	4	5
	Kimi	4	4	5	5
4	xf	3	2	3	2
	db	4	3	4	3
	DeepSeek	2	4	5	4
	Kimi	5	4	5	5
5	xf	4	4	4	3
	db	5	4	5	5
	DeepSeek	3	3	3	2
	Kimi	5	4	4	5
6	xf	4	2	4	3
	db	5	5	5	5
	DeepSeek	3	3	3	2
	Kimi	5	5	5	5
7	xf	3	3	3	3
	db	5	4	5	5
	DeepSeek	2	2	4	2
	Kimi	4	5	4	4
8	xf	2	1	3	3
	db	4	4	5	5
	DeepSeek	3	4	4	3
	Kimi	5	5	5	5
9	xf	5	4	4	3
	db	5	4	5	4
	DeepSeek	2	2	3	5
	Kimi	4	4	4	4
10	xf	3	2	3	3
	db	5	4	4	4

DeepSeek	4	2	5	4
Kimi	4	4	4	5

Notes: xf: iFLYTEK spark AI, db: Doubao AI, the same below.

3.2 Statistical Results of Four GAI

3.2.1 Descriptive Statistics

Descriptive statistical analysis was carried out on the scores of the ten questions of the four GAI (full score is 50), and the results are shown in Table 3.

Table 3. Descriptive statistical results of GAI score data

GAI	Average	Median	Total	Standard deviation
db	4.45	4.5	45	0.422
Kimi	4.50	4.5	45	0.333
DeepSeek	3.35	3.5	34	0.568
xf	3.05	3.0	31	0.538

(1) Accuracy: the scores of Kimi and Doubao are significantly higher than those of other GAI (the average scores are 4.50 and 4.45, respectively, with a median of 4.5), and the total scores are 45 and 45, respectively, indicating that they perform best in the accuracy of answers.

(2) The stability of accuracy score: Kimi's standard deviation is the smallest (0.333), the score fluctuation is the smallest, and the stability is the best; Doubao followed (standard deviation 0.422), while DeepSeek and iFLYTEK were less stable (standard deviation > 0.5).

3.2.2 Normality Test

For the overall data, Shapiro Wilk test showed that all 160 original scores did not meet the normal distribution ($w=0.979$, $p=0.018 < 0.05$). For the 10 item average score of each GAI, the average scores of the four GAI were in line with the normal distribution (P values > 0.05) after respective tests. Table 4 and Figure 1 show the results.

Table 4. Overall data and score test results of each GAI

Variable	Obs	W	V	z	Prob>z
xf	10	0.97644	0.363	-1.583	0.94332
db	10	0.93547	0.994	-0.009	0.50378
DeepSeek	10	0.9409	0.911	-0.159	0.5631
Kimi	10	0.95751	0.655	-0.697	0.75714
Overall	160	0.97948	2.523	2.105	0.01763

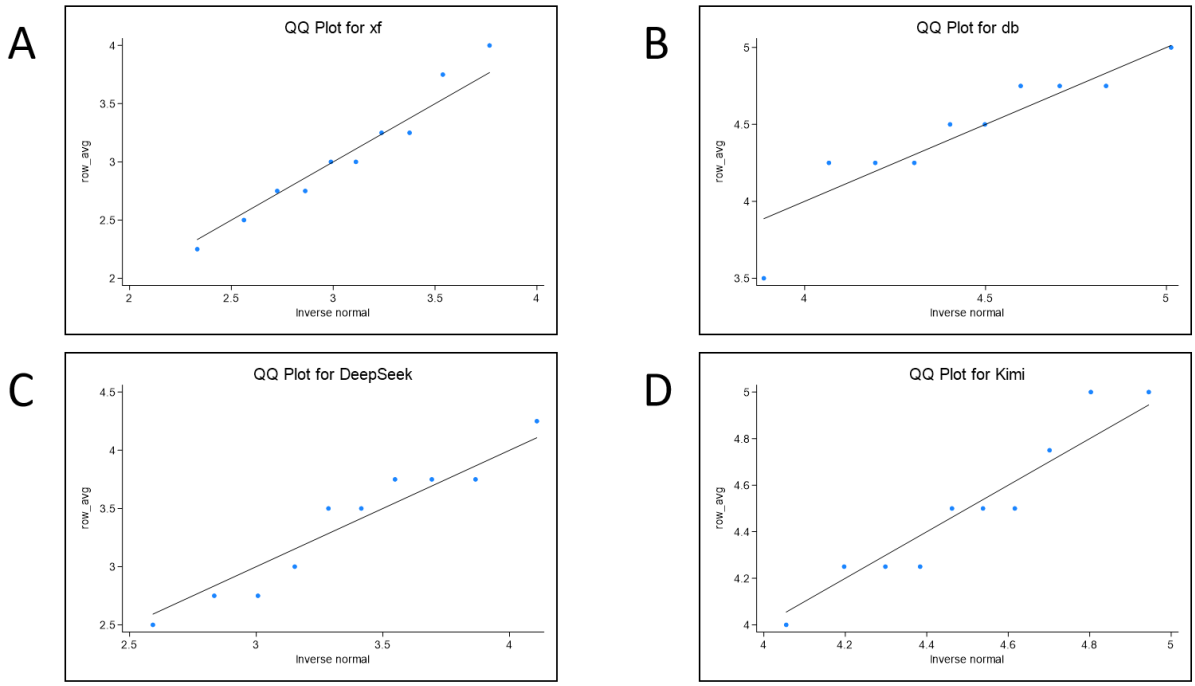

Figure 1. QQ plot for score test of four GAI

Notes: Score test QQ plot of four GAI (A) QQ plot of iFLYTEK spark AI score data; (B) QQ plot of Doubao AI score data; (C) QQ plot of DeepSeek score data; (D) QQ plot of Kimi score data.

3.2.3 Friedman Test and Pairwise Comparison

(1) Friedman test: the results showed that the scores of different GAI were significantly different ($\chi^2 = 29.4$, df=3, p<0.001).

(2) Pairwise comparisons after Bonferroni correction are shown in Table 5. The P value was compared with the corrected significance level (α =0.0083).

$$\alpha_{corrected} = \frac{0.05}{\text{Number of comparisons}} = \frac{0.05}{6} \approx 0.0083$$

Table 5. Statistical analysis results of GAI pairwise comparison

Comparison object	P value	significant（α=0.0083）
xf vs db	0.0001	Ture
xf vs DeepSeek	0.0012	Ture
xf vs Kimi	0.0001	Ture
db vs DeepSeek	0.0023	Ture
db vs Kimi	0.87	False
DeepSeek vs Kimi	0.0015	Ture

Significant difference group: Doubao AI vs iFLYTEK spark AI (p=0.0001), Doubao AI vs DeepSeek (p=0.0023), Kimi vs iFLYTEK spark AI (p=0.0001), Kimi vs DeepSeek (p=0.0015), DeepSeek vs iFLYTEK spark AI (p=0.0012).

There was no significant difference between Doubao AI and Kimi (p=0.87).

In summary, through Friedman test and Bonferroni correction, it was confirmed that Doubao and Kimi were significantly better than other GAI (p<0.0083).

3.2.4 Comprehensive Ranking

According to the comprehensive performance of accuracy (average score, total score) and stability (standard deviation), the ranking is as follows:

No.1 Kimi: The accuracy was the highest (average score is 4.50, total score is 45.0), and the stability of accuracy score was the best (standard deviation is 0.3333).

No.2 Doubao AI: The accuracy is slightly inferior to Kimi (average score is 4.45), and the stability of accuracy score is suboptimal (standard deviation is 0.4216), but there is no significant difference with Kimi.

No.3 DeepSeek: The accuracy was low (mean score is 3.35), and the stability of accuracy score was poor (standard deviation is 0.5676).

No.4 iFLYTEK spark AI: The accuracy is the lowest (average score is 3.05), and the stability of accuracy score is the worst (standard deviation is 0.5375).

3.3 Statistical Results of "Diagnosis and Evaluation", "Control and Treatment" Dimension

3.3.1 Descriptive Statistics of Two Dimensions

Table 6. Descriptive statistical analysis results of "diagnosis and evaluation", "control and treatment" dimensions

Dimension	GAI	Average	Median	Total	Standard deviation
Diagnosis and evaluation	DeepSeek	3.33	3.0	40	0.888
	Kimi	4.67	5.0	56	0.492
	xf	3.08	3.0	37	0.900
	db	4.50	4.5	54	0.522
Control and treatment	xf	3.10	3.0	62	0.788
	db	4.40	4.5	88	0.681
	DeepSeek	3.15	3.0	63	1.137
	Kimi	4.45	4.0	89	0.510

"Diagnosis and evaluation" dimension:

(1) Kimi's average score was the highest (4.67), indicating that the accuracy of his answer was the best; Doubao AI was the second (4.50), and its performance was also relatively excellent; The average scores of DeepSeek and iFLYTEK spark AI are low (3.33 and 3.08, respectively), and their performance is relatively poor.

(2) The median of Kimi and Doubao AI were 5 and 4.5, respectively, indicating that their score distribution was biased towards high scores; The median score of DeepSeek and iFLYTEK spark AI is 3, indicating that their score distribution tends to be medium or low.

(3) Kimi's total score was the highest (56), followed by Doubao AI (54), which was significantly better than DeepSeek (40) and Xunfei spark AI (37).

(4) Kimi's standard deviation was the smallest (0.492), indicating that its score fluctuation was the smallest and its stability was the best; The Doubao AI was the second (0.522), and its stability was good; The standard deviations of DeepSeek and iFLYTEK spark AI are relatively large (0.888 and 0.900, respectively), indicating that their scores fluctuate greatly and have poor stability.

"Control and treatment" dimension:

(1) Kimi's average score was the highest (4.45), indicating that the accuracy of his answer was the best; The Doubao AI was the second (4.4), and its performance was also relatively excellent; DeepSeek and iFLYTEK spark AI have low average scores (3.15 and 3.1, respectively) and relatively poor performance.

(2) The median of Doubao and Kimi were 4.5 and 4, respectively, indicating that their score distribution was biased towards high scores; The median score of DeepSeek and iFLYTEK spark AI is 3, indicating that their score distribution is biased towards medium or low scores.

(3) Kimi's total score was the highest (89), followed by Doubao AI (88), which performed significantly better than DeepSeek (63) and Xunfei spark AI (62).

(4) Kimi's standard deviation is the smallest (0.510), indicating that its score fluctuation is the smallest and its stability is the best; Doubao AI was the second (0.681), and its stability was good; The standard deviations of DeepSeek and iFLYTEK spark AI are relatively large (0.788 and 1.137, respectively), indicating that their scores fluctuate greatly and have poor stability.

3.3.2 Normality Test of Two Dimensions

The results of analyzing the normality of each GAI separately are shown in Figure 2.

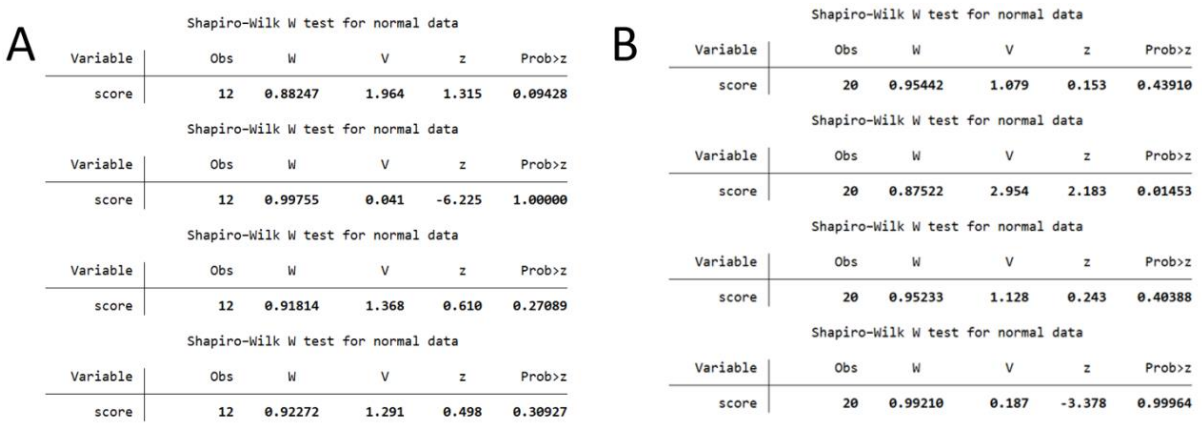

Figure 2. Normality test results of each GAI (A) Normality test results of "diagnosis and evaluation" dimension; (B) normality test results of "control and treatment" dimension

Notes: From top to bottom: iFLYTEK spark AI, Doubao AI, DeepSeek, Kimi.

"Diagnosis and evaluation" dimension: In the Shapiro Wilk W test normal test, the P values of the four GAI are > 0.05, and the original hypothesis is accepted, so the score distribution of the four GAI meets the normal distribution at the 0.05 significance level; Among them, the P value corresponding to Doubao AI is as high as 1.00, indicating that it is very close to normal and has good stability; In contrast, the P value corresponding to iFLYTEK spark AI is only 0.09428, indicating that its distribution may be skewed or abnormal, with poor stability.

"Control and treatment" dimension: In Shapiro Wilk W test normal test, iFLYTEK spark AI, DeepSeek and Kimi have P values > 0.05, and accept the original hypothesis, so the score distribution of these three GAI meets the normal distribution at the 0.05 significance level; The P value corresponding to Kimi is as high as 0.99964, indicating that it is very close to normal and has good stability; However, the P value of AI in Doubao =0.01453 < 0.05 rejected the original hypothesis, so its distribution did not conform to the normal distribution, indicating that its distribution may be skewed or abnormal, with poor stability.

3.3.3 Significance of Differences Between Two Dimensions by Friedman Test

Table 7. Friedman test results

Inspection statistics[a]		
Dimension		
	Diagnosis and evaluation	Control and treatment
Number of cases	12	20
Chi-square	21.471	25.575
Free degree	3	3
Asymptotic significance	0.000	0.000

Notes: a. Friedman test.

"Diagnosis and evaluation" dimension: Chi square value is 21.471, P value < 0.001, rejecting the original hypothesis, so there are significant differences in different GAI scores.

"Control and treatment" dimension: Chi square value is 25.575, P value < 0.001, rejecting the original hypothesis, so there are significant differences in different GAI scores.

3.3.4 Pairwise Comparison of Two Dimensions After Bonferroni Correction (Corrected α =0.0083)

Table 8. GAI pairwise comparison results

Inspection statistics[a]

		db - xf	DeepSeek - xf	Kimi - xf	DeepSeek - db	Kimi - DeepSeek	Kimi - db
Diagnosis and evaluation	Z	-3.002[b]	-0.540[b]	-2.840[b]	-2.547[c]	-2.676[b]	-1.000[b]
	Asymptotic significance (two tailed)	0.003	0.589	0.005	0.011	0.007	0.317
Control and treatment	Z	-3.841[b]	-0.354[b]	-3.582[b]	-3.065[c]	-3.265[b]	-0.258[b]
	Asymptotic significance (two tailed)	0.000	0.724	0.000	0.002	0.001	0.796

Notes: A. Wilcoxon signed rank test, B. based on negative rank, C. based on positive rank.

“Diagnosis and evaluation” dimension:

Comparing the P value in the pairwise comparison results with 0.0083, the P values corresponding to Doubao and iFLYTEK spark AI, Kimi and iFLYTEK spark AI, Kimi and DeepSeek are all less than 0.0083, so there is a significant difference between them, while the P values corresponding to DeepSeek and iFLYTEK spark AI, DeepSeek and Doubao AI, Kimi and Doubao AI are all bigger than 0.0083, so there is no significant difference between them.

“Control and treatment” dimension:

Comparing the P value in the pairwise comparison results with 0.0083, the P values corresponding to Doubao AI and iFLYTEK spark AI, Kimi and iFLYTEK spark AI, DeepSeek and Doubao AI, Kimi and DeepSeek are all less than 0.0083, so there is a significant difference between them, while the P values corresponding to DeepSeek and iFLYTEK spark AI, Kimi and Doubao AI are all bigger than 0.0083, so there is no significant difference between them.

3.3.5 Ranking of Two Dimensions

“Diagnosis and evaluation” dimension:

Score of this dimension: Kimi > Doubao AI > DeepSeek > iFLYTEK spark AI

Score stability of this dimension: Kimi > Doubao AI > DeepSeek > iFLYTEK spark AI

“Control and treatment” dimension:

Score of this dimension: Kimi > Doubao AI > DeepSeek > iFLYTEK spark AI

Score stability of this dimension: Kimi > Doubao AI > DeepSeek > iFLYTEK spark AI

Kimi has no significant difference with Doubao AI, but it is significantly better than DeepSeek and iFLYTEK spark AI (there is also no significant difference between them).

4. Discussion

This study shows that, in general, the Moonshot model (represented by Kimi) and the Lark model (represented by Doubao AI) perform best in answering questions related to older diabetes, with high accuracy and stability, and are recommended to be used preferentially in medical consultation. The performance of SparkDesk model (represented by iFLYTEK spark AI) and DeepSeek LLM (represented by DeepSeek) is relatively weak, and the answer logic needs to be optimized. In addition, in the dimensions of “diagnosis and evaluation” and “control and treatment”, the Moonshot model has better performance than the Lark model and the DeepSeek LLM model. The analysis of this study is based on strict statistical tests, ensuring the scientificity and reliability of the conclusions.

The reason for this phenomenon is the difference between the algorithm of generative AI and knowledge updating. Therefore, this study also provides a foundation for the in-depth study of generative AI. At present, there are also many researches on the algorithm of GAI, such as the discussion on the innovation and optimization of DeepSeek series models in large model training (Zhang, 2025), and for six serum tumor markers, eight different joint detection models are built in the modeling cohort and test cohort by combining eight different AI algorithms, and the joint detection model with the best performance is selected (Ren et al., 2025). This research is beneficial to the algorithm research and knowledge updating research of GAI.

At present, with the rapid development of artificial intelligence technology, its deep integration with the medical

and health field has become an important frontier direction of current research. As for the relevant research on the performance comparison of different AI in medicine, the current number of studies is relatively small, and the scoring method is human doctors' evaluation. Foreign researchers put forward ten common anesthesia questions to three AI chat robots: chatGPT4 (openAI), Bard (Google) and Bing chat (Microsoft). Five resident program directors from 15 medical institutions in the United States evaluated the answers of each chat robot in a randomized, blinded order (NGUYEN et al., 2024). Domestic researchers have also studied the differences between a variety of large-scale language models and the answers of ophthalmologists (Hu, 2023). Compared with them, this study formulated the reference answer according to the comprehensive evaluation standard of health status of elderly diabetic patients in China (2024), and used AI to score based on the reference answer and the comparison, which greatly reduced the influence of subjectivity. In addition, this study summarized the problems into two dimensions, "diagnosis and evaluation" and "control and treatment", and compared the two dimensions to enhance the depth of the study. In addition, the research object of this study is four AI large-scale language model chat robots (iFLYTEK spark AI, Doubao AI, DeepSeek, Kimi) with high popularity in China, which has greater significance for the current Chinese people's choice of AI.

The reliability of the application of artificial intelligence in the medical field has also received close attention. Current research focuses on whether artificial intelligence is reliable for disease detection. Some studies have evaluated the clinical safety of AI supported screen reading scheme compared with standard screen reading after mammography by radiologists, and found that compared with standard double reading, AI supported mammography screening produced similar cancer detection rate and greatly reduced screen reading workload, indicating that AI is safe to use in mammography screening (LåNG et al., 2023). Some researchers conducted a cluster randomized cross-over controlled trial to evaluate the impact of artificial intelligence — based diagnostic support software on the detection of proximal caries on wing X-rays, and proposed that AI could improve the diagnostic accuracy of dentists (MERTENS et al., 2021). As well, a randomized comparative effectiveness trial showed that AI-cbt-cp (cognitive behavioral therapy for chronic pain using artificial intelligence) was not inferior to the telephone CBT-CP (cognitive behavioral therapy for chronic pain) provided by the therapist, and the time needed by the therapist was greatly reduced (PIETTE et al., 2022). And, according to the Chinese and English nursing suggestions given by ChatGPT, some researchers evaluated its application value in chronic disease nursing (Yin et al., 2024).

In addition, this study also triggered the research team's thinking on the relationship between AI and traditional medical industry. AI technology is reshaping the medical industry, and there are questions like "Will the application of AI in the medical field replace doctors in the future?" (Zhu et al., 2025). The research team believes that the appropriate application of AI can promote the development of the medical industry. However, AI still faces many challenges in medical practice, including ethical dilemmas, data privacy issues and the lack of humanistic care. These limitations indicate that AI cannot completely replace the role of traditional doctors. The two promote each other and advance hand in hand is the ultimate solution of "AI+ medical" in the future.

There is also room for improvement in this study, such as evaluating the response performance of the generative AI large language model only from the dimension of "accuracy", and exploring the theme of "older diabetes". In addition, the evaluation system of the generative AI large language model is not absolutely scientific and accurate. More research dimensions, research topics, and research numbers will help enhance the value of research.

Author Contribution Statement

Ainingkun Xiang is responsible for the design of questions, the collection of scores and the writing of the first draft. Jingxue Tian is responsible for the statistical analysis of the original score data, and participated in the writing and revision of the article. Haixia Liu and Dehua Hu provided important guidance for this study in terms of topic selection, implementation, article revision, and detail optimization.

Declaration of Interest

All authors declare that there are no conflicts of interest.

Acknowledgements

This work was supported by National Social Science Foundation of China (Project No.: 20BTQ081); Research and development project in key fields of Hunan Province (Project No.: 2021WK2003).

References

DENG J P, ZHAO Y S., (2025). The breaking and changing situation of DeepSeek: on the regulatory direction of generative AI. *Journal of Xinjiang Normal University (Edition of Philosophy and Social Sciences)*, (04), 1-10.

FENG C Q, MENG L X, LUO G Q, et al., (2024). Research progress on the acquisition behavior of network health

information of elderly diabetic patients. *Chinese Medical Sciences*, *14*(21), 40-3.

HU C L., (2023). The application of the large language models in ophthalmic consultation. Guangdong: Shantou University.

LåNG K, JOSEFSSON V, LARSSON A M, et al., (2023). Artificial intelligence-supported screen reading versus standard double reading in the Mammography Screening with Artificial Intelligence trial (MASAI): a clinical safety analysis of a randomised, controlled, non-inferiority, single-blinded, screening accuracy study. *Lancet Oncol*, *24*(8), 936-44.

LEI C., (2024). ByteDance Doubao is very popular, and the AI industry chain is collectively restless. *21st Century Business Herald*, 012.

LI T, ZHANG J, LI Y Z, et al., (2025). Innovative Applications, Risk Challenges and Governance Countermeasures of Artificial Intelligence in the Field of Healthcare. *Journal of Medical Informatics*, *46*(01), 2-8+16.

LING X X., (2025). DeepSeek Ushers in the Post-ChatGPT Era: On Digital Paradigm Innovation and Its Operational Philosophy. *Journal of Northwestern Polytechnical University (Social Sciences)*, 1-9.

LIU Q F., (2024). The latest development and industrial application of Spark model technology. *China Economic Report*, (04), 130-3.

MERTENS S, KROIS J, CANTU A G, et al., (2021). Artificial intelligence for caries detection: Randomized trial. *J Dent*, *115*, 103849.

NGUYEN T P, CARVALHO B, SUKHDEO H, et al., (2024). Comparison of artificial intelligence large language model chatbots in answering frequently asked questions in anaesthesia. *BJA Open*, *10*, 100280.

PIETTE J D, NEWMAN S, KREIN S L, et al., (2022). 0 Patient-Centered Pain Care Using Artificial Intelligence and Mobile Health Tools: A Randomized Comparative Effectiveness Trial. *JAMA Intern Med*, *182*(9), 975-83.

REN N N, ZHANG H P, JIN S Y., (2025). Value of a combined detection model of six serum tumor markers and artificial intelligence algorithm in the diagnosis of lung cancer. *Zhejiang Medicine*, *47*(03), 268-73+339.

YIN B Q, LIU S Y, WANG H R, et al., (2024). Review on ChatGPT in Chronic Disease Nursing Care. *Military Nursing*, *41*(02), 83-5.

ZHANG H M., (2025). How DeepSeek-R1 was created? *Journal of Shenzhen University (Science and Engineering)*, 1-7.

ZHAO H., (2024). Domestic AI model Kimi's "debut" aims at the long text track. *China Strategic Emerging Industry*, (13), 72-5.

ZHU J L, ZHANG H, CHEN H., (2025). Will AI replace doctors? *Yangcheng Evening News*, A04.

Paradigm Academic Press
Journal of Innovations in Medical Research
ISSN 2788-7022
APR. 2025 VOL.4, NO.2

Metal Artifact Reduction MR Imaging After Arthroplasty: Advances and Clinical Applications

Zhangyan Xu[1]

[1] Department of Radiology, The First Affiliated Hospital of Chongqing Medical University, Chongqing, China

Correspondence: Zhangyan Xu, Department of Radiology, The First Affiliated Hospital of Chongqing Medical University, Chongqing, China.

doi:10.63593/JIMR.2788-7022.2025.04.009

Abstract

Total joint arthroplasty was an effective treatment for end-stage joint diseases, with rapid increasement and widely applied in clinical practice. Periprosthetic joint infection remains the most severe periprosthetic complications. MRI is the preferred imaging modality for evaluating musculoskeletal infections. However, conventional MRI in post-joint arthroplasty patients was significantly hindered by severe prothesis-induced artifacts, limiting the assessment of periprosthetic structures. Metal artifact reduction imaging has been developed to mitigate metal artifacts and enhance visualization of periprosthetic tissues, improving the detection and characterization of periprosthetic complications. This review systematically examines the advancements in metal artifact reduction imaging and its clinical applications in the assessment of periprosthetic complications.

Keywords: metal artifacts reduction, MRI, joint arthroplasty, periprosthetic complication

1. Introduction

Total joint arthroplasty is the most effective therapeutic intervention for managing advanced-stage osteoarthritis, with surgical volumes increasing annually in recent decades (Hamel, Toth et al., 2008; Melvin, Karthikeyan et al., 2014). The average rate of total hip arthroplasty (THA) and total knee arthroplasty (TKA) surged by 22% and 35%, respectively, across Organization for Economic Co-operation and Development (OECD) countries from 2009 to 2019 (OECD, 2021). According to the Annual Data Report on Artificial Joints in China, the number of THA and TKA witnessed a substantial increase, rising from 221,920 to 951,986 between 2011 and 2019, representing an average annual increase of 19.96% (Feng, Zhu et al., 2020). Periprosthetic complications increased gradually with the rising number of procedures, including aseptic loosening, periprosthetic fracture, linear wear, osteolysis, and periprosthetic joint infection (PJI). Among them, PJI stands as the foremost cause of TKA revision and the third leading cause for THA revision, 33% TKA revisions were attributed to PJI from a study based on national database in China (Kamath, Ong et al., 2015; Koh, Zeng et al., 2017; Long, Xie et al., 2023). PJI represents one of the most devastating complications, with associated mortality rates ranging from 2.7% to 18% (Voigt, Mosier et al., 2015), often requiring complex and challenging treatment with a result of poor prognosis (Bassetti, Castaldo et al., 2019; Long, Xie et al., 2023).

There is no single preoperative technique that can reliably diagnose PJI. Some patients exhibited nonspecific clinical manifestations, serum markers such as the erythrocyte sedimentation rate (ESR) and C-reactive protein (CRP) have only been reported with an accuracy of 76.47% and 75.00% for diagnosing PJI (Cheng, Yang et al., 2024). In addition, up to 50% of patients with aseptic periprosthetic complications also show elevated ESR and CRP (Jacobs, Cooper et al., 2014; Plummer, Berger et al., 2016). Invasive synovial fluid analysis by joint aspiration has been reported to identify about 65% of PJI cases (Abdel Karim, Andrawis et al., 2019). Microbiological and histological analyses are often limited due to low sensitivity of synovial microbiology and the fact that samples for histology are generally not available prior to revision surgery (Bassetti, Castaldo et al.,

2019; Romanò, Petrosillo et al., 2020).

Radiograph examinations play a crucial role in the follow-up of patients after joint replacement surgery. Existing imaging modalities have demonstrated limited sensitivity and accuracy in detecting PJI and were not yet to be incorporated into the PJI definition (Parvizi, Zmistowski et al., 2011; Osmon, Berbari et al., 2013; Romanò, Khawashki et al., 2019; McNally, Sousa et al., 2021). Magnetic resonance imaging (MRI) plays a vital role in the evaluation of musculoskeletal diseases, however, extensive metal artifacts around joint-prostheses often hinder the visualization of periprosthetic structures. Recent advancements in MRI metal artifact reduction techniques have reported which can minimize prosthesis-induced artifacts and distortion, improving the delineation of periprosthetic tissues (Sutter, Hodek et al., 2013; Liebl, Heilmeier et al., 2015). These developments offer new possibilities for MRI-based assessment of periprosthetic complications. This review provides an advanced analysis of MRI metal artifact reduction imaging and its clinical applications in the evaluation of periprosthetic complications.

2. MRI Metal Artifact Reduction Imaging

2.1 Optimization of Conventional Sequence Parameters

The severity of MR image distortion and metal artifacts in patients after joint arthroplasty was influenced by multiple factors, including the size, shape, material, and positioning of prosthesis, as well as the field strength of main magnetic, prosthesis orientation, bandwidth, voxel size, and slice thickness etc. Studies have demonstrated that lower field strengths, prosthesis orientation parallel to the main magnetic field, and diamagnetic materials of prosthesis result in relatively fewer metal artifacts (Ariyanayagam, Malcolm et al., 2015; Jungmann, Agten et al., 2017). Additionally, adjusting sequence parameters, such as increasing bandwidth, reducing voxel size or increasing matrix resolution, and decreasing slice thickness can effectively mitigate metal artifacts, among aforementioned strategies, increasing bandwidth was the most effective in metal artifact reduction, otherwise, these adjustments may compromise image signal-to-noise ratio and prolong scan time (Toms, Smith-Bateman et al., 2010; Jiang, He et al., 2016; Talbot & Weinberg, 2016; Feuerriegel & Sutter, 2024).

2.2 View Angle Tilting (VAT)

Significant magnetic susceptibility difference between joint-prosthesis and periprosthetic tissues was existed, which leaded to the inhomogeneities of main magnetic field and caused to shifts in resonance frequencies, finally resulting in metal artifacts and distortion in both the slice selection and frequency-encoding directions. Cho et al. (Cho, Kim et al. 1988) introduced the View Angle Tilting (VAT) technique, which applies an additional frequency-encoding gradient during signal readout. This induced a tilted readout trajectory, helping correct distortion and effectively reducing metal artifacts induced by field inhomogeneities. However, the VAT technique is constrained the duration of radiofrequency excitation, the added gradient may compromise signal-to-noise ratio and blurring of image edges. Moreover, VAT was useful in mitigating in-plane metal artifacts but has limited effectiveness in addressing through-plane distortions or signal voids (Popowski, Hiltbrand et al., 2000; Reichert, Ai et al., 2015).

2.3 Slice Encoding for Metal Artifact Correction (SEMAC)

Slice Encoding for Metal Artifact Correction (SEMAC) is an advanced spin-echo sequence that extends beyond high-bandwidth and the View Angle Tilting (VAT) technique. SEMAC introduced an additional phase-encoding gradient in the third dimension (Z-phase encoding gradient) to capture signals from off-resonance tissues and quantify the extent of image distortion. These signals are later reconstructed using a dedicated reconstruction algorithm, realigning displaced structures to their true anatomical positions, ultimately producing images with significantly reduced through-plane artifacts and geometric distortions and improved imaging quality (Talbot & Weinberg, 2016).

SEMAC has been proven to mitigate not only in-plane but also through-plane metal artifacts. Studies by Ma et al. (Ma, Zuo et al., 2018) and Jawhar et al. (Jawhar, Reichert et al., 2019) demonstrated that SEMAC outperforms conventional MRI sequences by substantially reducing metal artifacts and enhancing visualization of periprosthetic bone and soft tissue. However, the primary limitation of SEMAC is its prolonged scan time, which is directly proportional to the number of slice-encoding steps (SES). The required SES is determined by the severity of field inhomogeneity, as well as the size and shape of the prosthesis (Feuerriegel & Sutter, 2024). Research suggests that achieving clinically acceptable artifact reduction in MRI following total hip arthroplasty typically requires 11-19 SES (Lee, Lim et al., 2013; Germann, Nanz et al., 2021). The other limitations of SEMAC were increased computational load and potential signal-to-noise ratio reduction.

2.4 Multi-Acquisition Variable-Resonance Image Combination (MAVRIC)

The Multi-acquisition Variable-resonance Image Combination (MAVRIC) technique employed a three-dimensional fast spin echo acquisition with multi-spectral approach to capture signals from off-resonance

protons, and is designed to reduce both in-plane and through-plane metal artifacts resulting from susceptibility differences between metallic implants and surrounding tissues.

MAVRIC excited and acquired multiple overlapping narrow frequency bands, each targeting a different resonance shift, capturing signals from tissues that would otherwise be distorted or lost. Moreover, unlike traditional two-dimensional sequences, MAVRIC uses full-volume coverage, preventing slice misregistration and signal loss in areas affected by strong susceptibility gradients. Then, each individual spectral images are combined using post-processing algorithms to generate a final image with reduced metal artifacts and improved visualization of periprosthetic bone and soft tissue (Koch, Lorbiecki et al., 2009). A study by Hayter et al. (Hayter, Koff et al., 2011) demonstrated that MAVRIC significantly reduces periprosthetic metal artifacts in patients after hip, knee, and shoulder joint arthroplasty, enhancing the visualization of periprosthetic synovium, bone, and tendons, this improvement facilitates the detection of synovitis, periprosthetic osteolysis, and tendon ruptures. Additionally, a phantom study by Filli et al. (Filli, Jud et al., 2017) reported that MAVRIC outperforms SEMAC in metal artifact reduction; however, its major limitation is a prolonged scan time. Conversely, a study by Chen A et al. (Chen, Chen et al., 2011) on post-total knee arthroplasty MRI found that both MAVRIC and SEMAC significantly reduced periprosthetic metal artifacts, with no statistically significant difference between the two techniques in artifact reduction efficacy.

2.5 Multi-Acquisition Variable-Resonance Image Combination Selective (MAVRIC-SL)

The Multi-acquisition Variable-Resonance Image Combination Selective (MAVRIC-SL) technique was an advanced hybrid MRI technique, which combined MAVRIC's spectral selection technique with SEMAC's Z-phase encoding technique. By acquiring multiple spectral images across different frequency bands and subsequently reconstructing through post-processing, achieving significantly reduced metal artifacts MRI images (Koch, Brau et al., 2011). A small-sample prospective study by Nardo et al. (Nardo, Han et al., 2015) demonstrated that MAVRIC-SL effectively reduces metal-induced artifacts and enhances visualization of periprosthetic structures in both 1.5 T and 3.0 T MRI scanners. Similarly, studies by Choi et al. (Choi, Koch et al., 2015) and Kretzschmar et al. (Kretzschmar, Nardo et al., 2015) on MRI imaging of patients after hip joint arthroplasty confirmed that, compared to conventional two dimensional spin-echo sequences, MAVRIC-SL significantly minimizes metal artifacts and geometric distortions. This technique enhances the depiction of abnormal imaging findings around prosthetic joints and improves radiologists' confidence in diagnosing prosthesis-related complications.

2.6 Propeller Technology

The Propeller technique refers to a method in which signals are acquired in parallel to fill the K-space after each radiofrequency pulse excitation. Signals from multiple excitations are collected and fill the K-space in a radial pattern with a specific angle, resulting in the oversampling of the K-space center and improving the signal in the local spatial region. Different manufacturers have various names for the Propeller technique, including PROPELLER (the proprietary name for sample k-space in a rotating fashion in GE MR system), BLADE (the proprietary name for sample k-space in a rotating fashion in Siemens MR system), and ARMS (the proprietary name for sample k-space in a rotating fashion in United Imaging Healthcare MR system). This technique was mainly used as a motion resistant MRI technique to reduce motion artifacts and improve image quality (Fair, Wang et al., 2020). Additionally, the Propeller technique can also reduce magnetic susceptibility artifacts, and it has been demonstrated to outperform conventional sequences in imaging of the skull base and nasopharyngeal region (Mavroidis, Giankou et al., 2024; Xu, Liu et al., 2024). With the increasing number of metal implants and the severe interference of metal artifacts in postoperative MR imaging, which complicates the observation of surrounding structures, researchers have applied the Propeller technique to MRI imaging of patients with metal implants. A study by Li et al. (Li, Shi et al., 2022) demonstrated that the Propeller technique could reduce metal artifacts around dental implants and improve image quality. In a study on prostate diffusion-weighted imaging (DWI) following total hip replacement, it was shown that, compared to planar echo DWI, Propeller DWI significantly reduced metal artifacts and imaging distortion, providing better visualization of prostate lesions (Czarniecki, Caglic et al., 2018).

3. Clinical Applications of Metal Artifact Reduction Imaging

Metal artifact reduction MRI overcomes the limitations of traditional MRI, significantly reducing signal pile-up, signal loss, and imaging distortion around the prosthesis, improving the visualization of periprosthetic bone and soft tissues. This facilitates the detection of periprosthetic joint complication and helps differentiate between periprosthetic infections and non-infectious complications.

3.1 The Application of Metal Artifact Reduction Techniques in Structural Imaging

Serious studies have found MR imaging features, acquiring based on metal artifact reduction imaging, are beneficial for differentiating infectious from non-infectious periprosthetic complications. Schwaiger et al.

(Schwaiger, Gassert et al., 2020) investigated the usage of metal artifact reduction MRI (VAT) for distinguishing PJI from aseptic loosening after total hip arthroplasty, the results suggested that soft tissue swelling, abnormalities in both the acetabular and femoral components, and enlarged lymph nodes were more common in patients with PJI compared to those with aseptic loosening, aiding in the differentiation and guiding clinical treatment to improve prognosis. Fritz et al. (Fritz, Meshram et al., 2022) evaluated the feasibility and diagnostic efficacy of metal artifact reduction MRI (SEMAC) in diagnosing PJI after shoulder joint arthroplasty. Their study showed statistical differences between the infection and non-infection groups in joint effusion, complex joint effusion, edematous synovitis, extra-articular fluid accumulation, enlarged lymph nodes, periprosthetic bone marrow edema, and rotator cuff muscle swelling. Among these, complex joint effusion, enlarged lymph nodes, and edematous synovitis were the most effective in diagnosing PJI, with AUC values of approximately 0.91, 0.95, and 0.94, respectively, and sensitivity >85% and specificity >90%. Gao et al. (Gao, Jin et al., 2020) explored the diagnostic efficacy of metal artifact reduction (SEMAC) MRI imaging signs-layered synovitis-in determining periprosthetic infection after total hip arthroplasty, finding high sensitivity (0.80-0.88) and specificity (0.84-0.92). Galley et al. (Galley, Sutter et al., 2020) demonstrated that metal artifact reduction (SEMAC) MRI imaging features such as periosteal reaction, joint capsule swelling, and adjacent muscle edema showed significant differences between the PJI group and control groups, helping to differentiate infectious from non-infectious complications, with accuracy rates ranging from 86% to 91%. Levack et al. (Levack, Koch et al., 2022) found that metal artifact reduction (MAVRIC) MRI images were effective in diagnosing periprosthetic infection, displaying high specificity (99.6%). Inaoka et al. (Inaoka, Kitamura et al., 2022) also reported that after joint arthroplasty, metal artifact reduction (MAVRIC-SL) MRI imaging signs, including joint capsule thickening, soft tissue fluid accumulation, soft tissue swelling, pericapsular edema, and joint effusion, were indicative factors of periprosthetic infection.

3.2 The Application of Metal Artifact Reduction Techniques in Functional Imaging

Diffusion-weighted imaging (DWI) helps assess cell membrane integrity and the movement of water molecules in local tissues, providing quantitative apparent diffusion coefficient values, which are valuable for differentiating infectious from non-infectious lesions. However, clinically used-widely DWI sequences are mostly echo-planar imaging DWI, which is highly susceptible to magnetic field inhomogeneity. In patients after joint arthroplasty, EPI DWI imaging suffered from severe metal artifacts and geometric distortions, making it difficult to visualize peri-prosthetic bone and soft tissues. Previous studies have shown that Propeller (periodically rotated overlapping parallel lines with enhanced reconstruction) techniques can reduce susceptibility artifacts and improve the visualization of peri-prosthetic structures.

Currently, the application of DWI in patients after total knee/hip/shoulder joint arthroplasty remains limited. Gao et al. (Gao, Tan et al., 2023) proposed the two-dimensional multi-spectral Propeller DWI sequence, which integrated two-dimensional multi-spectral imaging and Propeller scanning techniques with diffusion-weighted imaging. In a study of 48 patients who underwent total hip arthroplasty, aforementioned sequence was used to acquire DWI images and analyze the differences in ADC values among different types of synovitis. The results showed no statistically significant differences in ADC values among the synovitis subtypes. Research on metal artifact reduction DWI sequences in patients after joint arthroplasty remains scarce, and further investigation is needed urgently.

4. Conclusions

In summary, MRI metal artifact reduction imaging has progressively evolved, with advanced techniques significantly reducing metal artifacts around prostheses and enhancing the visualization of periprosthetic bone and soft tissues. This progress plays a crucial role in detecting and differentiating periprosthetic joint complications in clinical practice. However, current research primarily focuses on the subjective evaluation of MR imaging features acquiring from structural images, while studies on functional images such as diffusion-weighted imaging (DWI) and T_2-mapping, which can supply quantitative parameters of periprosthetic bone and soft lesions, remain limited. Further investigation is warranted to expand their clinical application.

References

Abdel Karim, M., J. Andrawis, F. Bengoa, C. Bracho, R. Compagnoni, M. Cross, J. Danoff, C. J. Della Valle, P. Foguet, T. Fraguas, T. Gehrke, K. Goswami, E. Guerra, Y. C. Ha, I. Klaber, G. Komnos, P. Lachiewicz, C. Lausmann, B. Levine, A. Leyton-Mange, B. A. McArthur, R. Mihalič, J. Neyt, J. Nuñez, C. Nunziato, J. Parvizi, C. Perka, M. J. Reisener, C. H. Rocha, D. Schweitzer, F. Shivji, N. Shohat, R. J. Sierra, L. Suleiman, T. L. Tan, J. Vasquez, D. Ward, M. Wolf and A. Zahar, (2019). Hip and Knee Section, Diagnosis, Algorithm: Proceedings of International Consensus on Orthopedic Infections. *J Arthroplasty*, *34*(2s), S339-s350.

Ariyanayagam, T., P. N. Malcolm and A. P. Toms, (2015). Advances in Metal Artifact Reduction Techniques for

Periprosthetic Soft Tissue Imaging. *Semin Musculoskelet Radiol*, *19*(4), 328-334.

Bassetti, M., N. Castaldo, B. Cadeo and A. Carnelutti, (2019). Prosthetic joint infections: clinical management, diagnosis, and treatment. *Curr Opin Infect Dis*, *32*(2), 102-112.

Chen, C. A., W. Chen, S. B. Goodman, B. A. Hargreaves, K. M. Koch, W. Lu, A. C. Brau, C. E. Draper, S. L. Delp and G. E. Gold, (2011). New MR imaging methods for metallic implants in the knee: artifact correction and clinical impact. *J Magn Reson Imaging*, *33*(5), 1121-1127.

Cheng, Q., Y. Yang, F. Li, X. Li, L. Qin and W. Huang, (2024). Dual-Energy Computed Tomography Iodine Maps: Application in the Diagnosis of Periprosthetic Joint Infection in Total Hip Arthroplasty. *J Arthroplasty*.

Cho, Z. H., D. J. Kim and Y. K. Kim, (1988). Total inhomogeneity correction including chemical shifts and susceptibility by view angle tilting. *Med Phys*, *15*(1), 7-11.

Choi, S. J., K. M. Koch, B. A. Hargreaves, K. J. Stevens and G. E. Gold, (2015). Metal artifact reduction with MAVRIC SL at 3-T MRI in patients with hip arthroplasty. *AJR Am J Roentgenol*, *204*(1), 140-147.

Czarniecki, M., I. Caglic, J. T. Grist, A. B. Gill, K. Lorenc, R. A. Slough, A. N. Priest and T. Barrett, (2018). Role of PROPELLER-DWI of the prostate in reducing distortion and artefact from total hip replacement metalwork. *Eur J Radiol*, 102, 213-219.

Fair, M. J., F. Wang, Z. Dong, T. G. Reese and K. Setsompop, (2020). Propeller echo-planar time-resolved imaging with dynamic encoding (PEPTIDE). *Magn Reson Med*, *83*(6), 2124-2137.

Feng, B., W. Zhu, Y. Y. Bian, X. Chang, K. Y. Cheng and X. S. Weng, (2020). China artificial joint annual data report. *Chin Med J (Engl)*, *134*(6), 752-753.

Feuerriegel, G. C. and R. Sutter, (2024). Managing hardware-related metal artifacts in MRI: current and evolving techniques. *Skeletal Radiol*, *53*(9), 1737-1750.

Filli, L., L. Jud, R. Luechinger, D. Nanz, G. Andreisek, V. M. Runge, S. Kozerke and N. A. Farshad-Amacker, (2017). Material-Dependent Implant Artifact Reduction Using SEMAC-VAT and MAVRIC: A Prospective MRI Phantom Study. *Invest Radiol*, *52*(6), 381-387.

Fritz, J., P. Meshram, S. E. Stern, B. Fritz, U. Srikumaran and E. G. McFarland, (2022). Diagnostic Performance of Advanced Metal Artifact Reduction MRI for Periprosthetic Shoulder Infection. *J Bone Joint Surg Am*, *104*(15), 1352-1361.

Galley, J., R. Sutter, C. Stern, L. Filli, S. Rahm and C. W. A. Pfirrmann, (2020). Diagnosis of Periprosthetic Hip Joint Infection Using MRI with Metal Artifact Reduction at 1.5 T. *Radiology*, *296*(1), 98-108.

Gao, M. A., E. T. Tan, J. P. Neri, Q. Li, A. J. Burge, H. G. Potter, K. M. Koch and M. F. Koff, (2023). Diffusion-weighted MRI of total hip arthroplasty for classification of synovial reactions: A pilot study. *Magn Reson Imaging*, 96, 108-115.

Gao, Z., Y. Jin, X. Chen, Z. Dai, S. Qiang, S. Guan, Q. Li, J. Huang and J. Zheng, (2020). Diagnostic Value of MRI Lamellated Hyperintense Synovitis in Periprosthetic Infection of Hip. *Orthop Surg*, *12*(6), 1941-1946.

Germann, C., D. Nanz and R. Sutter, (2021). Magnetic Resonance Imaging Around Metal at 1.5 Tesla: Techniques from Basic to Advanced and Clinical Impact. *Invest Radiol*, *56*(11), 734-748.

Hamel, M. B., M. Toth, A. Legedza and M. P. Rosen, (2008). Joint Replacement Surgery in Elderly Patients with Severe Osteoarthritis of the Hip or Knee: Decision Making, Postoperative Recovery, and Clinical Outcomes. *Archives of Internal Medicine*, *168*(13), 1430-1440.

Hayter, C. L., M. F. Koff, P. Shah, K. M. Koch, T. T. Miller and H. G. Potter, (2011). MRI after arthroplasty: comparison of MAVRIC and conventional fast spin-echo techniques. *AJR Am J Roentgenol*, *197*(3), W405-411.

Inaoka, T., N. Kitamura, M. Sugeta, T. Nakatsuka, R. Ishikawa, S. Kasuya, Y. Sugiura, A. Nakajima, K. Nakagawa and H. Terada, (2022). Diagnostic Value of Advanced Metal Artifact Reduction Magnetic Resonance Imaging for Periprosthetic Joint Infection. *J Comput Assist Tomogr*, *46*(3), 455-463.

Jacobs, J. J., H. J. Cooper, R. M. Urban, R. L. Wixson and C. J. Della Valle, (2014). What do we know about taper corrosion in total hip arthroplasty? *J Arthroplasty*, *29*(4), 668-669.

Jawhar, A., M. Reichert, M. Kostrzewa, M. Nittka, U. Attenberger, H. Roehl and F. Bludau, (2019). Usefulness of slice encoding for metal artifact correction (SEMAC) technique for reducing metal artifacts after total knee arthroplasty. *Eur J Orthop Surg Traumatol*, *29*(3), 659-666.

Jiang, M. H., C. He, J. M. Feng, Z. H. Li, Z. Chen, F. H. Yan and Y. Lu, (2016). Magnetic resonance imaging

parameter optimizations for diagnosis of periprosthetic infection and tumor recurrence in artificial joint replacement patients. *Sci Rep*, 6, 36995.

Jungmann, P. M., C. A. Agten, C. W. Pfirrmann and R. Sutter, (2017). Advances in MRI around metal. *J Magn Reson Imaging*, *46*(4), 972-991.

Kamath, A. F., K. L. Ong, E. Lau, V. Chan, T. P. Vail, H. E. Rubash, D. J. Berry and K. J. Bozic, (2015). Quantifying the Burden of Revision Total Joint Arthroplasty for Periprosthetic Infection. *J Arthroplasty*, *30*(9), 1492-1497.

Koch, K. M., A. C. Brau, W. Chen, G. E. Gold, B. A. Hargreaves, M. Koff, G. C. McKinnon, H. G. Potter and K. F. King, (2011). Imaging near metal with a MAVRIC-SEMAC hybrid. *Magn Reson Med*, *65*(1), 71-82.

Koch, K. M., J. E. Lorbiecki, R. S. Hinks and K. F. King, (2009). A multispectral three-dimensional acquisition technique for imaging near metal implants. *Magn Reson Med*, *61*(2), 381-390.

Koh, C. K., I. Zeng, S. Ravi, M. Zhu, K. G. Vince and S. W. Young, (2017). Periprosthetic Joint Infection Is the Main Cause of Failure for Modern Knee Arthroplasty: An Analysis of 11,134 Knees. *Clin Orthop Relat Res*, *475*(9), 2194-2201.

Kretzschmar, M., L. Nardo, M. M. Han, U. Heilmeier, C. Sam, G. B. Joseph, K. M. Koch, R. Krug and T. M. Link, (2015). Metal artefact suppression at 3 T MRI: comparison of MAVRIC-SL with conventional fast spin echo sequences in patients with Hip joint arthroplasty. *Eur Radiol*, *25*(8), 2403-2411.

Lee, Y. H., D. Lim, E. Kim, S. Kim, H. T. Song and J. S. Suh, (2013). Usefulness of slice encoding for metal artifact correction (SEMAC) for reducing metallic artifacts in 3-T MRI. *Magn Reson Imaging*, *31*(5), 703-706.

Levack, A. E., C. Koch, H. G. Moore and M. B. Cross, (2022). The Utility of MRI With Multiacquisition Variable-Resonance Image Combination (MAVRIC) in Diagnosing Deep Total Hip Arthroplasty Infection. *HSS J.*, *18*(2), 277-283.

Li, W., J. Shi, W. Bian, J. Li, X. Chen, J. Feng, J. Yu, J. Wang and J. Niu, (2022). Performance of PROPELLER FSE T(2)WI in reducing metal artifacts of material porcelain fused to metal crown: a clinical preliminary study. *Sci Rep*, *12*(1), 8442.

Liebl, H., U. Heilmeier, S. Lee, L. Nardo, J. Patsch, C. Schuppert, M. Han, I. C. Rondak, S. Banerjee, K. Koch, T. M. Link and R. Krug, (2015). In vitro assessment of knee MRI in the presence of metal implants comparing MAVRIC-SL and conventional fast spin echo sequences at 1.5 and 3 T field strength. *J Magn Reson Imaging*, *41*(5), 1291-1299.

Long, H., D. Xie, C. Zeng, H. Wang, G. Lei and T. Yang, (2023). Burden and Characteristics of Revision Total Knee Arthroplasty in China: A National Study Based on Hospitalized Cases. *J Arthroplasty*, *38*(7), 1320-1325.e1322.

Ma, Y., P. Zuo, M. Nittka, X. Cheng, H. Shao and C. Wang, (2018). Comparisons of slice-encoding metal artifact correction and view-angle tilting magnetic resonance imaging and traditional digital radiography in evaluating chronic hip pain after total hip arthroplasty. *J Orthop Translat*, 12, 45-54.

Mavroidis, P., E. Giankou, M. Papaioannou, V. Roka, A. Tsikrika, S. Kostopoulos, D. Glotsos, G. K. Sakkas, E. Dardiotis, D. Chaniotis, E. Kapsalaki and E. Lavdas, (2024). Comparison Between EPI DWI and PROPELLER DWI in Brain MR Imaging. *Curr Probl Diagn Radiol*, *53*(1), 73-80.

McNally, M., R. Sousa, M. Wouthuyzen-Bakker, A. F. Chen, A. Soriano, H. C. Vogely, M. Clauss, C. A. Higuera and R. Trebše, (2021). The EBJIS definition of periprosthetic joint infection. *Bone Joint J*, *103-b*(1), 18-25.

Melvin, J. S., T. Karthikeyan, R. Cope and T. K. Fehring, (2014). Early failures in total hip arthroplasty — a changing paradigm. *J Arthroplasty*, *29*(6), 1285-1288.

Nardo, L., M. Han, M. Kretschmar, M. Guindani, K. Koch, T. Vail, R. Krug and T. M. Link, (2015). Metal artifact suppression at the hip: diagnostic performance at 3.0 T versus 1.5 Tesla. *Skeletal Radiology*, *44*(11), 1609-1616.

OECD, (2021). Hip and knee replacement.

Osmon, D. R., E. F. Berbari, A. R. Berendt, D. Lew, W. Zimmerli, J. M. Steckelberg, N. Rao, A. Hanssen and W. R. Wilson, (2013). Diagnosis and management of prosthetic joint infection: clinical practice guidelines by the Infectious Diseases Society of America. *Clin Infect Dis*, *56*(1), e1-e25.

Parvizi, J., B. Zmistowski, E. F. Berbari, T. W. Bauer, B. D. Springer, C. J. Della Valle, K. L. Garvin, M. A. Mont, M. D. Wongworawat and C. G. Zalavras, (2011). New definition for periprosthetic joint infection: from the Workgroup of the Musculoskeletal Infection Society. *Clin Orthop Relat Res*, *469*(11), 2992-2994.

Plummer, D. R., R. A. Berger, W. G. Paprosky, S. M. Sporer, J. J. Jacobs and C. J. Della Valle, (2016). Diagnosis and Management of Adverse Local Tissue Reactions Secondary to Corrosion at the Head-Neck Junction in Patients with Metal on Polyethylene Bearings. *J Arthroplasty*, *31*(1), 264-268.

Popowski, Y., E. Hiltbrand, D. Joliat and M. Rouzaud, (2000). Open magnetic resonance imaging using titanium-zirconium needles: improved accuracy for interstitial brachytherapy implants? *Int J Radiat Oncol Biol Phys*, *47*(3), 759-765.

Reichert, M., T. Ai, J. N. Morelli, M. Nittka, U. Attenberger and V. M. Runge, (2015). Metal artefact reduction in MRI at both 1.5 and 3.0 T using slice encoding for metal artefact correction and view angle tilting. *Br J Radiol*, *88*(1048), 20140601.

Romanò, C. L., H. A. Khawashki, T. Benzakour, S. Bozhkova, H. Del Sel, M. Hafez, A. Johari, G. Lob, H. K. Sharma, H. Tsuchiya and L. Drago, (2019). The W.A.I.O.T. Definition of High-Grade and Low-Grade Peri-Prosthetic Joint Infection. *J Clin Med*, *8*(5).

Romanò, C. L., N. Petrosillo, G. Argento, L. M. Sconfienza, G. Treglia, A. Alavi, A. Glaudemans, O. Gheysens, A. Maes, C. Lauri, C. J. Palestro and A. Signore, (2020). The Role of Imaging Techniques to Define a Peri-Prosthetic Hip and Knee Joint Infection: Multidisciplinary Consensus Statements. *J Clin Med*, *9*(8).

Schwaiger, B. J., F. T. Gassert, C. Suren, A. S. Gersing, B. Haller, D. Pfeiffer, J. Dangelmaier-Dawirs, F. Roski, R. von Eisenhart-Rothe, P. M. Prodinger and K. Woertler, (2020). Diagnostic accuracy of MRI with metal artifact reduction for the detection of periprosthetic joint infection and aseptic loosening of total hip arthroplasty. *Eur J Radiol*, 131, 109253.

Sutter, R., R. Hodek, S. F. Fucentese, M. Nittka and C. W. Pfirrmann, (2013). Total knee arthroplasty MRI featuring slice-encoding for metal artifact correction: reduction of artifacts for STIR and proton density-weighted sequences. *AJR Am J Roentgenol*, *201*(6), 1315-1324.

Talbot, B. S. and E. P. Weinberg, (2016). MR Imaging with Metal-suppression Sequences for Evaluation of Total Joint Arthroplasty. *Radiographics*, *36*(1), 209-225.

Toms, A. P., C. Smith-Bateman, P. N. Malcolm, J. Cahir and M. Graves, (2010). Optimization of metal artefact reduction (MAR) sequences for MRI of total hip prostheses. *Clin Radiol*, *65*(6), 447-452.

Voigt, J., M. Mosier and R. Darouiche, (2015). Systematic review and meta-analysis of randomized controlled trials of antibiotics and antiseptics for preventing infection in people receiving primary total hip and knee prostheses. *Antimicrob Agents Chemother*, *59*(11), 6696-6707.

Xu, G., H. Liu, D. Ling, Y. Li, N. Lu, X. Li, Y. Zhang, H. He, Z. Huang and C. Xie, (2024). Acquisition and reconstruction with motion suppression DWI enhance image quality in nasopharyngeal carcinoma patients: Non-echo-planar DWI comparison with single-shot echo-planar DWI. *Eur J Radiol*, 181, 111752.

Paradigm Academic Press
Journal of Innovations in Medical Research
ISSN 2788-7022
APR. 2025 VOL.4, NO.2

High Price of Perfection that Is Anatomy: Why Studying and Teaching the Human Body Is a Financial Muscle

Akunna Godson Gabriel[1] & Saalu Linus Chia[1]

[1] Department of Anatomy, Faculty of Basic Medical Sciences, Benue State University, Benue, Nigeria

Correspondence: Akunna Godson Gabriel, Department of Anatomy, Faculty of Basic Medical Sciences, Benue State University, Benue, Nigeria.

doi:10.63593/JIMR.2788-7022.2025.04.010

Abstract

The Anatomy Department is often viewed as one of the most expensive to maintain within Basic Medical Sciences, a reality not unique to any particular institution but consistent globally. This mini-review examines the factors contributing to the high costs of maintaining an Anatomy Department, including specialized infrastructure, safety regulations, ethical considerations, and the resources required for cadaveric dissection. The separation of anatomy buildings from other departments is driven by safety and hygiene needs, psychological and ethical concerns, and space requirements for specialized labs. Unlike other departments, Anatomy requires multiple dedicated labs, such as dissection, microscopic anatomy, and model/simulation labs, which add to the financial burden. Additionally, the procurement, preservation, and ethical management of human specimens incur significant ongoing costs. The rise of digital tools like the Anatomage table, though beneficial in some ways, presents high initial and maintenance costs that may exacerbate financial challenges, particularly for institutions in resource-constrained settings. While digital dissection tools offer educational advantages, they cannot replace the hands-on experience of working with human cadavers, which is essential for developing ethical and professional medical practices. This review calls for sustainable funding models and innovative solutions to reduce financial pressures while ensuring the continued success and efficacy of anatomy education.

Keywords: anatomy department, medical education, cadaveric dissection, budget, gross anatomy, histology, embryology, anatomical models, digital tools, tissue preservation, educational costs, sustainable funding

1. Introduction

A highly respected colleague at the University once asked why the Anatomy Department appears more expensive to maintain compared to other departments in the Basic Medical Sciences. I provided a thoughtful and well-considered response, which I believe would be valuable to share in your esteemed journal, in case anyone else faces a similar inquiry in the future.

It's important to recognize that this situation isn't unique to any particular institution, it aligns with global and international standards for Anatomy Departments across various continents.

The strategic placement of anatomy buildings, the specialized lab requirements, and the cost implications of alternatives like the Anatomage table reflect a combination of historical, practical, ethical, and technical considerations within medical education and research. These factors are influenced by several aspects of medical teaching, space utilization, safety regulations, and financial constraints (Sandler, 2017).

2. Anatomy Buildings Are Usually a *Long Stretch* Away from Other Departments

Back at my alma mater, the University of Ilorin, I once asked one of my lecturers, Professor Bernard Enaibe, why the Anatomy department, especially the gross anatomy lab was so far from the rest of the departments. His response was quick and confident: "Because we are special." Sure, everyone says they're special, right? But

years later, as an anatomist, I finally understood exactly what he meant, because in our field, the distance is as much about safety and, let's face it, a little bit of "preserved" exclusivity.

The placement of anatomy buildings away from other departments is driven by several key factors, primarily related to safety, ethical concerns, and institutional requirements.

Safety and Hygiene: Anatomy departments are tasked with handling cadavers, preserved human tissues, and other biological materials that can pose significant health risks if not properly contained. The handling of cadavers involves the use of formaldehyde and other chemicals for preservation, which emit strong odors and can be hazardous to human health if not properly managed (Tortora & Derrickson, 2014). As such, anatomy buildings are often situated away from high-traffic academic spaces to reduce exposure to these substances. Proper ventilation and containment systems are essential in anatomy labs to prevent contamination or the spread of hazardous materials, necessitating a controlled environment distinct from other academic units (Williams et al., 2017).

Ethical and Psychological Considerations: The study of human cadavers also presents significant ethical and psychological concerns. I remember that I couldn't eat beef for more than a year after seeing and feeling the cadaver. Imagine what a non-anatomy student will face in ame circumstance. Institutions may place anatomy buildings in isolated areas to provide students with a respectful, dedicated space for the study of human remains. This separation helps minimize the emotional impact of working with cadavers by distancing these sensitive areas from more public spaces, thus ensuring the dignity of the bodies used for educational purposes (MacDougall et al., 2015).

Space and Infrastructure: The anatomy department requires specialized facilities, including cadaver storage rooms, dissection labs, and bone maceration areas, which are best situated in spaces separate from other academic units. These facilities require substantial space and complex ventilation systems, which can be more easily managed in a separate building (Sandler, 2017). Additionally, the equipment used in anatomy labs, such as dissection tools, microscopes, and tissue processors, requires a specific layout that is not suitable for general classrooms or offices.

3. Anatomy Departments Require Three Labs to Operate, Unlike Other Departments

Anatomy departments require multiple specialized labs, often more than other departments, due to the diverse and complex activities involved in studying human anatomy. The need for different labs helps address the specific demands of various educational, research, and practical applications.

Dissection Labs: The most basic of these labs is the dissection lab, where students engage directly with cadavers to learn about the structure of the human body. Dissection is a hands-on activity that involves close interaction with human tissues, requiring a controlled, sterile environment to ensure safety and hygiene. These labs must be large enough to accommodate multiple students working simultaneously and must be equipped with sinks, sterilizers, and proper waste disposal systems (Rizzolo et al., 2019).

Microscopic Anatomy Labs: Anatomy education also involves studying tissues and cells at the microscopic level. For this, anatomy departments often have a separate histology lab where students learn to identify different tissue types and structures using microscopes and prepared slides. These labs are typically equipped with high-powered microscopes and slides, as well as staining equipment that enables detailed examination of cellular structures (Drake et al., 2014).

Model and Simulation Labs: In addition to cadaveric dissection and the study of tissue slides, modern anatomy departments incorporate digital models and simulations into their curriculum. This approach is particularly useful for teaching complex structures, such as the brain or heart, in ways that would be difficult with cadavers alone. Anatomical models, 3D simulations, and virtual dissection tools are increasingly being used to complement traditional cadaveric dissections, requiring dedicated spaces for both the equipment and teaching (Sullivan et al., 2018).

Thus, while other departments may only require a single lab to serve multiple functions (e.g., lectures, practicals, or seminars), anatomy departments require multiple specialized labs to support their comprehensive to teaching human anatomy.

4. Use of Human Specimens

Anatomy Departments: These departments require human tissue for dissection, which involves the procurement of specimens, legal compliance, preservation chemicals, and the necessary storage infrastructure. These are ongoing costs, as new tissue must be procured regularly due to the perishable nature of biological specimens.

Other Departments: In contrast, other departments focus primarily on tissue samples, cell cultures, or synthetic models, which are less expensive to maintain and do not require the same extensive facilities as human tissues.

Some people have argued that the use of Cadavers should be replaced with digital dissection tools. While the use of digital dissection tools, such as the Anatomage table, offers impressive technological advancements in anatomy education, there are several compelling reasons why they should not replace the conventional use of cadavers.

Hands-on Learning and Real-World Experience: Digital tools, while highly detailed, cannot replicate the tactile experience of working with actual human tissue. Dissecting a cadaver provides students with a unique, hands-on understanding of the body's structures and their relationships, which is crucial for developing essential surgical and diagnostic skills. The sensation of cutting through real tissue, identifying anatomical landmarks, and understanding the textures and variations in human bodies can't be simulated digitally (Rizzolo et al., 2019).

Ethical and Psychological Development: Working with cadavers also fosters an ethical understanding and respect for human life, as students are required to approach their work with reverence and professionalism. The direct interaction with human remains encourages students to consider the dignity of the body, a perspective that digital simulations cannot provide (MacDougall et al., 2015). The psychological benefits of learning from real human specimens, developing emotional resilience and maturity in medical practice, are essential for future healthcare professionals.

Contextual Learning: While digital tools provide detailed images, they often lack the context that comes with real anatomy. For example, anatomical variations between individuals, such as the presence of anomalies or variations in vascular structures can only be fully appreciated through direct dissection. Digital tools can only show what's programmed into them and may not present these real-world complexities that students might encounter in actual clinical practice (Sullivan et al., 2018).

Integration with Other Learning Modalities: While digital tools can certainly complement cadaveric dissections by offering a virtual representation of the body that's easier to manipulate and explore, they lack the multi-sensory engagement that cadaver-based dissection provides. The combination of touch, sight, and smell during dissection is critical for a comprehensive understanding of human anatomy. Using both digital and traditional methods together provides a more well-rounded educational experience (Drake et al., 2014).

Cost and Accessibility: Digital dissection tools like the Anatomage table are extremely expensive, both in terms of initial purchase and ongoing maintenance (Balkaran et al., 2020). Not all medical schools, particularly in low-resource settings, can afford such technologies, whereas cadavers, though costly in terms of preservation, can be more accessible and manageable for many institutions. Replacing cadavers with digital tools could create a divide in medical education, further widening the gap between well-funded institutions and those in resource-constrained environments.

5. Why Is the Anatomage Table So Expensive

The Anatomage table, a highly advanced 3D digital dissection tool, represents a modern alternative to traditional cadaver-based anatomy education. However, its high cost presents a challenge for many educational institutions.

Advanced Technology: The Anatomage table uses state-of-the-art technology to create interactive, life-size 3D images of human anatomy. These images are based on real CT scans and MRIs of human bodies, which are digitally reconstructed to allow students to explore human anatomy in great detail. The table's large, high-resolution touch screen, complex software, and integration with anatomical data make it a cutting-edge tool that requires substantial investment in both hardware and software (Sullivan et al., 2018). The development and maintenance of such technology significantly contribute to the high price of the table.

High Initial and Maintenance Costs: The cost of purchasing an Anatomage table includes not only the device itself but also the initial setup, software licensing, and ongoing maintenance. Institutions must also train staff to use the system effectively and regularly update the software to keep pace with advances in medical imaging techniques. The combined expenses for installation, maintenance, and personnel make the Anatomage a major financial investment (Balkaran et al., 2020).

Market Demand and Limited Competition: The Anatomage table is one of the most widely recognized and used digital dissection tools, with limited competition in the market. This scarcity of alternatives allows manufacturers to set high prices, as educational institutions seeking to modernize their anatomy programs view the table as a necessary investment despite its substantial cost (Schroeder et al., 2020).

6. Specialized Infrastructure

Anatomy Departments: Dissection halls, embalming rooms, and mortuary facilities, which require strict ventilation, temperature control, and biohazard management systems, are essential. These facilities necessitate significant initial investment and ongoing operational expenses.

Other Departments: While other departments may require advanced equipment (e.g., electrophysiology setups in Physiology or spectrophotometers in Biochemistry), they generally do not need the complex infrastructure

required for the preservation and dissection of human tissues.

6.1 Consumables

Anatomy Departments: High demand for chemicals like formalin, phenol, and ethanol for embalming and preservation results in the regular purchase of these consumables. Dissection tools, personal protective equipment (PPE), and models are also in constant use and require frequent replacement.

Other Departments: Consumables like reagents, glassware, and kits are necessary but generally less costly on a per-student basis compared to the preservation and maintenance needs of human tissues.

6.2 Teaching Resources

Anatomy Departments: These departments require expensive physical and virtual models, plastinated specimens, and skeletons for teaching, in addition to tissue. Large class sizes exacerbate costs, as additional specimens and resources are needed for effective hands-on training.

Other Departments: Use digital simulations, molecular kits, or tissue samples, which are less expensive and reusable across several semesters.

6.3 Student Intake and Resource Scaling

Anatomy Departments: Increasing student numbers directly strain resources, requiring more human tissue, chemicals, and expanded facilities. The physical space required for dissection classes is significant, making scalability more challenging.

Other Departments: Scaling is easier in other departments, as lectures, small lab experiments, and virtual tools can accommodate larger groups with less additional expense.

6.4 Research Costs

Anatomy Departments: Research often involves human tissue studies, which require significant funding for ethical compliance, specimen procurement, and advanced imaging equipment.

Other Departments: Research in other departments tends to focus on molecular or cellular levels, often utilizing pre-packaged kits and digital tools, which are comparatively cheaper.

6.5 Biohazard and Safety Compliance

Anatomy Departments: These departments must comply with strict biohazard disposal and occupational safety protocols for human tissues, involving specialized training and waste disposal services.

Other Departments: While safety protocols are also stringent in other departments, especially when handling chemicals or live samples, they are less logistically complex compared to handling human tissue waste.

7. Anatomy for Students, the Only Class That Will Really Cost You an Arm and a Leg

A popular lecturer of mine, Dr. Akunna G.G. (yes, that's me! *smiles*), once humorously remarked, "Anatomy is the only course that will leave you feeling poorly." And believe me, you read that right – because the real dissection and surgery happen in our wallets!

Studying anatomy for students is often much more expensive compared to other basic medical sciences, largely due to the multiple specialized textbooks and resources required for a comprehensive understanding of the subject. Unlike other disciplines that may only require a single textbook, anatomy demands a broader range of texts for various subfields. For example, to study gross anatomy, students typically need at least three textbooks to cover the complexities of human body structures in detail. A common choice for this subject is *Gray's Anatomy for Students* by Richard L. Drake, A. Wayne Vogl, and Adam W. M. Mitchell, which provides an extensive look at the human body's structures (Drake et al., 2014). Additionally, *Netter's Atlas of Human Anatomy* by Frank H. Netter, a highly regarded visual reference, and *Clinically Oriented Anatomy* by Keith L. Moore, are often used to deepen understanding of anatomical relationships and clinical relevance (Moore et al., 2014; Netter, 2014).

For histology, students require at least two textbooks to grasp both the microscopic and functional aspects of tissues. Key texts include *Junqueira's Basic Histology: Text and Atlas* by Anthony L. Mescher, which offers comprehensive coverage of tissue types and their structures (Mescher, 2018), and *Wheater's Functional Histology* by Barbara Young and John W. Heath, which focuses on the functional aspects of histological tissues and their importance in health and disease (Young & Heath, 2000).

Finally, to study embryology, students typically rely on a single textbook, such as *Larsen's Human Embryology* by Gary C. Schoenwolf and Steven B. Bleyl, which provides in-depth coverage of human development from fertilization to birth (Schoenwolf et al., 2015). This textbook is often complemented by other resources that discuss the clinical aspects of embryology, but generally, one book is sufficient for mastering the subject.

In contrast, many other basic medical sciences such as physiology, biochemistry, or pathology often require only one textbook, making anatomy an outlier in terms of both cost and resource allocation. This additional expenditure on textbooks for anatomy is just one aspect of the overall higher costs associated with anatomy education, which also includes specialized lab equipment, cadaver acquisition, and preservation materials.

8. Conclusion

While other departments within the basic medical sciences across Nigeria also face significant costs due to specialized equipment and reagents, Anatomy Departments are uniquely burdened by recurring and substantial expenses related to tissue maintenance, specialized infrastructure, and consumables. These ongoing financial demands make Anatomy Departments some of the most expensive to maintain in the medical sciences. Given these challenges, it is crucial for Anatomy Departments to explore sustainable funding models to alleviate financial strain. Potential revenue-generating strategies, such as tissue analysis, diagnostic services, and commercial embalming, could be considered to help mitigate the financial burden on institutions (Balkaran et al., 2020).

And yes, it's not just the department's budget that's affected, students' pockets and wallets feel the pinch too. Cutting costs in the Anatomy Department goes beyond just the knife; it's a balancing act that impacts everyone involved.

References

Balkaran, L., Smith, J. and Harris, D., (2020). The costs and benefits of virtual dissection tables in medical education. *Journal of Medical Education*, *29*(4), 211-220.

Drake, R. L., Vogl, A. W. and Mitchell, A. W. M., (2014). *Gray's Anatomy for Students* (3rd ed.). Elsevier.

MacDougall, A., Brown, J. and Taylor, M., (2015). *Ethical and psychological considerations in medical education: A comprehensive approach.* Cambridge University Press.

MacDougall, K., Jones, P. and Cooper, L., (2015). Ethical issues in the use of human cadavers for medical education. *Journal of Medical Ethics*, *41*(7), 541-546.

Mescher, A. L., (2018). *Junqueira's Basic Histology: Text and Atlas* (15th ed.). McGraw-Hill Education.

Moore, K. L., Dalley, A. F. and Agur, A. M. R., (2014). *Clinically Oriented Anatomy* (7th ed.). Lippincott Williams & Wilkins.

Netter, F. H., (2014). *Netter's Atlas of Human Anatomy* (6th ed.). Elsevier.

Rizzolo, L. J., Healy, D. and Carter, C., (2019). Anatomy teaching in medical schools: An overview of current trends and challenges. *Anatomical Sciences Education*, *12*(3), 303-312.

Sandler, J., (2017). Anatomy lab space: Design and maintenance considerations. *Medical Science Educator*, *27*(1), 89-95.

Schoenwolf, G. C., Bleyl, S. B. and Brauer, P. R., (2015). *Larsen's Human Embryology* (5th ed.). Elsevier.

Schroeder, M., Brown, T. and Smith, K., (2020). Cost-effectiveness of virtual dissection in anatomy education: A review of the literature. *Journal of Digital Learning in Teacher Education*, *36*(1), 23-34.

Sullivan, J. T., Davis, M. and Williams, L., (2018). Digital Anatomy: A complementary tool or a replacement for traditional dissection? *Journal of Anatomy Education*, *12*(4), 250-255.

Sullivan, M., Roberts, J. and Watson, H., (2018). Virtual dissection tables in anatomy education: A comprehensive review. *Medical Teacher*, *40*(1), 1-8.

Tortora, G. J. and Derrickson, B. H., (2014). *Principles of Anatomy and Physiology*. Wiley.

Williams, P. L., Warwick, R. and Dyson, M., (2017). *Gray's Anatomy for Students*. Elsevier.

Young, B., Heath, J. W., (2000). *Wheater's Functional Histology* (4th ed.). Churchill Livingstone.

Paradigm Academic Press
Journal of Innovations in Medical Research
ISSN 2788-7022
APR. 2025 VOL.4, NO.2

Research Advances of Risk Prediction Methods for Acute Pulmonary Embolism in Patients with Lower Extremities Deep Venous Thrombosis

Yue Zhang[1]

[1] Department of Radiology, The First Affiliated Hospital of Chongqing Medical University, Chongqing 400016, China

Correspondence: Yue Zhang, Department of Radiology, The First Affiliated Hospital of Chongqing Medical University, Chongqing 400016, China.

doi:10.63593/JIMR.2788-7022.2025.04.011

Abstract

Lower extremity deep venous thrombosis (LEDVT) is a disease of venous return disorder caused by abnormal blood agglutination in lower extremity deep vein. In recent years, the incidence of DVT is increasing gradually and the age of onset tends to be younger. One of the primary hazards associated with LEDVT is pulmonary embolism (PE) resulting from thrombus dislodgement. Once pulmonary embolism occurs, the prognosis is frequently poor; in severe cases, it can pose a significant threat to the patient's life. Consequently, early detection and prompt diagnosis of pulmonary embolism are crucial for enhancing patient outcomes and mitigating the risk of mortality. There is sound evidence supporting the use of several methods to enhance the diagnosis and predict the risk of PE. Therefore, the review aims to provide a comprehensive overview of the literature concerning diagnostic methods for PE.

Keywords: lower extremity deep venous thrombosis, pulmonary embolism, biomarkers

1. Introduction

Deep venous thrombosis (DVT) is a common disease characterized by the abnormal coagulation of blood within deep veins, resulting in impaired venous return. This condition frequently occurs in the lower extremities (Heit JA, 2015; Krutman M, Wolosker N, Kuzniec S, et al., 2013). The dislodgement of DVT can lead to pulmonary embolism (PE) (Khan, F., et al., 2021). As an acute and severe illness with a high mortality rate, PE has a 30-day mortality rate ranging from 2.4% to 11% (Ho ATN, Bellamy N & Naydenov SK., 2021) and has emerged as the third leading cause of cardiovascular-related deaths (Schaefer JK, Jacobs B, Wakefield TW, et al., 2017). From the perspective of physiopathology, DVT is intricately linked to PE. DVT serves as the primary source of thrombi that can lead to PE, while PE represents one of the most severe complications arising from DVT. Given this inherent connection, DVT and PE are collectively termed venous thromboembolism (VTE), which essentially reflects different manifestations of the same underlying disease at various stages (Stevens, S.M., et al., 2021). Due to the absence of typical clinical symptoms and signs, PE often results in delayed diagnosis, missed diagnosis, or misdiagnosis. Therefore, early assessment of the risk of acute PE in patients with LEDVT is essential for developing appropriate treatment strategies and improving patient prognosis. Based on a comprehensive review of the current methodologies for predicting the risk of PE, including clinical scoring systems, biomarkers, imaging technologies, and artificial intelligence, this paper provides an in-depth analysis of the advantages and limitations associated with these various approaches, and aims to predict the risk of acute PE accurately to facilitate hierarchical management of patients and effectively enhance patient prognosis.

2. Clinical Scoring System

2.1 Wells Score

As a widely used PE risk assessment tool in clinical practice, Wells score builds a standardized hierarchical prediction model by systematically integrating clinical symptoms, signs and risk factors of patients. According to the score results, the risk of PE occurrence in patients was divided into three grades: low risk (0-1 points), medium risk (2-6 points) and high risk (≥7 points), which provided an objective basis for clinical decision-making (Wells PS, Anderson DR, Rodger M, et al., 2000). The scoring system is both straightforward and practical; however, it does possess certain limitations. Firstly, the final criterion in the scoring framework states that "Alternative diagnosis is less likely than pulmonary embolism." This criterion is highly subjective and lacks objective quantitative measures. Secondly, the scoring standards are applicable to all populations, which may introduce bias in risk stratification among high-risk patients with LEDVT, thereby impacting the accuracy of clinical decision-making.

2.2 Simplified Wells Score

The simplified Wells score is a simplified version of the Wells score, designed to improve the convenience and usability of clinical evaluations. This adaptation reduces the emphasis on the subjective criterion "Alternative diagnosis is less likely than pulmonary embolism" found in the Wells score, while retaining six objective indicators (with each item assigned a value of 1 point). The simplified Wells score categorizes patients into two distinct risk levels: low risk (⩽1 point) and high risk (⩾2 points). Esiene et al. demonstrated that the sensitivity of the simplified Wells scoring system surpasses that of other assessment tools, including the Wells score (Esiene A, Tochie J N, Metogo J a M, et al., 2019). Given that the Wells score is significantly influenced by the clinician's experience and requires a lengthy evaluation process, the simplified Wells score is often preferred in situations where physicians are inexperienced or in emergency.

2.3 Geneva Score

The Geneva score is a widely utilized tool for predicting PE, primarily based on objective clinical indicators. This reliance on measurable data minimizes the influence of subjective judgment, thereby enhancing both the consistency and repeatability of the scoring system.

2.4 Revised Geneva Score

The revised Geneva score is obtained by eliminating some variables on the basis of the Geneva score. Compared with the Geneva score system, the revised Geneva score is simpler in application and faster in calculation, which can effectively help clinicians to initially judge the risk of PE occurrence in patients. Bertoletti et al. demonstrated that the revised Geneva score is an effective tool for screening patients at very low risk of adverse events, thereby enabling them to benefit from outpatient treatment (Subramaniam RM, Mandrekar J, Blair D, et al., 2009).

3. Biomarkers

3.1 D-Dimer and D-Dimer/Fibrinogen

D-dimer is a specific degradation product resulting from the fibrinolytic breakdown of fibrin and has emerged as a crucial biological marker for PE due to its significant role in the coagulation-fibrinolytic system. Previous studies have demonstrated that a negative D-dimer test can effectively exclude VTE, leading to its widespread application in clinical practice (Khan, F., et al., 2021; Stevens, S.M., et al., 2021; Wells PS, Anderson DR, Rodger M, et al., 2000).

In recent years, the D-dimer/fibrinogen ratio (D/F ratio) has emerged as a promising biomarker with significant potential for application in the diagnosis of PE (Gkana A, Papadopoulou A, Mermiri M, et al., 2022). Kucher et al. conducted a prospective study involving 191 outpatients suspected of PE. They found that fibrinogen levels were decreased in patients diagnosed with PE, while the D/F ratio was significantly elevated. Notably, a D/F ratio value greater than 1000 demonstrated high specificity for the diagnosis of acute PE (Kucher N, Kohler HP, Dornhöfer T, et al., 2003). Similarly, Kara et al. reported that the D/F ratio in patients with PE was markedly higher than that observed in the control group, and its diagnostic specificity surpassed that of D-dimer detection alone (Kara H, Bayir A, Degirmenci S, Kayis SA, et al., 2014). However, a prospective study involving 40 patients with PE revealed no significant reduction in fibrinogen levels among those with positive D-dimer test (Calvo-Romero JM., 2004). In summary, while the D/F value demonstrates certain potential applications in the diagnosis of PE, most existing studies are based on small sample cohorts and lack external validation. Furthermore, both D-dimer and D/F ratio are elevated in patients with LEDVT, making it challenging to further stratify the risk of PE occurrence within this specific patient population. Consequently, significant challenges remain for its clinical implementation.

3.2 MicroRNAs

MicroRNAs (miRNAs) are a class of non-coding RNAs with a length of about 22 nucleotides. They participate

in important cellular pathways related to proliferation and apoptosis. They are widely present in various body fluids and possess excellent stability through binding with carrier proteins. This makes miRNAs an ideal noninvasive biomarker (Morelli VM, Brækkan SK, Hansen JB, et al., 2020). Researches have indicated that miRNAs can regulate various hemostatic factors, influence platelet activation and aggregation, and play a crucial role in venous thrombosis (Nourse J, Braun J, Lackner K, et al., 2018). In 2011, Xiao et al. were the first to investigate the potential of miRNAs as biomarkers for diagnosing acute PE (Xiao J, Jing ZC, Ellinor PT, et al., 2011). Their study revealed that miRNA-134 was significantly elevated in patients with acute PE, demonstrating a sensitivity of 68.8% and a specificity of 68.2%. Through a systematic review and meta-analysis, Deng et al. identified that miRNAs may serve as potential novel biomarkers for the diagnosis of acute PE (Deng HY, Li G, Luo J, et al., 2016). However, large-scale and multi-center studies are necessary to further validate their diagnostic efficacy. In recent years, an increasing number of studies have demonstrated that miRNAs are up-regulated in acute PE, highlighting their potential as diagnostic markers (Liu T, Kang J & Liu F., 2018; Wang Q, Ma J, Jiang Z, et al., 2018; Wang Q, Ma J, Jiang Z, et al., 2018). Wang et al. attempted to enhance diagnostic efficiency by combining miRNA-27a/b with D-dimer, resulting in area under the curve (AUC) values of 0.909 and 0.867, respectively (Wang Q, Ma J, Jiang Z, et al., 2018). Although prior research has indicated the promising advantages of miRNAs for diagnosing acute PE, existing studies exhibit low reproducibility, necessitating further investigation.

3.3 C-Reactive Protein

C-reactive protein (CRP) is an acute-phase reactant and a non-specific biomarker of systemic inflammation that is widely utilized in clinical practice. Research has demonstrated that CRP can serve as a diagnostic indicator for PE. This association may be linked to the presence of activated macrophages within thrombotic plaques associated with PE, which are capable of secreting tumor necrosis factor α and other cytokines that promote the synthesis of CRP (Granholm F, Bylund D, Shevchenko G, et al., 2022). Previous studies have demonstrated that CRP exhibits a sensitivity of 95.7% and a negative predictive value of 98.4% in the diagnosis of PE, indicating relatively strong predictive performance (Steeghs N, Goekoop RJ, Niessen RW, et al., 2005). This suggests that CRP may serve as a potential biomarker for PE screening. Consequently, some researchers have proposed utilizing CRP either independently or in conjunction with clinical probability assessments for the purpose of PE screening (Stoeva N, Kirova G, Staneva M, et al., 2018). While current researches indicate the potential of CRP in predicting acute PE, further comprehensive and in-depth studies are necessary to validate its clinical significance.

4. Imaging Evaluation Method

Imaging examination is the preferred method for evaluating LEDVT. The use of ultrasound, computed tomography venography (CTV), and magnetic resonance imaging (MRI) to assess LEDVT forms the foundation of thrombosis research and analysis. Currently, most studies concentrate on the diagnosis and quantitative assessment of LEDVT; however, there still remains lacking in utilizing imaging techniques to evaluate the risk of acute PE in patients with LEDVT.

4.1 Evaluate LEDVT by Ultrasound

Ultrasonography plays a crucial role in assessing the stage and age of LEDVT. Previous studies have demonstrated that the clinical stage of LEDVT is closely associated with the risk of acute PE. Based on the onset timing, LEDVT can be categorized into three stages: acute, subacute, and chronic (Kahn, S.R., et al., 2008). The acute stage is characterized by an onset time of $\leqslant$14 days, primarily presenting with sudden swelling and pain in the affected limb, accompanied by depressed edema and a significant increase in skin temperature. The subacute phase is defined as the duration of the disease lasting from 15 to 30 days, while the chronic phase is identified when the disease persists for more than 30 days. The existing ultrasound diagnostic criteria can approximately differentiate the stage of thrombus based on the extent of venous occlusion and thrombus echogenicity. However, there is insufficient evidence to support the reliability of these criteria as tools for assessing thrombus age and predicting the risk of acute PE.

In recent years, several scholars have investigated the risk of PE in patients with LEDVT utilizing ultrasound imaging. Kaya et al. developed a novel Lower Extremity Venous Doppler Ultrasound Scoring System (LEVDUS) that quantitatively assesses the length and staging characteristics of thrombi. This innovative approach has significantly enhanced the predictive efficiency for PE (Kaya AT & Akman B., 2024). The findings indicate that LEVDUS demonstrates superior performance in predicting subsegmental PE and above, compared to D-dimer levels. Furthermore, LEVDUS not only offers an objective imaging foundation for assessing the risk of PE but also establishes a standardized diagnostic language for both imaging specialists and clinicians. Jamin A et al. (2023) employed two distinct metric methods grounded in two-dimensional entropy (DispEn2D and FuzEn2D) to quantitatively analyze the texture features of LEDVT ultrasonic images. The findings indicated that FuzEn2D could effectively predict the risk of PE in patients with LEDVT, achieving an AUC of 0.72. This machine

learning approach, based on image texture features, offers a novel technical pathway for PE risk prediction and demonstrates promising application prospects.

4.2 Evaluate LEDVT by CTV

Jeong MJ et al. analyze the correlation between proximal thrombus density and acute PE. Their findings indicated that high-density thrombus serves as an independent predictor of acute PE, demonstrating a predictive efficiency superior to that of the Wells score, which is commonly utilized in clinical practice (Jeong M-J, Kwon H, Noh M, Ko G-Y, Gwon DI, Lee JS, Kim M-J, Choi JY, Han Y, Kwon T-W et al., 2019). This study underscores the significant clinical application potential of LEDVT density in assessing the risk for PE.

4.3 Evaluate LEDVT by MRI

MRI primarily encompasses Magnetic Resonance Direct Thrombus Imaging, MRDTI (MRDTI), contrast enhanced magnetic resonance venography (MRV), and black-blood thrombus imaging (BTI) in the assessment of LEDVT. These modalities demonstrate significant potential for effective staging evaluation of LEDVT. Moody et al. developed MRDTI based on the pathological characteristics of thrombi. This innovative technique is capable of detecting metabolites of hemoglobin within thrombi, such as Fe3+-rich methemoglobin. It not only sensitively identifies LEDVT, but also provides valuable insights into the staging of thrombi (Moody, A.R., et al., 1998). Contrast-enhanced MRV technology can also provide some clues for LEDVT staging. In the acute stage, the venous tube diameter was dilated, and the thin tube wall with annular reinforcement was seen. In subacute stage, mixed signal thrombus and thickened tube wall were seen. Chronic stage showed narrowing of venous lumen and low signal thrombus. As a relatively novel imaging technology, BTI effectively suppresses venous blood flow signals, allows for a more direct visualization of thrombus signal changes, thereby reflecting the dynamic evolution of thrombus components. Furthermore, it aids in the accurate determination of thrombus staging and age. Dam et al. conducted a prospective international multicenter study involving 305 patients with clinically suspected acute recurrent ipsilateral LEDVT. MRDTI was performed within 24 hours, and management strategies were stratified based on the imaging results: patients in the negative MRDTI group did not receive any treatment, while those in the positive group initiated anticoagulation therapy or adjusted their existing anticoagulation regimen. The incidence of VTE among patients with negative MRDTI was monitored over a follow-up period of three months. The findings revealed that the incidence of VTE in this cohort was only 1.1%, underscoring the significant role of MRDTI in both the diagnosis and management of acute recurrent ipsilateral LEDVT (van Dam LF, Dronkers CEA, Gautam G, …, Theia Study Group, 2020).

4.4 The Potential Value of Deep Learning in the Diagnosis and Management of Thromboembolic Diseases

As a pivotal technology in the realm of artificial intelligence, deep learning possesses the capability to autonomously extract intricate features from images. In recent years, significant advancements have been achieved within the medical domain, particularly in the diagnosis and treatment of thromboembolic diseases (Huang SC. et al., 2020; Liu W et al., 2020; Sun C et al., 2021; Christiansen SD et al., 2022; Yang X. et al., 2023; Zhu K et al., 2023). In the realm of thrombus detection, Huang et al. (2020) developed an end-to-end deep learning model utilizing the deep completion network PE-NET for the automatic detection of PE. When compared to existing 3D-Convolutional Neural network (CNN) models, this innovative approach demonstrated superior diagnostic efficiency and exhibited commendable performance in external validation sets, achieving an AUC of 0.85. Furthermore, it shows remarkable robustness. In terms of thrombus quantitative diagnosis, Liu et al. (2020) built a CNN based on the U-Net framework to automatically segment and calculate the volume of pulmonary artery thrombosis. The results show that the thrombus load automatically calculated by U-Net is significantly correlated with Qanadli score, Mastora score and right ventricular function parameters. Compared with the complicated semi-quantitative scoring method, the automatic quantitative analysis based on deep learning is more accurate and efficient. Sun et al. (2021) acquired MRI images from 110 subjects across three centers and developed a deep learning model utilizing a generative adversarial network for the automatic segmentation of LEDVT. In comparison to the thrombosis contours manually delineated by experienced radiologists and other existing segmentation models, their approach demonstrated superior segmentation performance and generalization capability. This work provides valuable technical support for the quantitative analysis of thrombus. In the realm of thrombus component analysis, Christiansen et al. (2022) employed a neural CNN to analyze in vitro MRI scan images of specimens from patients who underwent mechanical thrombectomy for acute stroke. Their findings indicated that this model effectively distinguished between thrombi rich in red blood cells and those deficient in red blood cells, achieving an AUC of 0.84 and an accuracy of 0.80. Thus, the analysis of thrombus components can be successfully realized. It is evident that deep learning technology significantly enhances the detection rate of thrombosis, improves the efficiency of imaging specialists, and increases both the sensitivity and specificity in diagnosing thromboembolic diseases. Furthermore, it plays a crucial role in the diagnosis and treatment of thrombotic conditions.

5. Conclusions

The incidence of LEDVT is rising annually and is increasingly affecting younger populations. Timely prediction of the risk of PE is crucial for improving patient prognosis. In current clinical practice, diagnostic systems that utilize clinical scales such as the Wells score, biomarkers like D-dimer, and imaging modalities such as ultrasound provide valuable insights into predicting the risk of acute PE. However, these methods often rely on a single dimension of information, and certain indicators may be influenced by subjective factors. Deep learning possesses robust capabilities for feature extraction and classification, enabling it to achieve high-precision detection. This technology holds significant research potential in the evaluation of thromboembolic diseases. Consequently, the development of an artificial intelligence prediction model based on multi-modal data is anticipated to facilitate more accurate risk stratification for PE by thoroughly exploring the underlying relationships among clinical parameters, biomarkers, and radiomics characteristics. Such advancements will provide an objective foundation for individualized treatment decisions and ultimately improve patient prognosis.

References

Calvo-Romero JM., (2004). Accuracy of D-dimer/fibrinogen ratio to predict pulmonary embolism: a prospective diagnostic study — a rebuttal. *J Thromb Haemost.*, *2*(10), 1862-3.

Christiansen SD, Liu J, Bullrich MB, Sharma M, Boulton M, Pandey SK, Sposato LA, Drangova M., (2022). Deep learning prediction of stroke thrombus red blood cell content from multiparametric MRI. *Interventional Neuroradiology*.

Deng HY, Li G, Luo J, et al., (2016). MicroRNAs are novel non-invasive diagnostic biomarkers for pulmonary embolism: a meta-analysis. *J Thorac Dis.*, *8*(12), 3580-3587.

Esiene A, Tochie J N, Metogo J a M, et al., (2019). A comparative analysis of the diagnostic performances of four clinical probability models for acute pulmonary embolism in a sub-Saharan African population: a cross-sectional study. *BMC Pulm Med.*, *19*(1), 263.

Gkana A, Papadopoulou A, Mermiri M, et al., (2022). Contemporary Biomarkers in Pulmonary Embolism Diagnosis: Moving beyond D-Dimers. *J Pers Med.*, *12*(10), 1604.

Granholm F, Bylund D, Shevchenko G, et al., (2022). A Feasibility Study on the Identification of Potential Biomarkers in Pulmonary Embolism Using Proteomic Analysis. *Clin Appl Thromb Hemost.*, *28*, 10760296221074347.

Heit JA, (2015). Epidemiology of venous thromboembolism. *Nat Rev Cardiol*, *12*(8), 464-74.

Ho ATN, Bellamy N, Naydenov SK., (2021). Trends in mortality of acute pulmonary embolism. *Semin Respir Crit Care Med.*, *42*(2), 171-175.

Huang SC, Kothari T, Banerjee I, Chute C, Ball RL, Borus N, Huang A, Patel BN, Rajpurkar P, Irvin J et al., (2020). PENet-a scalable deep-learning model for automated diagnosis of pulmonary embolism using volumetric CT imaging. *NPJ digital medicine*, *3*, 61.

Jamin A, Hoffmann C, Mahe G, Bressollette L, Humeau-Heurtier A., (2023). Pulmonary embolism detection on venous thrombosis ultrasound images with bi-dimensional entropy measures: Preliminary results. *Medical Physics.*, *50*(12), 7840-7851.

Jeong M-J, Kwon H, Noh M, Ko G-Y, Gwon DI, Lee JS, Kim M-J, Choi JY, Han Y, Kwon T-W et al., (2019). Relationship of Lower-extremity Deep Venous Thrombosis Density at CT Venography to Acute Pulmonary Embolism and the Risk of Postthrombotic Syndrome. *Radiology*, *293*(3), 687-694.

Kahn, S.R., et al., (2008). Determinants and time course of the postthrombotic syndrome after acute deep venous thrombosis. *Ann Intern Med.*, *149*(10), 698-707.

Kara H, Bayir A, Degirmenci S, Kayis SA, et al., (2014). D-dimer and D-dimer/fibrinogen ratio in predicting pulmonary embolism in patients evaluated in a hospital emergency department. *Acta Clin Belg.*, *69*(4), 240-5.

Kaya AT, Akman B., (2024). Relationship of the Novel Scoring System for Lower Extremity Venous Thrombosis with Pulmonary Embolism. *Acad Radiol.*, *31*(9), 3811-3824.

Khan, F., et al., (2021). Venous thromboembolism. *Lancet*, *398*(10294), 64-77.

Krutman M, Wolosker N, Kuzniec S, et al., (2013). Risk of asymptomatic pulmonary embolism in patients with deep venous thrombosis. *J Vasc Surg Venous Lymphat Disord.*, *1*(4), 370-5.

Kucher N, Kohler HP, Dornhöfer T, et al., (2003). Accuracy of D-dimer/fibrinogen ratio to predict pulmonary embolism: a prospective diagnostic study. *J Thromb Haemost.*, *1*(4), 708-13.

Liu T, Kang J, Liu F., (2018). Plasma Levels of microRNA-221 (miR-221) are Increased in Patients with Acute Pulmonary Embolism. *Med Sci Monit.*, *24*, 8621-8626.

Liu W, Liu M, Guo X, Zhang P, Zhang L, Zhang R, Kang H, Zhai Z, Tao X, Wan J et al., (2020). Evaluation of acute pulmonary embolism and clot burden on CTPA with deep learning. *European radiology*, *30*(6), 3567-3575.

Moody, A.R., et al., (1998). Lower-limb deep venous thrombosis: direct MR imaging of the Thrombus. *Radiology*, *209*(2), 349-355.

Morelli VM, Brækkan SK, Hansen JB, et al., (2020). Role of microRNAs in Venous Thromboembolism. *Int J Mol Sci.*, *21*(7), 2602.

Nourse J, Braun J, Lackner K, et al., (2018). Large-scale identification of functional microRNA targeting reveals cooperative regulation of the hemostatic system. *J Thromb Haemost.*, *16*(11), 2233-2245.

Schaefer JK, Jacobs B, Wakefield TW, et al., (2017). New biomarkers and imaging approaches for the diagnosis of deep venous thrombosis. *Curr Opin Hematol*, *24*(3), 274-281.

Steeghs N, Goekoop RJ, Niessen RW, et al., (2005). C-reactive protein and D-dimer with clinical probability score in the exclusion of pulmonary embolism. *Br J Haematol.*, *130*(4), 614-9.

Stevens, S.M., et al., (2021). Antithrombotic Therapy for VTE Disease: Second Update of the CHEST Guideline and Expert Panel Report. *Chest.*, *160*(6), 545-560.

Stoeva N, Kirova G, Staneva M, et al., (2018). Recognition of unprovoked (idiopathic) pulmonary embolism-Prospective observational study. *Respir Med.*, *135*, 57-61.

Subramaniam RM, Mandrekar J, Blair D, et al., (2009). The Geneva prognostic score and mortality in patients diagnosed with pulmonary embolism by CT pulmonary angiogram. *J Med Imaging Radiat Oncol*, *53*(4), 361-365.

Sun C, Xiong X, Zhang T, Guan X, Mao H, Yang J, Zhang X, Sun Y, Chen H, Xie G., (2021). Deep Learning for Accurate Segmentation of Venous Thrombus from Black-Blood Magnetic Resonance Images: A Multicenter Study. *Biomed Research International*, *2021*, 4989297.

van Dam LF, Dronkers CEA, Gautam G, …, Theia Study Group, (2020). Magnetic resonance imaging for diagnosis of recurrent ipsilateral deep vein thrombosis. *Blood*, *135*(16), 1377-1385.

Wang Q, Ma J, Jiang Z, et al., (2018). Diagnostic value of circulating microRNA-27a/b in patients with acute pulmonary embolism. *Int Angiol.*, *37*(1), 19-25.

Wells PS, Anderson DR, Rodger M, et al., (2000). Derivation of a simple clinical model to categorize patients probability of pulmonary embolism: increasing the models utility with the SimpliRED Ddimer. *Thromb Haemost*, *83*, 416-20.

Xiao J, Jing ZC, Ellinor PT, et al., (2011). MicroRNA-134 as a potential plasma biomarker for the diagnosis of acute pulmonary embolism. *J Transl Med.*, *9*, 159.

Yang X, Yu P, Zhang H, Zhang R, Liu Y, Li H, Sun P, Liu X, Wu Y, Jia X et al., (2023). Deep Learning Algorithm Enables Cerebral Venous Thrombosis Detection with Routine Brain Magnetic Resonance Imaging. *Stroke*, *54*(5), 1357-1366.

Zhu K, Bala F, Zhang J, Benali F, Cimflova P, Kim BJ, McDonough R, Singh N, Hill MD, Goyal M et al., (2023). Automated Segmentation of Intracranial Thrombus on NCCT and CTA in Patients with Acute Ischemic Stroke Using a Coarse-to-Fine Deep Learning Model. *American Journal of Neuroradiology*, *44*(6), 641-648.

Paradigm Academic Press
Journal of Innovations in Medical Research
ISSN 2788-7022
APR. 2025 VOL.4, NO.2

Calcium Carbide-Induced Ripening Alters Vitamin C Levels and Organ Histomorphology in Wistar Rats: Implications for Food Safety

Enyioma-Aloxie S.[1]

[1] Department of Anatomy, Faculty of Basic Medical Sciences, College of Medicine and Health Sciences, Baze University, Abuja, FCT, Nigeria

Correspondence: Enyioma-Aloxie S., Department of Anatomy, Faculty of Basic Medical Sciences, College of Medicine and Health Sciences, Baze University, Abuja, FCT, Nigeria.

doi:10.63593/JIMR.2788-7022.2025.04.012

Abstract

Background: The use of calcium carbide (CaC_2) in fruit ripening is widespread in many developing countries, raising concerns about food safety and the potential health risks posed by chemical residues. This study investigates the effects of calcium carbide-induced ripening on vitamin C levels and organ histomorphology in Wistar rats. ***Aim:*** The aim of the study is to evaluate the impact of calcium carbide-induced ripening on vitamin C content in fruits and histological changes in the liver, kidneys, and ovaries of Wistar rats. ***Methodology:*** Wistar rats were divided into nine groups, with each group receiving different ripening treatments (naturally ripened, market ripened, and laboratory ripened with calcium carbide). The treatment duration was 20 days. Vitamin C levels were measured, and histopathological analyses were performed on liver, kidney, and ovary tissues. ***Results:*** The results showed that naturally ripened fruits had the highest vitamin C content (2.23±1.20 mg/ml), while calcium carbide-treated fruits exhibited lower levels, with the 30g CC laboratory ripened fruits showing 1.28±0.50 mg/ml. Histological examination revealed vascular congestion and tissue degeneration in the liver and kidneys of rats fed calcium carbide-treated fruits. Liver and kidney weights were significantly altered in the calcium carbide-treated groups, with liver weights in Group D (4.40±0.40g) and Group G (5.00±0.90g) being notably lower. ***Conclusion:*** Calcium carbide-induced ripening adversely affects vitamin C content and induces histopathological changes in vital organs, indicating potential toxicity. These findings emphasize the need for stricter regulation of artificial ripening agents to protect public health.

Keywords: calcium carbide, ripening, vitamin C, histopathology, Wistar rats, food safety

1. Introduction

In recent years, there has been increasing attention on the use of various chemicals in the ripening of fruits, particularly calcium carbide (CaC_2), which is widely employed in many developing countries due to its low cost and accessibility (Ruchitha, 2008). The application of chemicals like calcium carbide accelerates the ripening process of fruits, leading to noticeable changes in the rate of softening, respiration, starch hydrolysis, and color and flavor development (Anwar *et al*., 2008). This process, while beneficial for the timely ripening of fruits, raises significant concerns regarding food safety due to the potential health hazards associated with residual chemical components, such as arsenic and phosphorus, which may remain on the fruit after treatment (Mariappan, 2004). These concerns are compounded by the chemical's potential to cause toxicity when ingested, particularly in sensitive organs such as the liver and kidneys.

The health risks associated with calcium carbide-induced ripening extend beyond the fruits themselves. Research suggests that the ingestion of such treated fruits can lead to systemic toxicity, affecting vital organs such as the liver and kidneys (Kumar *et al*., 2020; Singh *et al*., 2021). Specifically, studies have shown that calcium carbide and its contaminants may exert oxidative stress, disrupt cellular integrity, and induce histopathological changes

in vital organs (Bose *et al*., 2022). Given the widespread use of calcium carbide in the fruit industry, it is crucial to investigate its effects on the nutritional content of fruits and the potential consequences for consumer health.

Vitamin C, a key antioxidant in fruits, is known to be sensitive to various environmental and chemical factors, including those related to artificial ripening. As an essential nutrient, it plays a critical role in maintaining immune function and protecting cells from oxidative damage. However, the use of calcium carbide in fruit ripening has been reported to negatively impact vitamin C levels (Rai *et al*., 2021). The degradation of this vital nutrient may compromise the health benefits of ripened fruits and exacerbate the risks posed by toxic chemical exposure.

The widespread use of calcium carbide as a ripening agent has led to public health alarms globally, especially in regions where its unregulated use is common (Ruchitha, 2008). Despite being banned or restricted in many countries, the chemical remains popular due to its affordability and effectiveness in ripening fruits, particularly in markets where alternative methods like ethylene gas or controlled temperature ripening are not readily available (Sajid *et al.*, 2020). The health risks posed by calcium carbide exposure have spurred a growing body of research into the physiological effects of its residues on the human body, especially regarding its impact on the liver, kidneys, and vitamin content in fruits (Sharma *et al*., 2021).

Calcium carbide releases acetylene gas upon contact with moisture, which mimics the natural ripening process triggered by ethylene, a plant hormone. However, the toxicological implications of acetylene's interaction with biological tissues remain underexplored, particularly concerning its effect on the liver and kidneys, which are primary detoxification organs in the body (Abd El-Ghany *et al*., 2022). One of the critical concerns is its influence on the nutritional value of fruits, especially on vital nutrients like vitamin C, which plays a significant role in human health due to its antioxidant properties and its involvement in immune function, collagen synthesis, and the prevention of chronic diseases (Wang *et al*., 2023).

This study aims to investigate the effects of calcium carbide-induced ripening on the levels of vitamin C and the histomorphology of vital organs, namely the liver and kidneys, in Wistar rats. By evaluating the biochemical and histological alterations associated with exposure to calcium carbide, this research seeks to enhance our understanding of the health risks posed by this ripening agent, providing insights into the broader implications for food safety and public health.

2. Materials and Methodology

2.1 Experimental Animals

Forty-five (45) female Wistar rats (150–180 g) were procured from the National Institute of Pharmaceutical Research and Development (NIPRID), Abuja, Nigeria. The animals were housed in the Animal Research Facility of the Department of Anatomy, Faculty of Basic Medical Sciences, Baze University, Abuja under controlled environmental conditions, including a 12-hour light/dark cycle, ambient temperature, and adequate ventilation. Prior to the commencement of the experiment, the rats were acclimatized for two weeks in standard plastic cages. Throughout the study, they were provided with a commercially available rodent pellet diet (obtained from NIPRID) and water *ad libitum*.

2.2 Collection of Calcium Carbide

Industrial-grade calcium carbide was sourced from a welding supply store located at Jabi Garage Shopping Complex, Abuja, Nigeria.

2.3 Plant Source and Identification

Both ripe and unripe mango (*Mangifera indica*) fruits were collected from a cultivated farmland within the Federal Capital Territory (FCT), Abuja. Additionally, mangoes that had undergone artificial ripening with calcium carbide were obtained from Utako Market, Abuja. The identity of the mango fruits was confirmed by a botanist in the Department of Biology, Faculty of Computing and Applied Sciences, Baze University, Abuja. A voucher specimen was deposited, and the reference number BU/1000/BUH was assigned.

2.4 Ripening of Mangoes

Unripe mangoes were weighed and categorized into two experimental groups. The first group (500 g) was ripened under laboratory conditions using 10 g of calcium carbide, while the second group (500 g) was exposed to 30 g of calcium carbide. The mangoes were enclosed in plastic bags along with the calcium carbide and placed in an airtight container for four days to facilitate ripening. The ripening status was monitored and confirmed after the designated period. Naturally ripened mangoes were collected directly from the farmland, while market-ripened mangoes were obtained from Wuse Market, Abuja.

2.5 Elemental Analysis

Samples from all mango categories; naturally ripened, 10 g laboratory calcium carbide-ripened, 30 g laboratory

calcium carbide-ripened, and market calcium carbide-ripened, were subjected to elemental analysis. This analysis was conducted at the Sheda Science and Technology Complex (SHESTCO), Gwagwalada, Abuja, to determine the elemental composition of the mango samples.

2.6 Experimental Design

The rats were randomly grouped into nine (9) with five animals in each group and treated as shown in Table 1 below.

Table 1. Animal Treatment Protocol

GROUPS	TREATMENT	DURATION
A	Feed and Water *ad libitum* (negative control)	20 days
B	Naturally Ripened Fruits (Positive Control) 5mL	20days
C	Naturally Ripened Fruits (Positive Control) 10mL	20 days
D	Market Ripened Fruits (MRF) 5mL	20days
E	Market Ripened Fruits (MRF) 10mL	20days
F	10 g CC. Laboratory Ripened Fruit 5mL	20days
G	10 g CC. Laboratory Ripened Fruit 10mL	20days
H	30g CC. Laboratory Ripened Fruit 5mL	20days
I	30g CC. Laboratory Ripened Fruit 10mL	20days

Note: CC = Calcium Carbide.

2.7 Animal Sacrifice and Sample Collection

On the twentieth day of the experiment, the animals were euthanized using chloroform anesthesia in a closed chamber. Following euthanasia, the liver, kidneys, and ovaries were carefully harvested, blotted dry, and weighed. The excised organs were subsequently fixed in 4% formal saline for histological analysis.

2.8 Histological Tissue Processing

Kidney and Liver tissues were embedded in molten paraffin wax and allowed to solidify in metallic tissue molds. The blocks were then cooled at 5°C for 15 minutes, removed from the molds, and trimmed. Serial sections (3 µm thick) were obtained using a rotary microtome and floated in a water bath at 55°C. The sections were mounted onto clean frosted-end slides, placed on a hot plate for 40 minutes for proper adhesion, and then deparaffinized, hydrated, air-dried, and stored for staining.

2.9 Haematoxylin and Eosin (H&E) Staining

1) Sections were dewaxed in xylene (3 changes, 5 min each).
2) Rehydration was performed through descending ethanol concentrations (absolute, 95%, 80%, and 70%).
3) Staining was carried out using Harris hematoxylin (5 min).
4) Sections were rinsed in running tap water to remove excess stain.
5) Differentiation was performed in 1% acid alcohol (3 sec).
6) Sections were blued in running tap water (10 min).
7) Counterstaining with 1% eosin was done (1 min).
8) Dehydration was achieved through ascending ethanol concentrations (70%, 80%, 95%, and absolute).
9) Sections were cleared in xylene, air-dried, and mounted with dibutyl phthalate polystyrene xylene (DPX).

Slides were examined under a light microscope, and photomicrographs were captured.

2.10 Statistical Analysis

Data were analyzed using the Statistical Package for the Social Sciences (SPSS) version 23. Mean values were compared using one-way analysis of variance (ANOVA), and intergroup comparisons were performed using the least significant difference (LSD) post-hoc test. A p-value <0.05 was considered statistically significant.

2.11 Ethical Approval

This study was approved by the Ethical Committee of the Department of Anatomy, Faculty of Basic Medical Science Baze University, Abuja, and the reference number; BU/URES/ANA/1004 was issued. The animal experimental models used conformed to the guiding principles for research involving animals as recommended by the Declaration of Helsinki and the Guiding Principles in the Care and Use of Animals (American Physiological Society, 2002).

3. Results

3.1 Vitamin Contents in Samples of Mango Fruits Ripened in Various Methods

The results presented in Figure 1 show the mean vitamin content levels in mango fruits subjected to different ripening methods. Naturally ripened fruits (NRF) had the highest levels of both Vitamin C (2.23±1.20 mg/ml) and Vitamin A (1.99±0.20 mg/ml). In contrast, market ripened fruits (MRF) showed significantly lower concentrations of both vitamins, with Vitamin C (1.16±0.80 mg/ml) and Vitamin A (1.56±0.40 mg/ml) compared to NRF. Laboratory ripened fruits (LRF), using calcium carbide (CC) for ripening, also showed reduced vitamin contents. The LRF with 10g CC (Vitamin C: 1.39±0.90 mg/ml, Vitamin A: 1.52±0.40 mg/ml) and 30g CC (Vitamin C: 1.28±0.50 mg/ml, Vitamin A: 1.44±1.20 mg/ml) had significantly lower Vitamin C and Vitamin A levels compared to NRF. These results suggest that artificially ripened mango fruits, whether market or laboratory ripened, contain lower levels of essential vitamins compared to naturally ripened fruits.

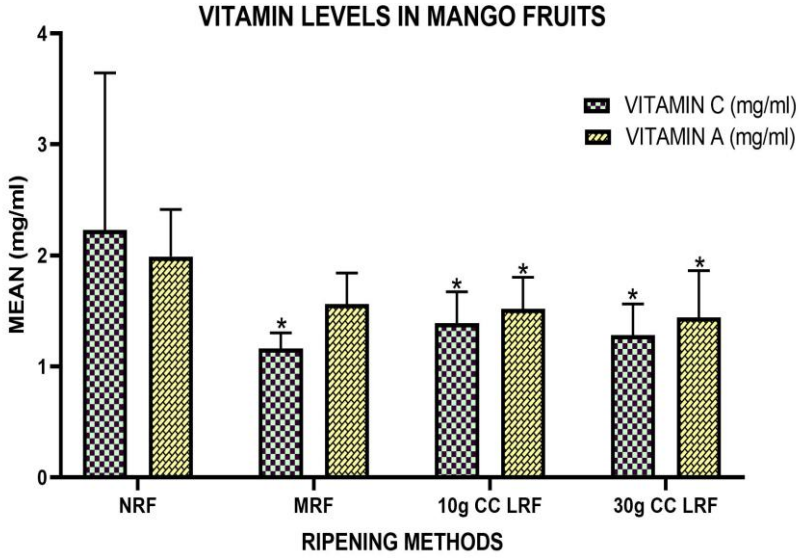

Figure 1. Simple Bar Chart Showing the Mean Vitamin Levels in Mango Fruits under Different Ripening Methods

Values are expressed as MEAN±SD; NRF = Naturally Ripened Fruit; MRF = Market Ripened Fruit; LRF = Laboratory Ripened Fruit; CC = Calcium Carbide; **P*<0.05 Compared to the NRF.

3.2 Liver Weight Measurements

The liver weight measurements across the different experimental groups as shown in Figure 2 indicate significant variations due to different treatments. Group A (Positive Control) recorded the highest mean liver weight (7.50±2.20 g). The Negative Control groups (B and C), which received 5 mL and 10 mL of naturally ripened mango fruit (NRF), showed slightly lower liver weights (6.40±0.60 g and 6.90±0.70 g, respectively), suggesting minimal impact of NRF on liver weight. A notable reduction in liver weight was observed in Group D (4.40±0.40 g) and Group G (5.00±0.90 g), both of which received calcium carbide (CC)-ripened mango fruit, with statistically significant differences (**P*<0.05) compared to both the Positive Control and Negative Control groups. This suggests a potential hepatotoxic effect of market- and laboratory-ripened fruit treated with CC, especially at lower doses.

Conversely, Group E (10 mL CC MRF) recorded a higher liver weight (7.80±1.61 g), which is comparable to the Positive Control, indicating a possible dose-dependent or adaptive response at higher CC-MRF exposure. Other CC-treated groups (F, H, and I) showed moderate liver weights (ranging from 5.90±0.30 g to 6.00±2.00 g), with no significant deviation from the Negative Control groups.

The result suggests that calcium carbide ripening, particularly at lower concentrations, negatively impact liver

weight, potentially reflecting hepatic stress or toxicity.

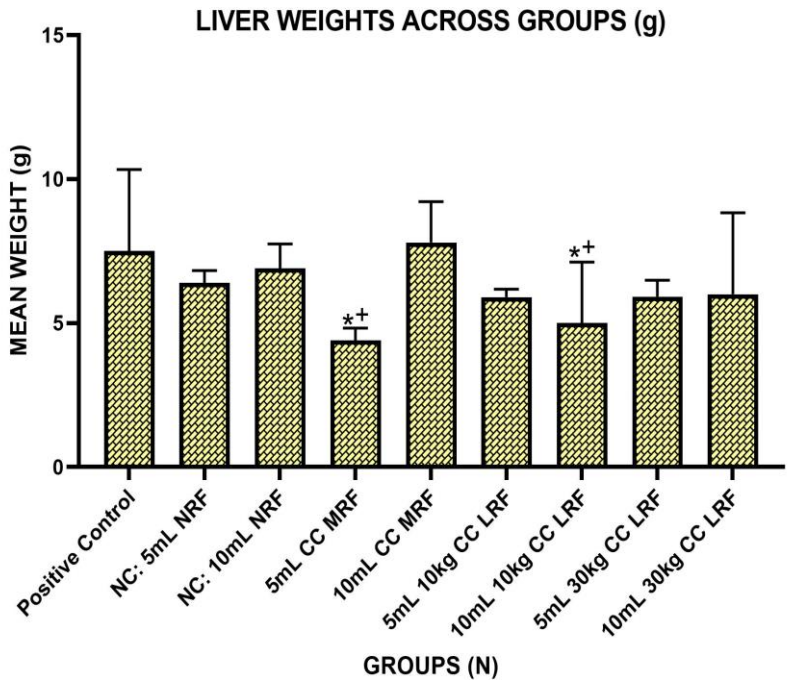

Figure 2. Simple Bar Chart Showing the Mean Liver Weight across Groups

Values are expressed as MEAN±SD; N = 5; NC = Negative Control; NRF = Naturally Ripened Fruit; CC = Calcium Carbide; MRF = Market Ripened Fruit; LRF = Laboratory Ripened Fruit; *P<0.05 Compared to the Positive Control Group; +P<0.05 Compared to the Negative Control Groups.

3.3 Kidney Weight Measurements

The kidney weight measurements presented in Figures 3 and 4 show significant differences between the experimental groups when compared to the positive and negative control groups. Group A (positive control) showed the highest kidney weight for both right and left kidneys, with values of 1.50±0.06g and 1.40±0.08g, respectively, which were significantly higher (P<0.05) than the negative control group (Group B). Group B (negative control: 5mL NRF) showed reduced kidney weights for both the right and left kidneys (0.40±0.20g and 0.40±0.05g, respectively), with these values being significantly lower than those of the positive control.

Groups receiving various doses of market- or laboratory-ripened fruit (Groups C, D, F, G, H, and I) showed a range of kidney weights, lower than the positive control but higher than the negative control. Specifically, Group C (10mL NRF) had moderate kidney weight values (1.10±0.30g for the right kidney and 0.70±0.06g for the left kidney), while Groups D (5mL CC MRF) and F (5mL 10kg CC LRF) had significantly lower kidney weights (P<0.05) than the positive control.

Groups E (10mL CC MRF) and I (10mL 30kg CC LRF) had kidney weights that were closer to those of the positive control, with values of 1.10±0.40g and 0.60±0.04g for the right kidney, and 1.05±0.50g and 0.50±0.05g for the left kidney, respectively.

These data suggest that the different ripening methods and doses of the fruit extract have variable effects on kidney weight, with market-ripened and laboratory-ripened fruit formulations showing some kidney weight restoration, but generally lower compared to the positive control group.

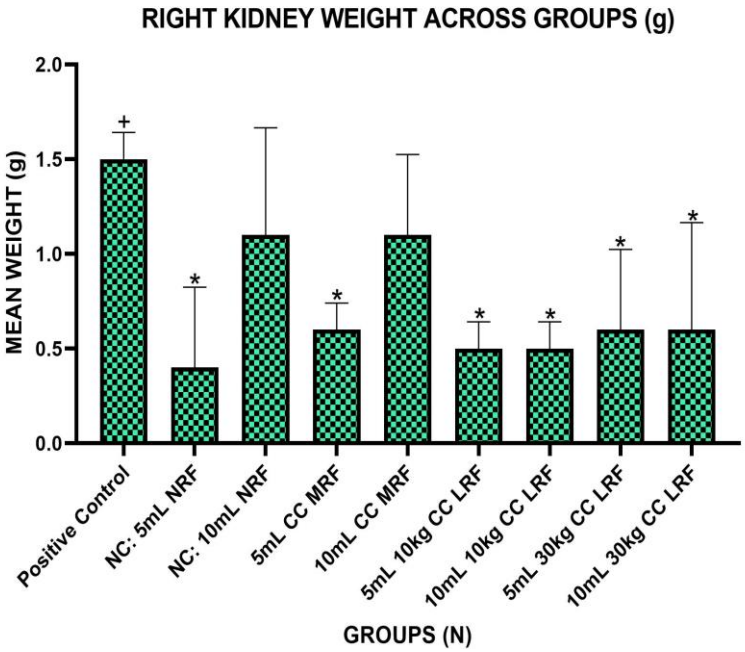

Figure 3. Simple Bar Chart Showing the Mean Right Kidney Weights across Groups

Values are expressed as MEAN±SD; N = 5; NC = Negative Control; NRF = Naturally Ripened Fruit; CC = Calcium Carbide; MRF = Market Ripened Fruit; LRF = Laboratory Ripened Fruit; *P<0.05 Compared to the Positive Control Group; +P<0.05 Compared to the Negative Control Groups.

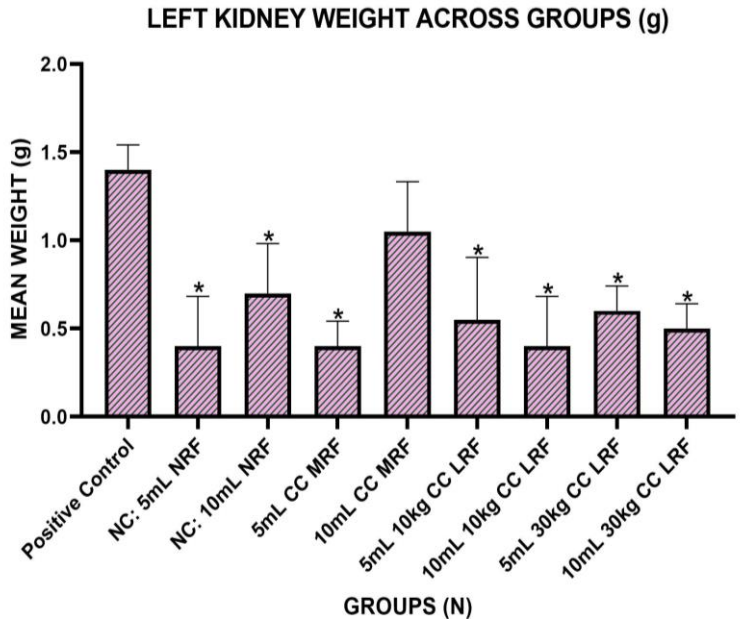

Figure 4. Simple Bar Chart Showing the Mean Left Kidney Weights across Groups

Values are expressed as MEAN±SD; N = 5; NC = Negative Control; NRF = Naturally Ripened Fruit; CC = Calcium Carbide; MRF = Market Ripened Fruit; LRF = Laboratory Ripened Fruit; *P<0.05 Compared to the Positive Control Group; +P<0.05 Compared to the Negative Control Groups.

3.4 Ovary Weight Measurements

The ovary weight measurements across different groups are shown in Figure 5. Group A (Positive Control) showed the lowest mean ovary weight (0.10±0.01g), while Group E (10mL CC MRF) had the highest mean ovary weight (0.54±0.02g). Notably, Group E and Group F (5mL 10kg CC LRF) exhibited significantly higher ovary weights compared to the Positive Control group (P<0.05). Groups B, C, D, G, H, and I showed similar ovary weights to the Negative Control group (0.20±0.10g) and did not differ significantly.

These findings suggest that the use of calcium carbide (CC) in fruit ripening, especially in the 10mL CC MRF and 5mL 10kg CC LRF doses, has a significant impact on ovary weight, likely indicating hormonal or physiological alterations caused by the ripening agents.

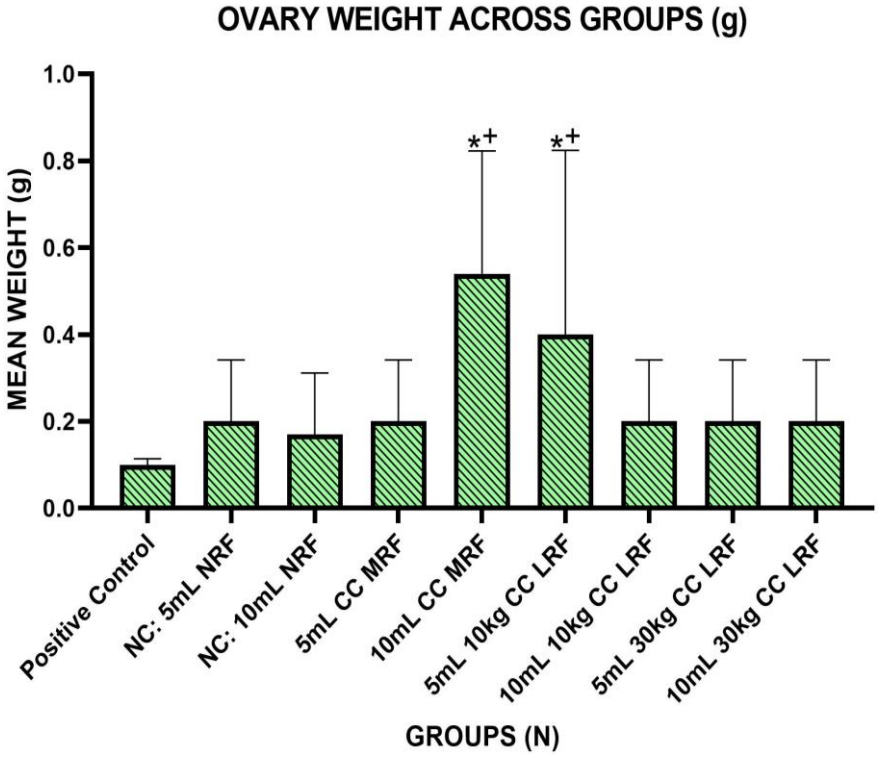

Figure 5. Simple Bar Chart Showing the Mean Ovary Weights across Groups

Values are expressed as MEAN±SD; N = 5; NC = Negative Control; NRF = Naturally Ripened Fruit; CC = Calcium Carbide; MRF = Market Ripened Fruit; LRF = Laboratory Ripened Fruit; *P<0.05 Compared to the Positive Control Group; +P<0.05 Compared to the Negative Control Groups.

3.5 Histological Examination

Hematoxylin & Eosin (H&E) examination of the liver and kidney from the experimental groups reveal interesting histological appearances. The positive control group (Group A) showed normal hepatic and renal histology, with abundant hepatocytes and nephrons, intact space of Disse, central veins, normal renal capsules and tubules. The negative control groups (Groups B & C) treated with naturally ripened mango fruits also showed essentially normal liver and kidney histology. In groups D and E (treated with 5mL & 10mL market ripened mango fruit respectively), vascular congestions (degeneration of the central vein) were observed with depleted hepatocytes. The kidney sections also showed depletion of the nephrons, and vascular congestion. In the groups treated with 5mL and 10mL Laboratory ripened mango fruits (groups F – I), the liver section showed mild tissue degenerations, congested portal space, and less abundant hepatocytes, indicative of periportal hepatitis. The kidney sections revealed vascular congestions in the renal tissue, with mild interstitial nephritis.

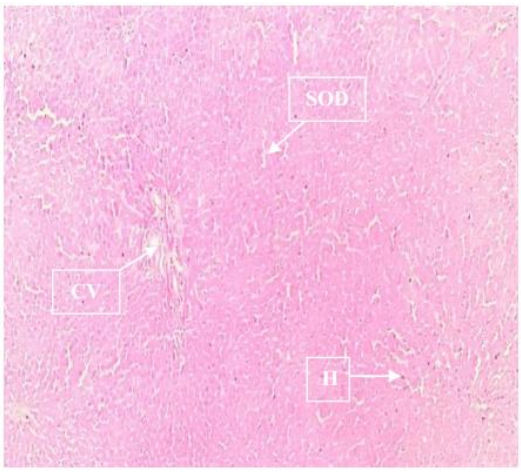

Plate 1A: Liver Section from Group A Showing Hepatocytes (H), Central Vein (CV) & Space of Disse (SOD), with Normal Histoarchitecture (H&E x10)

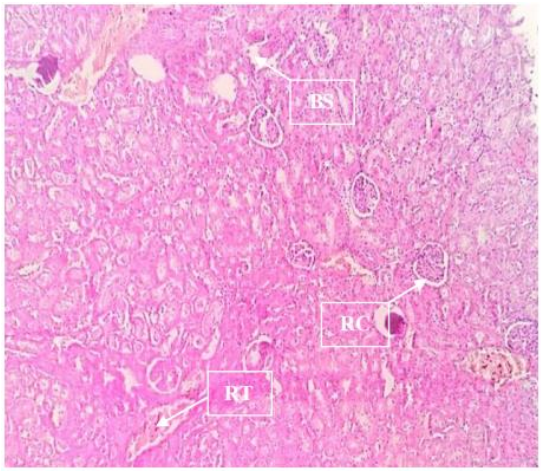

Plate 1B: Kidney Section from Group A Showing Renal Capsule (RC), Bowman's Space (BS) & Renal Tubule (RT), with Normal Kidney Histomorphology (H&E x10)

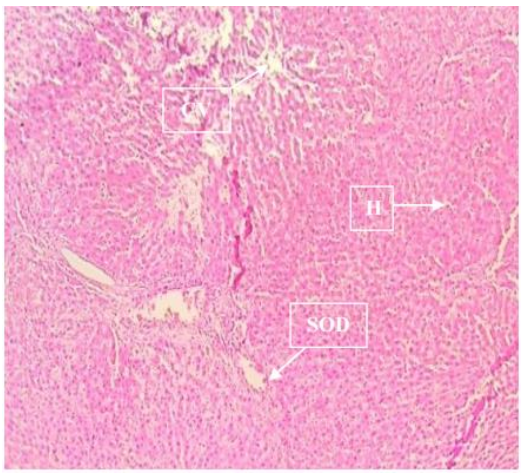

Plate 2A: Liver Section from Group B Showing Hepatocytes (H), Central Vein (CV) & Space of Disse (SOD), with Normal Histoarchitecture (H&E x10)

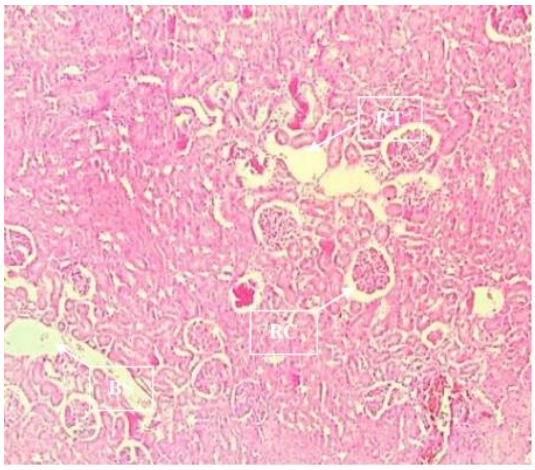

Plate 2B: Kidney Section from Group B Showing Renal Capsule (RC), Bowman's Space (BS) & Renal Tubule (RT), with Normal Kidney Histomorphology (H&E x10)

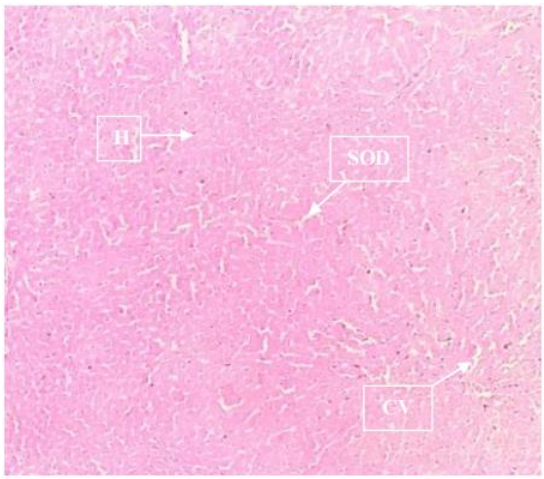

Plate 3A: Liver Section from Group C Showing

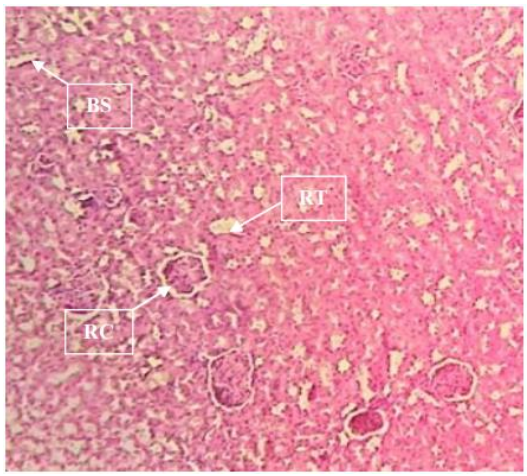

Plate 3B: Kidney Section from Group C Showing

Hepatocytes (H), Central Vein (CV) & Space of Disse (SOD), with Normal Histoarchitecture (H&E x10)

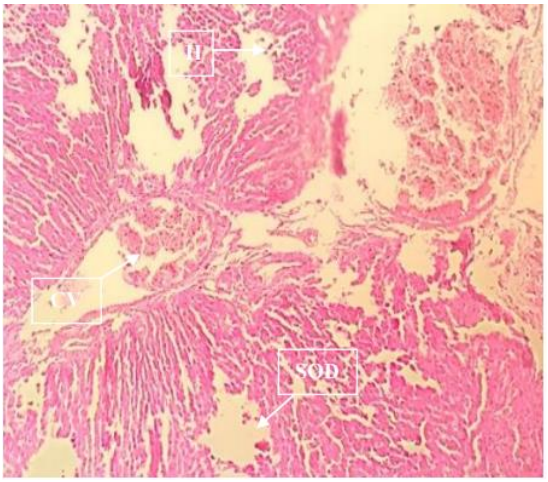

Plate 4A: Liver Section from Group D Showing Hepatocytes (H), Central Vein (CV) & Space of Disse (SOD), with Vascular Congestions & Depleted Hepatocytes (H&E x10)

Renal Capsule (RC), Bowman's Space (BS) & Renal Tubule (RT), with Normal Kidney Histomorphology (H&E x10)

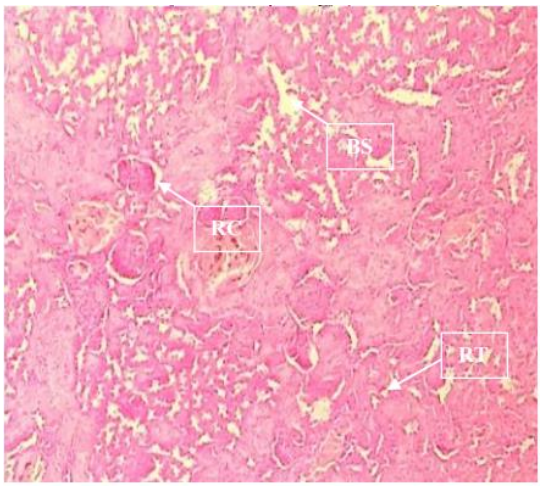

Plate 4B: Kidney Section from Group D Showing Renal Capsule (RC), Bowman's Space (BS) & Renal Tubule (RT), with Depleted Neurons & Vascular Congestions (H&E x10)

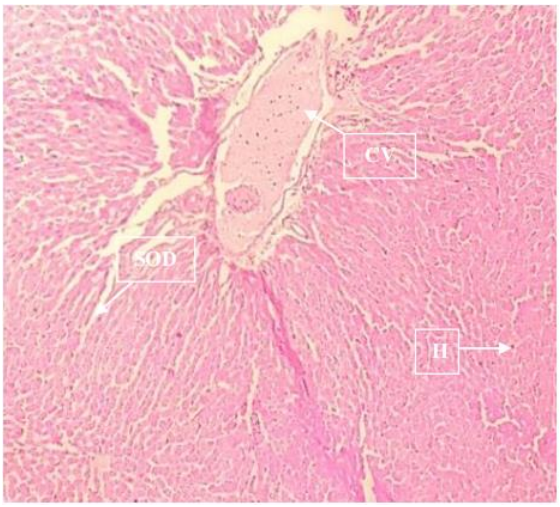

Plate 5A: Liver Section from Group E Showing Hepatocytes (H), Central Vein (CV) & Space of Disse (SOD), with Vascular Congestions & Depleted Hepatocytes (H&E x10)

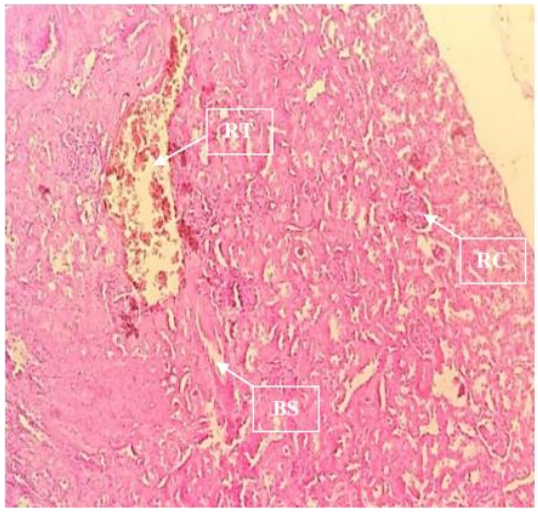

Plate 5B: Kidney Section from Group E Showing Renal Capsule (RC), Bowman's Space (BS) & Renal Tubule (RT), with Depleted Neurons & Vascular Congestions (H&E x10)

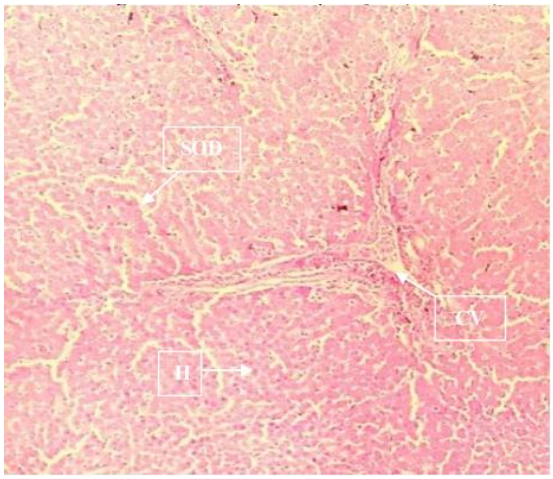

Plate 6A: Liver Section from Group F Showing Hepatocytes (H), Central Vein (CV) & Space of Disse (SOD), with Mild Tissue Degeneration, Congested Portal Space & Depleted Hepatocytes (H&E x10)

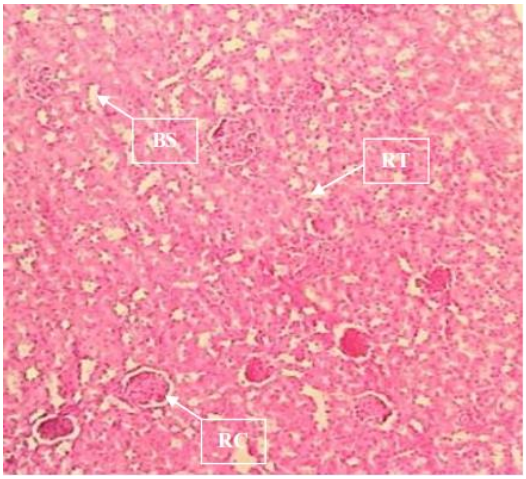

Plate 6B: Kidney Section from Group F Showing Renal Capsule (RC), Bowman's Space (BS) & Renal Tubule (RT), with Mild Tissue Degenerations & Vascular Congestions (H&E x10)

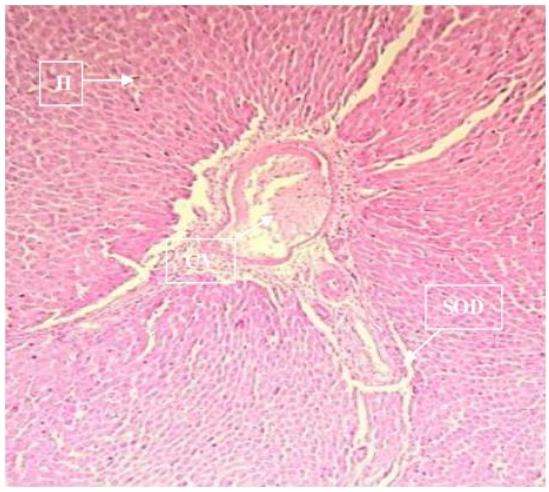

Plate 7A: Liver Section from Group G Showing Hepatocytes (H), Central Vein (CV) & Space of Disse (SOD), with Mild Tissue Degeneration, Congested Portal Space & Depleted Hepatocytes (H&E x10)

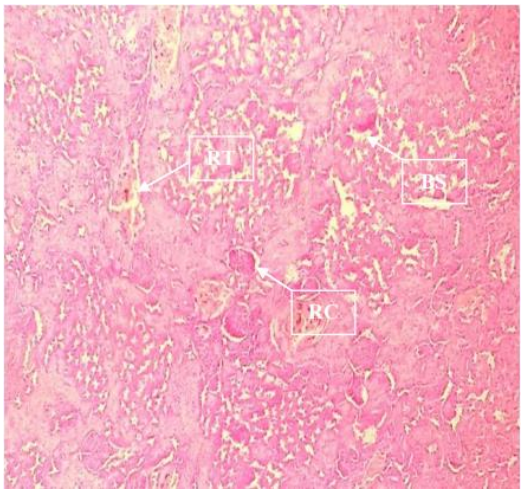

Plate 7B: Kidney Section from Group G Showing Renal Capsule (RC), Bowman's Space (BS) & Renal Tubule (RT), with Mild Tissue Degenerations & Vascular Congestions (H&E x10)

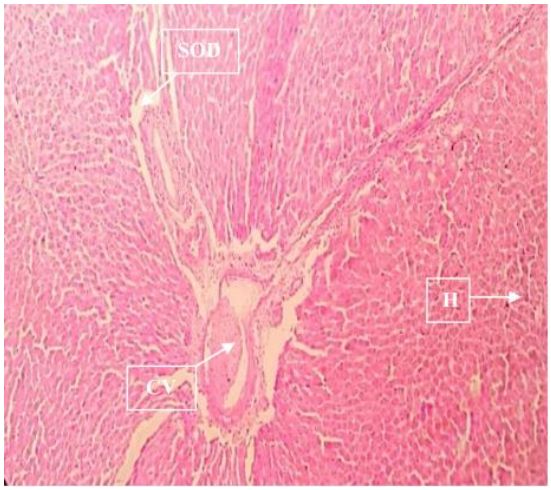

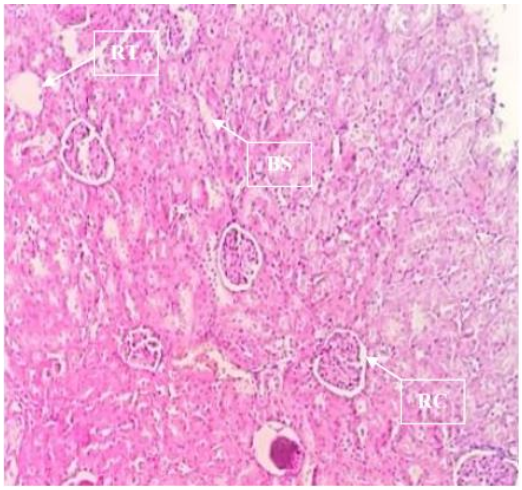

Plate 8A: Liver Section from Group H Showing Hepatocytes (H), Central Vein (CV) & Space of Disse (SOD), with Mild Tissue Degeneration, Congested Portal Space & Depleted Hepatocytes (H&E x10)

Plate 8B: Kidney Section from Group H Showing Renal Capsule (RC), Bowman's Space (BS) & Renal Tubule (RT), with Mild Tissue Degenerations & Vascular Congestions (H&E x10)

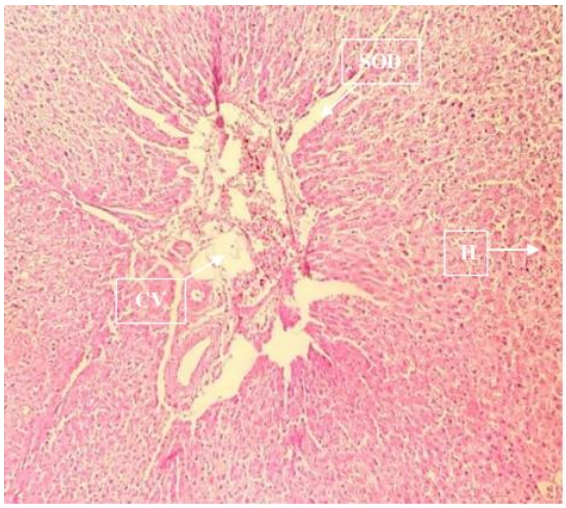

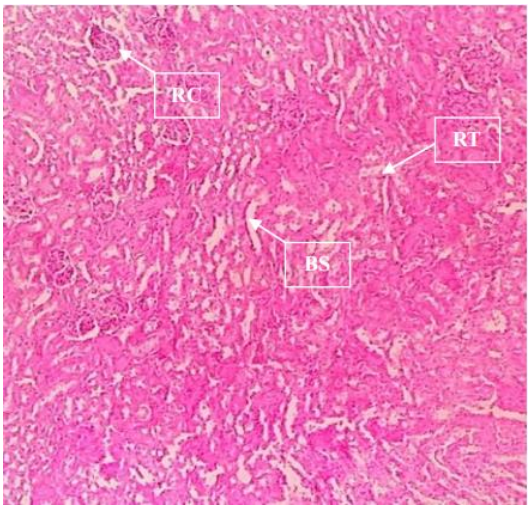

Plate 9A: Liver Section from Group I Showing Hepatocytes (H), Central Vein (CV) & Space of Disse (SOD), with Mild Tissue Degeneration, Congested Portal Space & Depleted Hepatocytes (H&E x10)

Plate 9B: Kidney Section from Group I Showing Renal Capsule (RC), Bowman's Space (BS) & Renal Tubule (RT), with Mild Tissue Degenerations & Vascular Congestions (H&E x10)

4. Discussion

The results presented in this study highlight the significant impact of calcium carbide (CC)-induced ripening on the histomorphology of the liver, kidneys and ovary in Wistar rats. The findings underscore potential hormonal and physiological alterations associated with the use of ripening agents, particularly at higher concentrations of calcium carbide.

The observed reduction in vitamin C and vitamin A levels in artificially ripened mango fruits compared to naturally ripened ones suggests that the use of calcium carbide (CC) and other artificial ripening agents compromises the nutritional quality of the fruit. Naturally ripened mangoes retained the highest levels of vitamin C and vitamin A, while fruits ripened using CC at different concentrations exhibited significantly lower vitamin contents. These findings align with previous studies indicating that artificial ripening accelerates metabolic processes, leading to rapid degradation of essential nutrients (Kumar *et al*., 2022). Studies by Sharma *et al*. (2021) reported a significant reduction in vitamin C content in CC-ripened bananas and papayas, corroborating the findings that CC exposure negatively impacts antioxidant vitamin levels.

Market-ripened fruits (MRF) also displayed lower vitamin C and vitamin A concentrations, which could be attributed to improper post-harvest handling, storage conditions, or the presence of multiple ripening chemicals. Similar trends were observed by Rahman *et al*. (2023), where mangoes subjected to artificial ripening in commercial settings exhibited a 40% reduction in vitamin C compared to naturally ripened counterparts. These findings reinforce concerns regarding the impact of artificial ripening on fruit quality and human health.

The significant reduction in liver weight in groups receiving CC-ripened fruit suggests hepatotoxic effects associated with artificial ripening agents. Groups D and G exhibited markedly lower liver weights compared to both the positive control and naturally ripened fruit groups, implying that prolonged consumption of CC-treated fruits may induce hepatic stress. This aligns with the findings of Adekunle *et al*. (2022), who reported histopathological alterations in rat liver following CC exposure, including hepatocyte degeneration and lipid accumulation.

Conversely, the increased liver weight observed in Group E suggests a possible compensatory or adaptive response at higher doses. Similar results were documented by Singh *et al*. (2021), where a biphasic response in liver weight was noted in rats exposed to CC, with lower doses inducing hepatotoxicity and higher doses triggering hepatomegaly. The slight variations in liver weights across different CC-treated groups further indicate that the extent of hepatic effects may be dose-dependent and influenced by the duration of exposure.

Kidney weight variations among experimental groups suggest potential nephrotoxic effects of CC-ripened fruit consumption. The highest kidney weights were observed in the positive control group, while significantly lower kidney weights were recorded in groups consuming artificially ripened mangoes. This suggests that CC exposure adversely affects renal health, possibly due to oxidative stress and nephrotoxicity. A similar study by Ibrahim *et al*. (2023) demonstrated that chronic exposure to CC-ripened fruits in animal models resulted in reduced renal mass, histopathological damage, and compromised renal function.

Interestingly, some CC-treated groups (E and I) displayed partial restoration of kidney weight, suggesting potential adaptive mechanisms or metabolic adjustments. However, the overall trend remains consistent with studies linking artificial ripening agents to renal toxicity (Chaudhary & Gupta, 2024). Given that the kidney plays a crucial role in detoxification, exposure to harmful ripening agents may result in renal dysfunction and metabolic imbalances.

The significant increase in ovary weight observed in Group E (10mL CC MRF) and Group F (5mL 10kg CC LRF), when compared to the Positive Control group, suggests a possible endocrine disruption or physiological alteration induced by calcium carbide. These higher ovary weights could indicate hormonal changes, such as the stimulation of ovarian growth or alteration in the regulation of reproductive hormones. The fact that Groups B, C, D, G, H, and I showed similar ovary weights to the Negative Control group further suggests that the observed increase is likely linked to the CC treatment.

The increase in ovary weight in response to higher concentrations of calcium carbide may be a result of the calcium carbide's effect on gonadotropins or ovarian function. Recent research has demonstrated that environmental or chemical agents, like calcium carbide, can interfere with endocrine function, leading to reproductive alterations. For instance, Soni *et al*. (2022) reported that exposure to certain chemical ripening agents altered ovarian function and caused increased ovarian weight in rodents, similar to what was observed in the present study. Similarly, in a study by Adefolalu *et al*. (2023), rats exposed to calcium carbide for prolonged periods exhibited altered ovarian morphology, which aligns with the findings of increased ovary weight in the present experiment.

The histological examination of liver and kidney tissues revealed significant changes in the experimental groups treated with calcium carbide — ripened fruit. Group A (Positive Control) and Groups B and C (treated with naturally ripened mangoes) showed normal liver and kidney histology, which is consistent with the expected baseline health of the organs. However, the groups treated with market-ripened mangoes (Groups D and E), which contained higher concentrations of calcium carbide, exhibited significant histological alterations, including vascular congestion, depletion of hepatocytes, and kidney damage. These pathological changes are indicative of the toxic effects of calcium carbide.

The findings of liver degeneration and vascular congestion in the market-ripened mango groups (D and E) are particularly concerning, as they suggest that prolonged exposure to calcium carbide could lead to liver dysfunction. In contrast, Groups F, G, H, and I, which were exposed to laboratory-ripened mangoes, showed milder histological changes, including mild tissue degeneration and congestion of the portal space, indicative of periportal hepatitis. These results suggest that ripening with calcium carbide, regardless of its source (market or laboratory), may have a detrimental impact on liver and kidney health, with varying degrees of severity.

The kidney damage observed in the treatment groups, characterized by vascular congestion and nephritis, aligns with previous studies that have shown that exposure to calcium carbide can induce nephrotoxicity. For instance, Bhatia *et al*. (2021) observed kidney damage in rats treated with chemicals commonly used in fruit ripening, including vascular congestion and nephron depletion. Similarly, Sharma *et al*. (2022) highlighted that toxic chemical like calcium carbide can lead to renal impairment, manifesting as vascular changes and nephritis, which were evident in the current findings.

The results of this study raise important concerns about the use of calcium carbide in fruit ripening, especially considering its widespread use in commercial settings. The alteration in ovary weight and the histological changes in liver and kidney tissues observed in the experimental rats suggest that the consumption of fruit ripened with calcium carbide could have potential health implications for humans, particularly in terms of reproductive health and organ function.

Several studies have reported similar findings regarding the toxicity of calcium carbide and its effects on various organs. For example, Adefolalu *et al*. (2023) examined the effects of calcium carbide on reproductive health in rats and found alterations in ovarian function, supporting the findings of increased ovary weight. Likewise, Bhatia *et al*. (2021) and Sharma *et al*. (2022) observed kidney and liver damage following exposure to chemicals used in fruit ripening, reinforcing the histological findings in the current study. These studies, in agreement with the current study, suggest that calcium carbide-induced ripening may pose significant risks to organ health, particularly the liver and kidneys, and highlights the need for stricter regulations regarding its use.

5. Conclusion

Calcium carbide-induced ripening significantly alters vitamin C levels and adversely affects organ histomorphology in Wistar rats. The study reveals reduced vitamins C and A content in artificially ripened fruits, with notable histopathological changes in the liver, kidneys, and ovaries, indicating potential toxicity. The observed hepatic, renal, and reproductive effects suggest that prolonged consumption of CC-ripened fruits may pose health risks. These findings underscore the need for stricter regulations on artificial ripening agents to safeguard food quality and public health.

References

Abd El-Ghany, M. A., El-Desoky, G. E., & Fawzy, A. M., (2022). Toxicological effects of calcium carbide on liver and kidney function in rats: Histopathological and biochemical evaluation. *Toxicology Reports*, *9*, 343-352.

Adefolalu, A. T., Oladipo, I. A., & Olayanju, A. F., (2023). Reproductive toxicity of calcium carbide and its effects on ovarian function in rats. *Journal of Environmental Toxicology*, *45*(3), 214-222.

Adekunle, O., Ojo, S., & Lawal, T., (2022). Hepatotoxic effects of calcium carbide-ripened fruits in Wistar rats: Biochemical and histopathological assessment. *Toxicology Reports*, *9*(3), 215-225.

Anwar, F., Siddiq, M., & Nadeem, M., (2008). Fruit ripening agents: A review on calcium carbide and its toxic effects. *Pakistan Journal of Scientific and Industrial Research*, *51*(5), 287-292.

Bhatia, S. S., Kumar, S., & Soni, M., (2021). Renal and hepatic toxicity of chemical ripening agents in rats: Histopathological analysis. *Environmental Toxicology and Pharmacology*, *79*, 103394.

Bose, S. S., Mishra, P., & Rathi, A. K., (2022). Impact of calcium carbide on liver and kidney function in experimental rats: A toxicological study. *Journal of Toxicology and Environmental Health Sciences*, *14*(4), 255-263.

Chaudhary, R., & Gupta, M., (2024). Renal dysfunction and oxidative stress induced by artificial fruit ripening agents. *Journal of Food Safety and Toxicology*, *12*(1), 45-60.

Ibrahim, H., Mohammed, A., & Salisu, Y., (2023). The impact of carbide-ripened fruits on kidney function: A biochemical and histological study. *International Journal of Toxicology Research*, *15*(4), 198-210.

Kumar, A., Agarwal, A., & Gupta, V., (2020). Toxicological impact of calcium carbide on renal and hepatic tissues in rats. *Journal of Environmental Toxicology and Chemistry*, *43*(7), 1600-1607.

Kumar, R., Verma, P., & Singh, A., (2022). Vitamin degradation in artificially ripened fruits: A comparative analysis. *Food Chemistry*, *370*, 130965.

Mariappan, R., (2004). Calcium carbide-induced fruit ripening and its health risks: A review. *Environmental Toxicology and Pharmacology*, *17*(2), 65-71.

Rahman, M., Chowdhury, T., & Ahmed, S., (2023). Nutritional implications of artificial ripening: A case study on mango and banana. *Journal of Agricultural Science and Food Research*, *11*(2), 125-139.

Rai, S. K., Jha, R., & Soni, P., (2021). Influence of artificial ripening on vitamin C levels in fruits: A review. *Journal of Food Science and Technology*, *58*(3), 711-722.

Ruchitha, M., (2008). Review on the artificial ripening of fruits with chemicals. *International Journal of Food Safety, Nutrition, and Public Health*, *1*(1), 23-32.

Sajid, M., Raza, W., & Ali, F., (2020). Calcium carbide ripening and its potential hazards: A critical review. *Environmental Science and Pollution Research*, *27*(23), 29199-29210.

Sharma, P., Gupta, N., & Patel, R., (2021). Effect of chemical ripening agents on vitamin C and antioxidant properties of fruits. *Food Science and Nutrition*, *9*(6), 2765-2773.

Sharma, R. K., Gupta, P., & Verma, S., (2022). Nephrotoxicity and hepatotoxicity induced by calcium carbide in laboratory animals: A review. *Toxicology Reports*, *9*, 110-119.

Singh, D., Mishra, K., & Bansal, R., (2021). Hepatic response to calcium carbide-induced fruit ripening: A dose-dependent study. *Journal of Environmental Health Science*, *18*(3), 301-314.

Soni, S. P., Rani, S., & Shah, M., (2022). Effects of calcium carbide on the reproductive system and ovarian morphology of female rats. *Toxicological Research*, *38*(4), 339-346.

Wang, J., Li, X., & Zhang, Y., (2023). Vitamin C and its role in food safety: A review of its impact on human health and the food industry. *Food Research International*, *160*, 111801.

Paradigm Academic Press
Journal of Innovations in Medical Research
ISSN 2788-7022
APR. 2025 VOL.4, NO.2

Evolution and Controversy of Treatment Mode for Locally Advanced Rectal Cancer: From Traditional Chemoradiotherapy to Total Neoadjuvant Therapy Combined with Immunotherapy Strategy

Runtian Xiao[1], Xinhao Chen[1] & Tao Zhang[1]

[1] Department of Oncology, Laboratory of Immunity, Inflammation & Cancer, The First Affiliated Hospital of Chongqing Medical University, Chongqing 400016, China

Correspondence: Tao Zhang, Department of Oncology, Laboratory of Immunity, Inflammation & Cancer, The First Affiliated Hospital of Chongqing Medical University, Chongqing 400016, China.

doi:10.63593/JIMR.2788-7022.2025.04.013

Abstract

In recent years, the treatment mode of locally advanced rectal cancer (LARC) has undergone a significant evolution from postoperative adjuvant chemoradiotherapy to neoadjuvant chemoradiotherapy, and then to total neoadjuvant therapy (TNT). Although the traditional mode of "preoperative chemoradiotherapy + surgery + adjuvant chemotherapy" reduces the local recurrence rate, the distant metastasis rate is still high, and the compliance of postoperative adjuvant chemotherapy is poor. By advancing postoperative chemotherapy to preoperative period, TNT has formed "induction chemotherapy + concurrent chemoradiotherapy + surgery" or "concurrent chemoradiotherapy + consolidation chemotherapy + surgery" mode, which has significantly improved the completion rate of treatment and the rate of pathological complete response (pCR). Many studies have shown that induction chemotherapy has the potential to improve disease free survival (DFS) and metastasis control, while consolidation chemotherapy has advantages in organ preservation rate. In addition, breakthroughs have been made in immunotherapy for patients with Mismatch Repair Deficiency (dMMR). Single-agent PD-1 inhibitors can lead to clinical complete response (cCR) in some patients. However, the immunotherapy response of patients with Microsatellite stability (MSS) still needs a breakthrough. The current controversies focus on the selection of chemotherapy timing in TNT mode, the synergistic mechanism of radiotherapy and immunotherapy, and the optimization of precise stratification strategy. In the future, it is necessary to integrate multi-omics data and artificial intelligence models, combined with dynamic efficacy evaluation, to promote individualized treatment decisions, and ultimately achieve the dual goals of survival benefit and function preservation.

Keywords: total neoadjuvant therapy, treatment mode, chemoradiotherapy, immunotherapy

1. Introduction

LARC refers to rectal cancer with full-thickness tumor invasion (T3-4 stage) or regional lymph node metastasis (N+) but without distant metastasis. The standard treatment model of LARC has been changed several times. Before the 1970s, LARC patients were mainly treated with surgery alone. In order to overcome the high local recurrence rate after surgery alone, people began to explore postoperative adjuvant radiotherapy and chemotherapy. In the 1990s, the National Institutes of Health (NIH) issued a consensus, which established "TME surgery + adjuvant chemoradiotherapy" as the standard treatment for LARC. However, the local recurrence rate of LARC patients is still high, and it cannot meet the needs of sphincter preservation. The reason is that the completion rate of postoperative chemotherapy is low, and the downstaging effect of radiotherapy cannot be taken advantage of. Therefore, investigators began to explore the use of postoperative long-course concurrent chemoradiotherapy (LCCRT) before surgery. Subsequently, in the early 20th century, the German

CAO/ARO/AIO-94 study (Sauer R, Becker H, Hohenberger W, et al., 2004) established the important position of preoperative LCCRT (50.4 Gy + 5-FU/ capecitabine) in the treatment of LARC, and then entered the era of neoadjuvant chemoradiotherapy. However, although the current standard treatment (LCCRT + TME surgery + adjuvant chemotherapy) reduces the local recurrence rate of LARC patients, the distant metastasis rate of LARC patients is still high. This is partly due to poor compliance with postoperative adjuvant chemotherapy. Therefore, researchers began to add postoperative adjuvant chemotherapy to preoperative treatment, and since then the treatment of LARC has entered the era of TNT. In addition, the high response rate to immunotherapy has led researchers to look at combining it with chemoradiotherapy. This article systematically reviews the evidence-based progress of treatment modalities, analyzes the current controversy, and provides theoretical basis for the precise treatment of LARC.

2. Evolution of Treatment Modalities

2.1 Era of Postoperative Adjuvant Chemoradiotherapy

Before the 1970s, surgery alone was the main treatment for LARC patients, but the local recurrence rate was high. Therefore, since 1970, people have begun to explore postoperative adjuvant therapy to reduce the local recurrence rate. However, most of the early studies used radiotherapy alone, and the effect was limited. Since 1980, postoperative adjuvant chemoradiotherapy has been gradually developed. The GITSG 7175 trial compared surgery alone, postoperative radiotherapy, postoperative chemotherapy, and postoperative concurrent chemoradiotherapy, and found that postoperative concurrent chemoradiotherapy was significantly superior to surgery alone, chemotherapy alone, or radiotherapy alone in local recurrence control (Thomas P R & Lindblad A S., 1988). In 1990, based on the GITSG 7175 trial, the NIH adopted postoperative concurrent chemoradiotherapy as the standard treatment for LARC, marking the official establishment of the “surgery + adjuvant chemoradiotherapy” model.

2.2 Era of Neoadjuvant Chemoradiotherapy

The advantage of postoperative chemoradiotherapy lies in the clear scope of pathology and tumor bed. However, the poor blood supply of tumor bed, less intestinal peristalsis, and the corresponding high toxic reactions lead to poor compliance with postoperative chemoradiotherapy and high local recurrence rate. Therefore, some scholars began to study preoperative radiotherapy. In the early 21st century, the German CAO/ARO/AIO-94 study compared the “LCCRT+TME surgery” mode with the “TME surgery +LCCRT” mode and found that the preoperative LCCRT combined surgery group had higher overall compliance rate, better local control rate, lower toxicity and higher sphincter preservation rate in patients with low tumors (Sauer R, Becker H, Hohenberger W, et al., 2004). Based on the German CAO/ARO/AIO-94 trial, “LCCRT (50.4 Gy + 5-FU/ capecitabine) +TME surgery + adjuvant chemotherapy” has been listed as the standard treatment mode for LARC, and since then LARC has entered the era of neoadjuvant therapy. The popularity of neoadjuvant therapy marks the shift of the focus of treatment from “postoperative rescue” to “preoperative optimization”, which lays a foundation for subsequent models (such as total neoadjuvant therapy and combined immunotherapy).

2.3 Era of Total Neoadjuvant Therapy

2.3.1 Total Neoadjuvant Therapy and Quasi-Total Neoadjuvant Therapy

Although the local recurrence rate of LARC patients under the standard treatment mode is controlled below 10% (Azria D, Doyen J, Jarlier M, et al., 2017; Bosset J F, Collette L, Calais G, et al., 2006; Martling A L, Holm T, Rutqvist L E, et al., 2000; Dahlberg M, Glimelius B & Pahlman L., 1999), the distant metastasis rate is still as high as about 30% (Azria D, Doyen J, Jarlier M, et al., 2017; Sauer R, Liersch T, Merkel S, et al., 2012; van Gijn W, Marijnen C A, Nagtegaal I D, et al., 2011; Kitz J, Fokas E, Beissbarth T, et al., 2018). Furthermore, moving postoperative chemoradiotherapy to preoperative therapy does not improve the OS of LARC patients. This is in part due to poor adherence to and completion of postoperative adjuvant chemotherapy. Therefore, researchers tried to shift postoperative chemotherapy to preoperative chemotherapy, which derived the concept of induction chemotherapy and consolidation chemotherapy. Since then, the treatment of LARC has entered the era of TNT. TNT refers to bringing all postoperative adjuvant treatment to preoperative treatment, that is, from the traditional “preoperative chemoradiotherapy + surgery + adjuvant chemotherapy” to “induction chemotherapy + preoperative chemoradiotherapy + surgery” or “preoperative chemoradiotherapy + consolidation chemotherapy + surgery” treatment mode. However, some studies only add a part of postoperative chemotherapy to preoperative treatment, forming two mixed modes: one is “chemoradiotherapy/radiotherapy + consolidation chemotherapy + surgery + adjuvant chemotherapy” mode, and the other is “induction chemotherapy + chemoradiotherapy/radiotherapy + surgery + adjuvant chemotherapy” mode. These two modes are called TNT -like (Xiao W W & Chen G., 2019). For example, the SCRT group in the POLISH II study (Jin J, Tang Y, Hu C, et al., 2022; Bujko K, Wyrwicz L, Rutkowski A, et al., 2016) and STELLAR study received the mode of “SCRT+ consolidation chemotherapy + TME surgery + (selective) adjuvant chemotherapy”, while the induction

chemotherapy group in the PROGIGE 23 study (Conroy T, Bosset J F, Etienne P L, et al., 2021) received the mode of “induction chemotherapy + LCCRT + TME surgery + adjuvant chemotherapy”. At present, the concept of TNT-like mode only appears in a review by Xiao et al. (2019), while some existing clinical studies confuse the two concepts of TNT mode and TNT-like mode, and generally refer to TNT mode.

2.3.2 Mode of Induction Chemotherapy

Induction chemotherapy refers to the addition of postoperative adjuvant chemotherapy before neoadjuvant chemoradiotherapy. It eliminates subclinical metastatic lesions through early intervention, thereby improving the pCR rate and finally achieving the therapeutic goal of sphincter preservation. The administration mode of induction chemotherapy under the framework of TNT can provide a basis for dynamic adjustment of subsequent concurrent chemoradiotherapy through the evaluation of drug response in vivo. This staged treatment strategy not only contributes to the development of individualized radiotherapy regimens, but also creates a feasibility space for subsequent radiation dose reduction or selective exemption of radiotherapy by screening chemotherapy-sensitive patients, thereby effectively reducing the risk of radiation-related complications (Ominelli J, Valadao M, Araujo R O C, et al., 2021). Grupo Cancer de Recto 3 (GCR3) study from Spain was one of the early systematic studies to explore the application of preoperative induction chemotherapy in rectal cancer. GCR3 study compared the induction chemotherapy group (induction chemotherapy + LCCRT + TME surgery) with the standard treatment group (LCCRT + TME surgery + adjuvant chemotherapy) and found that the two groups of patients had similar OS, DFS, DM, LRR efficacy, but the induction chemotherapy group had lower acute toxicity and higher compliance (Fernandez-Martos C, Garcia-Albeniz X, Pericay C, et al., 2015). Based on GCR3 and Cercek (2014) studies, NCCN guidelines added “induction chemotherapy + LCCRT + TME surgery” as one of the treatment recommendations for LARC in 2015. The subsequent PRODIGE 23 study compared the neoadjuvant chemotherapy group (induction chemotherapy + LCCRT + TME surgery + adjuvant chemotherapy) with the standard treatment group (LCCRT + TME surgery + adjuvant chemotherapy) and found that the neoadjuvant chemotherapy group was significantly better than the standard treatment group in terms of overall DFS(P=0.034), overall MFS(P=0.017), pCR (28% vs. 12%, P < 0.0001), serious adverse events during adjuvant chemotherapy (11% vs. 23%, P=0.0049), neurotoxicity(12% vs. 21%, P= 0.032), and tumor regression score(median: 8.4 vs 15.0, p<0.0001), but there was no significant difference in overall OS and overall LRR (Conroy T, Bosset J F, Etienne P L, et al., 2021). Cercek (2018) et al.’s GCR3 study compared the TNT group (induction chemotherapy + LCCRT + TME surgery) with the standard treatment group (LCCRT + TME surgery + adjuvant chemotherapy) and found that the overall CR rate of the TNT group (36% vs. 21%, P < 0.001) was better than that of the standard treatment group. And this advantage still existed after eliminating the confounding factor of operation time (41% vs. 27%, P=0.004). In addition, Cercek et al. found that patients in the TNT group were significantly better than those in the standard-care group in terms of ostomy closure time (median: 89 days vs. 192 days, P < 0.001) and the proportion of minimally invasive surgery (72.2% vs. 47.3%, P < 0.001). Chotard et al. (2021) compared the induction chemotherapy group (induction chemotherapy + LCCRT + TME surgery) with the standard therapy group (LCCRT + TME surgery + adjuvant chemotherapy) and found that the induction chemotherapy mode significantly increased the proportion of pN0 patients (75% vs. 625, P=0.03). In conclusion, induction chemotherapy may improve pCR, MFS and DFS of LARC patients compared with standard treatment.

2.3.3 Consolidation Chemotherapy Mode

Consolidation chemotherapy refers to the advance of postoperative adjuvant chemotherapy to neoadjuvant chemoradiotherapy and surgery, which improves the efficacy through the late reaction of radiotherapy and the addition of systemic chemotherapy. The clinical goal of consolidation chemotherapy is to achieve significant tumor volume reduction, pathological stage improvement, and occult micrometastasis clearance in the neoadjuvant stage. Based on the consolidation chemotherapy regimen of TNT strategy, after the completion of concurrent chemoradiotherapy, the tumor response can be dynamically monitored by imaging and molecular markers, and then the individualized continuous treatment plan can be formulated. Our data show that the prolongation of consolidation chemotherapy cycles is positively correlated with the pCR rate, while there is no statistically significant difference in the incidence of perioperative complications and adverse event spectrum, suggesting that the consolidation chemotherapy mode may provide a new direction (Kim SY, Joo J, Kim T W, et al., 2018; Wang Y, Lou Z, Ji L Q, et al., 2023) for improving the long-term prognosis of patients. The RAPIDO study (Bahadoer R R, Dijkstra E A, van Etten B, et al., 2021) compared the experimental group (SCRT + consolidation chemotherapy +TME) with the standard treatment group and found that the 3-year disease-related treatment failure rate (23.7% vs. 30.4%, P=0.019) and 3-year distant metastasis rate (20.0% vs. 26.8%, P=0.0048) in the experimental group were significantly better than those in the standard treatment group. The POLISH II study (Bujko K, Wyrwicz L, Rutkowski A, et al., 2016) compared the preoperative SCRT plus consolidation chemotherapy group with the standard therapy group and found that the preoperative SCRT plus consolidation chemotherapy group had a better 3-year OS rate than the standard therapy group (73.0% vs.

65.0%, P=0.046). Based on RAPIDO study and POLISH II study, NCCN guidelines recommend SCRT combined with consolidation chemotherapy (CAPOX or FOLFOX) as the recommended regimen for patients with LARC. The subsequent STELLAR study (Jin J, Tang Y, Hu C, et al., 2022) compared the TNT group (SCRT + consolidation chemotherapy + TME surgery) with the CRT group (LCCRT + TME surgery + adjuvant chemotherapy) and found that the TNT group had a better 3-year OS rate (86.5% vs. 75.1%, P=0.033) and overall pCR rate (21.8% vs. 12.3%, P=0.033). TNT was superior to CRT in terms of OS (86.5% vs. 75.1%, P=0.033) and overall PCR rate (21.8% vs. 12.3%, P=0.002). TNT was noninferior to CRT in terms of overall DFS (P < 0.001), while there was no significant difference in 3-year MFS and LRR. In conclusion, consolidation therapy may have a certain value in improving the OS, pCR and DM rates of LARC patients compared with standard therapy.

2.3.4 Comparison Between Induction Chemotherapy and Consolidation Chemotherapy

In terms of some prognostic indicators, induction chemotherapy and consolidation chemotherapy show the possibility of being better than the standard treatment, but whether there is a difference in efficacy between induction chemotherapy and consolidation chemotherapy is still controversial. The CAO/ARO/AIO-12 trial is the first prospective study (Fokas E, Schlenska-Lange A, Polat B, et al., 2022) to report the head-to-head comparison between induction and consolidation chemotherapy. It compared the induction chemotherapy group (chemotherapy +LCCRT+TME surgery) with the consolidation chemotherapy group (LCCRT + consolidation chemotherapy + TME surgery) and found that the consolidation chemotherapy group had a significantly better pCR rate (25% vs. 15%, $P < 0.001$) than historical data. However, direct comparison between the consolidation chemotherapy group and the induction chemotherapy group did not show statistically significant difference (25% vs 17%, P=0.071). These results suggest that consolidation chemotherapy is a better choice for improving pCR rate, but further phase III trials are needed to verify the long-term survival benefit. However, the 3-year follow-up of the CAO/ARO/AIO-12 study (Fokas E, Schlenska-Lange A, Polat B, et al., 2022) showed that the higher pCR rate in the consolidation chemotherapy group did not bring long-term survival benefit. The next CAO/ARO/AIO-18 study will further compare the efficacy of preoperative SCRT combined with consolidation chemotherapy and preoperative LCCRT combined with consolidation chemotherapy. In addition, the OPRA study (Garcia-Aguilar J, Patil S, Gollub M J, et al., 2022) compared LARC patients who received induction chemotherapy (chemotherapy + LCCRT + selective TME surgery) with those who received consolidation chemotherapy (LCCRT + chemotherapy + selective TME surgery) and found that patients who received consolidation chemotherapy achieved a higher 3-year organ preservation rate (41% vs. 53%, P=0.01). However, there were no significant differences in 3-year DFS, OS, DM and LRR between the two groups. The preliminary results of OPRA study suggest that consolidation chemotherapy is more advantageous in tumor regression and organ preservation. The long-term follow-up results of OPRA study showed that the 5-year surgery-free survival rate of the consolidation chemotherapy group was significantly higher than that of the control group (54% vs 39%, P=0.012), but there was no significant difference in 5-year OS, DFS, LRR, and DM between the two groups. This further confirmed that the consolidation chemotherapy mode had the advantage of organ preservation in terms of organ preservation rate, and the survival outcome was not affected by the treatment sequence. In conclusion, for patients with a strong desire for organ preservation, TNT is recommended as the preferred consolidation chemotherapy.

3. Exploration of Neoadjuvant Immunotherapy

3.1 Current Evidence

Approximately 5% to 10% of rectal adenocarcinomas have dMMR, and these patients have a poor response to standard chemotherapy regimens (CercekA, Dos Santos Fernandes G, Roxburgh C S, et al., 2020; Alex A K, Siqueira S, Coudry R, et al., 2017; Alatise O I, Knapp G C, Sharma A, et al., 2021). The use of immune checkpoint blockade alone as a first-line treatment for patients with metastatic colorectal cancer and refractory disease with dMMR has been shown to improve objective response rates and prolong overall survival in such patients (Andre T, Shiu K K, Kim T W, et al., 2020; Le D T, Uram J N, Wang H, et al., 2015; Overman M J, Lonardi S, Wong K Y M, et al., 2018). Based on this finding of benefit in metastatic colorectal cancer, Cercek et al. (2022) explored the use of anti-PD-1 monoclonal antibody alone followed by standard chemoradiotherapy followed by surgery in patients with LARC and dMMR, depending on whether the patient achieved cCR. All 12 patients achieved cCR and were recurrence-free with at least 6 months of subsequent follow-up. The study by Cercek et al. is a pioneer study to explore PD-1 inhibitors as neoadjuvant therapy in LARC with dMMR at an early stage, which lays the foundation for subsequent immunotherapy application. The VOLTAGE-A study (Bando H, Tsukada Y, Inamori K, et al., 2022) is the first clinical study to integrate an immune checkpoint inhibitor (Nivolumab) into the TNT framework in patients with LARC. The treatment model of “LCCRT+ immunotherapy +TME surgery ± adjuvant chemotherapy” has significantly improved the pCR rate of patients with MSS and Microsatellite instability- high (MSI-H), and clarified the predictive value of PD-L1 and

CD8/CTreg ratio. These results provide an important evidence-based basis for the application of immunotherapy in LARC patients, and mark substantial progress in precision immunotherapy in this field.

3.2 Challenges

There are still many challenges in the immunotherapy of LARC. First, the molecular heterogeneity of LARC patients significantly affects the efficacy and universality of immunotherapy. Based on MSI status, LARC patients can be divided into two major subtypes, dMMR/MSI-H and MSS. Although dMMR/MSI-H patients are sensitive to immunotherapy, they account for only 5% to 10% of patients with rectal adenocarcinoma, and some patients are still at risk of drug resistance. However, MSS subtype accounts for more than 90% of patients with rectal adenocarcinoma and has a low response rate to immunotherapy. In addition, the dynamic changes of immune microenvironment (such as up-regulation of PD-L1 expression after radiotherapy) and genomic instability (such as POLE/POLD1 mutation) further increase the complexity of efficacy prediction. Second, the timing of radiotherapy and immunotherapy remains to be resolved. Whether preoperative radiotherapy followed by immunotherapy, preoperative immunotherapy followed by radiotherapy, or radiotherapy combined with immunotherapy is more beneficial to patients and how long the interval between radiotherapy and immunotherapy remains controversial.

4. Conclusions and Prospects

With the continuous evolution of treatment modalities for LARC, individualized treatment strategy has become the core orientation of clinical practice. Current studies have shown that multi-dimensional factors such as tumor anatomical location, stage, molecular characteristics, functional status and willingness to preserve anus should be comprehensively considered in the formulation of treatment plans for LARC. For example, for patients with large tumors or low rectal cancer, consolidation chemotherapy may significantly improve the organ preservation rate by enhancing tumor regression effect. In contrast, for patients at high risk for metastasis (e.g., N2 stage or vascular invasion), induction chemotherapy may improve disease-free survival through early systemic control. In addition, dMMR/MSI-H patients can significantly benefit from neoadjuvant immunotherapy, while MSS patients need to explore the synergistic strategy of radiotherapy combined with immunotherapy. Adaptive treatment adjustment based on dynamic response evaluation (e.g., imaging response, changes in molecular markers), such as the “watch and wait” strategy of adjusting radiotherapy dose according to chemotherapy sensitivity or waiving surgery, further promotes the realization of personalized precision medicine. In the future, the integration of multi-omics data and artificial intelligence prediction models is expected to achieve more refined risk stratification and treatment optimization.

References

Alatise O I, Knapp G C, Sharma A, et al., (2021). Molecular and phenotypic profiling of colorectal cancer patients in West Africa reveals biological insights. *Nature Communications*, *12*(1), 6821.

Alex A K, Siqueira S, Coudry R, et al., (2017). Response to Chemotherapy and Prognosis in Metastatic Colorectal Cancer with DNA Deficient Mismatch Repair. *Clinical colorectal cancer*, *16*(3), 228-39.

Andre T, Shiu K K, Kim T W, et al., (2020). Pembrolizumab in Microsatellite-Instability-High Advanced Colorectal Cancer. *The New England Journal of Medicine*, *383*(23), 2207-18.

Azria D, Doyen J, Jarlier M, et al., (2017). Late toxicities and clinical outcome at 5 years of the ACCORD 12/0405-PRODIGE 02 trial comparing two neoadjuvant chemoradiotherapy regimens for intermediate-risk rectal cancer. *Annals of Oncology: Official Journal of the European Society for Medical Oncology*, *28*(10), 2436-42.

Bahadoer R R, Dijkstra E A, van Etten B, et al., (2021). Short-course radiotherapy followed by chemotherapy before total mesorectal excision (TME) versus preoperative chemoradiotherapy, TME, and optional adjuvant chemotherapy in locally advanced rectal cancer (RAPIDO): a randomised, open-label, phase 3 trial. *The Lancet Oncology*, *22*(1), 29-42.

Bando H, Tsukada Y, Inamori K, et al., (2022). Preoperative Chemoradiotherapy plus Nivolumab before Surgery in Patients with Microsatellite Stable and Microsatellite Instability-High Locally Advanced Rectal Cancer. *Clinical Cancer Research: An Official Journal of the American Association for Cancer Research*, *28*(6), 1136-46.

Bosset J F, Collette L, Calais G, et al., (2006). Chemotherapy with preoperative radiotherapy in rectal cancer. *The New England Journal of Medicine*, *355*(11), 1114-23.

Bujko K, Wyrwicz L, Rutkowski A, et al., (2016). Long-course oxaliplatin-based preoperative chemoradiation versus 5 × 5 Gy and consolidation chemotherapy for cT4 or fixed cT3 rectal cancer: results of a randomized phase III study. *Annals of Oncology: Official Journal of the European Society for Medical Oncology*, 27(5), 834-42.

Cercek A, Goodman K A, Hajj C, et al., (2014). Neoadjuvant chemotherapy first, followed by chemoradiation and then surgery, in the management of locally advanced rectal cancer. *Journal of the National Comprehensive Cancer Network: JNCCN*, *12*(4), 513-9.

CercekA, Dos Santos Fernandes G, Roxburgh C S, et al., (2020). Mismatch Repair-Deficient Rectal Cancer and Resistance to Neoadjuvant Chemotherapy. *Clinical Cancer Research: An Official Journal of the American Association for Cancer Research*, *26*(13), 3271-9.

CercekA, Lumish M, Sinopoli J, et al., (2022). PD-1 Blockade in Mismatch Repair-Deficient, Locally Advanced Rectal Cancer. *The New England Journal of Medicine*, 386(25), 2363-76.

CercekA, Roxburgh C S D, Strombom P, et al., (2018). Adoption of Total Neoadjuvant Therapy for Locally Advanced Rectal Cancer. *JAMA Oncology*, *4*(6), e180071.

Chotard G, Capdepont M, Denost Q, et al., (2021). Effects of neoadjuvant chemotherapy plus chemoradiotherapy on lymph nodes in rectal adenocarcinoma. *Virchows Archiv: An International Journal of Pathology*, *479*(4), 657-66.

Conroy T, Bosset J F, Etienne P L, et al., (2021). Neoadjuvant chemotherapy with FOLFIRINOX and preoperative chemoradiotherapy for patients with locally advanced rectal cancer (UNICANCER-PRODIGE 23): a multicentre, randomised, open-label, phase 3 trial. *The Lancet Oncology*, *22*(5), 702-15.

Dahlberg M, Glimelius B, Pahlman L., (1999). Changing strategy for rectal cancer is associated with improved outcome. *The British Journal of Surgery*, *86*(3), 379-84.

Fernandez-Martos C, Garcia-Albeniz X, Pericay C, et al., (2015). Chemoradiation, surgery and adjuvant chemotherapy versus induction chemotherapy followed by chemoradiation and surgery: long-term results of the Spanish GCR-3 phase II randomized trial †. *Annals of Oncology: Official Journal of the European Society for Medical Oncology*, *26*(8), 1722-8.

Fokas E, Schlenska-Lange A, Polat B, et al., (2022). Chemoradiotherapy Plus Induction or Consolidation Chemotherapy as Total Neoadjuvant Therapy for Patients with Locally Advanced Rectal Cancer: Long-term Results of the CAO/ARO/AIO-12 Randomized Clinical Trial. *JAMA Oncology*, *8*(1), e215445.

Garcia-Aguilar J, Patil S, Gollub M J, et al., (2022). Organ Preservation in Patients with Rectal Adenocarcinoma Treated with Total Neoadjuvant Therapy. *Journal of Clinical Oncology: Official Journal of the American Society of Clinical Oncology*, *40*(23), 2546-56.

Jin J, Tang Y, Hu C, et al., (2022). Multicenter, Randomized, Phase III Trial of Short-Term Radiotherapy Plus Chemotherapy Versus Long-Term Chemoradiotherapy in Locally Advanced Rectal Cancer (STELLAR). *Journal of Clinical Oncology: Official Journal of the American Society of Clinical Oncology*, *40*(15), 1681-92.

Kim SY, Joo J, Kim T W, et al., (2018). A Randomized Phase 2 Trial of Consolidation Chemotherapy After Preoperative Chemoradiation Therapy Versus Chemoradiation Therapy Alone for Locally Advanced Rectal Cancer: KCSG CO 14-03. *International Journal of Radiation Oncology, Biology, Physics*, *101*(4), 889-99.

Kitz J, Fokas E, Beissbarth T, et al., (2018). Association of Plane of Total Mesorectal Excision With Prognosis of Rectal Cancer: Secondary Analysis of the CAO/ARO/AIO-04 Phase 3 Randomized Clinical Trial. *JAMA Surgery*, *153*(8), e181607.

Le D T, Uram J N, Wang H, et al., (2015). PD-1 Blockade in Tumors with Mismatch-Repair Deficiency. *The New England Journal of Medicine*, *372*(26), 2509-20.

Martling A L, Holm T, Rutqvist L E, et al., (2000). Effect of a surgical training programme on outcome of rectal cancer in the County of Stockholm. Stockholm Colorectal Cancer Study Group, Basingstoke Bowel Cancer Research Project. *Lancet (London, England)*, *356*(9224), 93-6.

Ominelli J, Valadao M, Araujo R O C, et al., (2021). The Evolving Field of Neoadjuvant Therapy in Locally-advanced Rectal Cancer: Evidence and Prospects. *Clinical Colorectal Cancer*, *20*(4), 288-98.

Overman M J, Lonardi S, Wong K Y M, et al., (2018). Durable Clinical Benefit with Nivolumab Plus Ipilimumab in DNA Mismatch Repair-Deficient/Microsatellite Instability-High Metastatic Colorectal Cancer. *Journal of Clinical Oncology: Official Journal of the American Society of Clinical Oncology*, *36*(8), 773-9.

Sauer R, Becker H, Hohenberger W, et al., (2004). Preoperative versus postoperative chemoradiotherapy for rectal cancer. *The New England Journal of Medicine*, *351*(17), 1731-40.

Sauer R, Liersch T, Merkel S, et al., (2012). Preoperative versus postoperative chemoradiotherapy for locally advanced rectal cancer: results of the German CAO/ARO/AIO-94 randomized phase III trial after a median

follow-up of 11 years. *Journal of Clinical Oncology: Official Journal of the American Society of Clinical Oncology*, *30*(16), 1926-33.

Thomas P R, Lindblad A S., (1988). Adjuvant postoperative radiotherapy and chemotherapy in rectal carcinoma: a review of the Gastrointestinal Tumor Study Group experience. *Radiotherapy and Oncology: Journal of the European Society for Therapeutic Radiology and Oncology*, *13*(4), 245-52.

van Gijn W, Marijnen C A, Nagtegaal I D, et al., (2011). Preoperative radiotherapy combined with total mesorectal excision for resectable rectal cancer: 12-year follow-up of the multicentre, randomised controlled TME trial. *The Lancet Oncology*, *12*(6), 575-82.

Wang Y, Lou Z, Ji L Q, et al., (2023). Clinical application progress of total neoadjuvant therapy for locally advanced rectal cancer. *Chinese Journal of Practical Surgery*, *43*(4), 461-4.

Xiao W W, Chen G., (2019). Transition of treatment strategy for locally advanced rectal cancer towards “watch and wait”. *Zhonghua wei chang wai ke za zhi = Chinese Journal of Gastrointestinal Surgery*, *22*(6), 514-20.